INTERFACIAL COEFFICIENTS IN POWDER METAL COMPACTION

by

RICHARD FRANCIS MALLENDER B.Sc.(HONS)

Doctoral Thesis

Submitted in partial fulfilment of the requirements for the award of Doctor of Philosophy of Loughborough University of Technology

JANUARY 1974

Supervisors: Dr. D. S. COLEMAN
Mr. C.J. DANGERFIELD

Department of Materials Technology

INTERFACIAL COEFFICIENTS OF POWDER METAL COMPACTION

By R. F. MALLENDER

SYNOPSIS

A study has been made of the die compaction of metal powders and in particular the problems associated with friction between sliding surfaces have been examined. Friction, which results from adhesion or welding, plays an important role in powder consolidation and is greatly influenced by the condition of the surfaces concerned.

Attention has been focused upon the compact die interface and the interactions occurring within this region. In particular information has been obtained for friction coefficients between the sliding surfaces and the role of lubricants in affecting these parameters.

An assessment has been made of the effect of admixed lubricant level upon the laboratory scale compaction of a reduced iron powder. Ejection forces have been measured and the effects of lubricant content and characteristics evaluated. Die material and surface finish has been shown to be of importance during compaction and ejection. Compact surfaces and strengths have been examined and correlated with the ejection stress data.

Determination of friction coefficients necessitated calculations of the residual radial stress acting upon the compacts during ejection. This required determination of the elastic properties of the pressed compacts before coefficient of friction values between compact and die wall could be obtained for mixtures containing up to 2.0 w/o lubricant.

A production tableting press has been fully instrumented to allow measurement of the forces involved during high speed compaction and ejection. A comparison of stress values between production and laboratory scales has been made, and die radial stress measurements have been taken during the compaction cycle and compared with the calculated values.

The experimental data obtained were found to agree with existing pressure-density relationships. The energy involved in the rapid compaction of an iron powder has been determined and how this was influenced by lubricants.

Friction coefficients have also been determined with a "pin and disc friction testing apparatus, and compared with the coefficients measured dynamically on the production press. The effects of lubricant type, pin load, speed, temperature, and disc material upon the coefficient of friction and wear rate have been found. Worn surfaces have been examined using profilimeter and electron optical techniques, and possible wear mechanisms discussed.

ACKNOWLEDGEMENTS

The Author would like to thank Dr. D. S. Coleman and Mr. C. J. Dangerfield for their invaluable assistance and many helpful discussions during the course of this work. The Author also wishes to thank the British Metal Sinterings Association for their financial assistance to carry out this research. Thanks must also go to all the members of the Association for assistance with various items of equipment, as well as helpful advice and discussions during the progress of these studies. Shell Ltd., Thornton Research Centre must be thanked for their helpful advice and loan of the "Pin and Disc" machine, and likewise Durham Chemicals Ltd are thanked for their assistance in carrying out chemical analyses on the lubricants tested.

INDEX

1.00 INTRODUCTION

The field of Powder Metallurgy involves those industries which use powders as their raw material from which to press out components. The majority of powders used are metallic, though some industries use ceramic powders, such as ferrites for the electronics industries, or carbides for tool tips or friction materials in the engineering industries. The bulk of the powders used are iron or steel powders, however some bronze, copper and other non-ferrous powders are used, but to a far less extent.

Because a powder is pressed in a die to make the component the process lends itself to a wide range of shapes and types of components having use in a great number of industries. Those industries involved in making transport vehicles, such as cars, lorries, motor cycles, bicycles demand the bigger and stronger components based on iron powders. Other industries making sewing machines, typewriters, calculating and cash register machines require the smaller and sometimes more intricate parts.

The production of powder metal components relies on lubricants to reduce wear in the tooling, to aid ejection after compaction particularly after high pressure compaction, and in some cases to give strength to the green component prior to sintering.

Although a large research effort has been devoted to discover the most suitable lubricants and the amounts required to give the optimum results in terms of compacted components with the high density; little research has been devoted to study what role the lubricant really plays in the powder metallurgy process.

Ideally the addition of lubricants to produce a component is wasteful, in as far as the lubricant is burnt in the pre-heating prior to sintering. Furthermore, any residues of the lubricant can sometimes be detrimental to the component's properties. It certainly tends to increase the porosity of the sintered component, and it would be better therefore to do without the lubricant altogether, if it were possible. This is not possible because the wear on tooling and the extra energy required to eject the components would far offset the cost of the lubricant, even allowing for the extra cost of preheating or dewaxing furnaces; most certainly the overall production times would be increased and damage through jammed tooling would be involved.

Therefore, if the role the lubricant plays in the process can be evaluated and understood, alterations to the accepted procedure could possibly be devised and examined . Study of the process is restricted however, because it is extremely difficult to find the parameters which relate a lubricant's performance correctly. The amount and type of lubricant can easily be decided by considering the maximum pressed densities achieved in the components. Also the speed and pressures required to give the optimum results can be examined. However, these types of studies have been carried out before and have not really elucidated the part that a lubricant plays in the powder metallurgy compaction and ejection process.

We believe that this problem is a surface/surface or interfacial one. In the process we have interactions of lubricant, metal powder particles, dies and punches. These present interfaces such as lubricant/metal particle, metal particle/dieface, lubricant/dieface, all of which are involved in the process. For these reasons this thesis has set out to examine such interfacial reactions from the consideration of coefficients of friction at these combinations of surfaces. A study of friction at

these surfaces enables the efficiency of a lubricant type to be evaluated, as well as what effects interaction of the lubricant has with the range of surfaces presented in the compaction and ejection process.

Such a study of surfaces and friction phenomenon must be linked of course to real production conditions for a time evaluation to be considered. This raises problems of accurate scientific study on a large, mobile and complex system, such as presented by a typical powder metal compaction press.

To evaluate friction parameters, exact stress measurements at the interacting surfaces under study must be made. This is experimentally difficult and few researchers have attempted it. Those who have done so are recorded and discussed in the next chapter. This research has used these previous studies to assist in tackling the problem again and perhaps in a newer way. A simple consideration of the powder metal compaction and ejection process indicates that friction coefficients can only be obtained on stable sliding surfaces. Therefore, since compaction is a continuously changing process up to the attainment of the final pressed density, involving massive interparticle sliding as well as particle/die and punch interactions; only ejection can be studied properly because this involves sliding of complete and virtually unchanged surfaces.

This research records the study of the system on ejection. Here it is possible to measure accurately the stresses on the punch, die and compact, when ejection is in progress. Under these conditions, it is possible to examine also the lubricant films produced in the compaction process, the surface of the compacts, the surfaces of the tools, and determine the coefficient of friction for the interaction of these surfaces.

Ejection behaviour of metal powders with lubricants has been studied, and is reported here, in two distinct ways. Compaction and ejection has been performed and studied using a small die and laboratory sized equipment. This enabled these "Laboratory Studies" to be adapted and translated into "Pilot Scale Studies" using a full sized powder metallurgy mechanical compaction press which was fully instrumented for this research. This instrumentation was set up from experience gained in visits to industrial plants and therefore the results will have some direct relevance to "real" as opposed to "laboratory" conditions.

Because this research involves already a complex system, only one metal powder and one type of lubricant has been considered. These materials were used as "model" materials upon which the basic concepts of interfacial friction can be based. The metal powder was a commonly used reduced iron powder, typical of industrial materials presently in use in iron component manufacture. Lubricants given preference from industrial experience are those based on stearates, usually stearates of the alkali and alkaline earth metals such as lithium, sodium, calcium, magnesium stearates etc. In particular the zinc stearate has fairly universal use, therefore this research has concentrated on a reduced iron powder/zinc stearate combination; although other stearates have been examined cursorily during this work.

It will be seen that because we are considering a series of surface interactions, the study of these has been considerably helped by the use of the Scanning Electron Microscope, which gives a real insight into the type of surface conditions encountered on this process.

Further to the study of frictional surfaces, this research has been reinforced by some considerable study of rubbing surfaces and the resultant wear produced. Although no major evaluation of wear is considered in this

work, valuable insight into the powder metallurgy process has been gained by the use of a "Pin-and-Disc" friction apparatus. Reported in this thesis are some studies of a range of die materials and their corresponding surface interaction with iron/zinc stearate compacts and the resultant coefficients of friction for each system.

Finally, it is worth noting here that this research was carried out with the aid and assistance of the Members of the British Metal Sintering Association, from whom, by visits, discussions etc. this research was able to benefit from true industrial conditions, both in plant and from research and development areas. The research has already resulted in the presentation of a paper at the Powder Metallurgy Joint Group Annual Meeting held in Eastbourne in November 1972.

2.00 REVIEW OF FRICTION, WEAR AND LUBRICATION CONCEPTS

2.10 Surface and Contact Area

1. Contact Between Solids and Surface Interactions
2. Area of Contact Between Surfaces

2.20 The Nature of Friction

1. Mechanism of Friction
2. The Influence of Surface Properties Upon Friction

2.30 Boundary Friction and Lubrication

1. General Considerations
2. Effect of Lubricant Chain Length and Film Thickness upon Boundary Friction
3. Effect of Speed, Load and Temperature on Boundary Friction
4. Mechanisms of Boundary Lubrication

2.40 Metallic Wear

1. Lubricated and Unlubricated Wear
2. Mechanism of Unlubricated Wear
3. Mechanism of Lubricated Wear

2.50 Application of Modern Techniques in Friction and Wear Studies

2.00 REVIEW OF FRICTION, WEAR AND LUBRICATION CONCEPTS

2.10. Surfaces and Contact Area

1. Contact between solids and surface interactions. The surfaces of solids are never perfectly flat, but are irregular and rough. Even the best surface finishes that can be produced are far from being flat. For instance, coarse ground surfaces and superfinished surfaces can have irregularities of between 0.5-3.0 microns and between 0.04-0.1 microns respectively.

BOWDEN and TABOR [20] and HOLM [21] determined the real contact area of surfaces in contact using electrical resistance techniques. The measurements indicated that when two metal surfaces are placed together, contact occurs over only a very small fraction of the apparent contact area. For example, using two steel flats of 21cm^2 area under a load of 5 KN, the true area of contact was found to be 0.05cm^2. This fact has been of considerable importance in the development of friction theory [1].

When two metal surfaces are brought together, contact occurs at a few widely spaced areas. The number of contacts depends upon the nature of the surfaces and the load on the surfaces. As the load is increased the two surfaces approach, interacting regions at first deform elastically and as the yield stress is exceeded, then local plastic deformation occurs. New contact areas are formed as the existing ones grow in size. Equilibrium occurs when the total contact area has increased sufficiently to carry the load at the mean yield stress of the contacts [2].

When the load is removed there is a relaxation of elastic stress and the surfaces separate, the contact spots previously formed being destroyed. For clean metals particularly soft ones, separation may be

hindered by adhesion occurring between the surfaces when the load is applied. With harder metals or contaminated surfaces the junctions may break readily.

Under the action of combined normal and tangential forces, contact points are continually being made and broken, the contact points being referred to as adhesive bonds. The result of this is that the underlying material deforms and is changed compared with its original state. Friction and wear occurs from the formation, existence and destruction of the bonds and the bulk deformation of the material[1]. The important factors in the interactions between the surfaces will therefore be the characteristics of the adhesion bond and the influence of any surface protective layers.

2. Area of contact between surfaces. The approach of two ideal smooth curved surfaces was first considered by HERTZ[19]. If an asperity is considered as a portion of a sphere radius r and it rests upon a flat surface then at first the deformation is elastic. The diameter of the contact circle is given by

$$d = 1.1 \left[\frac{P r}{2} \left(\frac{1}{E_1} + \frac{1}{E_2} \right) \right]^{\frac{1}{3}} \quad \ldots\ldots\ldots\ldots\ldots\ldots \quad (1)$$

where E_1 and E_2 are Young's Moduli for the two surfaces, P is the normal load. This predicts therefore that for elastic deformation of the contact area: $A = \pi a^2$ is proportional to $P^{\frac{2}{3}}$. However, Bowden and Tabor[1] demonstrated that for most types and shapes of surface irregularity the real contact area is very nearly proportional to the load which agrees with plasticity theory. Bowden and Tabor[20] consider that the stresses acting upon the contacting surface asperities are equal to the hardness of the softer of the two metals, i.e. the pressure that can be

supported under the action of a localised deformation is equal to the indentation hardness.

The elastic deformation of asperities was discounted by a number of workers, because the single contact theory outlined above gives an area of contact proportional to $P^{\frac{2}{3}}$ and thus the kinetic frictional force should also be proportional to $P^{\frac{2}{3}}$ in contrast with the observed direct proportionality. However ARCHARD[9] has shown that by making assumptions regarding the distribution of contacting asperities and by application of the single contact theory to the multiple point contacts, then the first law of friction can be explained altogether in terms of elastic theory. By considering an increasingly complex topography ARCHARD[10] demonstrated that the relationship between contact area and elastically supported load approached linearity.

The formation of adhesive bonds has been investigated by a number of workers[3,4,5] who conclude that strong welded junctions, which result in a high coefficient of friction, are produced between metals forming solid solutions. Furthermore, MACFARLANE and TABOR[6] have shown that oxide films decrease the adhesive interaction.

2.20. The Nature of Friction

1. The Mechanism of Friction. Various views have been put forward regarding the mechanism of friction. It has been explained in terms of: lifting micro asperities over each other; molecular attraction forces between the two solids; deformation of a volume of one material by the asperities of the second, and various other composite theories.

Bowden and Tabor[1] have suggested that the frictional resistance results from the shear strength of metallic junctions formed under the

normal load P. Thus if A_c is the total area of contact and $\bar{s}$ is the mean shear strength of the junctions, then the static frictional force F_{stat} is given by the relationship:-

$$F_{stat} = A_c.\bar{s} = \frac{P.\bar{s}}{\bar{p}} \qquad \ldots\ldots\ldots\ldots\ldots\ldots (2)$$

where $\bar{p}$ is the mean yield strength of all the junctions.

Bowden and Tabor also claim that the junctions still weld together when the surfaces are slid over each other. The force required to maintain a constant sliding speed whilst forming and breaking asperity contacts is the kinetic frictional force F_{kin}. This assumes a negligible force for bulk deformation of the material.

In this case, $F_{kin} = \frac{P.\bar{s}}{\bar{p}}$ $\ldots\ldots\ldots\ldots\ldots\ldots (3)$

Thus since both shear strength and yeild stress are inherent properties of the material and their ratio is almost constant, the frictional force is proportional to the normal load. Also the real area of contact determines the frictional force. This is in accordance with the two basic laws of friction first recorded by LEONARDO da VINCI[7].

Now the kinetic coefficient of friction μ_{kin} is:

$$\mu_{kin} = \frac{F_{kin}}{P} = \frac{\bar{s}}{\bar{p}} \qquad \ldots\ldots\ldots\ldots\ldots\ldots (4)$$

Since shearing occurs in the softer material, Bowden and Tabor suggest that $\bar{s}$ will be approximately equal to the shear strength of the softer material. Hence we can write

$$\mu_{kin} = \frac{\text{shear strength of softer material}}{\text{yield pressure of softer material}} \qquad \ldots\ldots\ldots (5)$$

This idea is used to explain why μ_{kin} lies in a fairly narrow range for a large number of materials. More recently BOWDEN and TABOR[8] have shown that a more correct relationship is:-

$$\mu_{kin} = \frac{\text{critical shear stress at the interface}}{\text{plastic yield pressure of the underlying material}} \qquad (6)$$

A further factor contributing to the frictional force can also occur when one surface is harder than the other. The asperities of the harder surface will plough out the softer material. However for harder materials this ploughing term is considered to be small[1].

Archard[9,10,11] however, has obtained evidence that the plastic deformation and cold welding hypothesis is not valid under all conditions of sliding. He suggests instead that entirely elastic deformation can explain the proportionality between frictional force and load. The frictional force between the sliding surfaces results from the energy required to elastically deform the real contact areas. On the other hand, the plastic deformation hypothesis suggest that the frictional force results partly from the force required to break welded junctions formed between the two surfaces. In practice possibly both mechanisms occur to a greater or lesser degree depending upon the sliding conditions.

2. The Influence of Surface Properties Upon Friction. As stated earlier, friction is greatly affected by the conditions at the surfaces of the opposing materials. This is quite obvious since the strength of adhesion at the contact points is markedly influenced by the presence of surface films; because the mean shear strength of the junctions is decreased by these films and if the area of contact does not increase proportionately, then there will be a resultant decrease in the coefficient of friction.

A number of workers have shown the effects of environment on the frictional force. BOWDEN and HUGHES[12] and CAMPBELL[13] carried out research in vacuum and in controlled atmospheres and showed the dramatic effect of surface films in reducing the coefficient of friction of perfectly clean surfaces. Soft metal films, having low shear strengths,

have also been shown to reduce friction coefficients[14]. Film thickness is of importance and a number of workers have demonstrated its effects[1,13].

Soaps and soft waxes are often used to reduce friction coefficients since they produce thin films on the surfaces of the metals having low shear strengths[15], the contact area remaining constant. If deformation occurs entirely within the soap film the friction coefficient is the same as that on the solid soap. This is much greater than the value found when the load begins to deform the underlying metal.

Thus the presence and nature of surface films greatly influences surface interactions and the resultant friction coefficients.

2.30 Boundary Friction and Lubrication.

1. General Considerations. Boundary lubrication and its mechanisms is a complex subject involving surface interactions and reactions. Boundary lubrication is of considerable engineering importance since it controls the behaviour of most sliding systems. Boundary lubrication occurs under conditions of high load and/or low surface velocity. As the load increases the lubricant film becomes thinner and thinner until the asperities begin to penetrate the film. At these asperity tips the lubrication is of a boundary nature. Clean metal surfaces have friction coefficients of around 1.00, whereas surfaces lubricated with boundary films have coefficients of friction between 0.05 and 0.15. Dry sliding between surfaces is usually discontinuous involving a "stick-slip" type of motion, whose frequency is governed by the elastic characteristics of the testing machine used. "Stick-slip" motion also occurs under conditions of poor boundary lubrication, i.e. steel lubricated with paraffin or alcohol. A good boundary lubricant will normally prevent

such oscillations allowing the surfaces to glide over each other. Long chained molecules such as fatty acids, have been found to exhibit good boundary lubrication properties.

A considerable amount of work has been carried out in this area to understand the basic mechanisms responsible for boundary friction and adhesion between solids. Various factors have been shown to be of importance. These will be outlined below.

2. Effect of lubricant chain length and film thickness upon boundary friction. HARDY[22] has investigated this subject extensively and has shown that the friction coefficient and the molecular weight of a lubricant are related. Bowden and Tabor[1] and ZISMAN[27] found a similar relationship, but also found that the friction coefficient reaches a minimum limiting value as the lubricant molecular weight is further increased. Following the original work of Hardy a number of investigators have studied the effect of thin films of polar organic substances in reducing the coefficient of friction. LANGMUIR[23] found that a single molecular layer deposited onto glass using the Langmuir trough technique reduces the friction to the same value as that observed with excess lubricant. Some time later, it was demonstrated[24] that a multilayer of calcium or barium stearate was no more effective than a monolayer in reducing the friction. It was however shown that under conditions of repeated sliding a multilayer was very much more durable. Similar conclusions were reached by a number of other researchers[25,26]. Further work has shown that the film thickness necessary for good lubrication is related to the nature of the underlying materials, their surface characteristics and upon the loads used. HIRST[28] has shown that in processes where large amounts of surface deformation are involved then thicker films are necessary to protect the surfaces.

3. Effect of speed, load and temperature on boundary friction. Bowden and Tabor[1] have shown that for fatty acids the friction coefficient does not alter significantly with the speed of sliding (in the range 0.001cm/sec to 2 cm/sec) whilst the surfaces are under boundary lubrication conditions. Paraffins and alcohols show a decrease in friction coefficient with increasing speed down to a limiting value. The effects of speed have also been discussed by RABINOWICZ[29]. CLAYTON[30] has shown that between velocities of zero and 0.2 cm/sec the coefficient of friction for fatty acids increases with increasing velocity consistent with the fact that mechanical relaxation oscillations were not observed (Mechanical relaxation oscillations or "stick-slip" motion is associated with a falling friction-velocity relationship). FORESTER[31] also reports a slight increase in the coefficient of friction with speed for a steel-bronze combinations lubricated with oleic acid.

The effect of load on boundary friction has been investigated by a number of researchers,[1,32,33] all of whom have shown that as the load is increased the coefficient of boundary friction decreases to a limiting value. On further increasing the load it would be expected that the coefficient of friction would begin to rise again due to boundary friction at contacting asperities changing to dry friction.

HARDY and DOUBLEDAY[34] investigated the effect of temperature on boundary friction and showed that the coefficient of friction decreases with temperature increase until the melting point of the lubricant is reached, when there is a sudden rise in the friction coefficient. Bowden and Tabor[1] have also shown similar effects. Above this critical temperature, damage results to the boundary film and surfaces. It is also shown that where chemical reaction occurs between the lubricant and the surface layers, i.e. fatty acid reacting to produce a metal soap, effective lubrication

occurs up to the melting point of the metal soap. Boundary lubricants are only fully effective if they are solids or if they can react to form solids. Electron diffraction studies on monolayers of stearic acid has shown that the molecules are highly oriented but become less oriented as the temperature is increased. At the melting point the molecules in the monolayer become completely disoriented.

Bowden and Tabor also show that there is a good correlation between the chemical reactivity of a lubricant and the properties which it exhibits. In the case of fatty acids, those metals which are attacked by the acid have been shown to be the ones most effectively lubricated.

4. Mechanisms of Boundary Lubrication. The theory of metallic friction is obviously modified by the existence of a boundary lubricant. In the case of metallic friction it was proposed that the frictional force resulted from the shear of all contacting asperities (see equation 2). If the mean shear strength $\bar{s}$ of the interface is reduced, the friction zone will be reduced, provided that the contact area does not increase in proportion. ROWE[15] has demonstrated the principles involved in deformation of waxes and soaps at the boundary layer. Obviously the shear strength of the film is of considerable importance in reducing the coefficient of friction. Direct shear strength measurements have been made[34] for monomolecular soap films deposited onto cleaned mica sheet. Hardy considered that the frictional resistance under conditions of boundary lubrication was entirely due to interaction of the adsorbed layers of the boundary lubricant without any contact between the surfaces. Bowden and Tabor[1] however consider the mechanism as one in which lubricant film breakdown occurs over small localized regions. Thus the resistance to motion consists partly of the force necessary to break these junctions,

plus the force necessary to shear the lubricant film. This situation may be represented by supposing that there is metallic contact over some fraction x of the load bearing contact area A_c. The shear strength of the interface is therefore composed of two components, one due to metal shearing $\bar{s}_M$ and the other due to lubricant $\bar{s}_L$. Then the frictional force is:

$$F = A_c \left[x \bar{s}_M + (1-x)\bar{s}_L \right] \quad \text{.....(7)}$$

The fraction of metallic contact x has been measured using radioactive tracer techniques. For sliding copper surfaces it was found[34] that the wear reduced from 2×10^{-5} g/cm^2 for dry sliding to 2×10^{-8} g/cm^2 with a fatty acid lubricant. Calculations of percentage metallic contact based upon the above equation should be treated with respect since lubricant shear strengths vary with pressure. TABOR[35] considers that lubricants prevent metallic contact growth which would occur otherwise under the action of combined normal and tangential stresses. In fact equation 2 does not account for the fact that s_M (shear strength of metal junctions) and P_M (yield strength of metal junctions) are related. Macfarlane and Tabor[6] considered a two dimensional model to represent this. They demonstrated that under the action of a normal stress the contact area grows with the tangential force applied. COURTNEY, PRATT and EISNER[99] show that with clean surfaces junction growth continues indefinitely but with lubricant present growth stops at a particular shear stress level. Tabor[35] has taken account of this fact and suggests that junction growth occurs while the shear stress can be transmitted through the interface. Sliding occurs when the limiting shear strength of the film is reached. Tabor deduces a new friction coefficient relationship to account for the junction growth effect. When applied under boundary conditions this becomes approximately equal to the critical shear stress of the interface divided by the plastic yield stress of the substrate which is the simple expression for boundary friction.

2.40 Metallic Wear

1. Lubricated and Unlubricated Wear. It is useful to consider wear under either dry or lubricated conditions. Unlubricated systems may seem a little remote from the real life situation but an understanding of dry wear should lead to an understanding of lubricant failures. Some work[9,36,37] has been carried out to determine wear laws and this has been done using either no lubricant at all or an inert lubricant. Under both dry or lubricated conditions the asperities are subjected to stress cycling by either direct contact or via a lubricant film. This fatigue ultimately results in failure. Thus fundamentally, sliding under unlubricated conditions is not different from sliding under lubricated conditions and hence its understanding is of importance.

2. Mechanisms of Unlubricated Wear. It is generally agreed[1,33] that contact between surfaces occurs within a small fraction of the apparent contact area. Wear can take place by gradual removal of asperity tips due to mechanical interlocking. This however is thought to be less significant than that caused by shearing of adhesion welds between asperities whose formation is aided by the high pressures and high contact temperatures which may lead to softening or melting . This theory suggests that surface damage results from welding, whether hot or cold. Various other workers have examined this concept in greater detail. ERNST and MERCHANT[39] and also COFFIN[40] concluded that there was a relationship between metals exhibiting negligible solid solubility at a temperature and their antiscoring properties at that temperature. Relative positions of metals within the periodic table have also been found[41] of importance in determining scoring resistance. The strength of the metallic junction formed between sliding surfaces has a profound effect upon the wear process. The strength of the weld junction determines

whether shearing at the interface, shearing of bulk metal in one surface or shearing in bulk of both surfaces occurs. Bulk shearing processes usually involve high rates of wear.

A number of workers[38,42,43] have used "pin and ring" testing machines to determine the wear characteristics and mechanisms. These have shown that wear particles may be produced by material transfer oxidation and subsequent fragmentation or agglomeration and breakaway.

Various other mechanisms have been suggested to explain the wear process. For example BURWELL and STRANG[36] site the following mechanisms:

(1) Adhesion,

(2) Abrasion,

(3) Corrosion,

(4) Ploughing,

(5) Fatigue.

Investigations have been carried out concerned primarily with the study of particular types of wear but it is likely that several of these mechanisms may be operative in a real situation all contributing to wear. Holm[21] suggests that the real contact area is formed by plastic deformation of contacting asperities and wear results from atomic interactions. According to Holm:

$$W = \frac{zP}{H} \qquad \ldots\ldots\ldots\ldots\ldots\ldots \quad (8)$$

where W is the quantity of wear debris produced per unit distance of sliding, P is the load, H is the hardness and z is the probability for removal of an atom from the surface when it encounters another atom. This theory has been translated into macroscopic terms[37] assuming wear of particles rather than atoms. Archard[9] suggests a relationship between wear, sliding distance, load and hardness for plastic deformation

of:-

$$W = \frac{K\ s\ P}{p_m} \qquad \ldots\ldots\ldots\ldots\ldots\ldots \quad (9)$$

where K is constant related to probability of wear particle production per unit encounter, s is sliding distance and p_m is the flow pressure of the softer material.

Archard's original wear hypothesis[9] involved a rather complicated expression for the wear rate. Various relationships were proposed between wear rate and load under either elastic or plastic deformation conditions involving material removal in layers or lumps. A linear relationship between wear rate and load was only suggested for plastic deformation involving lump removal, i.e severe wear conditions. The mild wear rate was suggested to be proportional to the 4/5th power of load. ARCHARD and HIRST[38] however found that both mild and severe wear rates were proportional to load and K varied within the range 10^{-2} to 10^{-7}.
By assuming a much more complex surface geometry, ARCHARD[11] found that direct proportionality between wear rate and load was found under both elastic and plastic conditions. He proposed the relationship that wear $w = KA$ where A is real contact area elastic or plastic, and K is the proportion of contacts producing a wear particle.

QUINN[46] has suggested an oxidational hypothesis of wear after finding a correlation between oxidation temperature (as indicated by analysis of oxide wear debris) and calculated asperity flash temperatures[47]. This oxidation hypothesis leads to a theoretical interpretation of the K factor in terms of basic material properties and the conditions of sliding:

$$K = \frac{d\ A_o\ \exp(-Q/R_c T_c)}{\varepsilon^2 \rho^2 V} \qquad \ldots\ldots\ldots\ldots\ldots\ldots \quad (10)$$

where d is the distance along which a wearing contact is made, A_o is Arrehenius constant, Q is activation energy, R_c is gas constant, ε critical oxide film thickness before a wear particle is produced, ρ is the oxide

density and v is the speed of sliding. The contact temperatures T_c were estimated using this equation and found to be about 1400°K, considerably less than those predicted by Archard[48] of around 1800°K.

Various other theories and models have been suggested to describe the wear process[44,45].

3. Mechanism of Lubricated Wear. ROWE[49] and KINGSBURY[50,51] have examined boundary lubrication conditions and have produced a theory to describe the process. It is suggested that wear at an asperity depends on the time required for an adsorbed lubricant molecule to be desorbed compared with the time the asperity takes to travel the distance equivalent to the diameter of an adsorbed molecule. KINGSBURY[50,51] arrives at the following relationship:

$$x = 1 - \exp\left[-\frac{z}{v t_o}\exp.\ (-E/RT)\right] \quad \ldots\ldots\ldots\ldots \quad (11)$$

where x is the fractional film defect (see equation 7), z is the distance between lubricant sites, v is the relative sliding velocity, t_o is the period of vibration of an adsorbed molecule and E is the heat of adsorbtion. Also according to Kingsbury the fractional film defect x may be related with the friction coefficient and hence measurements of heat of adsorbtion may be made from temperature, sliding velocity and friction measurements.

ROWE[49] suggests that since x is often less than 10^{-2} then $\log_e(1-x)$ is approximately equal to -x. So

$$x = \frac{z}{v t_o} \cdot \exp(-E/RT) \quad \ldots\ldots\ldots\ldots\ldots\ldots \quad (12)$$

Rowe also proposes that wear under lubricated conditions w_L obeys the relationship:

$$w_L = (k_L x)A \quad \ldots\ldots\ldots\ldots\ldots\ldots \quad (13)$$

where k_L is a constant and A is the area of real contact. ($x = A_c/A$ where A_c is area of real contact without lubrication). Finally Rowe suggests that the wear rate constant for lubricated wear K_L may be found from the equation

$$K_L = \frac{z}{v t_o} \cdot \exp(-E/RT) \qquad \ldots\ldots\ldots\ldots\ldots\ldots \quad (14)$$

and fairly good agreement is found between calculated and determined K_L values. He makes the assumption that the probability of producing a wear particle is very high (between unlubricated colliding asperities) and his experiments show this to be nearly correct. The form of the equation is very similar to the K factor obtained for dry wear using the oxidation hypothesis of QUINN[46].

2.50. Application of Modern Techniques in Friction and Wear Studies

A number of experimental methods have been applied to the measurement of size and shape of the surface irregularities. Surface profilimeters have been used to give magnifications of 40,000. This method does not involve surface destruction but is limited by the size of the needle which is often too coarse for "microscopic" examination. YOUNG[16] has recently developed an instrument for measurement of metal microtopography having a resolution of 30 Å perpendicular to the surface. Worn surfaces may also be examined using optical, electron and scanning electron microscopy. Optical methods lack high resolution and electron microscopy normally involves the manufacture of replicas which are extremely fragile. Worn steel surfaces have however satisfactorily been examined using transmission electron microscopy[52] and the technique has been used for other systems[52]. This technique has the advantage that it is non destructive and the changes occurring on the same wearing surface may be examined. Reflection electron microscopy has also been used to examine wear surfaces[54]. Scanning electron microscopy however seems to combine

the advantages of all these techniques having great depth of focus, being easy to apply to bulk surfaces and possessing a wide range of magnifications. This technique has been used by a number of workers [17,18]. X-ray crystallography has found application in tribological research for examining crystallographic effects upon friction and wear, analysis of wear debris and lubricant orientation relationships. Electron diffraction techniques have also been used for examination of thin film or surface crystallography, and also in studies on wear.

Radioactive tracer techniques have been used for examining friction mechanisms under conditions of lubricated[34] and unlubricated[43,55] sliding. The technique has found application to both fundamental studies and technological problems for example, engine wear investigations.

Electrical techniques have been applied to tribology to measure oil film thickness[56] (capacitance methods) and to indicate metallic contact between sliding surfaces[57] (resistance methods). FUREY[59] has developed a method of studying metallic contact and friction between sliding surfaces. Instantaneous and average resistance values were used to determine the extent of metallic contact. Various electrical methods for assessing metallic contact, including Furey's method, have been examined by CHU and CAMERON[58]. Furey has also measured surface temperatures using a dynamic thermocouple. The experimental results were considerably lower than those theoretically calculated by BLOK[60], JAEGER[61] and ARCHARD[48].

These techniques have provided results to give us an even better understanding of the processes involved in sliding and the interactions occurring between surfaces mainly on a microscopic scale. These methods are of considerable value for the development of tribological research.

3.00 REVIEW OF FRICTION AND LUBRICATION IN POWDER METALLURGY

3.10 General Considerations

3.20 Powder Consolidation Theories and Friction Effects

3.30 The Effects of Lubricants during Compaction of Powder

3.40 The Effects of Lubricants during the Ejection of Metal Powder Compacts

3.50 The Effects of Lubricants on other Properties

3.60 Previous Instrumented Techniques for Lubricant Evaluation

3.00 REVIEW OF FRICTION AND LUBRICATION IN POWDER METALLURGY

3.10 General Considerations

In both powder metallurgy and in mechanical sliding systems, the problems of friction and lubrication are similar since they are both concerned with the interactions between surfaces. The particular difficulties which friction presents in powder metallurgy have been examined by a number of workers [62,63,64,65] who have contributed towards a general appreciation of the important factors, but who have not fully analysed them.

These studies have appreciated that friction in powder metal compaction involves powder/powder, powder/die, powder/lubricant, die/lubricant and die/punch surface interactions; and ejection also involves some of these interfaces. HAUSNER and SHEINHARTZ[65] consider that the major pressure loss during compaction results from friction between the powder particles and the die wall and that the friction depends upon a number of factors including particle type and characteristics, die surface finish and the applied pressure. Modification of the surface properties of powder and die by application of lubricants has a considerable effect upon the consolidation process. The lubricant serves to reduce wall friction, reduce interparticle friction, reduce the ejection force and prevent subsieve powder fractions from falling into the die clearances. However in considering the effects of a lubricant admixed to the metal powder, the effects of lubricant upon particle bonding must be examined. The lubricant is added primarily to reduce die wall friction but we also require cohesion between particles to allow the pressed component to hold together upon ejection from the die. Thus from this point of view the smaller the quantity of lubricant that can be added, the stronger will be the pressed component, assuming components to be pressed to the

same real density. Thus there exists a conflict of requirements in metal powder compaction using admixed lubricants.

Die wall friction exerts a considerable influence, both during compaction and ejection, and upon the finished component. Die wall friction produces a density distribution along the length of a compact which results in a variation of physical properties. This may lead to problems occurring during sintering, for example decarburization, or ultimately to service failure. Application of lubricants lowers the die wall friction loss and hence aids the production of more uniform components.

The powder metallurgy process involves the use of high cost complex tooling arrangements and the economy of the process therefore depends upon the life of such tools. The die wear is affected by powder properties, lubricant, tooling materials and design, and by the compacting variables. The evaluation of lubricants with respect to die wear rate is therefore of considerable importance. Also as wear occurs, the surface finish of the die changes and this affects the compaction and ejection forces as well as the compact properties.

3.20 Powder Consolidation Theories and Friction Effects.

Increased punch pressures on a mass of powder within a die results in increased density. However, as pointed out previously, friction between the die wall and particles results in density variations along the compact length. The cold compaction of indium and lead powders was studied by TRAIN and HERSEY[69] who used the friction theory of Bowden and Tabor to derive equations for the die wall friction of pressed powder. These equations enabled shear strength calculations to be made of the materials examined which agreed with those determined using a

punch penetration test. SHEINHARTZ et al[66] used a comparatively simple direct measurement method and determined a relationship between applied and transmitted forces. They showed that the majority of the total friction occurring during powder metal compaction develops along the die wall and the effects of die wall lubrication were also evaluated. The relationship between applied and transmitted forces has been studied by a number of workers[66,67,68] and various mathematical relationships have been suggested to take account of frictional forces and component shapes.

The majority of these theories during compaction use the concept of powder-die wall friction coefficient and a number of workers have shown that this friction coefficient may change along the length of the compact die wall interface.

Compaction occurs by a multi-stage process[70] which includes

(a) densification during filling the die;

(b) densification by particle rearrangement at low pressures before appreciable interparticle bonding;

(c) densification by compact deformation after appreciable interparticle bonding.

The various stages which occur during powder compaction are difficult to see from a plot of pressure versus density. However by plotting pressure versus relative porosity the stages become more clearly discernible[71]. TORRE[72] originally considered the isostatic compression of powders in terms of a hollow sphere subjected to an external hydrostatic pressure to provide theoretical confirmation to the formula proposed by other workers[73]. The applied pressure P and the resulting relative density of the compact D are related according to the equation:

$$\text{In} \quad \frac{1}{1-D} = KP + A \quad \ldots\ldots\ldots\ldots\ldots\ldots (15)$$

where K and A are constants. HECKEL[70] evaluated the values of K and A and also proposed that K (the slope of the linear portion of the graph) is given approximately by the equation:

$$K = \frac{1}{3\sigma_o} \quad \ldots\ldots\ldots\ldots\ldots\ldots (16)$$

where σ_o is the yield strength of the powder material. Heckel found that both die and powder lubrication generally resulted in only minor variations in the pressure density curve. KAWAKITA[74] found a more general empirical relationship between pressure and density which is applicable to a large number of powdered materials. He suggests that the relative reduction in compact volume C is related to the compaction pressure P by the equation:

$$C = \frac{V_o - V}{V_o} = \frac{a\,b\,P}{1+bP} \quad \ldots\ldots\ldots\ldots\ldots\ldots (17)$$

where V_o is the original powder volume, V is the volume at pressure P and a,b are constants. This theory however appears to neglect the effects of die wall friction as did HECKEL[70]. The relationships between powder properties and Kawakita constants and other fundamental aspects of powder consolidation have been fully reviewed by JAMES[68].

3.30 The Effects of Lubricants During Compaction of Powders

LEOPOLD and NELSON[75] investigated the effects of admixed and die wall lubrication upon the compaction of a sponge iron powder. The lubricant efficiency was assessed by measuring the difference between the applied and transmitted forces, F_a and F_t respectively. A linear

relationship was found between F_a and F_t which was represented by the equation:

$$K = \frac{F_t}{F_a} \qquad \text{..... (18)}$$

where K is the slope of the line and is independent of pressure. This relationship has been used by a number of workers[65,66,76]. They found that there is an optimum lubricant level for a given combination of compact weight and pressing pressure. They also show that at low pressures a greater amount of admixed lubricant is required to provide optimum lubrication, because the pressure is insufficient to force it to the die walls. Die wall lubrication is shown to be superior to admixed lubrication at high pressures whereas at a low pressure the reverse applies. LJUNGBERG and ARBSTEDT[77] have reported similar findings. YARNTON and DAVIES[78] investigated the effects of admixed lubrication upon the compaction of -300mesh electrolytic copper powder. They showed that the lubricant can either assist or retard densification depending upon the applied pressure and the lubricant content. At low pressures the lubricant had a beneficial effect but as the compaction pressure was increased a point was reached where the lubricant began to hinder compaction. Yarnton and Davies suggest that this is due to extrusion of lubricant into the pores. Similar results have been reported by other workers[77]. Comparisons have been made between die wall and admixed lubrication from which it was shown that die wall lubrication was superior and that where both die wall and admixed lubricant are used together exudation of the lubricant from the compact was retarded and densification was inhibited by the retained lubricant.

SAJDAK etal[78] investigated the effects of lubricant content, application and iron powder type upon the value of K at various compact

length to diameter ratios. They demonstrate that little advantage is to be gained by increasing the lubricant level above 1 w/o and that the punch force is more effectively transmitted when using electrolytic iron than atomised or sponge iron. Very few investigations have been carried out into the effects of the lubricant particle size upon the compaction of powders. HAUSNER and SHEINHARTZ[65] find that in pressing electrolytic iron powder at a given compacting pressure zinc stearate of fine particle size gives greater densities than a zinc stearate of coarse particle size. Similar effects have been noted by BOCKSTIEGEL and SVENSSON[79] compacting sponge iron powders and by FLIPOT et al[80] in the compaction of UO_2 pellets.

3.40 The Effects of Lubricants During the Ejection of Metal Powder Compacts.

A number of workers[77,78,81] have shown that increasing the admixed lubricant content reduces the force necessary to eject the compact from the die. However once the die walls become flooded with lubricant then the effects of increasing the lubricant content become small. LEOPOLD and NELSON[81] show that a small amount of die wall lubrication is much more effective in decreasing the ejection pressure than a large amount of admixed lubricant. For example they found that 0.012 mg/cm^2 die wall lubrication was more effective than 2.0% admixed lubricant. They also noted that the ejection pressure increased during ejection of the compact from the die where admixed lubricants were employed and that this effect is reduced with increasing lubricant content. These workers do not however note the speed of ejection which may be an important factor in determining the ejection forces.

Again few examinations of the effects of lubricant particle size upon ejection forces seem to have been made and those that have appear

to be contradictory. BOCKSTIEGEL and SVENSSON[79], HAUSNER and SHEINHARTZ[65] and FLIPOT etal[80] all show that fine particle size lubricants are better than coarse lubricants in reducing ejection forces, whereas GEIJER and JAMISON[82] appear to show the opposite effect. These workers also show that lubricant type is of importance in determining ejection forces.

LJUNGBERG and ARBSTEDT[77] found that the die surface finish affected their ejection forces but do not appear to have taken account of the fact that their dies of different surface finish were also of different materials. Geiger and Jamison using tungsten carbide and steel dies of similar surface finish (0.25 μm C.L.A) have shown that carbide dies give lower ejection forces than steel for compacts pressed under similar conditions. Many other workers however seem to either ignore the effects of die surface finish or measure it at the beginning of a series of tests and assume that it remains the same. BOCKSTIEGEL and SVENSSON[83] measured the ejection force changes which resulted from die wear but only Scanning Electron Microscope pictures were used to assess the die condition at the end of each run. It has been suggested[77] that ejection force measurements are a useful indicator of die wear. However they demonstrated that lubricants which yield low ejection pressures do not necessarily also give low die wear rates. They in fact found it impossible to correlate ejection forces and wear rates for different lubricants. An analysis was also made of influence of tool design and die materials on wear.

3.50 The Effects of Lubricants on other Properties

From the foregoing sections it is clear that die wall lubrication appears to offer great advantages over admixed lubricants. However due to the practical difficulties of using such a system during production,

admixed lubrication techniques are commonly used. This, however, does have an effect upon powder, compact, sintering and final finished properties.

HAUSNER[15] and LJUNGBERG and ARBSTEDT[77] demonstrate that lubricant addition reduces the flow rate of powders. This factor is of importance since during automatic pressing, where the die filling time is small, rapid flow is important. Also where intricate tool sections are used, powder flow into those die sections is vital. The flow rates were measured using a standard Hall flowmeter[84] and it was found that above a certain lubricant level flow ceased. The flow test does not always correlate with flow into a narrow die and to overcome this problem OAKLEY [85] devised a simple apparatus. The lubricant also influences the packing of particles following conditions of free fall, that is the packing or apparent density. YARNTON[86] demonstrated that a monomolecular layer of lubricant can increase the packed density by up to 20% relative to the unlubricated state. Additions in excess of that required to give monomolecular layer coverage resulted in reduced packed densities. HAUSNER [89] has shown that this effect continues with further lubricant additions up to 1.5%. The flow and packing behaviour of powders is dependant upon a number of powder properties such as particle size distribution and shape, surface films, additives etc., and Hausner suggests that the ratio of tap density (apparent density produced when the container is tapped under specified conditions) to apparent density indicates the friction conditions between powder particles.

Lubricant particle size has been shown[79,82] to be of importance in determining the flow and apparent density of powder mixes. Coarser lubricants were shown to have better flow properties than fine lubricants when mixed with powder.

The lubricant content affects both the springback which occurs when the compact is ejected from the die and the strength of the compact [77]. Increased lubricant contents were shown to increase the springback and reduce the strength of the compacts. The sintered properties have also been found to be dependent upon both type [87] and quantity [77] of lubricant used.

The burn off characteristics of common lubricants have also recently been investigated by MOYER [88], who showed that they often left traces of metal oxides in the sintered compacts and increased the compacts' porosity.

3.60 Previous Instrumented Techniques for Lubricant Evaluation

A considerable amount of research has been carried out on the measurement of friction during the compacting of metal powders. UNKEL [90] used a method in which part of the load was transmitted by friction through the die wall to three Brinell balls on which the die rested. The size of the impression made by these balls in a soft iron ring gave an assessment of the frictional forces. SHEINHARTZ, McCULLOUGH and ZAMBROW [66] used a simple method of hydraulically measuring top and bottom punch pressures whilst using a fixed die. The difference between the two measurements then gave the pressure loss due to die wall friction. Other workers, [75,81] have used a similar method, but modified by using strain gauge techniques to measure the punch forces.

The pressure which is applied to a metal powder is not transmitted hydrostatically to the die walls and a number of workers have used different techniques to measure these radial stresses. SHANK and WULFF [91] measured these radial pressures and then calculated friction values. DUWEZ and ZWELL [92] also attempted to determine friction values but these results seem to vary considerably from the previous workers.

KAMM, STEINBERG and WULFF[93] used a deformable lead grid to determine their friction coefficients and various other workers[94] attempt to correlate friction results with ejection pressure and density distribution. BUSTAMANTE and SHEINBERG[94] determined the hoop stresses produced in a cylindrical die during powder compaction using strain gauges around the die circumference. They showed that finer or softer particles transmitted more pressure than coarser or harder particles. For a given punch pressure the hoop stress in the die was shown to be considerably lower for powder compaction than for liquid compression. BOCKSTEIGEL and SVENSSON[79] show a similar effect with respect to radial stresses.

LONG[96] has developed a theory to explain the variation of radial pressure during compaction. It is suggested that during application and release of punch pressure, the radial pressure follows a cycle which is determined by the elastic and shear yield stress properties of the pressed material. Long also describes an apparatus for measurement of powder/die friction coefficients although no values are given.

The majority of the lubricant evaluation methods use very slow compaction and ejection speeds, far slower than would be used in commercial production and in a number of cases testing speeds are not given at all. A few workers have however used instrumented commercial presses in order to evaluate lubricant effects on compaction and ejection. HIGUCHI, NELSON and BUSSE[97] describe the design and construction of instrumented pharmaceutical tabletting machine. This was used later[98] to determine the relationship between upper and lower punch forces during compaction and the effects of lubricant upon the ejection force was assessed. Bockstiegel and Svensson also carried out work along these lines using an automatic mechanical compacting press capable of running up to 35 strokes/min. Radial stress measurements were determined during compaction and ejection, and friction coefficients measured.

4.00 MATERIALS CLASSIFICATION AND PREPARATION

4.10 Iron Powder

1. Apparent Density and Tapped Density Measurements
2. Powder Flow Determination
3. Particle Size Distribution
4. Particle Shape, Microstructure, Hardness and Chemical Analysis
5. Surface Area Determinations

4.20 Characterisation of Metal Stearates

1. Particle Shape and Size Distribution

   Coulter Counter Method
   Centrifugal Sedimentation Method

2. Other Lubricant Characteristics

4.30 Iron/Lubricant Blending and Characterisation.

1. Blending Technique
2. Assessment of Mixing Effectiveness
3. Mix Characteristics

4.00 MATERIALS CLASSIFICATION AND PREPARATION

This research examines the effects of lubricants on the pressing and ejection characteristics of metal powders. The majority of powder metal components are fabricated from iron powders generally using metal stearates as lubricants for the compaction operation. In view of this, those raw materials were selected for investigation.

4.10 Iron Powder

Various iron powders were classified according to apparent density, tapped density, flow rate, particle shape and size distribution etc. by the methods outlined below. One of these iron powders J.J. MAKINS 100 P1 was chosen for the research in order to reduce the number of possible variables.

1. Apparent Density and Tapped Density Measurements. These measurements were carried out in accordance with M.P.I.F. Standard 9-62[84]. The iron powder was allowed to flow through a standard Hall flowmeter into a 25 cm^3 standard density cup until iron powder began flowing over the sides of the cup. The excess iron powder was carefully scraped from the cup surface using a straight edge ensuring that no vibration of the cup occurred. If vibrations are allowed to occur, the powder settles and an incorrect value of apparent density results. The apparent density was found by weighing the powder contained within the cup and dividing this by the cup volume.

The tapped density was determined by allowing the iron powder to flow into a 25ml. measuring flask, filling it to a level of approximately 20ml. The flask was repeatedly tapped until the iron powder settled to a constant volume which was noted. The iron powder was weighed and hence from a knowledge of the volume the tapped density was found.

2. Powder Flow Determination. Fifty grams of iron powder were weighed and placed in a standard Hall flowmeter[84]. The time taken for the iron powder to completely flow through the flowmeter was measured.

3. Particle Size Distribution. The particle size distribution was determined by sieve analysis and the subsieve size distribution was found using the Quantitative Image Analysing Computer (100,101). The iron powder was scoop sampled[102] from several places and the samples cone mixed for 5 minutes. One hundred grams of iron powder were weighed from this sample and sieved through 100,150,200,240,300 and 350 B.S. mesh sizes for 30 minutes. The fractions of powder remaining on each sieve were weighed and the -350fraction saved for further particle size analysis. This was repeated three times and average values taken.

The applications of the Automated Image Analysing Computer have been reviewed by Allmand and Coleman[101] and this technique was selected for particle size distribution of the -350 mesh iron powder. This powder was very fine and agglomerated easily. Various methods were tried to overcome this problem and the method finally used consisted of pouring about 10 milligrams of the iron powder sample into 1ml of microscope oil The mixture was stirred and agitated ultrasonically to break down any agglomerates. A drop of the liquid was quickly placed on a slide before any settling occurred and a cover glass placed over it. Slight pressure was applied to remove any entrapped air and further separate the particles. Although a few agglomerates still occurred they could easily be recognised and the results from them ignored.

The "Quantimet B" utilizes a delay line memory which enables individual particles of powder to be separately counted. The particle size is determined using a system which only allows a count to be recorded if the line intercept is greater than a pre-selected value. Six sizing contro

are provided which can be set to different intercept lengths in order to measure the size distribution of the particles. The intercepts were set at 10,20,30,40,50 and 60 μm for this investigation and in order to obtain a statistically representative result 100 fields were examined on each of 4 samples from the same powder.

4. Particle Shape, Microstructure, Hardness and Chemical Analysis. In order to obtain information about the characteristics of the iron powder surface, particles were examined and photographed using a Cambridge Stereoscan Scanning Electron Microscope (S.E.M) at magnifications up to 20,000. Samples of the powder were also mounted in resin and polished. Micro hardness measurements were made of the bulk material and also any large inclusions.

Chemical analysis of the iron powder was carried out and hydrogen loss determinations were made to determine the surface oxide content. A weighed sample of iron powder was placed in a previously conditioned alumina boat. The boat was conditioned by allowing it to stand empty for 30 mins. within a furnace held at 1100°C. After cooling, the boat was weighed and the process repeated until two consecutive weights were found the same. This boat now containing the iron powder was weighed and then placed in a sealed furnace held at 1100°C. The furnace was purged with nitrogen and then dry hydrogen was allowed to pass over the iron powder for 30 minutes. The boat was allowed to cool and the furnace repurged with nitrogen. The boat with iron powder was reweighed and the percentage weight loss of the iron powder determined.

5. Surface Area Determinations. Determination of the surface area of iron powder was carried out using a permeametry technique devised by DONNELLY[111]. The method and theory used is given in Appendix 1.

4.20 Characterisation of Metal Stearates.

Various standard tests are used by lubricant manufacturers to assess the quality of their metal stearates. The tests may include such things as appearance, texture, fineness, gel strength etc, few of which may be of relevance to the powder metal component produced. The factors which are considered to be of importance and their methods of determination are outlined below.

1. Particle Shape and Size Distribution. Lubricants are mainly added to metal powder in the dry form and therefore particle shape is of importance in determining the mixing characteristics of the two materials. Lubricant particle shapes were examined using the S.E.M. Metal stearates are poor conductors and it was therefore necessary to vacuum coat the particles with gold-palladium before examination.

Particle size determinations were carried out using a Coulter counter and by centrifugal sedimentation methods. In both techniques problems were encountered with agglomeration of the fine stearate particles. The stearates were dispersed in a suitable liquid (water and iso-propyl alcohol were used) and surface active agents were added to reduce agglomeration ("Nonidet" was used for the water dispersions). Microscopic examination of slides prepared prior to test indicated that even after ultrasonic treatment and addition of surfactants some agglomeration was still present. Thus the results obtained do not give the exact particle size distribution of the lubricant.

Coulter Counter Method. The technique used for instrument set up and procedure is given in the Coulter Counter instruction manual. The counter determines the number and size of particles suspended in a conductive liquid, by forcing the suspension through an aperture having

an immersed electrode on either side. As the particle passes through the aperture, the resistance between the electrodes changes and a voltage pulse of size proportional to the particle size is produced. The series of pulses is then counted and scaled electronically.

Cumulative weight percent undersize curves were produced and the particle size given in the tables was determined at 50 percent weight undersize.

Centrifugal Sedimentation Method. A Simcar centrifugal sedimentation unit was used and the procedure and method for determination of the cumulative weight percent undersize curves is given in the Simcar manual.

The technique consisted of adding the suspension (0.2% V/V conc.) to a flat cylindrical container which was then rotated at constant speed. Samples of given volume were drawn off from the fixed sampling point at given times and the amount of solid contained within them determined. From this data, the particle size distribution curves were determined using the technique outlined in the manual.

2. Other Lubricant Characteristics. The techniques for carrying out the physical tests of apparent density, tap density and melting point determinations together with the chemical analysis methods for ash, moisture and free fatty acid contents are given in a Durham Chemical technical service bulletin[103].

4.30 Iron/Lubricant Blending and Characterization.

1. Blending Technique. Two techniques of mixing were examined and compared. Bottle mixing was used for mixing small quantities of powder (400g) and cone mixing was used for larger mixes (2000g). Iron powder

and lubricant in the desired proportions were first mixed together by hand before being passed through an 80 mesh sieve to break up any large agglomerates. Further mixing was carried out for 60 mins either in a 200 cm^3 bottle rotated at 36 r.p.m. (400g mixes) or in an 8,500 cm^3 double cone mixer rotated at 40 r.p.m. (2000g mixes).

A few mixes were prepared by dissolving the required amount of lubricant in a suitable volatile solvent. This mixture was poured onto the iron powder contained in the cone mixer and blended for 30 mins. The mixer was opened for 10 mins to allow some of the solvent to evaporate and remixed for a further 30 mins. The mixture was poured out and allowed to dry completely before use.

2. Assessment of Mixing Effectiveness. Microscopic examination of the mixes was carried out to determine the effectiveness of the mixing process in distributing the lubricant evenly within the iron. A simple test was devised to determine the amount of lubricant which was not attached to the iron powder. A clean glass slide was taken and weighed. A thin layer of iron-lubricant mix was sprinkled onto the glass slide which was weighed again. A powerful magnet was then drawn several times 10 min above the surface of the iron powder mix causing all the iron particles to be transferred to the surface of the magnet. The slide was reweighed and the amount of lubricant remaining determined.

A further assessment of mix behaviour was to examine the effect of lubricant mixing upon the surface characteristics of the iron powder. Several iron powder particles were taken and attached in known positions to the surface of a S.E.M. stub. Their surfaces were examined and photographed using an S.E.M. The stub was then fixed inside a cone mixer and an iron-lubricant mix prepared in the normal manner. Following

mixing the stub was removed and the iron particle surfaces re-examined.

3. Mix Characteristics. Apparent density, tapped density and flow determinations were carried out upon each mix using the techniques previously described in section 4.10. The effect of mixing time upon these properties was determined by sampling the mix and measuring the properties at various times. A standard mixing time of 60 mins was chosen for subsequent mixes. The green strength of compacts produced from these mixes was measured using the indirect tensile test described by CLAUSSEN and JAHN[104]. 10g compacts, 14.8mm diameter compacted at 410 MN/m^2 were used for this test. A Houndsfield tensometer with an automatic load recording device was used for measuring the compressive breaking strength of the compacts.

The mixing characteristics of a range of commercially produced zinc stearates was examined with respect to the iron powder used throughout the investigation. Bottle mixing was used at this time since the cone mixer was then not available. The results were subsequently repeated when the cone mixer was obtained. Flow, green strength, apparent density and tapped density values were determined for these mixes and in addition, a visual assessment of the mix appearance was made.

5.00 EXPERIMENTAL DETAILS AND PROCEDURES

5.10 Laboratory Scale Compaction and Ejection

1. Tooling Details
2. Compaction and Ejection
3. Compact Density Measurement

5.20 Die Surface Finish Measurement and Examination

5.30 Production Scale Compaction and Ejection

1. Press: General Description
2. Production Press Tooling
3. Instrumented Press Design Requirements
4. Press Instrumentation
5. Calibration of Punches and Dies
6. Assessment of System Accuracy
7. Dynamic Compaction and Ejection Studies
8. Pressed Compact Evaluation

5.40 Determination of the Stress/Strain Relationship for Unsintered Compacts

Modulus Value Used in Radial Stress Determination

5.50 "Pin and Disc" Friction Testing Apparatus

1. General Description of the "Pin and Disc" Machine
2. Calibration of Friction Force Measurement
3. Contact Resistance Measurement between Pin and Disc
4. Technique for Pin Temperature Variation
5. Test Procedure and Conditions
6. Wear Assessment Using the "Pin and Disc" Machine

5.00 EXPERIMENTAL DETAILS OF APPARATUS AND PROCEDURES

5.10 Laboratory Scale Compaction and Ejection.

1. Tooling Details. The simple top punch, bottom punch and die arrangement shown in Fig 1(a) was used for the laboratory scale studies. The die and punches were made from high carbon, high chromium die steel (typical composition Cr 13, C 2.10, Mo 0.5, Si 0.3%). The die was heat treated to 60-62 HRC and the top and bottom punches were heat treated to 57-60 HRC. The die bore was subsequently ground and lapped to a surface finish of 0.077 μm CLA.

2. Compaction and Ejection. The required amount of iron powder was weighed and carefully transferred to die and punch arrangement shown in Fig 1(b). Compaction was carried out by single end compression using a hydraulic 10^5N laboratory press. The single end compression technique using a punch placed in the same position was designed to make the compact move over the same die surface during each ejection stroke. A Houndsfield tensometer was used for ejection and the automatic recorder was employed to obtain a complete trace of the load-distance relationship during ejection. The arrangement used is shown in Fig. 2. Ejection speeds were varied by altering the tensometer cross head speed in the normal manner. When the compaction conditions were altered, ie. by varying the amount or type of lubricant within the mix, the punches and die were washed in xylene to remove any lubricant build up which may have occurred.

3. Compact Density Measurement. Density determinations were made by weighing and micrometer measurement. Any 'flash' occurring around the circumference of the compact was removed before the measurements were made. During subsequent processing the lubricant is burnt off and does not contribute towards the final density. True compact densities were therefore

calculated to give a more realistic indication of densification. The compaction reproducibility was found to be better than $\pm$ 0.01g/cm^3 when using the same powder mix and weight.

5.20 Die Surface Finish Measurement and Examination.

Die surface finish measurements were made using a "Talysurf". The topographical nature of the surface was indicated by a stylus which rested on the surface and was traversed across it. The vertical movement of the stylus was measured relative to a datum provided by a skid resting on the surface. The instrument carrying the stylus recorded and integrated the movements of the stylus over the sampling length and the "centre line average" (CLA) value was measured. The CLA value[105] is the arithmetic average of the departure of the whole of the profile both above and below the centre line throughout the prescribed cut off.

Surface finish measurements were made on the laboratory scale die at a distance of 2-12mm and 15-25mm within the bore. These measurements were repeated at 90° intervals around the die bore. Surface finish determinations were carried out upon the die after final lapping and polishing and the measurements were repeated during the experimental programme.

An assessment was made of the effect of surface finish upon compaction and ejection. A mix containing 1% zinc stearate was used for this purpose and compaction and ejection data were obtained for a series of true density compacts. The tests were repeated following each surface finish measurement.

"Talyrond" surface finish examinations were also carried out. This instrument enabled surface finish determinations of a cylindrical bore to be made and consisted of a stylus which was made to traverse around the

bore of the die. The bore surface topography was magnified up to 10,000 times before being automatically recorded. These techniques were also used for surface examination of the dies used during the production scale compaction and ejection studies.

Die surfaces were in addition examined using a replication technique. This had the advantage that inaccessible bore surfaces couldbe examined without having to destroy the die and that the changes in surface characteristics occurring during the life of the die could be easily followed. The replica material chosen was required to have the following properties:

(i) Good surface reproduction.

(ii) Easily removed from surface.

(iii) Capable of withstanding the electron beam during S.E.M. examination.

(iv) Fairly easy to use.

Two materials were found to be suitable for this purpose. "Araldite 219" and "Silicoset"; although "Araldite 219" was sometimes rather difficult to remove from the surface. The surface to be examined was thoroughly cleaned in iso-propyl alcohol. A plasticine ring was made and placed around the required area ensuring that it was pushed well down to prevent liquid leakage underneath it. The "Araldite 219" was mixed (Resin DY 219 100 parts, Hardener HY 219 50 parts, Accelerator CY 219 10 parts) and poured into the mould. The cast was left to set for 24 hours and then the replica removed from the surface. The replica was reduced to approximately 2mm thickness by linishing away the back taking care not to damage the replica face. It was mounted on a stub and vacuum coated with gold-palladium before S.E.M. examination. The replica was reduced to 2mm thickness to minimise the possibility of charging during examination i.e. by reduction of the distance electrons must travel before going to earth

potential.

5.30 Production Scale Compaction and Ejection

Accurate measurements of the forces involved during the compaction and ejection of metal powder can be made relatively easily during the slow closely controlled pressing of metal powder compacts. There is some doubt however whether these measurements can be directly related to high speed compaction and ejection conditions. In order to overcome this uncertainty a high speed production press was instrumented and the method used is described below.

1. Press: General Description. The automatic mechanical cam operated compaction press shown in Fig. 3 was used in this investigation. A pressing force of up to 350 kN could be progressively applied and a production rate of up to 1500 parts per hour could be obtained. During this investigation the press was operated on a single cycle basis although step by step operation was used during tool setting and automatic continuous cycling was available if required.

The bottom punch was fixed during compaction and the die table was supported by springs just strong enough to bear its weight. Thus as compaction took place the increasing frictional force between the powder and die wall caused the die to move downwards over the stationary lower punch. (floating die tooling). This gives the effect of double ended compaction.

During automatic compaction the die cavity was fed by a feed shoe that oscillated during fill. However during single cycling the feed shoe was removed and the die filled by hand being subsequently levelled with a straight edge. The pressed compact was ejected from the die by raising the lower punch.

The length of stroke of the upper punch was determined by the main operating cam profile, but the position of the stroke could be varied by adjustment of an eccentrically mounted roller which raised or lowered the contact point of the operating mechanism relative to the main cam. Fig. 4 shows graphically the relative movements of the punch, die table and feed shoe throughout a complete compaction and ejection cycle. The main operating cam profile was modified later to give a continual increase in compacting force throughout the compacting cycle.

2. Production Press Tooling. Details of the tool arrangement used in the pilot plant press are shown in Fig. 6. The punches were made from high carbon, high chromium steel (H.C.D) heat treated to 57-60 HRC. Two die materials were used in the production scale investigation, one made from H.C.D. and the other from tungsten carbide surrounded by a shrink fit collar. The HCD was heat treated to 60-62 HRC and was subsequently ground, lapped and polished to a surface finish of 0.07 μm CLA. The tungsten carbide die was lapped and polished to a surface finish of 0.05 μm CLA. The clearance between the die and punches was 0.010mm which is consistent with the clearances recommended by JONES[76].

3. Instrumented Press Design Requirements. The instrumented press with its associated equipment was required to measure the dynamic compressional variables to the following limits and degrees of accuracy: (a) the force exerted by the top punch to within $\pm$ 1% up to 350 kN; (b) the force exerted by the bottom punch to within $\pm$ 1% up to 350 kN; (c) the displacement of the top punch to an accuracy of $\pm$ 0.05mm; (d) the force to eject the compact from the die to within $\pm$ 1% up to 70 kN; (e) the radial stress acting upon the die in the compact zone during compaction and ejection to within $\pm$ 1% up to 500 MN/m^2.

The response speed of the measuring devices and the recording equipment was required to be fast since the time the top punch was actually compacting was between 1 and 2 seconds and the ejection time was less than 0.5 seconds. Thus a system having a response time better than 0.1 sec was desirable in order to measure dynamic punch forces with the required accuracy during the pressing cycle.

4. Press Instrumentation. The opening between the upper and lower rams of the press was insufficient to accommodate the tools and a load cell. Punch force measurements were therefore made with strain gauges bonded onto the punches as shown in Fig. 5 . Two T.M.L. type FCA-6-1 strain gauges were bonded to each punch diametrically opposite to each other and as close to the punch base flange as possible to avoid the die fouling them. The strain gauges were orientated so that the active gauges lay parallel to the punch length while the temperature compensating dummy gauges lay normal to the length. This arrangement is shown in Fig. 7. The active and dummy gauges were connected in a Wheatstone bridge circuit with active gauges in opposite arms of the bridge. This arrangement measured direct thrust independently of bending and/or torsion. The resistance changes in the active gauges due to compressive strains within the punch put the bridge out of balance and produce a potential difference across the output.

The "dummy" gauges are also strained during punch compression due to a Poissons ratio effect. However the calibration procedure accounts for these changes.

The H.C.D. die and the tungsten carbide die were both fitted with strain gauges designed to measure directly the internal stresses acting upon the die during compaction and ejection. Two T.M.L. type F.C.A-6-1 strain gauges were attached diametrically opposite each other

on the outside diameter of the die. They were positioned to lie at the centre of the compaction zone as shown in Fig. 8. The die holding plate was relieved to prevent it from fouling the strain gauges. The active gauges lay around the circumference of the die and measured the hoop strains resulting from application of an internal pressure. The temperature compensation gauges lay normal to the active gauges and again the bridge connection circuit shown in Fig. 7 was used.

These strain gauge transducers required a stable power supply and the output from them required amplification before being fed to a recorder. "Strainstall" 91A and 91B strain gauge amplifiers supplied by a stabilized D.C. voltage were used for both these purposes, to supply a stable 10 volt potential to the transducers and to amplify the output potential before feeding it to a high speed two pen recorder. This had a pen speed of 0.25 sec for full scale deflection, a maximum chart speed of 1600mm/min and an attenuator which enabled the voltage for full scale deflection to be varied between 1mV and 5V in ten steps.

Since the forces of compaction differed by at least an order of magnitude from those of ejection, a rapid scale change unit was needed to ensure that the ejection forces were recorded to the desired accuracy. Microswitches and cams were integrated with the press motion which along with the scale change unit allowed rapid scale changes at the required points during the pressing cycle.

Top punch and die movements were measured using a rectilinear potentiometer which was attached to the press frame, the slider being connected to either the top punch mechanism or the die bed. The potentiometer was connected as shown in Fig. 9. A constant voltage was supplied to the potentiometer and the output fed into a recorder. The system was calibrated with dial gauge capable of measuring deflections

of 0.0025 mm.

5. Calibration of Punches and Dies. Calibration of the punch strain gauges was performed on a 500kN Amsler mechanical testing machine using self aligning platens to avoid any bending effects. The system was allowed to stabilize for 1 hour before any readings were taken and then the load was cycled several times between 0 and 350kN. Calibration was then started and the strain gauge amplifiers were adjusted to give an output of about 50mV per kN of force applied to the punches. The bottom punch was further calibrated at low loads using an Instron mechanical testing machine to obtain the accuracy required for the much smaller ejection force measurements.

The strain gauges on the die were calibrated by two separate methods as follows:

(i) Using a Denison mechanical testing machine;

(ii) in situ within the press.

Method (i) Fig 10 shows the arrangement used for calibration using the Dension. Heavily plasticised P.V.C. as used by PENRICE[106] was placed in the position of the compact. This material behaves as a fluid under compression and transmits force equally in all directions. Hence the internal bore pressure is the same as the applied punch pressure. However at a pressure of 500 MN/m^2 the plasticised P.V.C. began extruding between the punch and die clearance; the clearances being enlarged by the pressure within the die. 'D' section neoprene seals were used to prevent this effect at high pressures. The die was calibrated in the die holding plate and the same procedure used as for punch calibration.

Method (ii). Further calibration curves were obtained with the die bolted in position on the press. Different heights of P.V.C. plug were used to assess the effect upon the calibration. The bottom punch position was adjusted so that the P.V.C. plug was in the same position as a powder compact after compaction to the same height. The eject motion of the press was removed during the calibration and the press stroke gradually adjusted to slowly increase the force applied to the P.V.C. plug. The force was measured with the previously calibrated top punch. It was found that the height of the P.V.C. plug affected the strain gauge output due to the change in the amount of die constraint. Compacts having standard heights of 10mm were therefore prepared in this investigation. (The calibration results for punches and dies are given in Appendix II).

6. Assessment of System Accuracy. The accuracy of force measurement using the punch load cell, amplifier system was found to be better than $\pm$ 0.5%. Ejection force measurements were determined using only 0.1 of the full scale deflection (time for full scale deflection was .25 secs) and therefore the response time of the system was 0.025 sec. A check was made using a storage oscilloscope, which proved that the maximum compaction and ejection forces were being recorded and that there was no significant system hysteresis. The die strain gauge calibration results indicated an accuracy of $\pm$ 3.0% and the punch movements could be recorded to an accuracy of $\pm$ 0.05mm.

These systems for force and displacement measurement on the various items of tooling, moving at production speeds were found to be adequate. A run of 30 identical compacts was produced and excellent reproducibility between results was obtained.

7. Dynamic Compaction and Ejection Studies. Pressure-density relationships produced at production speeds were obtained using the instrumented press. The outputs from the rectilinear potentiometer (connected to the top punch mechanism) and the top punch strain gauges were connected to the 'X' and 'Y' channels respectively of an 'XY' recorder. A continuous record was therefore obtained of the punch force-distance relationship which was then converted to a pressure-density relationship from a knowledge of the compact weight and dimensions. This however did not give the true pressure density relationship because the compact recovered elastically on ejection from the die and therefore its length whilst under pressure was unknown. This difficulty was overcome by cycling the press without any powder in it but with a packing piece of known length (10.00mm) placed above the top punch. The press was adjusted so that the top and bottom punches pressed against each other with a maximum pressure P during the cycle. The top punch packing piece was removed and the press returned to its fill position. A weight of the iron powder under investigation sufficient to produce a compact 10mm high and of density $6.8 g/cm^3$ was poured into the die. (Note: the punch pressure P is slightly lower than the pressure normally required to produce such a compact). The press was then cycled and a force-distance plot obtained. This was converted to a pressure-distance plot. Thus at pressure P on this diagram the compact height must be the same as the thickness of the punch packing piece (machine and punch strains all being equal in both cases at pressure P) and this point then can be used as a datum for determination of the true dynamic pressure-density relationship.

The effect of lubricant additions upon the pressure density relationship of the raw material was examined in this way. Also from a knowledge of the area under the force-distance curve the energy expended during the compaction process was determined.

A study was also made of the effects of density change, admixed lubricant content and type upon the ejection behaviour of metal compacts. The height of the compacts was kept at 10mm throughout these tests and a series of true densities between 5.8 and 6.8g/cm^3 was examined with lubricant contents varying between 0.2 and 2.0 wt.%. A number of metal stearate lubricants were examined. Six compacts were produced at each condition and the compaction and ejection forces measured along with die radial stress and top punch force-displacement determinations. When the compaction conditions were altered, i.e. by the amount or type of lubricant within the mix, the punches and die were washed in xylene to remove any lubricant build up that might have occurred.

The effects of using different die materials i.e. high chromium die steel, tungsten carbide and glass ceramic, were evaluated using a mix containing 1 wt.% admixed zinc stearate. Compacts of 10mm height were produced at true densities between 5.8 and 6.8 g/cm^3, and compaction and ejection data determined.

8. Pressed Compact Evaluation. The surfaces of selected compacts were examined following ejection from the die using the S.E.M. to reveal the presence of lubricant films. In some cases it was necessary to vacuum coat the surfaces to prevent charging. Green strengths were evaluated as described later in Section 5.40 and fracture surfaces examined again using the S.E.M.

The density distribution within a compact was examined by two methods. In the first method a mercury balance as shown in Fig. 11 was used for determining compact sectional densities. The specimen was weighed in air W_1 and the upthrust due to the specimen holder lowered to a constant position below the level of the mercury was measured W_2. This was determined by just making electrical contact between a needle placed

alongside the specimen holder and the mercury surface. The procedure was repeated with a specimen in position and the upthrust measured W_3. The difference between these weights (W_3-W_2) is the apparent upthrust of the displaced mercury due to the specimen. Thus the volume V of the specimen is found from the expression:-

$$V = \frac{W_1 + (W_3-W_2)}{\rho_T} \qquad \ldots\ldots\ldots\ldots\ldots\ldots \quad (19)$$

where ρ_T is the density of mercury at the testing temperature T. Hence the apparent density ρ_A can be found since

$$\rho_A = \frac{W_1}{V} = \frac{W_1 \rho_T}{W_1 + (W_3 - W_2)} \qquad \ldots\ldots\ldots\ldots\ldots\ldots \quad (20)$$

The compacts were weighed to $\pm$ 0.02g and an accuracy of $\pm$ 0.01g/cm^3 could be achieved.

Following density determination as previously described, a section was machined from the compact and the procedure repeated to give the density of the remaining piece. The density of the piece removed was found by difference. The technique was repeated a number of times to build up an outline of the compact density distribution.

Since this method required a large amount of time and some difficulty was encountered with machining the green iron powder compacts a second technique was investigated using the "Quantimet B" Automated Image Analysing Computer. It was proposed to diametrically section mount and polish the iron powder compacts for porosity distribution measurement with the "Quantimet B". Great difficulty was however experienced in preventing the pull out of iron powder from the compact surface during polishing. This effect would completely invalidate any quantitative measurement of surface features. Various unsuccessful methods were tried to impregnate

the porous iron compacts with "Araldite 219". A presintering treatment of 10 minutes at 800°C in an atmosphere of 97% N_2, 3% H_2 was finally used to overcome this problem. Polishing was carried out on 220,320, 400 and 600 grade carborundum papers finishing with 6 μm, 1μm and $\frac{1}{4}\mu$m grade diamond polishing. The $\frac{1}{4}\mu$m diamond polish was used on a paper pad to reduce relief polishing effects, and the specimens automatically polished for 30 minutes.

The distribution of porosity over the surface of the compact was determined using the automated specimen holder on the "Quantimet B" Ten fields were examined at 0.8mm intervals along the compact height and fourteen traverses were made at 0.8mm intervals to completely survey half of a compact. It was assumed that the compact density would be symmetrical at about its centre. A x10 eyepiece and a X3 objective were used with the blank frame set at 9999. Thus the percentage area porosity could be directly determined. Several compacts were examined in this way.

An assessment of green spring was made by measuring the outside diameter of the compacts with a micrometer to an accuracy of $\pm$0.002mm and comparing this value with the internal diameter of the die. The diameter of the compacts was carefully measured in three different positions along its height, the compact being turned by 90° around its axis between each two diameter readings. The mean value was taken over the total of six diameter measurements obtained.

The die bore was measured using spring callipers expanded against the die wall which were locked in position removed from the die and micrometer measured. A number of readings were taken around the pressing zone and the mean found. This was checked by making a casting of "Araldite 219" within the die bore and measuring it after removal from the die. The shrinkage of "Araldite 219" was previously determined by casting it into

a shape of known size and measuring it following removal.

These measurements of compact-die spring were also used to give an estimate of the residual radial stress occurring between the compact and die following withdrawal of the punches. This calculation was based upon thick cylinder theory[107] which requires however a knowledge of the elastic moduli and Poissons ratio for the compact and die materials. These values were available for the die, but no information was available about unsintered compacts, and the values therefore had to be determined. Strain gauges were attached to the die later to directly measure these stresses and evaluate the accuracy of the technique.

5.40 Determination of the Stress/Strain Relationship for Unsintered Compacts

The modulus of cylindrical compacts was determined in compression using an Instron mechanical testing machine. The method of testing is illustrated in Fig.12 (a). The system strain was first determined by obtaining a graph of load versus compression without a compact. The compact under investigation was then placed in position and quickly loaded to 2000 Kg. The compact was held under load for about 30 sec and then unloaded at a strain rate of 1mm/min. This technique for determining the stress/strain curve whilst unloading the compact was adopted because during loading an amount of strain occurs due to viscoelastic effects within the iron-lubricant system. The effects of such strains are removed by holding the load on the compact immediately before starting the test. This technique of determination was considered most applicable to the situation of a compact held under an interference fit within the die. The stress-strain diagram was determined after correction for initial take up strain and machine strain, this is shown in Fig 12(b).

These determinations were carried out on compacts 14.8mm dia. and about 10mm high (the exact height of the compacts was measured to determine the compressive stress-strain diagram). Compact densities in the range 5.8 to 6.8g/cm^3 were examined containing between 0.5 and 2.0 wt.% zinc stearate.

Modulus Value Used in Radial Stress Determinations. The equations used to calculate the radial stress assume constant modulus of elasticity values. However in the case of powder metal compacts the modulus was found to vary with strain. This must be accounted for in the radial stress determination. If the relative amounts of strain occurring in the compact and the die can be estimated then the modulus of elasticity of that strain can be found and its value used in the calculations. The graphical method shown in Fig. 13 was used to determine the appropriate modulus value. If the outside diameter of the compact Dc is larger than the inside diameter of the die D_D by an amount δD_c then the amount of strain in the compact can be shown to be $2\delta D_c/D_c$ (see Appendix III). From Fig. 13 the value of $\epsilon_2 - \epsilon_1$ is $2\delta D_c/D_c$. The modulus of the die material was drawn from ϵ_2 as shown to account for the die strain. The compact secant modulus value was obtained from the slope of the line joining ϵ_1 to the point of intersection of the die modulus and compact modulus lines. This secant modulus value was used in the calculation of die residual radial stress.

5.50 Pin and Disc Friction Testing Apparatus.

In order to provide a method for lubricant evaluation it was decided to use a "pin and disc" friction testing rig. This was used to provide a rapid method of lubricant assessment and to determine the effects of varying load, speed, temperature and disc material upon the measured value of coefficient of friction. The results from these tests were then compared

with those determined from laboratory and production scale tests. In addition to measurements of friction coefficient the pin and disc machine was used for wear assessment and contact resistance determinations.

1. General Description of the "Pin and Disc" Machine. The apparatus which is shown in Fig. 14 consisted of a pin made from one of the materials under investigation and carried by a horizontal arm. The pin was allowed to rub against the outer curved surface of a rotating disc. A vertical force could be applied to the pin by addition of weights to a hanger supported by the pin arm. The horizontal force resulting from the friction between the pin and rotating disc was measured using strain gauges. The horizontal arm supporting the pin was attached to the rest of the rig by a springy metal beam inclined at an angle of $\sim 20^{\circ}$ to the horizontal. Two strain gauges were attached to each of the upper and lower surfaces of this beam. These gauges were connected in a bridge circuit with the upper gauges in opposite arms of the bridge and similarly with the lower gauges. A bending force resulting from friction between the pin and the disc applied to the beam produced compression forces in the upper gauges and tensile forces in the lower gauges thus throwing the bridge circuit out of balance. The bridge circuit was supplied from a stabilized D.C. power unit and the output fed into a pen recorder. For small beam deflections there is a linear relationship between deflections and surface strain.

2. Calibration of Friction Force Measurement. The system was calibrated by attaching a nylon cord to the end of the horizontal pin arm containing a pin and supported by a disc. The cord was passed around a frictionless pulley and a pan of known weight attached to it. It was necessary to make sure that the cord between the arm and the pulley was horizontal otherwise vertical force components could be introduced during the calibration. The strain gauge circuit was balanced without

any load being applied to the arm. Loads were then applied in 200g increments up to a load of 2Kg. The mV output from the strain gauge was recorded after each addition and the procedure repeated for decreasing load increments. A graph of horizontal arm load versus strain gauge output was produced.

To avoid any possible frictional effects between pin and disc during calibration the disc was vibrated after each incremental load increase or decrease. The output from the strain gauges for a given load could be varied by adjusting the stabilized input voltage but for the purpose of the runs to be carried out 14.70 V was used which resulted in an output of 5mV/Kg. The friction force could be measured to an accuracy of $\pm$ 2.0%

3. Contact Resistance Measurement Between Pin and Disc. The method used for contact resistance measurement was similar to that described by FUREY[59] and the circuit used is shown in Fig. 15. The electrical resistance between the pin and disc was determined by a voltage drop method and a $1\frac{1}{2}$ volt dry cell was used as the voltage source. Resistors were used to reduce the input to about 60mV. The electrical path from the cylinder was through the shaft and a flexible copper wire sheathed with a polythene tube into a mercury bath. Contacts were made with the pin and the mercury. This technique gave a satisfactorily low constant resistance during operation. The instantaneous resistance was viewed using an oscilloscope and a pen recorder was used to record the average electrical resistance during a test. A plot of resistance at the junction between the two rubbing surfaces versus the voltage drop was made by connecting known resistances between the pin and the disc where the mid scale resistance was 200Ω. This is shown in Fig. 16 from which it is clear that one plot alone cannot be used to determine contact resistances over the range 0 - $\infty\Omega$

with the same degree of accuracy. This however was shown not to affect the results of the present investigation.

4. Technique for Pin Temperature Variation. A special pin holder was constructed to heat or cool the pin specimen. It was produced from copper sheet and tubing and was designed to allow either hot or cold liquids to be pumped through it so heating or cooling the pin. A thermocouple was used to measure the temperature of the liquid passing just above the pin and a second thermocouple was embedded within the pin to measure its bulk temperature. The disc was not heated but its temperature was measured both before and after a test.

For temperatures between ambient and 80°C hot water was pumped through the pin holder, between 80°C and 139°C heated glycol was used. Special silicone rubber tubing was also used at these temperatures. Temperatures down to -21°C were achieved with a mixture of dry ice and alcohol and for temperatures down to -196°C liquid nitrogen was poured directly into the copper pin holder tube using a funnel. At these low temperatures the tests were carried out within 30 sec of the correct temperature being achieved whilst the pin temperature was fairly stable. Pin temperatures were controlled to $\pm$ 1°C at temperatures above ambient and down to -21°C but at temperatures down to -196°C the control was $\pm$ 3°C.

5. Test Procedure and Conditions. The surface finish of the disc was measured before it was fixed in position on the machine. 12.5mm dia high iron powder compacts having an apparent density of 6.8 g/cm^3 were used as the pins. Surface finish measurements on this material was not very meaningful because of the surface porosity. The pin was mounted in

the pin holder so that there was a crossed cylinders relationship between the disc and the pin. The surfaces of the pin and disc were thoroughly cleaned with acetone and then isopropyl alcohol. The pin was carefully lowered onto the surface of the disc. The load between the pin and disc was obtained by counterbalancing the supporting arm and then adding the appropriate weights to the hanger. The applied loads could be varied between a few grams and several thousand. The arm was released from its spring retaining clamps, the strain gauges zeroed, and the test started. Tests were carried out for periods of between 10 minutes and 10 hours. Where a powdered metal stearate lubricant was applied during a test it was pressed into the form of a cylindrical compact and continuously rubbed against the disc. It was replaced whenever necessary.

The effects of changes in pin load, pin temperature, surfacevelocity, and lubricant type upon the coefficient of friction and contact resistance were examined using this rig. Pin loads were varied between 1Kg and 40Kg and pin temperatures in the range -196°C to +139°C were examined. Disc surface velocities were varied between 19 and 145 cm/sec by adjusting the pulley drive train between the motor and disc. All the above tests of 10mins duration were carried out using a high chromium die steel disc heat treated to 58 HRC with a pad of zinc stearate lubricant continuously rubbing against it.

A further series of 10 minute duration tests were carried out on a series of metal stearate lubricants using pin loads in the range 5 - 25Kg again using the high chromium die steel disc. Friction coefficients and contact resistances were measured.

A series of tests was performed using pieces of iron powder compacts containing lubricant instead of the plain iron powder pin. An examination was made of the change in coefficient of friction with sliding distance, at pin loads between 5 and 20Kg. A pen recorder having a fast chart speed

and rapid response was used for this purpose.

6. Wear Assessment Using the "Pin and Disc" Machine. Determinations of wear rate were made under both lubricated and unlubricated conditions. A crossed cylinder arrangement between pin and disc was again used. The pin dimensions were as previously described and wear rates were found by measuring the compact weight loss per unit time resulting from sliding at a known relative velocity under a given load.

Under conditions of unlubricated sliding it was found necessary to limit the pin load to 2 Kg. This was required because the excessive vibrations which occurred at higher loads resulted in fracture of the iron powder pin. Surface velocities of 19 and 156 cm/sec were used and wear rates measured under loads between 100g and 2Kg. Several pins made from different iron powders were also tested.

The effect of lubrication on the wear rate was found and in this case pin loads were increased in order to give measurable changes in weight. Difficulty was however still experienced in obtaining significant weight changes even using pin loads of 25Kg.

The wear behaviour of several different disc materials was studied in the unlubricated condition. The wear rate of iron powder pins upon their surface was measured at 100g and 1Kg and the change in coefficient of friction with running time found. Surface finish measurements were made across the disc surface using a "Talysurf" profilimeter at the start and at intervals during the test. "Araldite 219" replicas were also made to study the surface changes occurring in the wear scar region of the disc. The replicas were prepared and examined under the S.E.M. The surface of the disc was marked so that the surface finish measurements and replicas could be taken at the same place on successive occasions. Discs made from

high chromium die steel, tungsten carbide plasma sprayed onto the surface of a steel blank, and glass ceramic were all investigated in the above manner.

6.00 PRESENTATION AND INTERPRETATION OF RESULTS

6.10 Characterisation of Materials and Examination of Mix Properties

1. Characterisation of Iron Powder
2. Characterisation of Metal Stearates
3. Evaluation of Mixing Techniques
4. Effect of Lubricant Content on Mix Characteristics
5. Effect of Lubricant Type upon Mix Characteristics

6.20 Laboratory Scale Compaction and Ejection Studies

1. Compaction of Iron Powder Without Lubricant
2. Ejection of Iron Powder Compacts without Lubricant
3. Compaction of Iron Powder Containing Lubricant
4. Ejection of Iron Powder Containing Lubricant
5. Effect of Die Surface Finish upon Compaction and Ejection Behaviour.
6. Analysis of Iron Powder Compaction Behaviour
7. Analysis of Iron Powder Ejection Behaviour

6.30 Production Scale Compaction and Ejection Studies

1. Compaction of Iron Powder Containing Lubricant
2. Analysis of Iron Powder/Lubricant Compressibility behaviour
3. Measurement of the Energy Used During the Compaction of Iron Powder
4. Ejection of Iron Powder Compacts Containing Lubricants
5. The Effect of Die Material upon Compaction and Ejection Behaviour
6. Compact Properties

6.40 Calculation of the Residual Radial Stress During Ejection

1. Elastic Properties of Green Compacts
2. Comparison of Calculated and Determined Residual Radial Stresses and Derived Friction Coefficients.

6.50 Die Radial Stresses Measured During Compaction and Ejection

6.60 Effect of Lubricant Content, Lubricant Type and Die upon the Measured Values of Friction Coefficient During Ejection

6.70 Determination of Poissons Ratio for Compacts

6.80 Friction and Wear Test Results

1. Effect of Pin Load and Lubricant Type upon the Coefficient of Sliding Friction and Contact Resistance.
2. Variation of Contact Resistance with Friction Coefficient
3. Effect of Disc Surface Velocity upon Coefficient of Sliding Friction and Contact Resistance.
4. Effect of Temperature upon Coefficient of Sliding Friction
5. Friction Measurements upon Ejected Compacts
6. Effect of Various Factors upon the Wear of Iron Powder Compact Pins.

6.00 PRESENTATION AND INTERPRETATION OF RESULTS.

6.10. Characterisation of Materials and Examination of Mix Properties

1. Characterisation of Iron Powder. One iron powder was selected for this research J.J. Makins 100 Pl and the results of apparent density, tapped density, flow, screen analysis, surface area determination and particle hardness, are shown in Table 1. The results of chemical analysis and hydrogen loss determinations are also given here. Sieve analysis only gave the particle size distribution down to 45 microns, and below this size Quantimet analysis was used. The results of the two analyses are shown in Fig. 17 as a curve of wt %.undersize versus particle size.

The Quantimet gave a particle size frequency distribution which was then converted to a wt.% before inclusion on the graph. This was done by multiplying the frequency at each size fraction by the mean cube of the maximum and minimum size values of that fraction. For example, if there were an average of 5.15 particles in the range 10 to 20 microns in each field then this would be multiplied by $(10^3+20^3)/2$ to convert it to a weight fraction. Fig. 17 shows that there is some overlap in results between Quantimet and sieve analysis in the range 45 to 60 microns, although only the -45micron sieve fraction was used for Quantimet analysis. This can however be explained in terms of the particle shape characteristics. If for example we have a cylindrical particle 20 microns diameter and 60 microns long this could pass through a 45 micron sieve. When viewed on the Quantimet this may be seen as a particle of 20 microns or 60 microns size depending upon the orientation of the particle on the T.V. screen. It is therefore possible to measure particle sizes larger than the sieve size through which they passed. If sufficient numbers of particles having random orientation are examined then an average size would be found.

The surface characteristics of the iron powder play a vital role in determining its friction behaviour with respect to either itself or another surface. These surfaces were therefore carefully examined. The results of S.E.M. examination of the iron powder particle surfaces are shown in Fig. 18. It is apparent from examination of these photographs that the particles are angular and their surfaces irregular containing both pores and protuberances.

2. Characterisation of Metal Stearates. Table 2 shows the results of analyses upon the metal stearates used during the course of this investigation. All of the stearates used were of commercial quality some of which are currently being used within the U.K. powder metallurgy industry. The ash contents were generally around 14% for the range of zinc stearates chosen and for the other metal stearates ash contents varied between 6.1 and 41.3%. Free fatty acid contents were found to normally be less than 0.6% although zinc stearate No. 4 contained 1.8% and some of the other metal stearates varied up to 32.3%. Moisture contents of the zinc stearates were in the range 0.1 - 0.8%, but went up to 3.5% for aluminium stearate No. 2. The tapped densities of metal stearates vary depending upon the type of process used during their manufacture. The fusion process generally produces stearates of coarser particle size and higher tapped density. In comparison the precipitation process produces stearates having fine particle size and of lower tapped density. Table 2 also shows the results of particle size determinations carried out upon the stearates. The particle size at the 50% weight undersize level is given although particle size distribution curves were obtained. These are given in Appendix IV, Coulter counter and centrifugal sedimentation techniques were used for the range of zinc stearates examined. Comparison of results from the two methods shows reasonable agreement although the Coulter counter results are generally higher than those

determined by centrifugal sedimentation.

Fig. 19 shows the results of S.E.M. examination of several metal stearates. In general the stearates produced by fusion appear to be fairly solid and rounded whereas the particles produced by precipitation are flocculent and sometimes platelike in character. Estimates of stearate particle size were made from the photographs by measurement and the results included in Table 2. The particle size measured using a photographic technique is quite markedly less than that recorded using the other two techniques. The discrepancy must result from agglomeration which is difficult to account for unless using a visual method.

3. Evaluation of Mixing Technique. The effects of mixing time on both bottle mixing and cone mixing using different amounts of mix were evaluated in order to determine the standard mixing conditions to be used throughout the investigation. The results of this preliminary investigation are given in Table 3. This shows that cone mixing was far more effective in increasing the apparent density and reducing the flow time of the 400g mixes containing 1% zinc stearate. Increasing the double cone mix weight from 400g to 2000g also shows a similar effect. Visual examination of the mixes (prepared by bottle mixing and cone mixing) showed that there were a lot less free stearate particles after cone mixing than bottle mixing and in the 2000g cone mix there appeared to be no stearate agglomerates present.

Microscopic examination of the bottle mixed powder showed stearate agglomerates and stringers both of which would contribute towards reducing the apparent density and increasing the flow time. This however did not mean that in the case of cone mixing the lubricant was evenly covered over the surface of the iron powder. Magnetic separation of the iron powder from the free stearate revealed that as much as 36% of the zinc stearate

contained within a mix containing 1% zinc stearate was not actually attached to any iron powder. This therefore shows that although cone mixing reduces the amount of agglomerates present it does not necessarily produce a mix in which the zinc stearate is evenly covered over the iron powder surface.

The results of microscopic examination of individual iron powder particles both before and after cone mixing with 1% zinc stearate are shown in Fig. 20. From these pictures it would appear that some zinc stearate particles attach themselves within the porous structure of the iron powder (See Fig. 20(a)). However where the surface of the iron powder particles is not so irregular then only a few particles of zinc stearate can be seen (See Fig. 20(b)). The surface features of the iron powder therefore play an important role in determining whether the zinc stearate is attached to the iron powder or exists freely within the mix.

4. Effect of Lubricant Content on Mix Characteristics. Table 4 shows the effects of lubricant additions upon the mix characteristics. The results show the dramatic increase in apparent density of the mix resulting from an addition of only 0.1% zinc stearate 1. Further increases in the zinc stearate content above 0.1% do not markedly alter the apparent density until a 2.0% addition is made which decreases it. The flow times also show a similar trend. The tapped density values generally were decreased by increasing lubricant contents and the ratio of tapped density to apparent density is included in the Table. Green strength measurements upon compacts produced from these mixes are also indicated. Visual examination of the mix showed that there was no free zinc stearate present up to 1.0% but above that level some small stearate agglomerates were observed.

5. Effect of Lubricant Type Upon Mix Characterisiics. Table 5 shows the effect that various metal stearate additions have upon the mix properties. Apparent density, tapped density, flow and green strength values were determined and in addition various ratios involving apparent density D_a, tapped density D_t and compact density D_c are given. The value of compact density D_c used was that produced by compacting 10g of mix in a 14.8mm die at 410 MN/m^2. These compacts were subsequently used for green strength determinations.

6.20. Laboratory Scale Compaction and Ejection Studies.

1. Compaction of Iron Powder Without Lubricant. Fig. 21 shows the compressibility curves obtained for J.J. Makins 100 Pl iron powder without any lubricant additions. Each curve was produced by compacting the same weight of powder at different pressures and measuring the resultant compact density. The set of curves for different height to diameter ratios was obtained by altering the weight of powder compacted. The height/diameter ratio given was the average value for that range of compacts. The tolerance given upon this ratio should be added for compacts produced at the lowest compaction pressure and subtracted for compacts produced at the highest compaction pressures. This was necessary because the compact height varies when pressing to fixed pressure levels. This also applies to all subsequent laboratory scale studies whe-re height to diameter ratios are given.

2. Ejection of Iron Powder Compacts Without Lubricant. Fig. 22 shows a typical force/distance curve obtained during ejection of an unlubricated compact from the die. The maximum force measured during the ejection of a compact occurred at the beginning, and the ejection stresses were calculated by dividing the area of compact in contact with the die wall into the initial ejection load. Fig. 23 shows the effect of compact density

upon the ejection stress at ejection speeds of 5mm/min and 50mm/min.

3. Compaction of Iron Powder Containing Lubricant. The compressibility curves obtained for J.J. Makins 100P1 iron powder containing 1% admixed zinc stearate are shown in Fig. 24. Again compacts having different height/diameter ratios were produced but it was not possible to separate the curves for each particular height/diameter ratio. The results are therefore shown as an average line with upper and lower limits.

Compressibility curves were produced for a series of iron powder mixes containing up to 2.0% zinc stearate 1. The apparent density values of the compacts produced were converted to true metal densities by using the following equation:-

$$\text{True Compact Density} = \text{Green Compact Density} \times \frac{\% \text{ Metal in mix}}{100}$$

A plot was then made of true compact density versus zinc stearate content at a number of different compaction pressure levels. The results of this analysis are shown in Fig. 25.

Compressibility curves were also produced for a series of mixes containing zinc stearates from various sources. A 1% zinc stearate mix was used in each case and from these curves the compaction pressure required to produce compacts of given true density was determined. The results of this analysis together with the particle sizes of the zinc stearates used are shown in Table 6.

4. Ejection of Iron Powder Compacts Containing Lubricant. Since the height/diameter ratio was shown to influence the ejection behaviour of unlubricated compacts a similar series of tests was carried out using the same iron powder mixed with 1% zinc stearate 1. The initial force to start compact ejection was again used to determine the ejection stress values. The results of this investigation are shown in Fig. 26. which

for comparison also includes the values obtained when no lubricant was used.

The effects of zinc stearate 1 content upon the ejection stress for compacts at constant true density levels are shown in Fig. 27. These curves were obtained by determining the relationship between ejection stress and true compact density at various lubricant levels up to 2.0%. The ejection stress at a fixed true density level was then taken at each lubricant level considered and the curves shown in the figure deduced. This procedure was necessary because when compacting to fixed pressure levels the compact density varies as the mix properties change.

An examination of the effects of zinc stearate type upon the ejection behaviour of mixes containing 1% zinc stearate from various sources was carried out and the results shown in Fig. 28. The initial stress to start the 11 grm compacts moving was used to draw these graphs. Changes in the surface characteristics of the ejected compacts were also found between those of high and low densities. Fig. 29 shows S.E.M. photographs of the surfaces of a series of different density compacts produced from a 1% zinc stearate 1 mix. The relevant ejection stress versus compact density curve is included.

These curves all show a marked change in slope but this transition does not appear to be related to the lubricant characteristics such as particle size. The graphs however may be replotted using compaction pressure rather than the resultant compact density. The results of this are shown in Fig. 30. The transition point may be found by extrapolation of the two different parts of the curve. Table 7 shows the transition compaction pressure values and the respective zinc stearate particle sizes together with details of the slopes of the two parts of each graph.

5. Effect of Die Surface Finish Upon Compaction and Ejection Behaviour.

Fig 31 shows the effect of surface finish upon the ejection stress for compacts containing 1% zinc stearate 1 pressed to various true density levels. Variation of the die surface finish within the limits measured had little effect upon the compressibility behaviour of the powder. The surface finish of the die at a distance 15-25mm below the die mouth (i.e. within the compactiong region) improved from 0.078 μm CLA to 0.026μm CLA during the course of the trials. Typical examples of Talysurf traces obtained from this region of the die taken at various times throughout the series of trials are shown in Fig. 32. In the region from 2-12mm below the die mouth, the surface finish changed from 0.078 to 0.14μm CLA.

6. Analysis of Iron Powder Compaction Behaviour. A number of workers have attempted to find the mathematical relationship between pressure and density during the compaction of particulate materials. Of the pressure density relationships proposed KAWAKITA'S[74] empirical equation has been found of most general use and applicable to a wide range of powdered materials. The relationship is

$$C = \frac{V_o - V}{V_o} = \frac{a\,b\,P}{(1+bP)} \quad \ldots\ldots\ldots\ldots \quad (21)$$

where C is the relative reduction in volume, V_o the original powder volume V the volume at pressure P and a,b are constants. This equation may be rearranged[111] to give the following equation:-

$$KP = \frac{1}{1 - D} - C \quad \ldots\ldots\ldots\ldots\ldots\ldots \quad (22)$$

where D is the relative density at pressure P and K and C are constants. Thus plotting compacting pressure P versus the reciprocal porosity 1/ε should give straight lines. This analysis of the compressibility behaviour was carried out upon the data obtained for iron without lubricant additions at various height/diameter ratios and also upon the compressibility values

for iron with a 1% addition of zinc stearate. The results of this investigation are shown in Fig. 33. In addition an Olivetti desk computer programme (See Appendix V) was used to determine the constants in the equation and the results are given in Table 8. Reciprocal porosity values are also included based upon apparent and tapped density measurements.

7. Analysis of Iron Powder Ejection Behaviour. Typical results of the ejection behaviour of metal powder-lubricant compacts obtained using the Houndsfield tensometer are given in Fig. 34. Typical variations in ejection stress with compact movement are shown and it is quite apparent from the curves that a series of stress levels are being measured. Referring to Figs. 34 (a)-(d) the ejection stresses are defined as follows:

σ_B the 'break stress' i.e. the stress to overcome static friction

σ_{si} the 'initial slip stress' i.e. the stress at which sliding friction starts

σ_{smax} the 'maximum slip stress' i.e. the maximum stress at which slip can still continue without sticking.

σ_{smax} the 'maximum stick stress' i.e. the maximum stress achieved before slip occurs.

The results of this analysis for compacts (height/diameter ~.7). containing between 0.3 and 2.0% zinc stearate 1 are shown in Fig. 35.

Table 9 shows the change in slip stress with distance for zinc stearate 1 at various compaction pressures and lubricant contents. The initial slip stress σ_{si} and maximum slip stress σ_{smax} were taken from Fig. 35 and the compact sliding distance involved between these two stress values was determined from the tensometer traces. Hence the slip stress change per unit sliding distance was determined. Here it was assumed that there was a straight line relationship between the two stress values (See Fig. 34 Tensometer Ejection). Although this was not exactly true the general

trends are still indicated. This analysis was not possible for lubricant levels below 0.3% since only stick-slip motion was observed.

The ejection behaviour of the range of zinc stearates examined was also evaluated in terms of the 'break stress' σ_B, the 'initial slip stress' σ_{s1} and the maximum slip stress σ_{smax} for mixes containing 1% lubricant.

The results of this analysis for compacting pressures of 258, 360, 462 and 564 MN/m^2 are shown in Tables 10-12.

6.30 Production Scale Compaction and Ejection Studies

The laboratory scale compaction and ejection studies revealed that the height to diameter ratio was an important factor. Therefore in order to evaluate the lubricants this ratio was kept constant at 0.4 for all the production scale compaction and ejection tests. A number of different test series was carried out. The first series involved comparison between laboratory values and production values and following this, a method was determined for calculating friction coefficients during the ejection of compacts from the die. A second series of tests was carried out then using a die with strain gauges attached to actually determine the ejection stresses, from which the coefficient of friction during ejection could be calculated and compared with the theoretically predicted values. Various metal stearate lubricants were then evaluated using the fully instrumented punches and dies. Finally the effects of die materials were examined using a carbide die (shrunk fit into a steel bolster and strain gauged) and a glass ceramic die (again shrunk fit into a steel bolster, but without strain gauges attached).

1. Compaction of Iron Powder Containing Lubricant. Compressibility curves were produced for iron powder mixes containing between 0.2 and 2.0% zinc stearate 1. Curves of true compact density versus zinc stearate content at compacting pressures of 300, 400 and 500 MN/m^2 were evaluated from the compressibility data and the results are shown in Fig. 36. For comparison, this figure also includes the results of a similar series of laboratory scale tests which are shown in Fig. 25.

Compressibility curves were determined for a series of mixes containing 0.5% of various metal stearates and stearic acid. From these curves the compaction pressure required to produce compacts of given true density was determined. These results are shown in Table 13. Some die wall lubrication tests were also performed using stearic acid dissolved in diethyl ether wiped onto the surface of the die. These results are also included in Table 13.

2. Analysis of Iron Powder/Lubricant Compressibility Behaviour. Dynamic pressure density relationships were determined using the instrumented press with the top punch force and displacement measurements fed onto the two separate channels of an 'XY' recorder as previously described. The compressibility relationships were determined for iron powder without lubricant addition, zinc stearate 1 powder and iron powder containing 0.2% and 2.0% admixed zinc stearate 1. The curves were then analysed using Kawakita's relationship (See equation 22). and the results are shown in Fig. 37. Kawakita constants were determined and the results are given in Table 14. The values of reciprocal porosity based upon apparent and tapped density measurements are also included.

3. Measurement of the Energy Used During the Compaction of Iron Powder. The area under the dynamic force-displacement curves was measured to give the energy used during the compaction process. This was done by cutting

out the area contained beneath the force displacement curve and weighing it. This weight was then compared with the weight of a known area (corresponding to a given energy) of similar paper to determine the energy. Fig. 38 shows the effect of true compact density and zinc stearate 1 content upon the energy required for the compaction of J.J. Makins 100 PL iron powder.

4. Ejection of Iron Powder Compacts Containing Lubricant. A typical trace obtained during ejection of a compact from the die during the production scale studies is included in Fig. 34 for comparison with laboratory scale traces. The maximum slip stress value $\sigma_{s\max}$ was determined for each of the compacts produced and plots of stress versus true compact density achieved by each compaction were obtained at each lubricant level. From this data, the ejection stresses for density levels of 5.90, 6.20, and 6.50g/cm^3 were deduced and the results are presented in Fig. 39 which also includes the results of laboratory scale tests for comparison.

Whilst carrying out these runs the following observations were made:

1) Compacting to a true density of 6.80g/cm^3 from a mix containing 0.5% zinc stearate 1. resulted in tool seizure. This was caused by the cladding of 'flash' from the compacts onto the die between the punch and die clearance. A replica of the die surface was taken after seizure and this is shown in Fig. 40. The compact surface also showed severe scoring in this region.

2) At zinc stearate contents of 1.5 and 2.0% it proved impossible to produce compacts having true densities greater than 6.55 and 6.25 g/cm^3 respectively whilst operating the press at 25 strokes/min. This was due to laminar fracture of the compact on ejection from the die. However by stopping the press immediately after compaction and leaving the compact within the die for several seconds, the ejection could be performed without fracture.

The ejection behaviour of compacts produced from a number of different metal stearates and stearic acid mixes each containing 0.5% of the lubricant was examined. The results are shown in Fig. 41 (a)-(b) as plots of ejection stress versus compaction pressure. Die wall lubrication values are also included.

5. The Effect of Die Material Upon Compaction and Ejection Behaviour. Several different die materials were investigated in addition to the high chromium die steel. These were tungsten carbide and glass ceramic. Pressure/density curves were obtained from each of these materials using a mix containing 1.0% zinc stearate 1 and from the curves compaction pressures to give true densities in the range 5.9 to 6.7 g/cm^3 were deduced. The results are given in Table 15.

The effect of die material upon the ejection behaviour was also examined and the results are shown in Fig. 42. These results are also given in Table 16 for ease of comparison.

6. Compact Properties. Compact surfaces were examined with the S.E.M. immediately following ejection from the die. Fig. 43 shows the effect of lubricant content upon compact surfaces (true density 6.2 g/cm^3) for zinc stearate 1 contents in the range 0.5% to 2.0%. Fig 44 also shows the effect of 0.2% and 2.0% zinc stearate 1 additions upon the surface characteristics of compacts having densities of 5.8 and 6.6 g/cm^3. Some compact fracture surfaces were also examined to try and determine the distribution of lubricant after compaction. Occasionally free particles of zinc stearate were seen as shown in Fig. 45 but otherwise it was not possible to see where the lubricant was distributed.

A preliminary investigation was carried out to try and establish the effect, if any, of lubricant content upon density distribution within

a compact. Two compacts of similar density but pressed with 0.2% and 2.0% zinc stearate 1 lubricant were taken and their density distributions were determined using the mercury balance(as described in section 4.38). The results of this investigation are shown in Fig. 46. Some specimens were also examined using the Quantimet and the results are shown in Fig. 47 as % area porosity contours across a diametrical section of the specimen. Specimen preparation plays a major role in determining the accuracy of these results and it was felt that in some cases when the porosity fell to 1% then this was not representative of the true porosity level at that point. The results have however been included for comparison with the values obtained by machining and mercury balance measurement although more research is required into polishing technique before accurate values can be determined and any firm conclusions drawn.

The effect of lubricant content upon green strength was measured and the results are given in Fig. 48. Compact density levels of 5.8 and 6.6 g/cm^3 were considered using zinc stearate 1 contents in the range 0.2 to 2.0%

Assessment was made of the 'green spring' which occurs when the compact is ejected from the die. This is affected by both the lubricant level and the compact density. Fig. 49 shows the effect of these parameters upon the 'green spring' expressed as a percentage increase on the original die dimension.

6.40 Calculation of the Residual Radial StressDuring Ejection.

The residual radial stress is that compressive stress acting against the compact when the top punch has been withdrawn. During compaction the die expands elastically due to transmission of the vertical compacting force through the powder to the die wall. On release of the compacting

pressure the die begins to contract elastically, but cannot fully return to its dimensions when empty due to the compressive stress built up progressively in the powder compact within it. The final state therefore is analagous to an interference fit with the compact in compression and the die in tension. The dimension of the common interface between them is greater than the bore of the empty die and less than the outside diameter of the compact after ejection. Fig. 50 represents this balanced state acting at any cross section. At the interface, the radial compressive stress σ_D exerted by the die on the compact must be balanced by the radial stress σ_C exerted by the compact on the die. It is assumed that the interface diameter D_I remains unchanged throughout the height of the compact. This, however, is not completely valid because a powder under pressure does not act as a fluid and the compacting pressure varies with distance from the punch. The die expansion will therefore not be uniform from one cross section to the next resulting in a variation along the height of the compact of the 'interference fit' to be overcome during ejection. However where the compact height/diameter ratio is small < 0.5, for most practical purposes estimates ignoring this variation will be accurate enough.

Of the three diameters shown in Fig. 50 only two, D_D and D_c can be measured. The value of D_I is known only approximately, lying between D_c and D_D. However the difference $(D_C - D_D)$ corresponds to the interference taken up when making force fits.

Now if we consider the general case where the outside diameter of a solid cylinder (the compact) in the unstressed condition is larger than the inside diameter of a hollow outer cylinder (the die) by an amount δ then after assembly a radial stress σ_R is produced between the cylinders. The radial stress is found from the condition where the increase in the

inside diameter of the outer cylinder plus the decrease in the outside diameter of the inner cylinder equals δ. Thus from Timoshenko[107] and using Fig. 50 it may be shown that for the case of a solid internal cylinder:

$$\delta = \frac{D_c \sigma^-}{E_1} \left[\frac{D_o^2 + D_c^2}{D_o^2 - D_c^2} + \nu_1 \right] + \frac{D_c \sigma^-}{E_2} (1 - \nu_2) \quad \ldots\ldots(23)$$

where D_o - outside diameter of outer cylinder

D_c - outside diameter of inner cylinder

E_1 - modulus of elasticity of outer cylinder

E_2 - modulus of elasticity of inner cylinder

ν_1 - Poissons ratio for outer cylinder

ν_2 - Poissons ratio for inner cylinder

Therefore provided the elastic moduli and Poisson's ratios of the die and compact material are known the radial compressive stress can be determined.

1. Elastic Properties of Green Compacts. The elastic properties of the green compacts were determined in compression and it was found that the modulus of elasticity varied with strain. At low stress levels ($3 MN/m^2$) the compacts which contained lubricant were found to behave in a visco-elastic manner and a technique of stress cycling[108] was used to determine the elastic properties. This behaviour was not observed in compacts produced without lubricant. Fig. 51 shows the effects of compact density and lubricant content upon Youngs moudulus values determined at stresses of $3 MN/m^2$ and 120 MN/m^2. Since the modulus values were found to vary with strain it was necessary to use a secant modulus value in the calculation of residual radial stress. The method for determining this modulus value is given in Section 4.41. The calculation also requires

a knowledge of Poissons ratio and initially, since no values were available for green material, the values were determined from the variation of elastic moduli with porosity according to Hashin's[109,110] equations. Since $\nu = (E/2G - 1)$ values in the range 0.284 at density 6.85 to 0.279 at density 5.80 were used. However later work using an instrumented die has enabled Poissons ratio to be determined for green compacts. Table 17 shows the effect of compaction pressure and lubricant level upon the calculated values of residual radial stress. The Poisson ratio values used were those determined for the actual compacts and the secant modulus values were found from modulus determinations on com pacts having similar densities. Thus from these measurements coefficient of friction values were found.

2. Comparison of Calculated and Determined Residual Radial Stresses and Derived Friction Coefficients. Table 18 shows the comparison between calculated and experimentally measured residual radial stress values for the production scale studies. The experimentally determined values were found using the die having strain gauges attached to it. Ejection stress values are also shown and the friction coefficients during ejection were determined by dividing the ejection stress by the residual radial stress. The friction coefficients determined from calculated and measured residual radial stress values are also shown in Table 18. Similar calculations were performed for the laboratory scale studies and the results are shown in Table 19. Regular density intervals were used in this case; the values of interference, modulus and Poisson's ratio being found graphically at the densities shown.

The variation of friction coefficient with density for a number of different 1% zinc stearate mixes is shown in Tables 20-22 for the laboratory scale studies. Break stress, initial slip stress and maximum slip stress values were used to determine the friction coefficients. As

indicated by Fig. 31 surface finish variations affect ejection stress measurements. These curves were approximated to a linear relationship over the range used in these trials and the ejection stresses were corrected to one surface finish level (.052 μM CLA). A series of correction factors was deduced from Fig. 31 to allow for this adjustment. These were determined by measuring the ejection stress of a standard mix compacted to a series of true densities after each trial. The corrections decrease with fall in true density, as Fig. 31 shows, so that at a density of 5.90 g/cm^3 no correction factor was applied.

6.50 Die Radial Stresses Measured During Compaction And Ejection.

Strain gauges attached to the outside diameter of the die were used to measure the radial stresses occurring during compaction and ejection. Figs. 52 (a)-(d) show the changes in die radial stress with top punch pressure during compaction for lubricant contents in the range 0.2 - 2.0% These figures also show the changes in die residual radial stress which occurs during ejection of the compact from the die. These measurements were taken with the high chromium die steel die. Similar results were also obtained for the instrumented tungsten carbide die and these are shown in Figs. 53 (a) - (d). These values of residual radial stress during ejection were used to determine coefficients of friction during compact ejection.

All the relevent data from which these plots were made are given in Appendix VI.

6.60 Effect of Lubricant Content, Lubricant Type and Die Material Upon the Measured Values of Friction Coefficient During Ejection

The effect of lubricant content upon the ejection friction coefficient for the H.C.D. die at different true compact density levels is shown in Fig. 54. This graph was obtained by plotting friction coefficient versus

true compact density at different lubricant contents and then taking the friction values at fixed density levels to produce a second graph (Fig. 54). The data from which these plots were made and subsequent ones in this section are given in Appendix VI.

The effect of lubricant type upon the ejection friction coefficient at different true density levels, again using the H.C.D. die is shown in Table 23. These friction values were obtained in a similar way to the values obtained above.

Fig. 55 shows the effect of lubricant content upon ejection friction coefficient at different density levels using a tungsten carbide die and Table 24 compares the friction coefficients measured using the tungsten carbide die and the H.C.D. die at similar compact densities and zinc stearate l contents.

6.70 Determination of Poisson's Ratio for Compacts.

Poisson's ratio was evaluated using the traces obtained from the bottom punch and die strain gauges. When a material is strained in any direction, lateral strains of opposite sign are produced in directions at right angles to the original strain. The ratio of lateral strain to initial longitudinal strain is Poisson's ratio (ν).

If we consider a compact placed in a die, which is an exact fit with the die bore then initially there will be no radial stress at the die wall. If a compressive stress σ_c is now applied to the compact, it will decrease in length and try to increase in diameter producing a radial stress σ_R. As shown below the ratio of σ_R to $\sigma_R + \sigma_c$ gives Poisson's ratio directly.

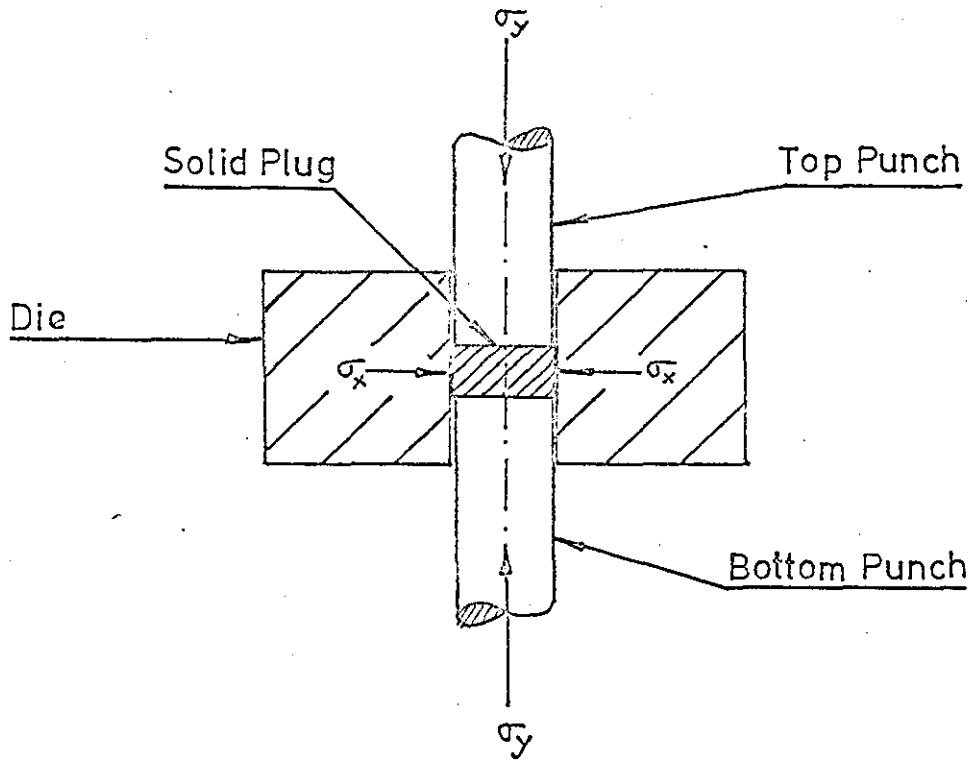

Consider a perfectly fitting solid cylindrical plug in the centre of a die assumed to be perfectly rigid.

Now in the case of a cube of material it can be shown that the following general equation applies:-

$$\varepsilon_x = \frac{1}{E}\left[\sigma_x - \nu(\sigma_y + \sigma_3)\right] \quad ;.....(24)$$

where ε_x is the strain in the x direction, E is Young's modulus for the material, ν is Poissons ratio and σ_x, σ_y and σ_3 are stresses applied to the cube face in the x,y and 3 directions respectively.

For a cylinder in the die as shown above $\sigma_x = \sigma_3$

Now since the die is assumed to be perfectly rigid then $\varepsilon_x = 0$

Thus using equation (24) above we obtain:-

$$0 = \frac{1}{E}\left[\sigma_x - \nu(\sigma_y + \sigma_x)\right] .....(25)$$

Hence:-

$$\nu = \frac{\sigma_x}{\sigma_y + \sigma_x} \qquad \text{.....(26)}$$

Now consider the typical traces obtained (Fig. 56) from which the maximum compacting stress and the die radial stresses values were measured. When the compacting stress is removed the die stress falls to the residual radial stress value σ_R. If we were now to recompact at the same stress σ_{cmax} the radial stress measurement would return to σ_{Rmax}. Thus a compacting stress of $\sigma_{c\ max}$ produces a radial stress of $(\sigma_{R\ max} - \sigma_R)$ and hence Poissons ratio can be determined i.e.

$$\nu = \frac{(\sigma_{R\ max} - \sigma_R)}{\sigma_{c\ max} + (\sigma_{R\ max} - \sigma_R)} \qquad \text{.....(27)}$$

Figs. 57 and 58 show the variation of calculated Poissons ratio with true compact density and lubricant content for compacts produced in the high chromium die steel and the tungsten carbide dies. The data from which the calculations were made are given in Appendix VI .

6.80. Friction and Wear Test Results.

1. Effect of Pin Load and Lubricant Type Upon the Coefficient of Sliding Friction and the Contact Resistance. A number of zinc stearates from various sources and other metal stearates were tested using the pin and disc machine. A high chromium die steel disc of surface finish 0.09μM CLA was used during these tests. Tables 25 and 26 show the effects of pin load and lubricant type upon the coefficient of sliding friction and the contact resistance measured between the pin and disc. The duration of these tests was 10 minutes and the friction values were measured when they became steady. The average, maximum and minimum values of contact resistance were measured during these tests.

2. Variation of Contact Resistance with Friction Coefficient. Whilst carrying out the above tests, it was noticed that whenever the contact resistance varied during a test there was an alteration in the value of the friction coefficient. This effect is shown graphically in Fig. 59 for two different zinc stearates with a pin load of 5 Kg.

3. Effect of Disc Surface Velocity Upon Coefficient of Sliding Friction and Contact Resistance. The changes in friction coefficient with velocity were examined and the results are given in Table 27. These tests were carried out to try and predict the changes in friction which may result from changes in the ejection velocity of metal powder compacts. A velocity of 19.1 cm/sec was selected for the majority of the pin and disc work since it corresponded approximately to the speed of ejection used during the production scale trials ($\sim$15 cm/sec).

4. Effect of Temperature Upon Coefficient of Sliding Friction. Fig. 60 shows the effect of pin temperature upon the measured value of friction coefficient. Zinc stearate 1 was used in these tests together with an H.C.D. disc.

5. Friction Measurements Upon Ejected Compacts. Pressed compacts containing 1 and 2% admixed zinc stearate were tested on the pin and disc machine to determine the initial value of friction coefficient when sliding started. A typical plot of friction coefficient versus sliding distance is shown in Fig. 61. An H.C.D. disc was used during these tests without any other lubricant being applied. Table 28 shows the values of initial coefficient of friction obtained for compacts containing up to 2% admixed zinc stearate. A compact containing no lubricant but having a mixture of acetone and zinc stearate evaporated onto its surface was also tested and the results shown. The friction coefficient soon changed from this initial sliding value and reached a maximum of about 0.3 in all tests. Contact resistance measurements

were also made during these tests and in all cases they were found to be zero.

6. Effect of Various Factors Upon the Wear of Iron Powder Compact Pins.

Load. The effect of load upon the unlubricated wear rate of a compact pin (density 6.3 g/cm^3) was measured and Fig. 62 shows the results obtained. The pin was rubbed against the H.C.D. disc (surface finish 0.09 μm CLA) rotating at 156 cm/sec. Pin loads between 100g and 2 Kg were used. Wear was determined by weight loss of the pin and then converted to volume of material removed by dividing by the density of the pin material. The figure shows an initial wear in period after which the volume of material removed per unit sliding distance becomes constant.

Velocity. The effect of velocity upon the volume of pin material removed per unit sliding distance during unlubricated wear is shown in Fig. 63. The results show similar wear rates at velocities of 19.1 and 156 cm/sec for pins under a load of 1 Kg.

Lubricant. In order to be able to obtain measurable rates of wear upon the pin during lubricated wear the pin load had to be increased to 25 Kg and even under such high loads wear rates were still small. Fig. 64 shows the results of this examination for pin loads of 5 and 25 Kg using zinc stearate 8 lubricant.

Disc material. H.C.D., tungsten carbide and glass ceramic disc materials were investigated and the results given in Fig. 65. The surface finishes of the three materials were H.C.D. 0.09 μM CLA, tungsten carbide 0.5μm CLA and glass ceramic 2.5 μmCLA. The surface finishes of the tungsten carbide and the glass ceramic, whilst not being as good as the H.C.D. were the best that could be achieved with the available equipment.

At intervals during these tests the surfaces of the discs were examined using Talysurf and replica techniques. Surface profiles and S.E.M. pictures of replicas taken during the wear tests are shown in Fig. 66 for a plain iron compact rubbing against an H.C.D. disc under a load of 100g. A brown powder was also produced in the region of the wear 'scar'. A similar type of effect, i.e. pick-up from the pin onto the disc and formation of brown powder, was observed during unlubricated wear tests at 1 Kg load using the H.C.D. disc and also when using the glass ceramic disc under similar conditions of load and speed. In contrast to this no pick up occurred at all on the surface of the tungsten carbide disc and the wear scar was undetectable using the S.E.M.

Coefficient of friction measurements were taken during these unlubricated wear tests and were as follows:

High Chromium Die Steel	0.35 - 0.50
Glass Ceramic	0.28 -0.60
Tungsten Carbide	0.16 - 0.28

7.00 DISCUSSION OF RESULTS

7.10 Materials and Mix Properties

1. Iron Powder and Lubricant Characteristics
2. Effectiveness of Mixing Technique
3. Effect of Lubricant Quantity upon Mix Properties
4. Effect of Lubricant Type upon Mix Properties

7.20 Laboratory Scale Compaction Studies

1. Unlubricated Compaction Studies
2. Lubricated Compaction Studies
3. Analysis of Laboratory Compaction Studies

7.30 Laboratory Scale Ejection Studies

1. General Considerations
2. Unlubricated Ejection Behaviour
3. Lubricated Ejection Behaviour
4. Effect of Lubricant Type upon Ejection Behaviour
5. Analysis of Iron Powder Ejection Behaviour
6. Effect of Die Surface Finish Upon Ejection Behaviour

7.40 Production Scale Compaction Studies

1. Comparison of Production Scale and Laboratory Scale Compaction Studies
2. Effect of Lubricant Type on Compressibility Behaviour
3. Analysis of Production Scale Compaction Studies
4. The Effect of Die Material Upon Compressibility Behaviour
5. Energy Involved During Compaction

7.50 Production Scale Ejection Studies

1. Comparison of Production Scale and Laboratory Scale Ejection Studies
2. Ejection of Lubricant Type and Die Material Upon Ejection Behaviour

7.60 Compaction Properties

7.70 Friction Coefficients During Compact Ejection

1. Comparison of Calculated and Determined Friction Coefficients for Production and Laboratory Scale Runs.
2. Coefficients of Sliding Friction and Lubricant Content
3. Coefficients of Sliding Friction and Correlation with other Values

4. Effect of Lubricant Type Upon Friction Coefficients for Laboratory Scale Tests

5. Effect of Lubricant type and Die Material Upon Friction Coefficients for Production Scale Tests

7.80. Pin and Disc Tests

1. Effect of Load and Lubricant Upon Friction Coefficient and Contact Resistance

2. Effect of Velocity and Temperature upon Friction Coefficient

7.00 DISCUSSION OF RESULTS

7.10 Materials and Mix Properties

In any study of friction lubrication and wear it is important to appreciate the nature and properties of the surfaces involved. During the lubricated compaction of iron powder, interactions occur between the three components involved in the system i.e. iron powder, lubricant and die wall, and the properties of these materials will determine the compact pressing and ejection behaviour.

1. Iron Powder and Lubricant Characteristics. Examination of the iron powder surfaces shown in Figs. 18 and 20 reveals that the particles are irregular some having spongy surfaces whilst others have plain surfaces. It is these surface characteristics which determine the iron powder/lubricant mixing behaviour which must ultimately affect the efficiency of lubrication during compaction and ejection.

In comparison to the iron powder, the metal stearate particles appeared less spongy and took the form of either solid more rounded particles, or of platelike particles. These result from different methods of manufacture. The fusion process produces more solid rounded particles and the precipitation process produces more flocculent platelike particles. This effect is reflected in the tapped density values shown in Table 2. Precipitated stearates had tapped densities of 0.16 - 0.28 g/cm^3 whereas fused stearates had tapped densities of 0.30 - 0.48 g/cm^3. Particle size of the lubricants also varies considerably as shown in Table 2.

All of these factors play an important part in determining mix effectiveness and characteristics.

2. Effectiveness of Mixing Technique. The mixing process is intended to blend the constituent parts completely together. In the case of iron powder and lubricant, the ideal situation would be to cover the individual iron powder particles with a thin layer of lubricant. However the evidence suggests that the laboratory scale mixing by either bottle or cone does not approach this ideal situation. Fig. 20 shows the effectiveness with which the lubricant is distributed over the iron powder surface. This suggests that rather than being smeared over the particle surface, the lubricant is attached as individual particles onto the surface. Where the iron surfaces are plane the lubricant coverage is not complete. The lubricant appears to be most readily held by mechanical entrappment within the irregular particle surface.

If we consider the case of an iron powder of specific surface area 500 cm^2/g covered with a monomolecular layer of stearate (thickness 25 Å assuming the molecules with their chains vertical from the surface) then this would require an addition of 0.013 wt % lubricant. Therefore in the case of a 1 wt % addition there would be sufficient for approximately 77 monomolecular layers if uniformly distributed over the surface.

However, as well as not completely covering the iron powder particles a large proportion of the lubricant is not even associated with the iron powder, but exists freely within the mix. Magnetic separation showed that as much as one third of the zinc stearate contained within a 1 wt % zinc stearate/iron powder mix was not associated with the iron powder.

Therefore cone mixing of iron powder and metal stearate in small quantities is ineffective in producing a uniformly distributed layer of lubricant over the particle surfaces. However it should be pointed out that in commercial practice quantities of the order of 5,000 - 10,000 Kg may be mixed where the mix shear stresses are greater. The effect of this upon mix effectiveness requires further investigation.

3. Effect of Lubricant Quantity Upon Mix Properties. Table 4 demonstrates the important effect of lubricant content upon the mix properties. The apparent density rises considerably following a 0.1 wt % addition of lubricant, but then remains constant or reduces with increasing lubricant additions. The results may best be analysed by considering the behaviour of the powder as it flows into the receptacle. The particles pack by sliding over each other and by reorientating themselves. The final packed density is therefore a delicate balance between the upward and downward forces and is related to particle characteristics such as size distribution, shape and surface properties, height of fall and receptacle characteristics. Addition of lubricant to the powder reduces the interparticle friction and the packing density is increased. Table 4 shows that this interparticle friction is reduced to a minimum after an addition of only 0.1 wt% lubricant, therefore suggesting at least monomolecular layer coverage of the particles, but not necessarily uniform coverage. As previously shown, 0.013% lubricant would be sufficient for a monomolecular layer. Increasing the lubricant content tends to either increase the film thickness or intersperse lubricant between the iron powder particles. Thus fewer particles occupy the same volume, decreasing the apparent density, as is observed. This would be shown more clearly if true density were used rather than apparent density which also includes the weight of the lubricant.

Tapping the receptacle provides additional energy for the particles to overcome the frictional forces and rearrange to produce a more closely packed condition. Therefore the tapped density is less dependent upon the surface condition of the powder than the apparent density. This is demonstrated in Table 4, which shows that the maximum tapped density is produced when there is no lubricant present within the iron powder. Again increasing the lubricant content reduces the tapped density for the same reason as above.

The ratio of tapped density D_t to apparent density D_a gives some indication of the friction conditions within the mass of powder as HAUSNER[89] suggests. Thus the value of D_t/D_a reduces from 1.46 to 1.22 and below as lubricant is added. This again shows that the interparticle friction is not reduced significantly for lubricant additions greater than 0.1 wt %.

4. Effect of Lubricant Type Upon Mix Properties. Examination of Table 5 shows that zinc stearate type affects the mix characteristics and using Table 2 suggests that zinc stearates of larger particle size give lower apparent densities and higher D_t/D_a ratios after mixing. Thus, either the surface friction conditions must be different or the lubricant is not being smeared over the particle surface, but is existing as discrete particles. This is in agreement with the previously observed results on mixing. If the lubricant were being smeared uniformly over the surface of the iron powder in both the cases the apparent density would be the same.

The tapped density values do not seem to be affected by the lubricant particle size which indicates similar packing in both cases. However if the lubricant particles were attached to the surface of the iron powder one might expect that the tapped density would decrease as the lubricant particle size increased. Attachment of a large lubricant particle to the iron particle surface would inhibit close packing more than uniform attachment of the same volume of small lubricant particles over the particle surface. This result therefore suggests that the lubricant is not attached to the iron powder, but exists as free particles.

Comparison of Tables 4 and 5 shows that cone mixing larger quantities of powder is more effective in increasing apparent density and reducing

the D_t/D_a ratio. Hence a better dispersal of lubricant over the particle surface is being obtained.

7.20 Laboratory Scale Compaction Studies.

1. Unlubricated Compaction Studies. The compaction behaviour of unlubricated iron powder was examined as well as that of lubricated iron powder. As Fig. 21 shows, the compressibility behaviour of unlubricated powder is greatly influenced by the height/diameter ratio of the compact. As this ratio increases an increased pressure is required to give the same compact density. This is due to the unproportionate increase in the effects of die wall friction as the height/diameter ratio increases and results in non uniform transmission of pressure through the particulate mass as demonstrated by DUWEZ and ZWELL[92]. UNCKEL[90] also showed that when compacting a quantity of powder half as large in the same die the pressure loss at the die wall drops to one third. Thus as the height/diameter ratio decreases the efficiency of pressure transmission between upper and lower punch increases and this is reflected in an improved compact density. Unckel related the applied and transmitted pressures, P_a and P_b, respectively for a cylindrical metal powder compact of height H and diameter D by the equation:

$$\frac{P_a}{P_b} = \exp. 4\mu\eta H/D \qquad \text{.....(28)}$$

where μ is the friction coefficient and η is the stress ratio i.e. the ratio between the radial stress σ_x and the axial stress σ_z. Thus it was thought that a plot of log applied pressure P_a versus H/D for compacts at constant true density may result in a straight line which could be extrapolated to zero H/D and hence give a pressure/density curve for the powder eliminating the effects of die wall friction. The results of this, determined from Fig. 21, are shown in Fig. 67. Although all the

points do not lie upon exactly straight lines, a straight line extrapolation to zero H/D ratio was carried out to give the pressure/density curve also shown on Fig. 67. This is compared with the pressure/density curve obtained for iron powder with 1 wt.% admixed zinc stearate (from Fig. 24). The curves appear to be rather contradictory in that a higher compaction pressure is required to produce a given compact density for the curve where H/D is zero i.e. where the die wall friction effects should have been eliminated.

However, as the height of the compact decreases the number of particles being pressed decreases. For instance with a final height of 1mm and an average particle diameter of 50 microns then there are only 20 particles stacked upon each other. Thus the probability of suitable particle rearrangement is reduced and the compact density drops. This type of effect has also been found by other workers[81], who showed that there was a weight of compact at which the maximum density occurred but it was not the smallest weight investigated.

2. Lubricated Compaction Studies. The effects of compact height/diameter ratio upon the pressure/density relationship are considerably reduced by the addition of 1 wt % zinc stearate as is clearly demonstrated in Fig. 24. However there is an optimum level of lubricant which should be added to give maximum densification at a given pressure level. Fig. 25 shows this fact. The initial rise in true density with lubricant content results from increased lubricant coverage of the iron powder surface aiding the motion of iron particles during compaction. As the lubricant level is further increased the density achieved at a particular compacting pressure reaches a maximum and then begins to fall, the rate of fall increasing with increased compacting pressure. Thus to achieve the best compaction properties it is necessary to provide adequate interparticle

and particle/die wall lubrication without causing density inhibition by addition of excess lubricant. The excess lubricant extrudes into the compact pores, filling them and therefore preventing further densification in that region. Similar effects have been shown by YARNTON and DAVIES[112], LJUNGBERG and ARBSTEDT[77] and others[65, 81].

Lubricant type also influences the density achieved at a given pressure level as shown in Table 6. There appears to be a relationship between the particle size of the zinc stearate used and the pressure required to produce a given true density. Zinc stearates of smaller particle size generally require less pressure to produce a given density than those of larger particle size. This may be related to the fact that it is easier for a large number of small particles to cover the iron powder surface than it is for a small number of large particles. This again suggests that the lubricant particles are not being broken down during the mixing process.

3. Analysis of Laboratory Compaction Studies. The compressibility behaviour of the lubricated and unlubricated mixes was analysed using Kawakita's relationship (Equation 22) and as Table 8 shows, the gradient of the lines (K) increased as the H/D ratio decreases. This again demonstrates the effect of die wall friction during the compaction process. Comparison of the gradients for an unlubricated compact of H/D ratio 0.037 with those of lubricated compacts in the range 0.165 - 0.675 shows almost identical values. This shows that 1 wt.%addition of lubricant considerably reduces the die wall friction effects during compaction.

BRACKPOOL[113] during his work using Kawakita's relationship found good agreement between the constant 'a' and reciprocal porosity values based upon the apparent density of the powder, being compacted. Table 8 does not always show this effect with respect to 'C' but this is probably due

to the limited number of results from which the plots were made. However in several cases the value of 'C' lay between the reciprocal porosity values based upon apparent and tapped density measurements. If the value of 'C' is related to the initial starting condition of the powder mass before any punch pressure is applied then it would be expected that its value lie inbetween the reciprocal porosity values based upon apparent and tapped density. The value of 'C' would then depend upon the degree of powder vibration prior to compaction.

7.30 Laboratory Scale Ejection Studies

1. General Considerations. Appraisal of a coefficient of sliding friction at a metal-compact/die-wall interface is dependent on an appreciation of the nature of that interface. It is not a continuous smooth surface, even approaching the 'smooth' surface of a highly polished metal. BOWDEN and TABOR[1], RABINOWICZ[29] and McCLINTOCK and ARGON[115] have shown that such 'smooth' surfaces are not truly planar but consist of a series of projecting peaks or asperities. Contact between two surfaces is made therefore at these asperities only. When a load P is applied to force these surfaces together, the asperities yield and work-harden to support the load. Thus, the interface is really a distribution of various sized metal/metal contact areas. The resultant total area of real contact is only a fraction of the geometrical area of the surface, and any coefficient of friction determined for such a system is dependent on the nature of such contacts and upon their area[115], since

$$F_1 = \sigma_{av} \cdot A_r$$

where F_1 = frictional force to shear metal/metal contacts

$\sigma_{av.}$ = average shear stress over the areas of contact

A_r = real area of contact

When a lubricant is introduced into this system, the valleys of the surfaces become filled with the lubricant, which, once the surfaces are sliding, can interpose itself between some metal/metal contacts. The resultant coefficient of friction is derived from a total frictional force that consists of the sum of the forces to slide the lubricant/metal interfaces, F_2, and the sum of the forces required to overcome the 'braking' action of the unlubricated surfaces, F_1, the coefficient of friction being the ratio

$$\frac{F_1 + F_2}{P} = \mu$$

When a thick film of lubricant is introduced between the two surfaces, part of the load becomes supported by the film. For the same load, P, the highest and sharpest asperities are more lightly loaded when lubricant is present, with consequently less plastic deformation of the asperities and a smaller contribution to the total frictional force from F_1. The film hardness is normally lower than that of the substrate and therefore the contribution from F_2 tends to be dependent on the film thickness. Increasing the load increases the fraction of the load supported by the substrate, so that for high loads appreciable film performation occurs giving increasing amounts of metal/metal contact; thus F_1 increases, resulting in an increase in μ

For compaction of metal powders with lubricants the system is further complicated by the porosity (or density) of the bulk material, which must affect the interface between such a powder-metal-lubricant compact and a die wall, particularly on ejection. Hence the sliding behaviour of such an interface system will be in some way dependent on the metal/metal contact area, lubricant film area, lubricant type (since this controls the nature and thickness of film), lubricant content of the compact (since this controls the extent of a lubricant film under given

conditions), and the density of the metal surface.

2. Unlubricated Ejection Behaviour. A 'stick-slip' type of motion as illustrated in Fig. 22 was observed during the ejection of unlubricated compacts. This behaviour is typical of systems which have high friction coefficients (μ = 1 to 1.5) and arises from the fact that the kinetic friction is less than the static friction, or when the friction decreases with increasing sliding velocity. The magnitude and frequency of the variations is dependent upon the sliding speed and the elastic behaviour of the tensometer. Therefore, the maximum ejection stress during the 'stick' phase was measured during the trials. This explains why velocity variation during the ejection of unlubricated compacts did not affect the maximum ejection stress values observed (see Fig. 23) since 'stick' stress values were being determined. H/D ratios however do seem to affect the ejection stress at given true compact density level. This can be explained in terms of density variations along the compact length. At small H/D ratios (less than 0.1) die wall friction effects have been shown to be reduced and hence large density variations along the compact length would not be expected. As the H/D ratio increases, die wall friction effects increase and therefore density variations occur along the compact length particularly during single ended compression. Therefore a compact having an overall density of 6.4 g/cm^3 may have densities of 6.1 and 6.7 at its ends if the H/D ratio is sufficient. Now since, from Fig. 23, the rate of change of ejection stress with true density increases with increasing true density any variation in compact end to end density will produce an ejection stress greater than that found for a compact having little or no end to end density variation.

3. Lubricated Ejection Behaviour. At low lubricant contents intermittent motion was still observed (Fig. 34(a)). i.e. there is insufficient lubricant at the die wall to give continuous sliding. However a higher lubricant

content (see Figs. 34 (b) and (c)) increases the lubricant film at the die wall, so that ejection becomes more continuous and occurs at progressively lower stress values as the lubricant content is raised. This effect is clearly shown in Fig. 27. The marked influence of a 1 wt.% addition of lubricant to iron powder upon the ejection stress is shown in Fig. 26. Here again under lubricated conditions compact aspect ratio (H/D) affects the value of ejection stress. Comparison of the slope of the curves for the unlubricated compacts with those for the compacts containing 1 wt.% zinc stearate (H/D of 0.640) suggests that above a true density of around 6.6 g/cm^3 the lubricant breaks down and the process reverts to the unlubricated condition. This effect is only noticeable at an H/D ratio of 0.640 which again most probably results from end to end density variations as the H/D ratio increases.

It was noticed that the compact surface finish deteriorated markedly at densities greater than 6.6 g/cm^3 (See Fig. 29) the surface then being typical of that found during unlubricated ejection. Thus, a marked transition exists in producing compacts containing 1 wt.% zinc stearate (H/D of 0.640) where lubrication fails and heavy wear of the compact surfaces occurs. This effect was used to evaluate the effectiveness of the lubricant being tested.

4. Effect of Lubricant Type Upon Ejection Behaviour. The marked change in ejection stress with density was observed for each of the zinc stearates tested, (See Fig. 28) and by plotting ejection stress versus compaction pressure a clearer indication of the transition point was found. This was done by extrapolation as previously described in Section 6.24. From Table 7 there appears to be a relationship between the lubricant particle size and the compaction pressure at transition. As the lubricant particle

size increases the transition pressure also tends to increase thus indicating that lubricants having larger particle sizes (up to 22.4 μm) are effective up to higher compaction pressures than those of smaller particle size. However, this effect tends to be nullified by the fact that in order to achieve a given true density for a mix containing 1 wt.% zinc stearate a greater pressure must be applied when the lubricant has a larger particle size (Table 6). This therefore explains why this effect was not noticeable from the plots of ejection stress versus density.

5. Analysis of Iron Powder Ejection Behaviour. Examination of Fig. 34 (a)(b) and (c) shows the transition observed between initial sliding followed by stick-slip motion to complete sliding throughout ejection at lower stress levels as the lubricant content is increased. This effect is shown for the actual values obtained in Fig. 35. As the break stress σ_B is reduced, the maximum slip stress values observed are also reduced. It is interesting to note that the initial break stress is not the maximum stress observed during ejection although as the lubricant content increases the two values approach each other. Immediately after the initial break stress point σ_B the ejection stress falls to the initial slip stress value σ_{si}, and this indicates the difference between the static and kinetic friction levels. From Fig. 35 it seems that the values of the initial slip stress σ_{si} do not vary markedly with lubricant content (in the range 0.3 - 2.0 wt.%) and therefore there is sufficient lubricant on the surface at 0.3 wt.% addition to initially give low slip stress values. However the rate at which the slip stress changes with sliding distance varies considerably with lubricant content (See Fig. 34).

Table 9 shows that the slip stress change per unit sliding distance generally increases as the compaction pressure increases for a given lubricant content and decreases as the lubricant content increases for a

given compaction pressure. These effects can be explained in terms of lubricant film thickness and wear behaviour. LANGMUIR[24] and other workers[25,2] have demonstrated that although a monomolecular layer of lubricant reduces the coefficient of friction to the same level as observed for multilayers, its wear resistance under conditions of repeated sliding is very much poorer. BOWDEN and TABOR[1] also show, under similar conditions, that a single molecular film of stearic acid is worn away very rapidly whilst a film of 53 molecular layers is scarcely worn away after 50 traversals of the same track. Therefore thicker films wear less rapidly. Now in increasing the lubricant content the thickness of lubricant layer at the compact/die wall interface would also be expected to increase, consequently increasing the life of the film under the given conditions. This is reflected in the reduction of maximum slip stress with increasing lubricant content whilst sliding over a fixed distance.

Lubricant films wear away as sliding takes place and the rate of wear increases as the load increases. It is therefore not surprising to find that the slip stress change per unit sliding distance generally increases with increased compaction pressure at a given lubricant content. However there does seem to be a notable exception to this at 1.0 wt.% lubricant addition. In the region of compaction pressure 462 - 564 N/m^2 there appears to be a transition zone where this rate at which the lubricant wears reduces with increasing compacting pressure. A possible explanation of this effect might be that lubricant already present on the surface of the iron powder provides lubrication at low pressures which breaks down more quickly as the compaction pressure is increased. Now at compaction pressures of 564 N/m^2 the true density of the compact produced is about 6.7 g/cm^3 (See Fig. 24). The porosity is about 14% and the lubricant occupies about 7.5% of the total volume. Therefore in regions of high density in the compact (7.25 g/cm^3) the lubricant will completely fill the

pores and for further densification in that region must extrude either to an adjacent pore or onto the die wall providing better lubrication during ejection and resulting in a decrease in slip stress change per unit sliding distance at higher pressures. This would also explain the form of the maximum ejection stress curve at 1 wt.% lubricant addition shown in Fig. 35. At low lubricant levels (0.3 wt.%) the quantity of lubricant on the compact surface was insufficient to allow continuous sliding of the compact through the die and 'stick-slip' motion occurred. The lubricant film had worn away and motion characteristics of unlubricated behaviour was observed. It was expected that the transition from 'slipping' to 'stick-slip' motion would occur at a constant stress level. However Fig. 35 shows that this transition increases with increasing compaction pressure and hence residual die wall pressure. This effect must be caused by the increase in shear strength of the lubricant as the pressure increases as shown by AKHMATOV[114] and resulting from the formation of a more condensed, stressed boundary layer structure.

Zinc stearate lubricant type does not appear to affect either break stress values σ_B or initial slip stress values σ_{si} (See Tables 10 and 11) However zinc stearate type does affect the maximum slip stress values observed. Lubricants of larger particle size generally give lower maximum slip stress values and therefore it must be concluded that such lubricants either provide a lubricant film having greater wear resistance or produce a thicker lubricant film which takes a longer time to wear away. In either case these lubricants provide better lubrication throughout the ejection period.

6. Effect of Die Surface Finish Upon Ejection Behaviour. As indicated in Fig. 31 the die surface finish improved during the testing programme which leads to changes in the measured values of ejection stress. This type of effect is not uncommon during the initial period of life of the

die. BOCKSTIEGEL and SVENSSON[83] show that the ejection force decreases during production of the first one or two thousand compacts and then it begins to increase again. This is due to 'conditioning' of the die in which the characteristics of the original ground and lapped surface are changed. Talysurf traces (See Fig. 32) show how the surface asperities change from an angular to a more rounded appearance as the die is used. This may be due to removal of die asperity tips or filling of the 'troughs' with material or a combination of both. The effect of the change in die surface finish upon the ejection stress was more pronounced at higher values of compact density and probably results from an increased contribution to the frictional force due to 'ploughing' out of the softer iron by the hardened die steel asperities.

7.40 Production Scale Compaction Studies.

1. Comparison of Production Scale and Laboratory Scale Compaction Studies. The compaction behaviour of mixes containing various amounts of zinc stearate, was studied on the production scale press in order to compare this with the laboratory scale studies. Such a comparison was necessary because of the difference in the time scales between the two processes; laboratory scale compaction taking about 10 secs whilst production scale compaction took between 1 and 2 secs. However Fig. 36 shows that the compacted true densities obtained by the two methods agree very closely. In all cases however the production scale densities are slightly lower than the laboratory scale densities which indicates the compaction velocity does affect the compressibility behaviour of the iron powder. This could be associated with the time required for either air to diffuse from the compact between the punch and die clearances or lubricant to extrude from pore to pore or pore to die wall. In the latter case it would be expected that the deviation between the two sets of results would be greater at higher lubricant contents. Fig. 36 does tend to show this effect at higher compaction pressures.

In Fig. 36 it can be seen that production scale values are not given for a mix containing 2.0 wt.% lubricant at compaction pressures of 400 and 500 MN/m^2. This was due to the fact that compacts produced under these conditions 'exploded' on ejection from the die, forming a series of laminar cracks around the compact. LONG[96] showed a similar effect during the compaction and ejection of talc. It was suggested by Long that this effect was due to the residual radial stress distribution occurring during ejection of the compacts. However, in the tests carried out during this research it was found that by holding the compact in the die for a few seconds after compaction and then ejecting at the same speed the compacts could be produced without fracture. This therefore suggests that there is some additional reason for this laminar fracture behaviour. If we consider a compact of apparent density 6.74 g/cm^3 containing 2 wt.% zinc stearate then the maximum solid density which can be achieved is 6.99 g/cm^3. Now LONG and ALDERTON[117] using powdered wax, tin and indium have shown that up to 83% of the gas initially present in the uncompacted powder may be trapped on compaction to about 90% theoretical density. Here compaction was up to 96% theoretical based upon 6.99 g/cm^3. If it is assumed that all the gas remains trapped during compaction, using Boyles Law it can be shown that the pressure of the air will rise to 17.5 ats. (about 1.8 KN/m^2). The measured green strength of this compact was 8.85 KN/m^2 and therefore the air pressure is unlikely to be the only cause for fracture. Since the compact fractured in a similar manner to that observed by Long a combination of residual radial stress effects and internal pressure due to entrappment of air is responsible for fracture of the compacts. At lower compaction pressures the residual radial stress is less and for a compact of density 5.80 g/cm^3 the air pressure falls to 0.38 KN/m^2. Under these conditions the compact is strong enough to be ejected without fracture. Permeability measurements carried out upon the compacts containing 2.0 wt.%. lubricant showed that the high density material (6.74 g/cm^3) was

two orders of magnitude less permeable than the low density material (5.80 g/cm^3), and therefore the air pressure would remain within the compact for a far greater length of time in the former case. Five seconds is sufficient time for the internal air pressure to reduce and allow ejection without fracture.

2. Effect of Lubricant Type on Compressibility Behaviour. As in the case of the laboratory studies, production scale compaction shows the effect of lubricant particle size upon the powder compressibility. The larger stearate particles of the same type showed poorer compressibility properties (See Table 13), in order to try and overcome some of the problems associated with lubricant dispersal, a mix was made by dissolving stearic acid in a volatile solvent and mixing this with the iron powder. Microscopic examination of the mix did not show any free particles of stearic acid and it was then assumed that the lubricant was dispersed uniformly over the iron powder surface. However no improvement in compressibility behaviour resulted and at lower densities it was slightly worse. (The results are not directly comparable since stearic acid is being compared with metal stearates).

Compaction of plain iron powder using stearic acid die wall lubrication was examined and as Table 13 shows, the compressibility is consistently worse at all densities than that obtained using admixed stearic acid although it is considerably better than that obtained without any lubricant (See Fig. 21, H/D 0.324). This must result from the reduction in ability of the particles to rearrange themselves under compression due to increased interparticle friction forces.

3. Analysis of Production Scale Compaction Studies. The dynamic compressibility of iron powder, zinc stearate and mixtures of the two was studied using Kawakita's and other derived relationships to establish more closely the effects of velocity upon compaction. Table 14 shows the results

of this analysis and comparison with Table 8 for the laboratory compressibility behaviour shows very good agreement in the values of the constant 'K'. The production scale tests produced compacts having an aspect ratio of 0.4 and for compacts without lubricant, 'K' was 0.0083, which lies in between the laboratory values found for aspect ratios of 0.324 and 0.675. Values for lubricated compacts show similar agreement. The values of 'C' for the iron powderand iron powder/lubricant mixes correspond closely to the tapped density values due to the vibrations which occur on the press prior to compaction (See Section 7.23). The relationship between reciprocal porosity and compaction pressure was not quite linear in the case of the iron powder containing 2.0 wt.% zinc stearate as reflected in the value of correlation coefficient obtained. This is due to excess lubricant within the pores inhibiting compaction at high pressure levels. This effect reduces the gradient of the line and results in an increased value of the constant 'C'. Zinc stearate 1 also obeys the derived relationship (equation 22) and demonstrates the general application of this relationship.

4. The Effect of Die Material upon Compressibility Behaviour. The only effects that die materials would be expected to exert upon the compressibility behaviour (assuming the same surface finish) result from die wall/particle/lubricant friction effects and die material modulus. It is shown later that high chromium die steel, and tungsten carbide exhibit similar friction behaviour while ejecting iron powder compacts and therefore similar effects would be expected during compaction. Increased die modulus, reduces the amount of die spring during compaction and subsequent 'springback' when the compacting pressure is removed. This effect would be expected to result in improved compact density at a given pressure.

Table 15 shows that high chromium die steel and glass ceramic die materials have similar compressibility behaviour but tungsten carbide is slightly worse. This is contrary to what was expected but a discrepancy of only 5% could have produced this effect.

5. Energy Involved During Compaction. Compaction energy determinations were made at a number of different density and lubricant levels. The results (See Fig. 38) show that at low densities lubricant content in the range 0.2 to 2.0 wt.% does not significantly alter the energy required for compaction. As the density increases the minimum energy used during compaction occurs at a lubricant content of 0.5 wt.%. At lower lubricant contents additional energy must be required to overcome increased inter-particle and die wall friction effects, whereas at higher lubricant contents exudation of lubricant into the pores inhibits further compaction and energy is expended in trying to compress incompressible material. This effect is particularly noticeable for high density compacts containing 2.0 wt.% lubricant.

STEIN et al[116] in their studies on high velocity compaction of metal powder showed that the compaction energy varied with ram velocity. For instance unlubricated electrolytic iron powder compacted to a density of 6.3 g/cm^3 required an energy of 40.6 J/g with a ram velocity of 5.18m/sec and only 15.2 J/g with a ram velocity of 76.20m/sec. The results from this research show values of 15J/g for lubricated iron powder compacted at about 0.030m/sec. (The top punch velocity varies during compaction according to the main cam profile).

7.50 Production Scale Ejection Studies.

1. Comparison of Production Scale and Laboratory Scale Ejection Studies. The number of different stress levels experienced during laboratory scale ejection studies makes the comparison with production-press ejection

results difficult, since there is no indication from Fig. 34(d) what the mode of ejection is. Assessment of the results obtained using each σ value showed that σ_{smax} had the greatest correlation with the production-press trials and it is this value that was used for comparison.

To further characterise the metal powder-zinc stearate system, the ejection stresses in the two methods were compared for the same zinc stearate (code number I). Fig. 39 illustrates the variation in σ_{smax} values for both methods with zinc stearate content. This demonstrates the similarity of these stress values in the two cases. The general shape of the family of curves follows the same form as shown by the ejection forces vs. stearic acid content for metal powders given by SAJDAK et al[78] ejection forces vs. zinc stearate content for sponge iron powders quoted by LJUNGBERG and ARBSTEDT[77] stripping forces vs. stearate content of metal powders discussed by GEIJER and JAMISON[82] and the ejection pressures measured by YARNTON and DAVIES[112] for metal powders with various levels of stearic acid.

The ejection stresses for a given density of compact must depend on the thickness and coherency of the lubricant film. Since these stresses are measured during ejection, i.e. in a kinetic system, the film can be imagined to change and probably rupture during the reaction between compact and die wall in the ejection process. At low lubricant levels the film is not covering the whole of the compact/die wall interface since the σ_{smax} values are high by both methods, as Fig. 39 shows. Examination of the surfaces of ejected compacts for 0.5 wt.% zinc stearate (see Fig. 43 (a)) shows a discontinuous lubricant film, i.e. a high number of metal/metal contact areas. This is borne out by Fig. 34 where the 'stick-slip' ejection behaviour, as measured for the compact of low lubricant content, is illustrated. The lubricant film area (and possibly its thickness) increases with increasing lubricant addition, since the ejection stresses

decrease towards a minimum value, as do the areas of metal/metal contact at the compact/die wall interface. The compact surfaces after ejection show this increasing coherency and degree of covering with the lubricant content, as examination of Figs. 43 (b)-(d) illustrates.

The differences in the curves for the laboratory and production-scale studies could be attributed to the different speeds of ejection. RABINOWICZ[29] quotes values of friction forces for various levels of lubrication vs. lower friction forces; this would account for the lower σ_{smax} values in the production-scale trials compares with the laboratory-scale experiments at zinc stearate contents below 1.0 wt %. For greater lubricant contents in this system, it is assumed that maximum lubrication is occurring above 2.0 wt.% zinc stearate.

The density-dependance of the curves in Fig. 39 can be explained by the greater compacting pressures or increased radial stresses needed to achieve higher densities. These cause perforation of the lubricant film when it has a limited thickness (i.e. at low lubricant contents), so increasing metal/metal contact which in turn raises the frictional resistance in proportion to the density level. This effect diminishes with increasing lubricant content. A similar effect is quoted by SCHEY[115] who shows how μ values for wire drawing with various lubricants increase with die pressure for a range of lubricants.

At high compact densities (6.8 g/cm^3) and low lubricant contents (0.5 wt.%) breakdown of the lubricant film occurred and tool seizure resulted. This was caused by 'cladding' of material from the compacts onto the die wall in the region of the clearance between punch and die (See Fig. 40). The compact surfaces also show the effects of lubricant breakdown (See Fig. 44).

2. Effect of Lubricant Type and Die Material upon Ejection Behaviour.

The ejection stress values were determined for a number of different stearate lubricants and as Fig. 41 shows they all behave in a similar manner and none of these lubricants appears to be particularly outstanding. Zinc stearate 8 appears slightly better than zinc stearate 1 as was found in the laboratory scale studies. Die wall lubrication seems to be just as effective as admixed lubrication as YARNTON and DAVIES[112] and LEOPOLD and NELSON[81] have also previously demonstrated. An approximate slope value was determined from the ejection stress/compaction stress curves (lubricant content 0.5 wt.%) which was found to be 0.03. This value is reduced to .012 when the lubricant content is increased to 1.0 wt.%. This value compares well with the values found during laboratory scale ejection studies (see Table 7). Die material seems to have little effect upon the ejection stress/compaction pressure relationship (see Fig. 42 and Table 16) and slope measurements appear very similar. Therefore, with a lubricant content of 1.0 wt.% the film produced must be sufficiently coherent to eliminate the effects of differences in the friction coefficients between iron powder particles and the three different die materials involved (See section 6.8.1). GEIJER and JAMISON[82] using steel and carbide dies to compact iron powder containing 1 wt.% zinc stearate found that the ejection pressures were similar although the carbide die tended to give lower values.

7.60 Compact Properties.

Examination of fracture surfaces did not reveal the distribution of lubricant following compaction (occasional free zinc stearate particles being seen; see Fig. 45) but green strength measurement gave an indication of the effectiveness of the lubricant in preventing interparticle adhesion. At low density (5.8 g/cm^3) increasing the lubricant content slightly reduced the green strength whereas this effect was much more marked at

higher density (6.6 g/cm^3). The green strength is a measure of the strength of cohesion between particles. If this strength resulted from simply cold welding of the powder particles then the influence of contaminant lubricant films would be to reduce the green strength considerably (Ref. influence of contaminant films on friction and welding: BOWDEN and TABOR[1]). The green strength is reduced on addition of a small quantity of lubricant (see Table 4) despite the fact that the density is increased as a result of lubricant addition but does not drop to zero on addition of excess lubricant. Thus mechanical interlocking must also be responsible for the bonding between adjacent particles. This occurs when the applied pressure forces metal of one particle into the pores of another.

It was thought that increased lubricant would reduce both interparticle and die wall friction, the latter effect being mainly responsible for producing density variations along the height of the compact. Figure 46 shows that increased lubricant content has virtually eliminated the outside end to end density variation however there is still a variation in compact outside to inside density. One of the samples examined using the Q.T.M. also shows this effect (See Fig. 47(a)) but two other samples examined (See Fig. 47 (b) and (C)) show the opposite effect, ie. dense core with a porous outside. This however is thought to be incorrect and due to polishing technique as already suggested (Section 6.3.6).

Following ejection, the compacts increase in size above the dimensions of the die. This results from the elastic stresses developed during compaction (See Section 6.40). This growth is dependent upon the characteristics of the powder being compacted, pressure, lubricant type and content and upon the elastic properties of the die. For a given powder, lubricant content and die, it was found that increasing the compacting pressure and hence the compact density increases the amount of

spring (See Fig. 49). Increasing the lubricant content also increases the amount of spring. HAUSNER and SHEINHARTZ[65] show similar effects during the compaction of electrolytic copper powder although YARNTON and DAVIES[112] find a minimum point in their spring versus compaction pressure relationship again using similar materials.

As the lubricant content is increased the powder mass begins to behave more as a fluid under compression. A greater amount of pressure is transmitted to the die (See Figs. 52 and 53) and therefore the elastic expansion of the die is greater. Thus the amount of spring measured on the ejected compact is greater also, provided that plastic deformation of the compact does not occur following removal of the compacting pressure. Modulus of the die material and its dimensions will also determine the amount of spring observed. The modulus of green compacts was measured and as shown in Fig. 51 it was found to vary with stress. As the stress applied to the compact increased so the modulus increased for compacts both with and without lubricant additions. In the case of unlubricated material compression of the compact may cause the formation of new junctions and the growth of existing ones[6]. Hence a larger area supporting the load and an increase in the modulus. However in the presence of a lubricant TABOR[35] considers that junction growth is prevented under the action of a combined tangential and normal stress and hence this mechanism cannot explain the observed behaviour where lubricant is present. AKHMATOV[114] however shows that the shear strength of organic substances increases exponentially with pressure and hence applying an increasing external pressure to a compact would have the effect of increasing the pressure between individual particles, increasing the lubricant shear strength and hence making deformation more difficult.

During the determinations of modulus at low stress it was noticed that the compacts containing zinc stearate behaved in a viscoelastic manner

during stress cycling[108]. This must result from the compression characteristics of the zinc stearate molecules since this effect was not observed when there was no lubricant present.

Poisson's ratio values were determined at different density and lubricant levels using the H.C.D. die and the tungsten carbide die. The values found lie in the range 0.23 to 0.38 as shown in Figs. 57 and 58. For solid steel a value of 0.30 is usually used but for sintered iron ARTUSIO et al[118] find values between 0.20 and 0.28 at porosities of 10 and 24%. Lubricant content as well as porosity affects Poisson's ratio and in general the higher the lubricant content the greater the value of the ratio.

Since Poisson's ratio is a material property it would be expected that its value would be independent of other factors such as die material. Examination of Figs. 58 and 59 reveals good agreement between the values obtained using the H.C.D. die and the tungsten carbide die, although there is a discrepancy at high lubricant and high density levels.

The method of Poisson's ratio determination (See Section 6.70) does not give absolute values because the theory assumes the die to be perfectly rigid. The die however does expand elastically and thus the value of ϵ_x is not zero. In fact from TIMOSHENKO[107] the strain within a die of infinite outside diameter subjected to an internal stress of σ_x is:-

$$e_x = \frac{\sigma_x}{Es} (1 + \nu_s) \qquad \text{.....(29)}$$

where E_s and ν_s are the modulus of elasticity and Poisson's ratio of the die material. Substituting equation (29) into equation (24) we obtain:-

$$\frac{\sigma_x}{E_s} (1 + \nu_s) = \frac{1}{E}\left[\sigma_x - \nu(\sigma_y + \sigma_z)\right] \qquad \text{.....(30)}$$

Rearranging gives:-

$$\frac{\sigma_x}{\sigma_x + \sigma_y}\left[1-(1+\nu_s)\left(\frac{E}{E_s}\right)\right] = \nu \quad \ldots\ldots\ldots\ldots\ldots\ldots (31)$$

Thus a correction factor of $\left[1-(1+\nu_s)\frac{E}{E_s}\right]$ must be applied to give the true Poisson's ratio values. Some corrected values are given in Table 17 along with the original values from which it is apparent that the Poisson's ratio values are reduced by between 5 and 15% by application of the corrections (The Poisson's ratio values given in Figs. 58 and 57 have not been corrected since the factor used depends upon the compact modulus which varies with stress).

The die radial stresses which occur during compaction are related to the compacting pressure (See Figs. 52 and 53) but do not follow it in an identical manner. This is due to the fact that the powder mass is not behaving as a liquid under pressure. Comparison of the ratio of radial stress to compaction stress with values determined by BOCKSTIEGEL and SVENSSON[79] for iron powders containing similar amounts of lubricant shows reasonably good agreement.

7.70 Friction Coefficients During Compact Ejection.

1. Comparison of Calculated and Determined Friction Coefficients for Production and Laboratory Scale Runs. The friction coefficients derived from direct radial stress measurement and by calculation show fairly good agreement in view of the assumptions made and the values used for the calculations (See Table 18). The friction values tend to increase with increased compacting pressure and reduce with increased lubricant content. This also generally follows from the results found during the laboratory scale tests (Table 19) and the friction values found there agree reasonably well with the values found during the production scale runs.

The calculated residual radial stress values found during laboratory scale compaction were greater than those either calculated or measured during the production scale runs, and therefore although the actual ejection stress values were different (See Fig. 39) the friction coefficients were similar. The difference between the radial stress values may be due to difference between the relative dimensions of the dies used. The very thick walled production scale die would be strained far less under the action of an internal pressure than the comparatively thin walled laboratory scale die. Therefore the compact would be strained by a smaller amount as a result of the die wanting to return to its original dimensions and the residual radial stress would also be correspondingly less.

2. Coefficients of Sliding Friction and Lubricant Content. Tables 18 and 19 and Fig. 54 illustrate the density dependence of the friction coefficients which must result from lubricant breakdown at higher pressures producing a high number of metal/metal contact areas. At lubricant levels of 2.0 wt.% the coefficient of friction drops as the lubricant film becomes more coherent (See Fig. 43) but even so the friction coefficient increases with increasing density and hence compacting pressure. This indicates that there are still areas present where metal/metal contacts are occurring although it has been shown that where friction coefficients of less than 0.1 occur the amounts of metal/metal contact and consequent surface damage are minimal when using a stearate lubricant. The dependence of these friction coefficients upon density must be due to the same causes as discussed in section 7.5.1.

3. Coefficients of Sliding Friction and Correlation with Other Values. BOWDEN and TABOR[1] present values and show that totally clean and pure metal surfaces will sieze in contact with each other in a vacuum. If gases or water vapour are admitted, coefficients of friction as high as 3.00

for platinum/platinum surfaces and 0.80 for molybdenum/molybdenum surfaces can be obtained. They quote a value of 0.80 for unlubricated steel on steel static friction, which falls to 0.10 for these surfaces lubricated with stearic acid. In general, kinetic friction is lower than static friction and they suggest that the kinetic coefficient of friction for the above system will fall to 0.07 or less, if the sliding speed is not too high. In comparison, lubricated tungsten carbide on steel can have values of sliding friction coefficients of 0.10 - 0.20 depending on the type of system.

Unlubricated surfaces of like metals are quoted by RABINOWICZ[27] as having coefficients of friction ranging from 0.07 for steels to 1.70 for indium at speeds of 1 cm/s. Hexagonal crystal lattice metals such as magnesium, titanium, zinc &c, appear to give lower but very close values of 0.06.

McCLINTOCK and ARGON[115] cite values of 0.05 - 0.10 for steel sliding on steel when lubricated fully with mineral oils or fatty acids.

The results quoted by BOCKSTIEGEL and SVENSSON[79] are more relevant to the present work since they give coefficients of sliding friction for iron powder/high speed steel systems with a number of lubricants-in particular, zinc stearate and stearic acid. However, for the ejection of sponge-iron powders compacted with 0.5 wt.% zinc stearate they quote coefficient of friction values ranging between 0.17 and 0.40 with a similar range for 0.5 wt.% stearic acid, for decreasing relative densities of compacts. Furthermore, even with an addition of 3.0 wt.% zinc stearate, over the same relative density range of 70-85%, they found coefficients of friction decreasing from 0.40 to 0.12, respectively. From values quoted by other workers, [29,115] these would appear high for such lubricated systems.

In the present research for 2.0 wt.% zinc stearate, coefficients of friction of between 0.03 and 0.14 were obtained.

Friction coefficients were determined for unlubricated compacts and values in the range 1.01 to 1.26 were found. This was however the static coefficient of friction rather than a dynamic value. Pin and disc measurements between H.C.D. and unlubricated iron powder compacts gave values in the range 0.35 - 0.50. Hence the coefficient of friction falls progressively with increasing zinc stearate content to the levels given above. Also, this fall was related to the true density of the compacts in a reverse manner to that found by BOCKSTIEGEL and SVENSSON[79] the lower density compacts giving a lower μ value; this is consistent with the suggested presence of a thicker, more coherent lubricant film that is disrupted and perforated at high densities owing to the greater stresses needed to compact the metal powder. HAUSNER and SHEINHART[65] give coefficients of friction for stainless-steel powders sliding on steel surfaces under low pressure in an unlubricated condition that vary between 0.62 and 0.37, depending on the size of the compact.

4. Effect of Lubricant Type upon Friction Coefficients for Laboratory Scale Tests. Comparison of Tables 20 and 21 shows that the friction coefficients based upon the initial break stress values are greater than those using the initial slip stress values. Hence the static friction coefficient is greater than the dynamic friction coefficient in this system. However comparison between Tables 20 and 22 shows that during ejection the friction coefficients approach and even exceed the static friction values. This effect results from the change in ratio between lubricated and unlubricated areas as ejection proceeds. Where ejection stresses and consequently friction coefficients are at their highest values (See Fig.29) the surface characteristics of the compacts show severe scoring indicating considerable amounts of metal/metal contact and consequent wear.

It was thought that the friction coefficients may be related to particle size particularly since from section 7.3.5 the zinc stearate type was shown to affect the maximum slip stress values. Comparison of Tables 20 and 21 to the particle size of the lubricants involved did not show any significant trend. However when using Table 21 a relationship did appear to exist and is shown in Fig. 68. The σ_{smax} values are shown to be related to the median particle size of the lubricant such that for a given lubricant content and true density level the larger the median particle size the lower is the maximum coefficient of sliding friction observed during ejection. This effect isfollowed for varying densities but a rise in the density level increases the coefficient of friction values presumably for the same reasons as discussed above; the higher pressures needed to produce the higher densities cause some breakdown of the lubricant film area and an increase in the metal/metal contact area.

It was previously shown (Section 7.12) that the lubricant does not spread uniformly over the surface of the iron powder but particles tend to adhere individually to the iron particles (See Fig. 20). Thus the larger zinc stearate particles seem to produce a more coherent lubricant film with better wear resistance which is more efficient in reducing the sliding friction under a given set of conditions.

5. Effect of Lubricant Type and Die Material upon Friction Coefficients for Production Scale Tests. The effects of lubricant particle size are again shown in the production scale runs between zinc stearates 1 and 8, (see Table 23) the difference showing more clearly at higher density levels. All the other metal stearate lubricants tested show fairly similar friction coefficients to zinc stearate 8. Stearic acid, admixed using a volatile solvent to give better lubricant coverage, did not give any significant improvement in friction behaviour. However by using only stearic acid die

wall lubrication (no admixed lubricant) the friction coefficient was reduced to 0.11 at all density levels. Measurement of ejection stress alone would not have revealed this since at comparative densities the ejection stresses are similar. However in the case of the die wall lubrication the residual radial stress values are greater, presumably due to the higher compacting pressures necessary to produce equivalent densities (see Table 13). The friction coefficients may be lower in this last case because during ejection of compacts containing admixed lubricant, the lubricant film is being continuously worn away and the maximum friction coefficient observed depends upon the wear resistance of the film originally present on the compact surface. However with die wall lubrication the lubricant is being continuously replaced during ejection and consequently lower friction coefficients result.

Comparison of friction coefficients observed using the high chromium die steel and the tungsten carbide dies show similar values although the tungsten carbide tends to give lower values at lower lubricant contents. This is not surprising since if it is assumed that the proportion of metal/die wall contacts is similar for the same compact density and lubricant content, then the friction coefficient will be determined by the unlubricated sliding behaviour between the die material and iron powder. Now it has been shown that the friction coefficient for an iron powder compact sliding against tungsten carbide is lower than when it slides against high chromium die steel (seeSection 6.8.6) and therefore it would be expected that ~~the~~ for a similar proportion of metal/die wall contacts the overall friction coefficient would be lower using the tungsten carbide die.

7.80 Pin and Disc Tests.

1. Effect of Load and Lubricant Upon Friction Coefficient and Contact Resistance. It was found in all cases that increasing the pin load reduced

the coefficient of friction. Loads of up to 40 Kg were used upon the pin but even this did not result in an increase in the measured friction coefficient (see Table 25). Contact resistance measurements were also taken and instantaneous values were examined using an oscilloscope (see Fig. 15). It was found that the instantaneous resistance was either infinite or extremely small and oscillated rapidly between these extremes. The low value was found to be approximately equal to the resistance between the pin and disc whilst the disc was static. This behaviour then must be due to the intermittent breakdown of the lubricant film resulting in metal/metal contact between the sliding surfaces. Fig. 59 shows that there appeared to be a relationship between the coefficient of friction and the contact resistance. These are the average contact resistance values determined by damping the rapid oscillations with a condenser and using a recorder to measure the output voltage (see Fig. 15). This behaviour is again explained in terms of lubricant film perforation i.e. at lower contact resistance values there is more metal/metal contact and shearing, thus the frictional force increases. Lubricant pad pressure affected the results, increasing the pressure increased the amount of lubricant transferred to the disc and consequently increased the contact resistance. (A pad load of 500g was used on the 14.7 mm.dia. lubricant pads). With pin loads of 25Kg it was found that the lubricants tested were capable of giving high contact resistance values, hence reducing metal/metal contact to very low levels. In some cases it was noticed that lubricant film breakdown did occur i.e. zero contact resistance, which was then repaired with resulting increase in resistance value.

The variation in friction coefficient with load for materials lubricated by thin films, has been observed by a number of workers [1,32,33]. This effect is thought to be due to the changing proportions of load supported by the lubricant and metal as the film thickness changes. This has been described by Lancaster[119] who

suggests that the friction is lowest when the film is very thin and all the load is supported by the surface asperities. The current investigation shows friction coefficients of 0.07 with a pin load of 40 Kg. A pin was made from zinc stearate rather than iron powder and an H.C.D. disc also lubricated with zinc stearate was slid over it. A friction coefficient of 0.9 was found thus demonstrating the effect of a thick film upon friction behaviour.

A number of different lubricants were examined using short 10 minute tests to provide friction and contact resistance data for comparison with similarly lubricated compact ejection behaviour. Comparison of Tables 25 and 26 with Table 23 shows that the friction coefficients observed during compaction with 0.5 wt.% admixed lubricant are much greater than those observed when a coherent lubricant film exists i.e. where the contact resistance is appreciable. Contact resistance measurements between the compact and die during laboratory scale ejection gave zero values even for compacts containing 2.0 wt.% lubricant. Hence even with a high quantity of lubricant metal/metal contacts are not completely eliminated and therefore during ejection of compacts at lubricant levels of 2.0 wt.% or less a mixed system of lubricated and unlubricated areas exists.

BOYD and ROBERTSON[120] have shown that at the yield strength of iron (150 MN/M^2) the shear strength of stearic acid was 7.5 MN/m^2 and this predicts a friction coefficient of 0.05 (see equation 6). Table 26 shows that for stearic acid this value is being approached as the pin load is increased. However using admixed stearic acid the friction coefficient is 0.15 - 0.16 and therefore shearing of metal junctions as well as lubricant is occurring. If we assume a pin load of 100N and the friction coefficient is 0.05 then the shear force is 5N. Therefore, for a lubricant of shear strength 7.5 N/mm^2, the load bearing contact area is 0.67 mm^2. Where the friction coefficient rises to 0.15 for a mixed

system, equation 7 may be used to determine the amount of metal contact. This gives a value of about 5% metallic contact for conditions outlined above.

2. Effect of Velocity and Temperature upon Friction Coefficient. The effects of velocity and temperature changes were examined in order to establish the effects that compact production speed and die temperature changes would have upon production ejection behaviour. Table 27 indicates that disc velocity did not have a very great effect upon the friction coefficient within the range tested. One effect of increasing press speed is to increase the energy expenditure per unit time. Energy is converted into heat during compaction and ejection, and consequently a rise in die temperature occurs when running for a long period of time. The effect of temperature variations was therefore examined on the pin and disc machine. The results (see Fig. 60) show a marked decrease in friction coefficient with temperature increase. Similar effects have been found for other solid lubricants and this effect can be explained almost entirely in terms of the shear strength-temperature relationship of the lubricant.

Fig. 60 appears to indicate low friction values at temperatures above the melting point of the lubricant (393°K). This is inconsistent with the observations of other workers[1] who show a marked increase in friction coefficient above the lubricant melting temperature. This must result from cooling due to the disc and the actual interface temperature must lie inbetween the pin and disc temperatures.

3. Friction Measurements on Ejected Compacts. Friction values on the die contact surfaces of ejected compacts compare very well with the values determined during ejection from punch and die stress data (see Tables 28 and 18). These measurements provide further support for the friction measurements obtained during production scale ejection. Immediately after initial sliding, the friction coefficient increased as wear of the

lubricant film occurred. The maximum value found was 0.30. Examination of the compact surfaces after test showed heavy wear scars similar to the surfaces of compacts ejected without lubricant.

4. Unlubricated Wear Behaviour. A number of different parameters were examined to assess their effects upon the wear behaviour and these are discussed below. The volume of material removed per unit sliding distance was determined and the values of K in equation 9 determined; K being a constant related to the probability per unit encounter that a wear particle will be produced. Load and Velocity Table 29 summarises the results taken from Figs. 62 and 63. When sliding begins, the wear rate was found to change with time, but after an initial running in period, the wear rate became constant. It has been shown that this occurs when an equilibrium condition occurs at the surface layers. This type of behaviour was observed when using different loads, speeds and materials. The wear rate therefore is independent of the apparent contact area, since this alters during wear, once equilibrium conditions have been obtained. In the load range 100-2000gms a linear relationship between wear rate and load was observed. Similar relationships have been observed by ARCHARD and HIRST[38] although simple relationships do not always occur, particularly where there is a transition from mild to severe wear conditions. The value of K for an iron powder compact sliding against tool steel (H.C.D.) lay in the range $5.2 - 5.9 \times 10^{-5}$.

Changes in surface velocity between 19 and 156 cm/sec did not alter the wear rates observed, therefore it is the number of encounters between asperities which determines the amount of wear in this particular case.

Disc Material. Fig. 65 and Table 30 show the effects of disc material upon wear behaviour. In the case of the H.C.D. and glass ceramic discs, detritus build up occurred upon their surfaces. Therefore the wear rate values do not truly represent the wear rates between the two materials but

the wear rate between a mixed disc-deritus system rubbing against an iron powder compact. This did not occur in the case of the tungsten carbide disc (see Fig. 65) and the wear rate observed in this case ($K = 1.3 \times 10^{-5}$) was less than for either H.C.D. or glass ceramic ($K = 5.4$ and 3.2×10^{-5}) respectively. This is not surprising since the wear rate usually decreases with increasing hardness and elastic modulus, tungsten carbide exhibiting both these properties.

Lubricant. Table 30 shows the ~~diameter~~ dramatic manner in which lubricant reduces the wear rate, the probability of wear particle production for encounter is reduced by more than 50 times when using zinc stearate 8. The wear rates under lubricated conditions were more difficult to measure due to the very small volumes of material removed. However using these values it is possible to try and estimate possible die lives. It would be expected that maximum wear would occur at the point of highest stress during compaction; ejection stresses are much lower but must also contribute to wear.

Now, say we are producing compacts of density ρ_c, diameter D and length L. The maximum radial stress during compaction is σ_{Rmax} and this occurs during the final part of compaction while the top punch travels a small distance x. Therefore the load on that region of the die will be $2\pi Dx\,\sigma_R$ and the sliding distance will be x. Thus using equation 9 the worn volume of iron W will be

$$W = \frac{K \times 2\pi Dx \sigma_{R\,max}}{P_M} \quad \ldots\ldots\ldots\ldots\ldots\ldots\ldots (32)$$

Now the worn volume W will be the sliding area ($2\pi Dx$) multiplied by the thickness of the worn layer (y). Therefore substituting in the above equation gives:-

$$2\pi Dxy = \frac{K \times 2\pi Dx \sigma_{R\,max}}{P_M} \quad \ldots\ldots\ldots\ldots\ldots\ldots\ldots (33)$$

$$y_{\text{Compaction}} = \frac{Kx\,\sigma_{R\,max}}{P_M} \qquad \ldots\ldots\ldots\ldots\ldots\ldots (34)$$

Wear also occurs during ejection, but in this case the stress acting upon the die is σ_R. The compact travels its whole length over the region nearest the top punch and therefore the thickness of the worn layer due to ejection will be:-

$$y_{ejection} = \frac{K\ L\ \sigma_R}{P_M} \qquad \ldots\ldots\ldots\ldots\ldots\ldots (35)$$

The total thickness of worn layer due to both compaction and ejection is:-

$$y_{total} = \frac{Kx\,\sigma_{Rmax}}{P_M} + \frac{KL\,\sigma_R}{P_M} \qquad \ldots\ldots\ldots(36)$$

This equation gives the amount of wear expected on the compact. Now it has been suggested that the relative amounts of wear occurring between two sliding materials are inversely proportional to their hardnesses (This is a very general statement since wear is also dependent upon a number of variable factors such as elasticity, plasticity, oxidation etc). However, let us assume that the relationship applies in this case and thus the thickness of the die worn layer will be:-

$$y_{die} = \frac{HV_{compact}}{HV_{die}} \left[\frac{Kx\,\sigma_{Rmax}}{P_M} + \frac{K\,L\,\sigma_R}{P_M} \right] \ldots.(37)$$

Now using the following values for a lubricant compact (6.6 g/cm^3) of length 10mm

HV compact	160
HV_{die}	850
K	0.096×10^{-5} (see Table 30)
σ_{Rmax}	300 N/mm^2
σ_R	50 N/mm^2
x	1 mm
L	10 mm
P_M	1570 N/mm^2

$$y_{die} = \frac{160}{850} \times \frac{0.096 \times 10^{-5}}{1570} \left[300 + 10.50 \right]$$

$$y_{die} = 3.57 \times 10^{-9} \text{cm}$$

Change in diameter = $2y_{die} = 7.14 \times 10^{-9}$cm.

Thus the number of compacts which can be pressed before the die diameter increases by 5×10^{-4} cm will be 70,000. This is in reasonable agreement with the wear rates determined by BOCKSTIEGEL and SVENSSON.[83] Using a chromium carbide steel of hardness 874 VPN to produce compacts of density 6.75g/cm^3 containing 0.5% zinc stearate they were able to produce 40,000 compacts for a die wear of 5×10^{-4}cm.

8.00 CONCLUSIONS AND SUGGESTIONS FOR FUTURE WORK

8.10 Mixing and Lubricants

8.20 Compaction, Height/Diameter Ratio and Densification

8.30 Compaction and Theoretical Considerations

8.40 Ejection and Ejection Stresses

8.50 Tool Materials, Tool Wear and Theoretical Predictions

8.60 Green Compacts

8.70 Friction Coefficients

8.80 Suggestions for future work

8.00 CONCLUSIONS AND SUGGESTIONS FOR FUTURE WORK

These are listed under the following headings:

8.10 Mixing and Lubricants

1. Laboratory scale mixing does not produce a uniform coverage of zinc stearate over the surface of the iron powder. The lubricant tends to attach itself as individual particles to the iron powder surfaces and the surface characteristics of these affect the amount of lubricant adhering to these surfaces. It is considered that this situation is not greatly improved with large weight mixes as used on an industrial scale.

2. A large proportion of the zinc stearate added to the iron powder exists freely within the mix. For example, as much as one third of the zinc stearate contained within a 1wt% zinc stearate/iron powder mix was not associated with iron powder.

3. Lubricant additions reduce the interparticle friction as measured by the ratio Tapped Density/Apparent Density, but additions greater than 0.1 wt% do not reduce this ratio further. It can be calculated that less than 0.1 wt% lubricant is required for complete coverage of the iron powder surfaces, however this does not happen in mixing.

4. Lubricant particle size affects the loose packing behaviour of iron powder. The loose packing behaviour is also influenced by the quantity of iron powder blended.

8.20 Compaction, Height/Diameter Ratio and Densification

1. Compact Height/Diameter ratio affects the density achieved during the compaction of unlubricated iron powder. The maximum

density achieved for compacts of Height/Diameter ratio approaching zero was less than that for compacts containing lubricant (H/D between 0.175 and 0.640). This was thought to be due to the increased difficulty for particle re-arrangement within very thin unlubricated sections.

2. There is an optimum level of lubricant required to give maximum densification at a given pressure level. Lubricants having smaller particle sizes generally require lower pressures to produce a given compact density than lubricants of larger particle size.

3. Good agreement was found between slow laboratory scale and rapid production scale compression studies. Increasing the compaction velocity tended to reduce the compressibility slightly.

4. Rapid compaction and ejection of compacts containing 2wt% lubricant or above, resulted in laminar fracture of the compacts upon ejection. This was due to a combination of residual radial stress and internal air pressure in the compacts.

5. Production scale compaction studies showed that larger stearate particles exhibit poorer compressibility properties than smaller stearate particles of the same type when mixed with iron powder. Die wall lubrication with stearic acid resulted in poorer compaction behaviour of iron powder than when compacting iron powders with admixed lubricant.

8.30 Compaction and Theoretical Considerations

1. The compaction of iron powders with lubricant can be predicted from the adapted theoretical equations deduced by KAWAKITA.

Laboratory scale studies could be followed using these relationships.

2. KAWAKITA's relationship was also found to be applicable to the dynamic compaction of iron powder and iron powder/lubricant mixes, as carried out on an industrial scale using a production type press. The constant 'C' in the relationship appears to be related to the density of the powder immediately before compaction.

3. Using the instrumented press it was possible to determine the energy consumed during dynamic powder compaction. In the range of 0.2 to 2.0 wt% lubricant content, the energy requirement was not affected at low density compaction but showed variations at high density compaction, probably due to variations in lubricant film distribution.

4. Thick cylinder stress theory has been used to determine the residual radial stress occurring between the compact and die wall immediately after compaction. The determinations used compact elastic properties evaluated during this work.

5. Residual radial stress values have been experimentally determined using the instrumented press and compared with the values obtained by calculation. Reasonable agreement was obtained between the two, considering assumptions made in the calculations.

6. Residual radial stress values, calculated and experimentally determined, have been used with ejection stress values to determine friction coefficients during compact ejection. These friction coefficients showed reasonable agreement when calculated from laboratory scale and production scale runs, and agreed with the values determined on the "pin and disc" apparatus.

8.40 Ejection and Ejection Stresses

1. Ejection stresses were inversely proportional to the quality of diesurface finish.

2. Unlubricated compact ejection stresses were found to be independent of ejection velocity in the range investigated, but were dependent upon the compact Height/Diameter ratio. "Stick-Slip" motion occurs during such unlubricated ejection.

3. Increased additions of lubricant to iron powder produce continuous sliding at progressively lower stress values. Under lubricated conditions, the compact Height/Diameter ratio affects the value of the ejection stress. At high compact densities the lubricant film may break down and the sliding process revert to the "stick-slip" motion of unlubricated ejection.

4. When "stick-slip" motion was observed during ejection poor compact surface finish was observed.

5. Plots of compaction pressure versus ejection stress indicate a transition point which appears to be related to the particle size of the lubricant used.

6. Reasonable agreement was found between ejection stress values determined with the production scale and laboratory scale equipment. and the small differences that occurred could be attributed to the different ejection speeds.

7. The density dependence of ejection stress was explained in terms of lubricant film thickness and coverage.

8. All of the stearates examined gave similar ejection stress values for comparable mixtures although coarser stearates appeared

to be slightly better. Die wall lubrication was just as effective as admixed lubrication in lowering the ejection stress.

9. Die material had little effect upon ejection stress when using a 1.0 wt% zinc stearate/iron powder mixture.

10. Compacts spring on ejection from the die and the amount of spring increased with increased compaction pressure and increased lubricant content.

8,50 Tool Materials, Tool Wear and Theoretical Predictions

1. High chromium steel and glass-ceramic dies have similar compressibility behaviour for a given powder compaction; but tungsten carbide dies gave slightly poorer compressibility performance.

2. Increasing the lubricant content in the iron powder increases the area of the lubricant film produced at the compact/die wall interface. The apparent "wear resistance" of this film increased with compaction pressure, presumably due to higher die radial stresses forcing the lubricant film over a greater area at the compact/die wall interface. These facts indicated that wear of the die wall is related to the coherency, thickness and wear resistance of this lubricant film at the compact/die wall interface.

3. Using a "pin and disc" apparatus it was found possible to estimate wear rates of various types of iron powder + lubricant compacts pins on different die material discs. The wear rate was independent of the apparent area of contact.

4. For an unlubricated system, the tungsten carbide disc/iron powder compact pin system showed the least wear.

5. Lubrication of such a system was shown to reduce the wear rate by up to 50 times or more depending on the conditions.

6. Theoretical predictions of die wear based upon wear rate data obtained using the "pin and disc" apparatus show good agreement with experimentally determined die wear rates.

8,60 Green Compacts

1. The elastic modulus of green compacts under compression has been determined and found to increase with increasing stress.

2. A theory has been developed to determine Poisson's ratio for green compacts from stress measurements taken on the instrumented press. Values have been found in the range 0.23 to 0.38 for compacts of true density 5.8 to 6.8 g/cm^3 and lubricant content 0.2 to 2.0 wt%.

3. A method has been developed to allow for elastic strains in the die during and after compaction which the original theory did not acoount for.

8.70 Friction Coefficients

1. The friction coefficient during ejection was dependant upon compact density and lubricant content. At low lubricant levels (0.2 wt%) and high density (6.6 g/cm^3), friction coefficients of 0.22 were found whereas at high lubricant levels (2.0 wt%) and low densities (5.8 g/cm^3) friction coefficients of 0.06 were found.

2. The lowest friction coefficients were obtained using zinc stearates of large median particle size. Die wall lubrication using only stearic acid gave low friction values of 0.11 at all density levels.

3. At low lubricant levels, ejection from the tungsten carbide die gave lower coefficient of friction values than when using the high chromium steel die. However at higher lubricant levels similar values were found.

4. Zinc stearate films are capable of giving separation of the sliding surfaces under the action of high point contact loads, as determined by contact resistance measurements.

5. During ejection of compacts from the die, friction coefficient was greater than the minimum values found using the pin and disc machine with a similar lubricant, i.e. where the contact resistance was large. Hence metal/metal contacts occur during the ejection of lubricated compacts from the die.

6. Zero contact resistance was found between compacts lubricated with 2.0 wt% zinc stearate and the die wall during their ejection: again showing metal/metal contacts exist even at this high level of lubrication.

7. Over the range 19-145 cm/sec, disc surface velocity did not affect the coefficient of sliding friction measured for the high chromium steel disc/zinc stearate lubricant/iron powder compact pin system. Pin temperature changes from 78 to 410^{o}K reduced the coefficient of sliding friction from 0.24 to 0.08 using the same system.

8. Friction measurement carried out on ejected compact surfaces, which were in contact with the die, agree very well with values determined during ejection from punch and die stress data.

8.80 SUGGESTIONS FOR FUTURE WORK

1. Continue studies of friction behaviour in powder metal-lubricant systems using the "pin and disc" apparatus, This could be used to obtain more detailed information on wear mechanisms in powder metallurgy tooling.

2. Investigate further die wall lubrication and its effect on production compaction behaviour using the instrumented press.

3. Continue a more detailed investigation of the effect of aspect ratio of powder metal compacts on ejection behaviour.

4. Develop suitable methods of compact surface preparation to show accurate pore size and distribution in green and sintered compacts. This would enable the porosity to be evaluated quantitatively on the Automated Image Analysing Computer.

9.00 REFERENCES.

1. Bowden E.P. and Tabor D., The Friction and Lubrication of Solids, Part I, Oxford 1950.

2. Tabor, D., Proc.Roy.Soc. 1948, A192,247.

3. Shaw, P. and Leavy, E. Phil.Mag. 1930,809.

4. Machlin E.S. and Yankee, J. J.Appl.Physics. 1954, 25,576.

5. Coffin, L.F., Lubrication Engineering 1956, 12 50.

6. Mcfarlane. J.S. and Tabor. D.P., Proc.Roy.Soc. 1950,202,244.

7. L. da Vince (1452-1519), Notebooks, Jonathan Cape, London 1938.

8. Bowden, F.P. and Tabor, D., The Friction and Lubrication of Solids, Part Oxford 1964.

9. Archard, J.F., J.Appl.Phys. 1953, 24, 981.

10. Archard, J.F., Proc.Roy.Soc., 1957, A243, 190.

11. Archard, J.F., J.Appl.Phys. 1961, 32, 1420.

12. Bowden, F.P. and Hughes, T.P., Proc.Roy.Soc. 1939, A172, 263.

13. Campbell, W.E., Trans.A,S.M.E. 1939, 61, 633.

14. Bowden, F.P. et al., J.Appl.Phys. 1943, 11, 80.

15. Rowe, G.W., Research 1960, 14,137

16. Young. R. et al., Rev.Sci.Inst. 1972, 43, (7), 999.

17. Fisher, J., Quinn, T.F.J. and Sullivan, J.F., Proceedings of the 3rd Conference on Industrial Carbon, London 1970.

18. Quinn, T.F.J., Proc.I.Mech.E. 1967-68, 182, Part 3N.

19. Hertz, H., J. reine angeur. Math. 1886, 92, 156.

20. Bowden, F.P. and Tabor, D., Proc.Roy.Soc. 1939, A169, 391.

21. Holm, R., Electrical Contacts, Almquist and Wiksells, Uppsala 1946.

22. Hardy, W.B., CollectedScientific Papers, Cambridge University Press 1936.

23. Langmuir, I., Trans.Faraday Soc. 1920, 15, 62.

24. Langmuir, J., J. Franklin Inst. 1934 218, 143.

25. Bowden, F.P. and Leben, L., Trans.Roy.Soc. 1940, A239, 1.

26. Frewing, J.J., Proc.Roy.Soc. 1942, A181, 23.

27. Zisman,W.A., Friction and Wear, Elsevier, Amsterdam 1959.

28. Hirst, W., Kerridge, M. and Lancaster, J.K., Proc.Roy.Soc. 1952, A212, 516.

29. Rabinowicz, E., Friction and Wear of Materials, John Wiley, New York and London 1965.

30. Clayton, D., Brit.J.Appl.Phys. 2nd Suppl. 1951, 1, 25.

31. Forrester, P.G., Proc.Roy.Soc. 1946, A187, 439.

32. Hardy, W.B. and Bircamshaw, Proc.Roy.Soc. 1925, A108, 1.

33. Milne, A.A., Wear, 1957-8, 1, 98.

34. Rabinowicz, E. and Tabor, D., Proc.Roy.Soc. 1951, A208, 455.

35. Tabor, D., Proc.Roy.Soc. 1960, A251, 378.

36. Burwell, J.T. and Strang, C.D., J.Appl.Phys. 1952, 23, 18.

37. Burwell, J.T. and Strang, C.D., Proc.Roy.Soc. 1952, A212, 470.

38. Archard, J.F. and Hirst, W., Proc.Roy.Soc. 1956, A236, 397.

39. Ernst, H. and Merchant, M.E., Proc.Spec.Summer Conf. on Friction and Surface Finish, M.I.T., Cambridge, June 1940.

40. Coffin, L.F., Friction and Wear, Elsevier, Amsterdam, 1959.

41. Roach, A.E., Goodzeit, C.L. and Hunnicutt, R.P., Trans. A.S.M.E. 1956, 78, 1659.

42. Kerridge, M., Proc.Phys.Soc. 1955, B68, 400

43. Kerridge, M. and Lancaster, J.K., Proc.Roy.Soc. 1956 A236, 250.

44. Davis, R., Friction and Wear, Elsevier, Amsterdam 1959.

45. Kragelskii, I., Friction and Wear, Butterworths, London 1965.

46. Quinn, T.F.J., A.S.L.E., Trans., 1967, 10, 158.

47. Quinn, T.F.J., Brit.J.Appl.Phys., 1962, 13, 33.

48. Archard, J.F., Wear, 1958-9, 2, 438.

49. Rowe, C. ., A.S.L.E. Trans. 1966, 9, 101.

50. Kingsbury, E.P., J.Appl.Phys., 1958, 29, 888.

51. Kingsbury, E.P., A.S.L.E. Trans. 1960, 3, 30.

52. Quinn, T.F.J., Proc.I.Mech.E. 1967-8, 182, Part 3N.

53. Scott, D. and Scott, H.M., Proc.Ist Int. Conf.on Lubrication and Wear, Paper 14, I.Mech.E., London 1957.

54. Halliday, J.S., ibid., Paper 40.

55. Rabinowicz, E., Proc. Phys.Soc. 1951, A64, 939.

56. Crook, A.W., Phil.Trans.Roy.Soc. 1958, A250.

57. Furey,M.J., A.S.L.E. Trans., 1961, 4, 1.

58. Chu, P.S.Y. and Cameron, A., ibid., 1967 10 , 226.

59. Furey, M.J., ibid., 1964, 7, 133.

60. Blok, H., I.Mech.E., Proc.General Discussion Lubrication and Lubricants, 1937, 2, 226.

61. Jaeger, J.C., Proc.Roy.Soc.New South Wales, 1942, 56, 203.

62. Greenwood, H.W. Metallurgia, 1948, 37, 283.

63. Kamm, R., Steinberg, M., and Wulff, J., A.I.M.E., Tech.Publ. 2133, 1947.

64. Seelig, R.P. and Wulff, J., A.I.M.E., Tech.Publ. 2044, 1946.

65. Hausner, H.H. and Sheinhartz, I. Proc. 10th Annual Meeting M.P.A. 1954, 6

66. Sheinhartz, I., McCullough, H.M. and Zambrow, J.L., J.of Metals 1954, 6, 515.

67. Kunin, N.F. and Uurchenko, B.D., Poroshkovaya Metallurgiya 1967, 12, 19.

68. James, P.J., Powder Met.Int. 1972, 4, 1.

69. Train, D. and Hersey, J.A., Powder Met. 1960, 6, 20.

70. Heckel, R.W., Progress Powder Met., 1961, 17, 66.

71. Donachie Jr. N.J. and Burr, M.F., J.of Metals 1963, 15, 249.

72. Torre, C., Berg-Huttenmann, Monatsh, Montan.Hochschule Leoben 1948 93, 62

73. Shapiro, I. and Koltholf, I.M., J.Phys. and Colloid Chem 1947, 51, 983.

74. Kawakita, K.. J.JapanSoc.Powder Met. 1963, 10, 236.

75. Leopold, P.M., and Nelson, R.C., Int.J.Powder Met. 1965, 1, 37.

76. Jones, W.D., Fundamental Principles of Powder Metallurgy, Edward Arnold, London 1960.

77. Ljungberg, I. and Arbstedt, P.G., Proc.12th Annual Meeting of M.P.A. 1956, 78.

78. Sajdak, R.J., et al., Int.J.Powder Metallurgy, 1970, 6, (2), 13.

79. Bockstiegel, G. and Svensson, O., "Modern Developments in Powder Metallurgy", Vol. 4. 'Processes', Plenum Press, New York 1971, 87.

80. Flipot, A.J., Gillisen, R. and Smolders, A., Powder Met. 1911, 14, 93.

81. Leopold, P.M. and Nelson R.C., Int.J.Powder Met. 1965, 1, (4), 37.

82. Geijer, E. and Jamison, R.S., 'Powder Metallurgy' ed.W.Leszynski, Interscience, New York and London 1961, 585.

83. Bockstiegel, G. and Svensson, D., Powder Met. 1969, 12, 316.

84. A.S.T.M. Standards B-243-61 and B-329-61; M.P.I.F. Standard 9-62

85. Oakley, J.

86. Yarnton, D., Metallurgia, 1962, 66, 153.

87. Meyer, R. Pillot, J. and Pastor, H., Powder Met., 1969, 12, 298.

88. Moyer, K.H., Int.J.Powder Met., 1971, 7, (3), 33.

89. Hausner, H.H., ibid, 1967, 3, (4), 7.

90. Unckel, H., Arch.Eisenhutlenw, 1944, 18, 125.

91. Shank, M.E. and Wulff, J., Trans.A.I.M.M.E. 1949, 185, 56.

92. Duwez, P. and Zwell, L., ibid, 1949, 185, 566.

93. Kamm, R., Steinberg, M.A. and Wulff, J., ibid, 1947, 171, 439

94. Seelig, R.P., and Wulff, J., Trans.A.I.M.M.E. 1946, 166, 492.

95. Bustamante, S.J. and Sheinberg, H., Powder Met., 1960, 6, 36.

96. Long, W.M., Powder Met., 1960, 6, 73.

97. Higuchi, T., Nelson, E. and Busse, L.W., J.Amer.Pharm.Assc'n. 1954, 43, 344.

98. Nelson, E., Nagri, S.M., Busse, L.W. and Higuchi, T., ibid, 1954, 43, 596

99. Courtney-Pratt, J.S. and Eisner, E., Proc.Roy.Soc. 1957, A238, 529.

100. Allmand, T.R. and Coleman, D.S., Metals and Materials, 1971, 5, 325.

101. Allmand, T.R. and Coleman, D.S., ibid, 1971, 5, 32.

102. Kaye, B.H., Powder Met., 1962, 9, 213.

103. Durham Chemical Group, Tech.Service Bulletin 8 (1) 6-10.

104. Claussen, N. and John, J., Powder Met.Int. 1970, 2, 87.

105. B.S. 1134.

106. Penrice, T.W., Powder Met. 1958, 2, 79.

107. Timoshenko, S., Strength of Materials, Part 2, Advanced Theory and Problems, Van Nostrand Reinhold, London 1969.

108. Instron Manual 10-70-1 (4), Section 6.11.5.

109. Hashin, Z., J.Appl.Mech., 1962, (3), 143.

110. Hashin, Z., Proc.Int.Conf.Mech.Composite Mat'ls, GE-ONR, Philadelphia, Pergammon Press 1967.

111. Donnelly, M., Ph.D. Thesis, Loughborough University of Technology 1974

112. Yarnton, D. and Davies, T.J., Powder Met. 1968, 11, 1.

113. Brackpool, J.L., M.Sc. Thesis, Loughborough University of Technology, 1970.

114. Akhmatov, A.S., Molecular Physics of Boundary lubrication, Israel Programme for Scientific Translations, Cat.No. 2108, Jerusalem 1966.

115. McClintock, F.A., and Argon, A.S., Mechanical Behaviour of Materials, Addison-Wesley, Reading Mass. 1966.

116. Stein, E.M., Van Orsdel, J.R. and Schneider, P.V., Perspectives in Powder Metallurgy Plenum Press, New York 1968, 13, 154.

117. Long, W.M. and Alderton, J.R., Powder Met. 1960, 6, 52.

118. Artusio, G. et al. ibid, 1966, 9, 89.

119. Lancaster, J.K. The Principles of Lubrication, Longmans 1961, Chapter 21

120. Boyd and Robertson, B. P., Trans. A.S.M.E., 1945, 67, (1), 51-56

APPENDIX I

An air permeameter to operate at atmospheric pressure has been constructed (Fig. 19). It consists of a 100 ml. burette inverted over a beaker of deionised water, on top of which is a cell 35mm long and 6.23mm diameter.

(i) Cell preparation

Two discs of filter paper $\frac{1}{4}$" diameter are made using an office punch. A 1/8" ring of p.v.c. tubing $\frac{1}{4}$" diameter is pushed into one end of the cell, and a disc of filter paper is pushed through from the other end of the cell, to rest on the p.v.c. ring. The powder to be tested is poured into the cell, taking care to avoid segregation; if necessary it is lightly compacted to give a porosity of about 50%. The remaining filter paper and p.v.c. ring are fitted to the open end. The cell is weighed to determine the weight of powder; the length of cell occupied by powder is measured (in the present case, by ruler) to establish the effective cell volume.

(2) Operation

Water is sucked up the burette using a pipette filler, to just below the tap, which must be kept well greased to prevent admission of air; the tap is then closed. The cell is connected to the top of the burette by a rubber tube, so that air entering the burette must do so via the cell. The tap is opened, and the water level in the burette falls, sucking air in through the cell. The time elapsed as the water falls past the 100ml mark, and at 10ml. intervals, is noted. A graph of time v. $\log_{10}$volume is plotted. The relationship of head of water (in cm) to volume indicated by the burette is measured.

The weight specific surface is calculated from the equation

$$Sw^2 = \frac{1}{K\eta\rho^2 L} \frac{\left(1 - \frac{4W}{\rho\pi D^2 L}\right)^3}{\frac{4W}{D^2 L}} \frac{T_2 - T_1}{\log_{10}V_1 - \log_{10}V_2} \frac{\rho_w g \pi D^2}{4.\ 2.303} \frac{H}{V} \quad \ldots\ldots(1)$$

Where S_w = weight specific surface, cm^2/gm

W = weight of powder, gm

ρ = density of powder, gm/cm^3

D = diameter of cell, cm

L = length of powder column, cm

$T_2 - T_1 / \log_{10}V_1 - \log_{10}V_2$ = slope of graph of time in seconds v. volume in cm^3

ρ_w = density of water, gm/cm^3

g = gravitational constant, cm/sec^2

V/H = volume of water (cm^3) per cm.water head in burette

K = aspect factor, assumed = 5

η = viscosity of air, poise

(3) Theory

Equation (1) is derived from Kozany's equation (10)

$$Sw^2 = \frac{1}{K\eta\rho^2 u} \cdot \frac{e^3}{(1-e)2} \cdot \frac{\Delta p}{L} \quad \ldots\ldots\ldots\ldots(2)$$

Where e = porosity

Δp = pressure drop across cell

u = volumetric flow rate/cross-sectional area of cell

e = (volume of cell) - (volume of metal)/volume of cell

$= 1 - \frac{4W}{\rho\pi D^2 L}$ $\ldots\ldots\ldots\ldots(3)$

$$u = \frac{dV}{dT} \cdot \frac{4}{\pi D^2} \quad \ldots\ldots\ldots\ldots(4)$$

$$\Delta p = H\rho w g \quad \ldots\ldots\ldots\ldots(5)$$

From (2), (4) and (5)

$$\frac{dV}{dT} = \frac{H \rho w\, g \pi D^2}{4K\eta \rho^2 L\, Sw^2} \cdot \frac{e^3}{(1-e)^2} \qquad \text{.....(6)}$$

$$\int_{V_2}^{V_1} \frac{dV}{dH} = \int_{T_1}^{T_2} \frac{dT\, \rho w\ \ g \pi D^2\ \ e^3}{4K\eta\ \ \rho^2 L\, Sw^2 (1-e)^2} = \int_{V_2}^{V_1} \frac{dV}{V} \cdot \frac{V}{H} \qquad \text{.....(7)}$$

V/H is a constant for the burette and beaker used: see section (4) below

$$\frac{V}{H} \cdot \log_{10}(V_1/V_2) \cdot 2.303 = \frac{(T_2 - T_1) \rho w\, g\, e^3 \pi D^2}{4K \eta \rho^2 L\, Sw^2 (1-e)^2} \qquad (8)$$

Rearranging

$$Sw^2 = \frac{(T_2 - T_1)}{(\log_{10} V_1 - \log_{10} V_2)} \cdot \frac{g \rho w\ \ e^3\ \pi\ D^2}{4K\eta\, \rho^2 L\, (1-e)^2\ 2.303} \cdot \frac{H}{V} \qquad (9)$$

Substituting for e from equation (3) gives equation (1)

(4) Experimental details

For the beaker and burette used, H/V was found to vary from 0.672 to 0.677, because of taper in the beaker. A mean value of 0.673 was used. The variation is not significant in view of the errors attributable to segregation - an error of -3% has been measured. The experiments were carried out at temperatures ranging from 21°C to 26°C; in calculation ρ_w = 0.9975, and η = 0.000182 were used. ρ was taken as 7.84. The graphs of $\log_{10} V$ v.t. are plotted and the surface areas and the porosities calculated.

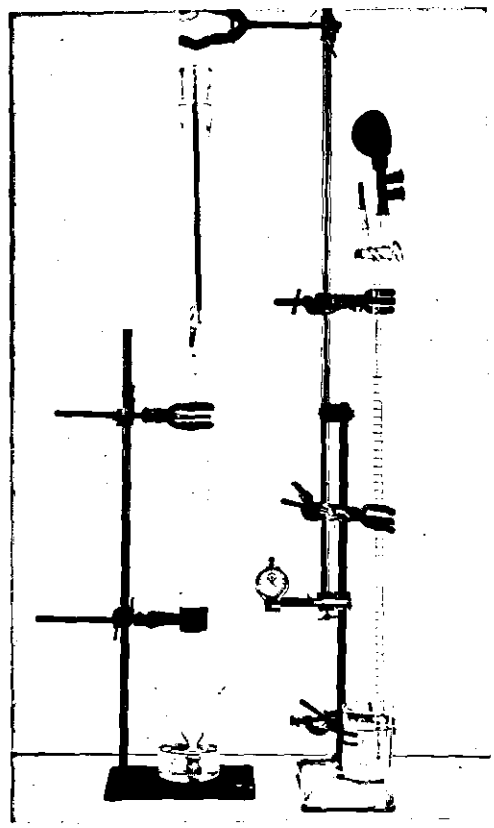

FIGURE I*

APPENDIX II

CALIBRATION OF INSTRUMENTED PRESS

(a) Calibration of Top Punch Strain Gauges

Top Punch Load (KN)	MV Output
0	0
50	252
100	499
150	746
200	993
250	1238
300	1484
350	1727

(b) Calibration of Bottom Punch Strain Gauges

Bottom Punch Load (KN)	MV output
0	0
50	250
100	500
150	748
200	997
250	1244
300	1488
350	1731

(c) Calibration of H.C.D. Die Strain Gauges

Top Punch Stress (Kg/mm^2)	Die Strain Gauge Output (mV)
2,2	17.6
4.6	30.0
7.2	41.6
15.6	86.4
32.0	171.0
34.2	184.0

(d) Calibration of W.C. Die Strain Gauges

Top Punch Stress (MN/m^2)	Die Strain Gauge Output (mV)
40	20
60	27
80	37
115	50
161	73
210	92
261	119
350	148
411	168
530	212

APPENDIX III

CALCULATION OF COMPACT STRAIN

Strain in Uniaxial Compression = $\frac{\delta L}{L}$

where δL = small change in total length L

However for a compact in a die we have the following situation:-

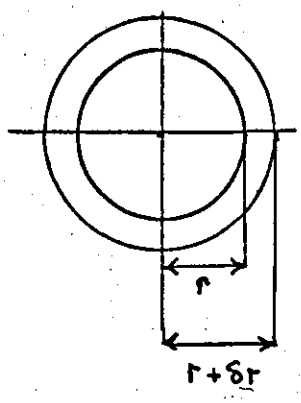

Now the area of the Annulus is:

$$\pi \left[(r + \delta r) + r\right]\left[(r + \delta r) - r\right]$$

$$= 2\pi r \delta r$$

$$\text{Strain} = \frac{\text{Change in Area}}{\text{Original Area}} = \frac{2\pi r \delta r}{\pi r^2}$$

$$= \frac{2\delta r}{r} = \frac{2\delta D}{D}$$

$D = 2r$

$\delta D = 2\delta r$

APPENDIX IV

LUBRICATION CODE NUMBERS AND MAKERS NAMES

ZINC STEARATES

Code Number	Makers Name & Grade
1	Durham: 'S' grade
2	Berk
3	Hardman & Holden
4	Witco
5	Albright & Wilson
6	Flexichem
7	Hardman & Holden, 'S' grade
8	Durham: 'A' grade

OTHER STEARATES

9	Calcium Stearate 'A' grade	Durham
10	Lithium Stearate 'A' grade	Durham
11	Aluminium Stearate 'G' grade	Durham
12	Aluminium Stearate 'N' grade	Durham
13	Aluminium Stearate G65 grade	Durham

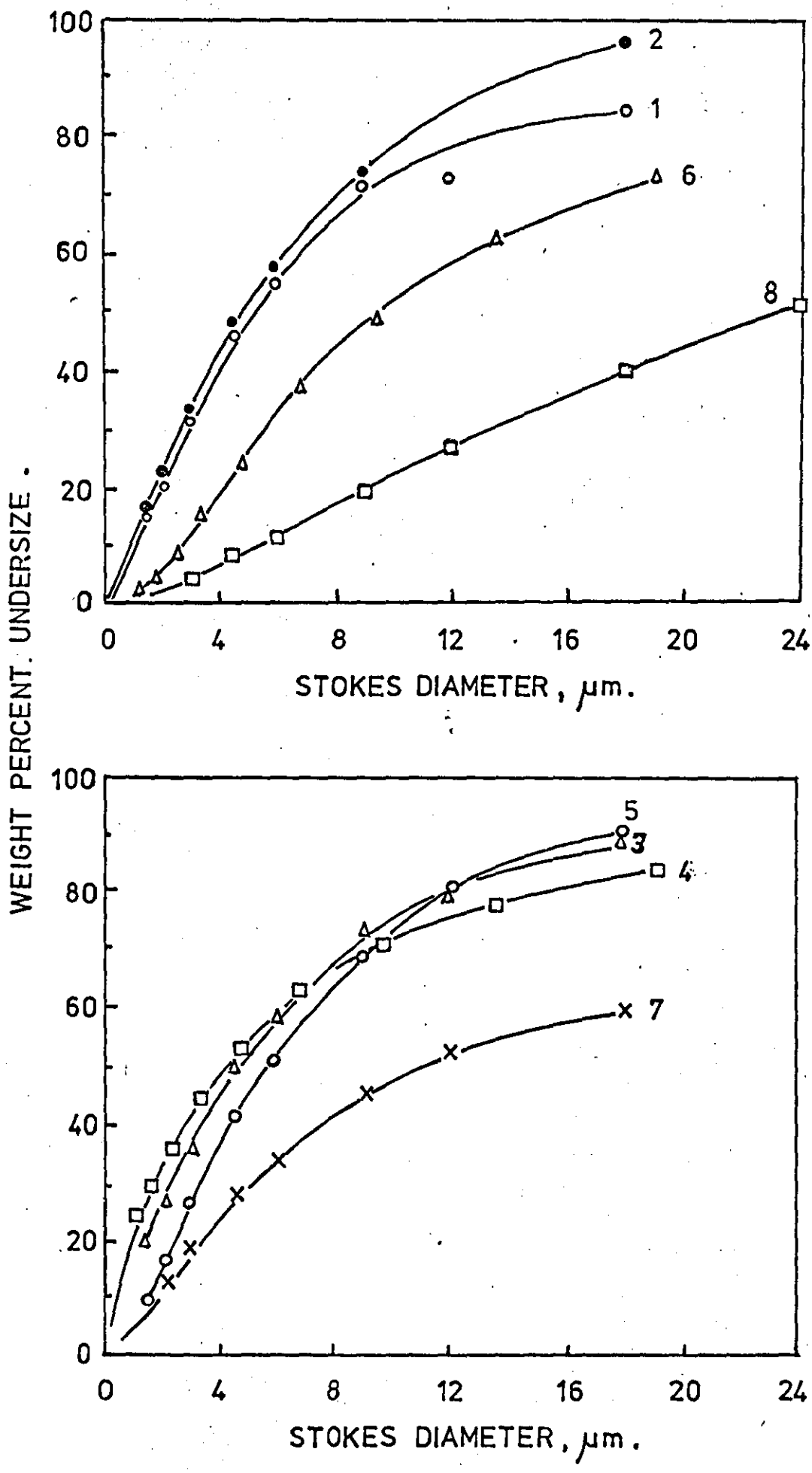
WEIGHT PERCENT. UNDERSIZE .
100
80
60
40
20
0
0
4
8
12
16
20
24
STOKES DIAMETER, μm.
2
1
6
8
5
3
4
7

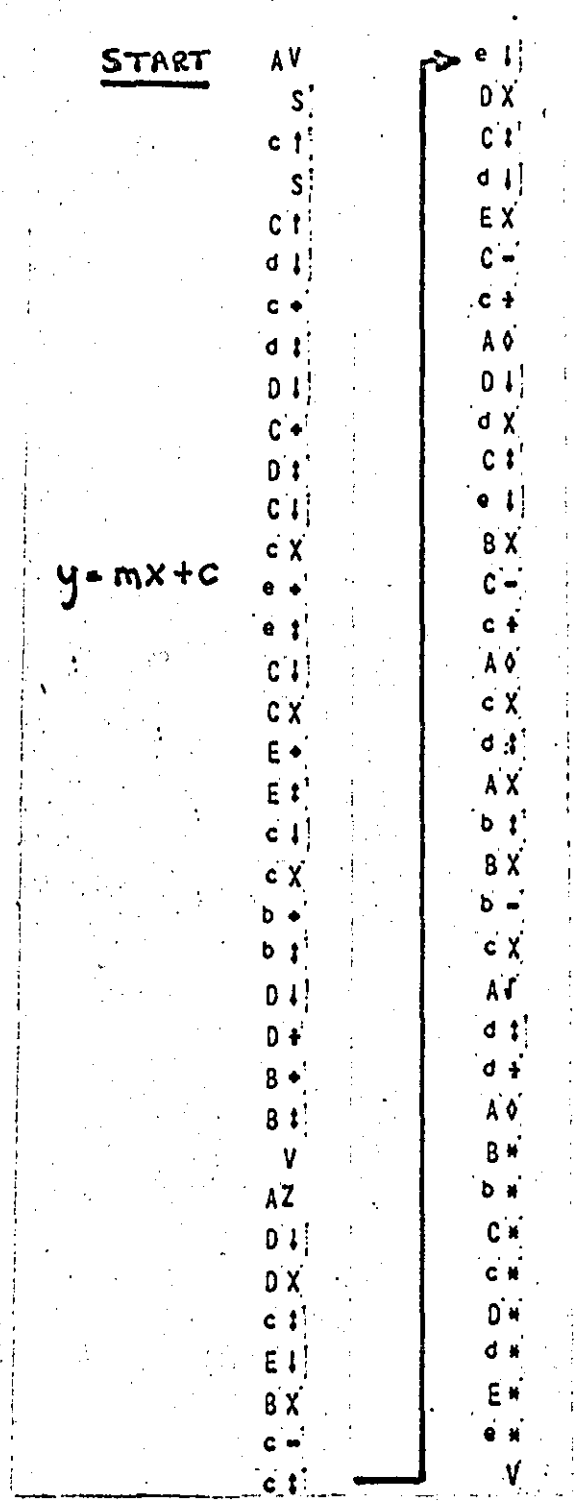
START
y = mx + c
AV
S
c ↑
S
C ↑
d ↓
c •
d ↕
D ↓
C •
D ↕
C ↓
c X
e •
e ↕
C ↓
C X
E •
E ↕
c ↓
c X
b •
b ↕
D ↓
D ↕
B •
B ↕
V
AZ
D ↓
D X
c ↕
E ↓
B X
c -
c ↕
e ↓
D X
C ↕
d ↓
E X
C -
c ↕
A ◊
D ↓
d X
C ↕
e ↓
B X
C -
c ↕
A ◊
c X
d ↕
A X
b ↕
B X
b -
c X
A ◊
d ↕
d ↕
A ◊
B *
b *
C *
c *
D *
d *
E *
e *
V

APPENDIX VI

Compacts Produced in Instrumented H.C.D. Die

Lubricant & Code No	Lubricant Content %	Pressing Pressure MN/m^2	True Compact Density g/cm^3	Maximum Radial Stress During Compaction MN/m^2	Residual Radial Stress During Ejection MN/m^2	Ejection Stress MN/m^2	Friction Coefficient During Ejection	ν	Compaction Energy Joules/grm
Zinc Stearate 1	0.2	232	5.85	90	21	3.05	0.142	0.23	8.5
"	0.2	286	6.09	122	31	5.01	0.161	0.24	10.6
"	0.2	412	6.48	224	60	10.44	0.172	0.28	17.2
"	0.2	462	6.61	260	65	15.46	0.240	0.30	17.0
Zinc Stearate 1	0.5	230	5.86	85	16	2.64	0.166	0.23	8.5
"	0.5	278	6.09	120	21	4.02	0.187	0.26	11.7
	0.5	368	6.39	191	39	6.76	0.173	0.29	15.1
	0.5	575	6.85	331	81	15.54	0.190	0.30	13.6
Zinc Stearate 1	1.0	204	5,78	78	11	1.59	0.144	0.25	8.5
"	1.0	277	6.12	126	24	3.72	0.155	0.27	11.5
"	1.0	349	6.36	176	33	5.33	0.159	0.29	13.9
"	1.0	446	6.58	266	52	7.39	0.140	0.32	15.1
Zinc Stearate 1	2.0	179	5.69	74	14	0.50	0.035	0.25	8.0
"	2.0	295	6.13	142	25	2.40	0.096	0.28	13.0
"	2.0	467	6.53	286	42	4.38	0.104	0.34	18.0
"	2.0	911	6.67	610	55	7.51	0.136	0.38	40.0

Compacts Produced in Instrumented H.C.D. Die

Lubricant & Code No	Lubricant Content %	Pressing Pressure MN/m^2	True Compact Density g/cm^3	Maximum Radial Stress During Compaction MN/m^2	Residual Radial Stress During Ejection MN/m^2	Ejection Stress MN/m^2	Friction Coefficient During Ejection
Zinc Stearate 8	0.5	220	5.78	99	15	2.25	0.145
	0.5	301	6.17	157	30	4.76	0.158
	0.5	400	6.40	219	44	6.80	0.154
	0.5	477	6.64	291	64	10.18	0.159
Calcium Stearate 9	0.5	234	5.87	97	20	2.72	0.136
	0.5	290	6.09	123	27	3.54	0.130
	0.5	389	6.42	195	47	6.96	0.148
	0.5	475	6.63	271	66	10.48	0.157
Lithium Stearate 10	0.5	205	5.74	79	14	1.53	0.104
	0.5	281	6.10	128	27	3.58	0.133
	0.5	372	6.41	200	45	6.48	0.143
	0.5	568	6.83	352	86	13.91	0.162
Aluminium Stearate 12	0.5	248	565	103	18	2.95	0.161
	0.5	294	6.14	152	26	4.12	0.159
	0.5	362	6.39	222	45	6.65	0.146
	0.5	550	6.80	356	79	13.68	0.166

Compacts Produced in Instrumented H.C.D. Die

Lubricant & Code No	Lubricant Content %	Pressing Pressure MN/m^2	True Compact Density g/cm^3	Maximum Radial Stress During Compaction MN/m^2	Residual Radial Stress During Ejection MN/m^2	Ejection Stress MN/m^2	Friction Coefficient During Ejection
Aluminium Stearate 13	0.5	195	5.76	86	13	1.62	0.127
	0.5	303	6.14	150	25	3.47	0.136
	0.5	401	6.43	205	44	6.00	0.136
Stearic Acid (dissolved in diethyl ether)	0.5	280	6.03	138	25	2.79	0.109
	0.5	360	6.32	215	44	7.33	0.166
	0.5	472	6.62	287	64	9.34	0.144
Stearic Acid (applied to the die wall)	0.0	294	5.94	148	44	5.07	0.114
	0.0	419	6.39	220	70	7.83	0.111
	0.0	489	6.58	267	89	9.52	0.106

Compacts Produced in Instrumented WC Die

Lubricant & Code No	Lubricant Content %	Pressing Pressure MN/m^2	True Compact Density g/cm^2	Maximum Radial Stress During Compaction MN/m^2	Residual Radial Stress During Ejection MN/m^2	Ejection Stress MN/m^2	Friction Coefficient During Ejection
Zinc Stearate 1	0.2	220	5.78	99	18	2.78	0.154
	0.2	271	6.01	125	24	4.24	0.177
	0.2	365	6.34	182	38	7.37	0.191
	0.2	495	6.67	256	62	13.44	0.210
Zinc Stearate 1	0.5	232	5.86	106	25	2.71	0.106
	0.5	265	6.03	126	29	4.30	0.148
	0.5	391	6.44	204	47	7.58	0.159
	0.5	534	6.76	289	72	11.46	0.160
Zinc Stearate 1	1.0	236	5.87	112	19	2.93	0.127
	110	346	6.32	181	35	5.60	0.160
	1.0	365	6.36	188	39	5.71	0.147
Zinc Stearate 1	2.0	237	5.81	110	22	1.75	0.079
	2.0	315	6.05	141	28	3.01	0.106
	2.0	493	6.40	214	39	5.69	0.145
	2.0	759	6.57	370	47	7.23	0.153

TABLE I

Iron Powder Characteristics

Physical Properties					
				Apparent Density:	2.40g/cm^3
				Tapped Density:	3.31g/cm^3
				Flow Rate:	46s
				Micro Hardness:	163 $HV_2$0.01
				Surface Area:	480 cm^2/g

Screen Analysis	B. S. Mesh	Micron Size	Weight% Retained
	+ 100	+ 152	0.0
	-100 + 150	-152 + 104	4.9
	-150 + 200	-104 + 75	28.5
	-200 + 240	-75 + 64	13.6
	-240 + 300	-64 + 53	11.1
	-300 + 350	-53 + 45	7.2
	-350	-45	34.7

Chemical Analysis	C %	H_2loss %	SiO_2 %	HCl insol. %	Others %
	<0.01	0.45			

TABLE 2

Characteristics of the Metal Stearates Used During This Investigation.

Metal Stearate	Code No.	Melting Point °C	Particle Size µm.			Tap Density g/cm³	Free Fatty Acid %	Moisture %	Total Ash %
			Coulter Counter	Centrifugal Sedimentation	Measured from S.E.M.				
Zinc Stearate	1	120	75	5.2	1 - 4	0.16	0.4	0.1	14.4
"	2	120	–	5.0		0.28	0.4	0.5	14.0
"	3	120	8.0	4.8		0.16	0.3	0.8	15.8
"	4	120	6.0	4.4		0.14	0.3	0.3	13.8
"	5	120	–	5.6		0.21	0.5	0.2	14.5
"	6		–	9.4		0.36	0.5	0.4	13.5
"	7		18.0	11.0		0.44	1.8	0.6	14.2
"	8		30.0	22.4	7 -14	0.48	0.6	0.2	14.5
Calcium Stearate	9		13.4	-	2 - 8	0.42	0.6	2.4	10.2
Lithium Stearate	10		5.3	-	2 - 7	0.30	0.0	0.1	15.9
Aluminium Stearate	11		11.4	-		0.29	5.4	0.6	9.0
"	12		7.0	-	1 - 4	0.17	2.1	3.5	41.3
"	13		9.5	-	1 - 5	0.42	32.3	0.7	6.1

TABLE 3

Mix Characteristics for Iron Powder Containing 1% Zinc Stearate 1

Mixing Time min	Bottle Mixing 200 cm^3 bottle rotated @ 36 r.p.m, 400g mix		Double Cone Mixing 8500 cm^3 cone rotated at 40 r.p.m,			
	Apparent Density g/cm^3	Flow s	Apparent Density g/cm^3	Flow s	Apparent Density g/cm^3	Flow s
0	2.27	66.8	2.27	66.8	2.27	66.8
5	2.41	64.8	2.56	60.8	2.57	60.1
10	2.47	62.5	2.60	56.0	2.61	59.2
20	2.52	62.1	2.62	52.7	2.65	57.1
30	2.55	60.9	2.65	55.9	2.69	55.9
40	2.57	61.1	2.66	49.8	2.73	56.4
60	2.59	61.0	2.68	48.9	2.74	53.6
120	2.67*	61.2*	2.72*	44.4*	2.80*	46.5*

* After standing for 24 hours

TABLE 4

The Effect of Lubricant Content on Mix Characteristics

Lubricant Content Zinc Stearate 1 %	Apparent Density D_a	Tapped Density D_t g/cm^3	Ratio D_t/D_u	Flow s	Green Strength Kg/mm^2	Mixability of Zinc Stearate and Iron Powder
0.0	2.27	3.31	1.46	66.8	1.46	-
0.1	2.70	3.30	1.22	44.0	1.27	Good
0.3	2.70	3.31	1.22	44.0	1.22	Good
0.5	2.68	3.24	1.21	43.0	1.16	Good
0.7	2.68	3.22	1.20	43.2	1.18	Good
1.0	2.71	3.28	1.21	44.7	1.02	Good
1.5	2.70	3.20	1.18	45.0	1.12	Small Stearate Agglomerates
2.0	2.65	3.20	1.21	61.8	1.01	Small Stearate Agglomerates

Note Mixes prepared by cone mixing 400g iron powder and lubricant for 60 mins

TABLE 5

The Effect of Metal Stearate Type on Iron Powder Mix Characteristics

Metal Stearate	Code No	Stearate Content in mix %	Apparent Density D_a g/cm^3	Tapped Density D_t g/cm^3	Ratio D_t/D_a	Flow s	Compact Density D_c g/cm^3	Comp Ratio D_c/D_a	D_c/D_t	Green Strength Kg/mm^2
Zinc Stearate	1	1.0	2.71	3.28	1.21	44.7	6.52	2.40	1.98	1.02
"	2	1.0	2.70	3.31	1.23	45.8	6.52	2.41	1.96	1.00
"	3	1.0	2.68	3.24	1.21	48.1	6.55	2.44	2.02	1.11
"	4	1.0	2.68	3.20	1.19	47.0	6.52	2.43	2.04	1.09
"	5	1.0	2.66	3.24	1.22	49.5	6.52	2.45	2.00	1.06
"	6	1.0	2.67	3.24	1.21	46.3	6.50	2.43	2.02	1.07
"	7	1.0	2.65	3.28	1.24	46.3	6.50	2.45	1.97	1.03
"	8	1.0	2.65	3.28	1.24	46.2	6.50	2.45	1.97	1.05
Zinc Stearate *	1	0.5	2.72	3.14	1.15	39.0	6.53	2.40	2.08	1.16
*	8	0.5	2.72	3.11	1.14	38.0	6.48	2.38	2.08	1.10
Calcium Stearate*	9	0.5	2.81	3.15	1.12	35.8	6.52	2.32	2.07	1.21
Lithium Stearate*	10	0.5	2.77	3.09	1.12	39.2	6.55	2.36	2.10	1.07
Aluminium Stearate*	12	0.5	2.79	3.18	1.14	38.2	6.54	2.34	2.06	1.12
"	13	0.5	2.40	2.90	1.21	50.0	6.46	2.69	2.20	1.05

Note 1. 2Kg mixes are marked *. The rest are 400g mixes
2. Compact densities are given for 10g compacts 14.8mm dia pressed @ 410 MN/m^2

TABLE 6

Compressibility Data for Various Zinc Stearate Mixes

Mix of J.J. Makins 100 Pl Iron Powder with 1% of the lubricant shown	Code No	Partice Size Centrifugal Sedimentation μm	Compacting Pressure (MN/m^2) to give the following true densities (g/cm^3)				
			5.9	6.1	6.3	6.5	6.7
Zinc Stearate	4	4.4	258	300	355	427	535
Zinc Stearate	3	4.8	-	302	352	424	527
Zinc Stearate	2	5.0	-	302	357	427	530
Zinc Stearate	1	5.2	255	303	360	427	540
Zinc Stearate	5	5.6	256	307	359	431	533
Zinc Stearate	6	9.4	261	307	362	439	553
Zinc Stearate	7	11.0	262	309	366	440	555
Zinc Stearate	8	22.4	262	310	368	444	558

TABLE 7

Ejection Data for Various Zinc Sterate Mixes

(Evaluated from Figs. 29 & 30)

Testing Order	Mix of J.J. Makins 100 Pl Iron Powder with 1% of the lubricant shown	Code No	Particle Size Centrifugal Sedimentation	Ejection Stress at Transition MN/m^2	Compaction Pressure at Transition MN/m^2	Initial Slope	Final Slope
2	Zinc Stearate	4	4.4	7.7	403	.014	.10
8	Zinc Stearate	3	4.8	7.8	440	.016	.08
6	Zinc Stearate	2	5.0	7.8	425	.017	.09
1	Zinc Stearate	1	5.2	10.0	443	.028	.10
5	Zinc Stearate	5	5.6	7.6	442	.010	..10
3	Zinc Stearate	6	9.4	8.3	450	.016	.11
4	Zinc Stearate	7	11.0	8.9	462	.017	.11
7	Zinc Stearate	8	22.4	7.8	493	.014	.10

TABLE 8

Analysis of Laboratory Compressibility Behaviour Following Kawakita
For Compacts of Various Height/Diameter Ratios

Powder	Lubricant Content %	H/D Ratio	Calculated Constants		Correlation Coefficient	Reciprocal Porosity Values Based Upon:-	
			C	K		Apparent Density	Tapped Density
J. J. Makins 100 Pl Iron Powder	0	0.037	1.025	0.0102	0.997	1.41	1.73
J. J. Makins 100 Pl Iron Powder	0	0.324	1.084	0.0090	0.996	1.41	1.73
J. J. Makins 100 Pl Iron Powder	0	0.675	1.659	0.0063	0.999	1.41	1.73
J. J. Makins 100 Pl Iron Powder with Zinc Stearate 1	1	0.165 to 0.675	1.535	0.0099	0.998	1.53	1.71

TABLE 9

Variation of Slip stress/Distance data for Zinc Stearate 1 Lubricant Films with Compaction Pressure and Lubricant Content

Lubricant Content wt.%	Compaction Pressure MN/m^2	Initial Slip Stress σ_{si} MN/m^2	Max Slip Stress σ^*_{smax} MN/m^2	Slip Stress Change $\sigma^*_{smax} - \sigma_{si}$ MN/m^2	Distance between σ_{si} and σ^*_{smax} points mm	Slip stress change per unit sliding distance $MN/m^2/mm$
0.3	258	4.9	7.6	2.7	2.0	1.35
0.3	360	8.3	13.7	5.4	3.0	1.80
0.3	462	11.3	17.6	6.3	4.0	1.58
0.5	258	3.9	8.3	4.4	6.0	0.73
0.5	360	6.4	13.7	7.3	7.8	0.94
0.5	462	9.8	18.1	8.3	6.5	1.28
0.5	564	15.2	21.1	5.9	3.3	1.79
1.0	258	3.6	3.9	0.3	14.0	0.02
1.0	360	5.9	6.3	0.4	14.0	0.03
1.0	462	9.8	19.6	9.8	9.0	1.09
1.0	564	15.2	18.6	3.4	10.0	0.34
2.0	258	3.1	3.5	0.4	14.0	0.03
2.0	360	4.4	4.6	0.2	14.0	0.01
2.0	462	6.1	7.0	0.9	14.0	0.01
2.0	564	8.3	9.8	1.5	7.0	0.21

Note: At lubricant levels below 0.3% there was no glide region

TABLE 10

Effect of Compaction Pressure upon Break Stress σ_b for various Zinc Stearate Mixes

Mix of J.J. Makins 100 Pl Iron Powder with 1% of the lubricant shown	Code No	Particle Size Centrifugal Sedimentation μm	Break Stress σ_b (MN/m^2) at the following compaction pressures (MN/m^2)			
			258	360	462	564
Zinc Stearate	4	4.4	5.91	7,55	14.31	23.95
Zinc Stearate	3	4.8	5.31	6.21	9.50	17.05
Zinc Stearate	2	5.0	4.91	6.56	10.79	19.91
Zinc Stearate	1	5.2	4.90	6.47	10.00	17.15
Zinc Stearate	5	5.6	5.60	6.72	10.05	19.20
Zinc Stearate	6	9.4	5.60	7,25	9.70	20.50
Zinc Stearate	7	11.0	5.26	7.12	9.21	20.09
Zinc Stearate	8	22.4	5.36	6.01	7.90	15.00

TABLE 11

Effect of Compaction Pressure upon Initial Slip Stress σ_{Si} for various Zinc Stearate mixes

Mix of J.J. Makins 100 Pl Iron Powder with 1% lubricant shown	Code No	Particle Size Centrifugal Sedimentation μm	Initial Slip Stress σ_{Si} (MN/m^2) at the following compaction pressures (MN/m^2)			
			258	360	462	564
Zinc Stearate	4	4.4	4.41	6.77	11.88	15.61
Zinc Stearate	3	4.8	3.91	5.53	10.10	14.01
Zinc Stearate	2	5.0	3.80	6.02	10.69	15.00
Zinc Stearate	1	5.2	3.61	5.93	9.80	15.21
Zinc Stearate	5	5.6	3.98	6.12	10.00	14.71
Zinc Stearate	6	9.4	4.09	6.55	9.40	15.21
Zinc Stearate	7	11.0	4.09	6.41	9.02	14.71
Zinc Stearate	8	22.4	3.82	5.61	7.75	13.01

TABLE 12

Effect of Compaction Pressure upon Maximum Slip Stress σ^*_{smax} for Various Zinc Stearate Mixes

Mix of J.J. Makins 100 Pl Iron Powder with 1% lubricant shown	Code No	Particle Size Centrifugal Sedimentation μm	Maximum Slip Stress σ^*_{smax} (MN/m^2) at the following compaction pressures (MN/m^2)			
			258	360	462	564
Zinc Stearate	4	4.4	4.61	7.24	16.28	18.61
Zinc Stearate	3	4.8	4.28	6.45	16.00	17.15
Zinc Stearate	2	5.0	4.12	6.81	16.95	17.08
Zinc Stearate	1	5.2	3.92	6.30	19.61	18.61
Zinc Stearate	5	5.6	4.31	6.86	17.18	16.49
Zinc Stearate	6	9.4	4.22	6.96	10.21	15.92
Zinc Stearate	7	11.0	4.05	6.86	10.39	15.30
Zinc Stearate	8	22.4	3.82	5.91	8.74	14.31

TABLE 13

Compressibility Data for Various Lubricant Mixes

Mix of J.J. Makins 100 Pl Iron Powder with 0.5% of the lubricant shown	Code No.	Particle Size Coulter Counter μm	Compacting Pressure (MN/m^2) to give the following true densities (g/cm^3)				
			5.9	6.1	6.3	6.5	6.7
Zinc Stearate	1		235	280	337	410	495
Zinc Stearate	8		247	294	348	420	507
Calcium Stearate	9		240	290	345	416	505
Lithium Stearate	10		240	285	337	405	494
Aluminium Stearate	12		240	284	337	405	496
Aluminium Stearate	13		245	295	353	425	517
Stearic Acid*			250	305	362	428	502
Stearic Acid**			279	333	393	458	537

* Added to mix in di-ethyl ether

** Stearic acid in di-ethyl ether applied only to die walls

TABLE 14

Analysis of Dynamic Compressibility Relationships Following Kawakita

Powder	Calculated Constants		Correlation Coefficient	Reciprocal Porosity Values Based Upon:-	
	C	K		Apparent Density	Tapped Density
Makins 100 Pl Iron Powder	1.739	0.0083	0.999	1.41	1.73
Zinc Stearate 1	4.526	0.0772	0.980		1.18
Makins 100 Pl Iron Powder + 0.2% Zinc Stearate 1	1.761	0.0105	0.998	1.52	1.74
Makins 100 Pl Iron Powder + 2.0% Zinc Stearate 1	1.829	0.0096	0.980	1.50	1.72

TABLE 15

The Effect of Die Material Upon the Compressibility of Makins 100 Pl Iron Powder Containing 1.0% Zinc Stearate 1. (Height/Diameter Ratio 0.4)

Die Material	Compacting Pressure (MN/m^2) to give the following true densities:					
	5.9	6.1	6.3	6.5	6.7	g/cm^3
High Chromium Die Steel	225	271	331	405	505	
Tungsten Carbide	240	283	342	420	525	
Glass Ceramic	225	278	334	400	-	

TABLE 16

The Effect of Die Material Upon the Ejection of Compacts Produced From Makins 100 Pl Iron Powder Containing 1.0% Zinc Stearate 1 (Height/Diameter Ratio 0.4)

Die Material	Ejection Stress (MN/m^2) at the following compaction pressures (MN/m^2)				
	250	300	350	400	450
High Chromium Die Steel	2.9	4.2	5.3	6.4	7.5
Tungsten Carbide	3.2	4.4	5.5	6.5	7.5
Glass Ceramic	2.5	3.7	4.9	6.4	

TABLE 17

Residual Radial StressCalculations for Compacts Containing 0.5, 1.0 and 2.0% Zinc Stearate 1 lubricant

Lubricant	Compaction Pressure MN/m^2	True Density g/cm^3	Interference δD_c mm	Compact Strain $\frac{2\delta D_c}{D_c} \times 10^2$	Secant Modulus $MN/m^2 \times 10^2$	Poisson's Ratio Original Values	Poisson's Ratio Corrected Values	Calculated Residual Radial Stress MN/m^2
0.5	225	5.88	0.038	0.301	61.7	0.23	0.22	11.5
0.5	281	6.11	0.042	0.332	184.2	0.25	0.22	35.2
0.5	375	6.40	0.050	0.448	238.0	0.29	0.25	54.5
0.5	575	6.85	0.061	0.482	260.0	0.29	0.25	71.0
1.0	212	5.83	0.031	0.246	113.9	0.25	0.23	16.9
1.0	270	6.14	0.037	0.293	155.0	0.26	0.23	26.4
1.0	361	6.40	0.042	0.332	243.0	0.30	0.25	46.8
1.0	461	6.63	0.053	0.417	233.5	0.32	0.27	58.9
2.0	190	5.72	0.033	0.260	63.7	0.25	0.24	10.5
2.0	299	6.13	0.040	0.316	110.0	0.27	0.25	21.6
2.0	450	6.49	0.045	0.356	137.1	0.32	0.29	31.8
2.0	911	6.67	0.062	0.490	164.1	0.38	0.34	55.2

TABLE 18

Comparison of Calculated and Determined Residual Radial StressValues and Derived Friction Coefficients for Production Scale Runs

Lubricant Content %	Compaction Pressure MN/m^2	True Density g/cm^3	Ejection Stress σ_E MN/m^2	Calculated Residual Radial Stress MN/m^2 $\sigma_{R\,calc}$	Measured Residual Radial Stress MN/m^2 $\sigma_{R\,max}$	Calculated Friction Coefficient μ calc	Measured Friction Coefficient μ meas
0.5	225	5.88	2.52	11.5	17	.22	.15
0.5	281	6.11	4.02	35.2	23	.11	.17
0.5	375	6.40	6.86	54.5	40	.13	.17
0.5	575	6.85	15.5	71.0	81	.22	.19
1.0	212	5.83	1.65	16.9	11	.10	.15
1.0	270	6.14	3.55	24.4	25	.15	.14
1.0	361	6.40	5.56	46.8	36	.12	.15
1.0	461	6.63	7.83	58.9	55	.13	.14
2.0	190	5.72	0.50	10.5	15	.05	.03
2.0	299	6.13	2.27	21.6	25	.10	.09
2.0	450	6.48	4.61	31.8	41	.14	.11
2.0	911	6.67	7.51	55.2	55	.14	.14

TABLE 19

Calculated Residual Radial Stress Values and Derived Friction Coefficients for Laboratory Scale Runs

Lubricant Content %	Compaction Pressure MN/m^2	True Density g/cm^3	Ejection Stress σ_{smax} MN/m^2	Calculated Residual Radial Stress MN/m^2	Calculated Friction Coefficient μ_{calc}
0.5	252	5.90	7.80	15.1	0.52
0.5	320	6.20	12.01	45.5	0.26
0.5	412	6.50	16.23	68.9	0.24
0.5	548	6.80	19.60	87.6	0.22
1.0	254	5.90	3.89	27.8	0.14
1.0	330	6.20	5.48	39.2	0.14
1.0	428	6.50	7.87	52.5	0.15
1.0	660	6.80	19.00	90.5	0.21
2.0	250	5.90	3.14	17.1	0.18
2.0	345	6.20	4.01	31.1	0.13
2.0	503	6.50	6.66	51.5	0.13

TABLE 20

Friction Coefficients Calculated Using Initial Break Stress Values for Compacts of Different Density (Laboratory Scale Studies)

Mix of J.J. Makins 100 Pl Iron Powder with 1% of Lubricant shown	Code No	Friction Coefficients Determined From Break Stress Values at the Following Densities (g/cm^3)			
		5.9	6.2	6.5	6.8
Zinc Stearate	1	.18	.15	.18	.22
Zinc Stearate	2	.17	.15	.15	.22
Zinc Stearate	3	.17	.14	.14	.21
Zinc Stearate	4	.17	.16	.18	.24
Zinc Stearate	5	.15	.16	.15	.20
Zinc Stearate	6	.20	.17	.15	.23
Zinc Stearate	7	.18	.17	.16	.26
Zinc Stearate	8	.17	.15	.14	.21

Table 21

Friction Coefficients Calculated Using Initial Slip Stress Values For Compacts of Different Density (Laboratory Scale Studies)

Mix of J.J. Makins 100 Pl Iron Powder with 1% of Lubricant shown	Code No	Friction Coefficients Determined From Initial Slip Stress Values at the following Densities (g/cm^3)			
		5.9	6.2	6.5	6.8
Zinc Stearate	1	.13	.13	.14	.18
Zinc Stearate	2	.13	.13	.15	.16
Zinc Stearate	3	.13	.13	.13	.16
Zinc Stearate	4	.15	.15	.17	.15
Zinc Stearate	5	.14	.14	.15	.16
Zinc Stearate	6	.15	.15	.14	.16
Zinc Stearate	7	.15	.15	.14	.17
Zinc Stearate	8	.13	.13	.14	.16

Table 22

Friction Coefficients Calculated Using Maximum Slip Stress Values for Compacts of Different Density (Laboratory Scale Studies)

Mix of J. J. Makins 100 P1 Iron Powder with 1% of lubricant shown	Code No.	Friction Coefficients Determined from Maximum Slip Stress Values at the following Densities (g/cm^3)			
		5.9	6.2	6.5	6.8
Zinc Stearate	1	.14	.14	.15	.21
Zinc Stearate	2	.16	.15	.21	.19
Zinc Stearate	3	.14	.14	.15	.19
Zinc Stearate	4	.17	.16	.18	.18
Zinc Stearate	5	.19	.16	.19	.16
Zinc Stearate	6	.16	.15	.15	.16
Zinc Stearate	7	.16	.15	.15	.16
Zinc Stearate	8	.14	.14	.15	.16

TABLE 23

Effect of Lubricant Type Upon Friction Coefficient At Various True Density Levels (H.C.D. die)

Lubricant and Code No.	Lubricant Content	Coefficient of Friction During Ejection at the following True Densities (g/cm^3)		
	%	5.8	6.2	6.6
Zinc Stearate 1	0.5	0.16	0.18	0.19
Zinc Stearate 8	0.5	0.15	0.16	0.16
Calcium Stearate 9	0.5	0.14	0.14	0.16
Lithium Stearate 10	0.5	0.11	0.14	0.15
Aluminium Stearate 12	0.5	0.16	0.16	0.15
Aluminium Stearate 13	0.5	0.13	0.14	0.14
Stearic Acid (Admixed)	0.5	-	0.15	0.15
" (Die Wall)	0.0	0.11	0.11	0.11

TABLE 24

Comparison of the Effect of Die Material Upon Friction Coefficient During Ejection

True Compact Density g/cm^3	Lubricant Content (Zinc Stearate 1)	Coefficient of Friction During Ejection	
		High Chromium Die Steel Die	Tungsten Carbide Die
5.8	0.2	0.15	0.16
6.2	0.2	0.16	0.18
6.6	0.2	0.22	0.21
5.8	0.5	0.16	0.13
6.2	0.5	0.18	0.16
6.6	0.5	0.19	0.17
5.8	1.0	0.15	0.11
6.2	1.0	0.16	0.14
6.6	1.0	0.14	0.15
5.8	2.0	0.06	0.08
6.2	2.0	0.10	0.12
6.6	2.0	0.12	0.15

TABLE 25

Effect of Pin Load and Zinc Stearate Type Upon The Coefficient Of Sliding Friction And The Contact Resistance

Lubricant Type	Code No	Pin Load Kg	Coefficient of Friction μ_{is}	Contact Resistance Ω Average	Maximum	Minimum	Testing Temp °C
Zinc Stearate	1	5	0.10	3000	15000	40	28,0
		15	0.07	500	6000	33	28.0
		25	0.07	230	2300	0	27.2
		40	0.07	-	-	-	25.0
Zinc Stearate	2	5	0.10	450	3000	35	24.0
		15	0.08	240	2300	36	24.0
		25	0.07	75	440	0	24.8
Zinc Stearate	3	5	0.09	1000	15000	0	23.0
		15	0.08	800	9000	240	23.0
		25	0.07	370	9000	90	23.0
Zinc Stearate	4	5	0.10	1300	15000	42	25.0
		15	0.08	1900	15000	240	25.0
		25	0.08	270	15000	0	25.0
Zinc Stearate	5	5	0.09	1500	15000	400	24.0
		15	0.08	1300	15000	500	24.0
		25	0.07	540	15000	88	24.0
Zinc Stearate	6.	5	0.09	2800	15000	0	25.0
		15	0.09	510	3000	0	25.0
		25	0.07	120	800	0	26.0
Zinc Stearate	7	5	0.12	2000	15000	0	25.0
		15	0.10	620	1600	0	27.0
		25	0.19	105	1300	0	27.0
Zinc Stearate	8	5	0.09	9000	15000	5800	25.0
		15	0.08	650	6000	170	33.0
		25	0.07	55	170	0	34.5
		40	0.07	-	-	-	25.0

TABLE 26

Effect of Pin Load and Lubricant Type Upon The Coefficient of Sliding Friction and The Contact Resistance

Lubricant Type	Code No	Pin Load Kg	Coefficient of Friction μ_{1S}	Contact Resistance Ω Average	Maximum	Minimum	Testing Temp °C
Calcium Stearate	9	5	0.06	4000	15000	1400	21.0
		15	0.04	660	1900	380	21.0
		25	0.05	500	15000	160	21.0
Lithium Stearate	10	5	0.05	4000	15000	1400	21.0
		15	0.05	500	15000	0	21.0
		25	0.04	2300	4000	41	21.0
Aluminium Stearate	11	5	0.07	80	180	47	21.0
		15	0.04	220	600	66	21.0
		25	0.05	250	2300	80	21.0
Aluminium Stearate	12	5	0.09	1000	2300	350	20.0
		15	0.06	9000	3000	66	20.0
		25	0.07	160	1100	40	20.0
Aluminium Stearate	13	5	0.07	800	4000	320	21.0
		15	0.04	1300	15000	560	21.0
		25	0.04	230	1300	54	21.0
Stearic Acid	-	5	0.09	-	-	-	26.0
		15	0.07	-	-	-	26.0
		25	0.06	-	-	-	26.0

Note: H.C.D. disc surface velocity 19.1 cm/sec

TABLE 27

Effect of Disc Surface Velocity Upon The Coefficient of Friction

Lubricant Type	Pin Load Kg	H.C.D. Disc Surface Velocity cm/sec	Coefficient of Friction μ_{1s}	Contact Resistance Ω			Temp °C
				Average	Maximum	Minimum	
Zinc Stearate 1	1	19.1	0.13	3000	6000	950	22.1
	5	19.1	0.10	3000	15000	40	28.0
	25	19.1	0.07	230	2300	0	27.2
Zinc Stearate 1	5	76.5	0.10	-	-	-	22.0
	1	145.0	0.15	1300	2300	400	22.0
Zinc Stearate 1	5	145.0	0.11	500	1900	120	22.0
	25	145.0	0.04	230	1300	80	22.0

TABLE 28

Friction Measurements on the Surfaces of Ejected Compacts

Lubricant Type and Amount (Compact Density 6.2g/cm^3)	Code No	Coefficient of Friction at Initial Sliding μ_{is} At the following Pin Loads (Kg)			
		5	10	15	20
Zinc Stearate 1%	1	0.15	0.16	0.16	0.16
Zinc Stearate 2%	1	0.16	0.16	0.14	0.15
Zinc Stearate (mixed with acetone and evaporated onto compact surface)	1	0.12	0.13	0.13	0.13
Zinc Stearate 1%	8	0.19	0.16	0.15	0.15

TABLE 29

Effect of Load and Velocity Upon Wear Characteristics

Disc Material	Disc Material	Lubricant	Disc Surface Velocity cm/s	Volume Remove per Unit Sliding Distance W/s cm^3/ $\times 10^{-9}$	Flow Pressure p_m of softer material $g/cm^2 \times 10^{-5}$	Applied Load P g.	K $\times 10^{-5}$
Makins 100P1 Iron Powder	H.C.D.	None	156	0.367	160	100	5.9
Makins 100P1 Iron Powder	H.C.D.	None	156	3.25	160	1000	5.2
Makins Iron Powder 100P1	H.C.D.	None	156	6.50	160	2000	5.2
Makins 100P1 Iron Powder	H.C.D.	None	119	3.47	160	1000	5.4

TABLE 30

Effect of Disc Material and Lubricant Upon Wear Characteristics

Pin Material	Disc Material	Lubricant	Disc Surface Velocity cm/sec	Volume Removed per Unit Sliding Distance W/s $cm^3/cm \times 10^{-9}$	Flow Pressure P_m of softer material $g/cm^2 \times 10^5$	Applied Load P	K $\times 10^{-5}$
Makins 100P1 Iron Powder	Tungsten Carbide	None	19	0.83	160	1000	1.3
Makins 100P1 Iron Powder	Glass Ceramic	None	19	2.00	160	1000	3.2
Makins 100P1 Iron Powder	H.C.D.	None	19	3.47	160	1000	5.4
Makins 100P1 Iron Powder	H.C.D.	Zinc Stearate 8	19	0.20	160	5000	0.064
Makins 100P1 Iron Powder	H.C.D.	Zinc Stearate 8	19	2.00	160	25000	0.096

FIGURE 1

Tool Arrangement used for laboratory scale studies

(a) Laboratory Compaction Tools

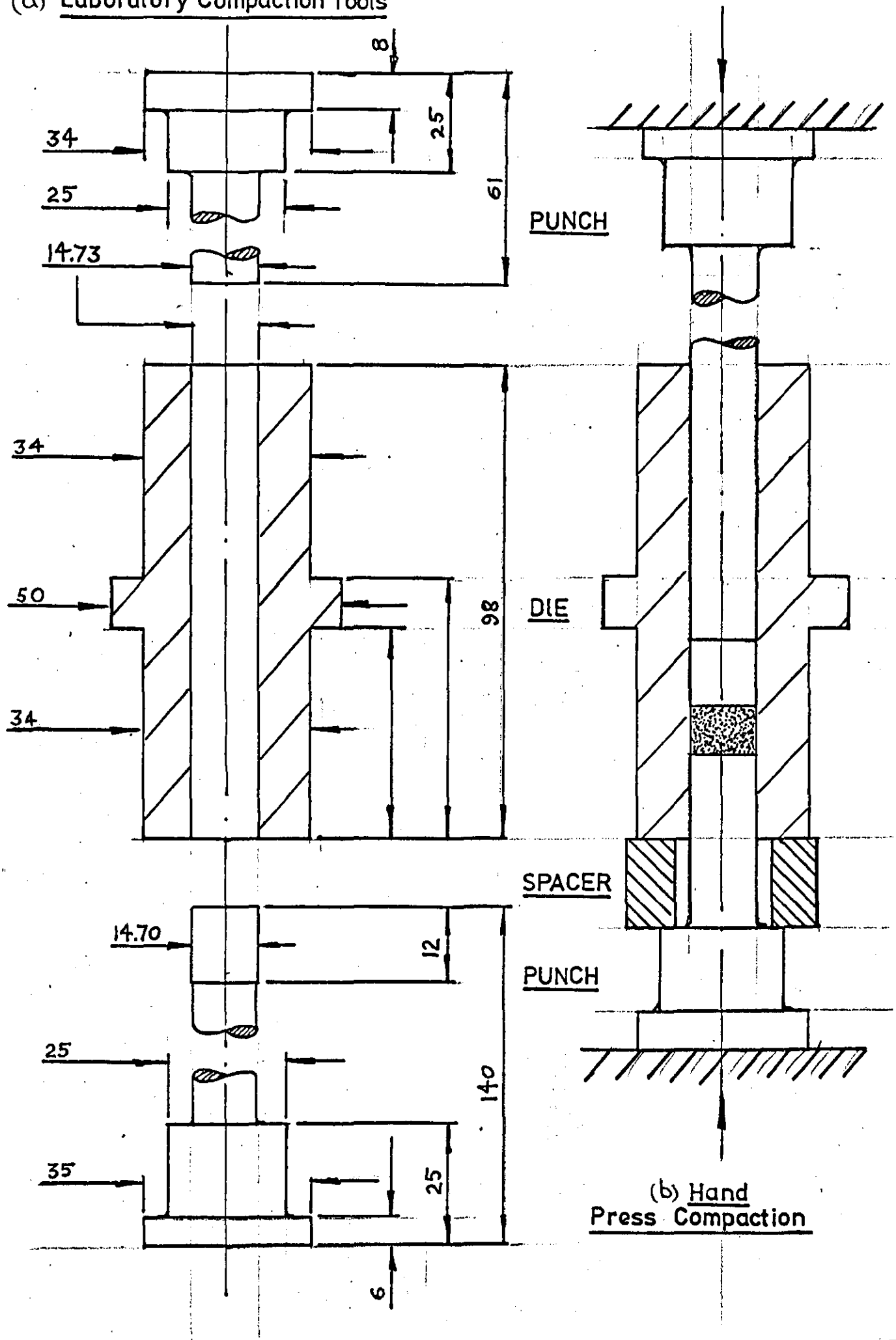

(b) Hand Press Compaction

FIGURE 2

Method of compact ejection on laboratory scale studies

COMPACT EJECTION

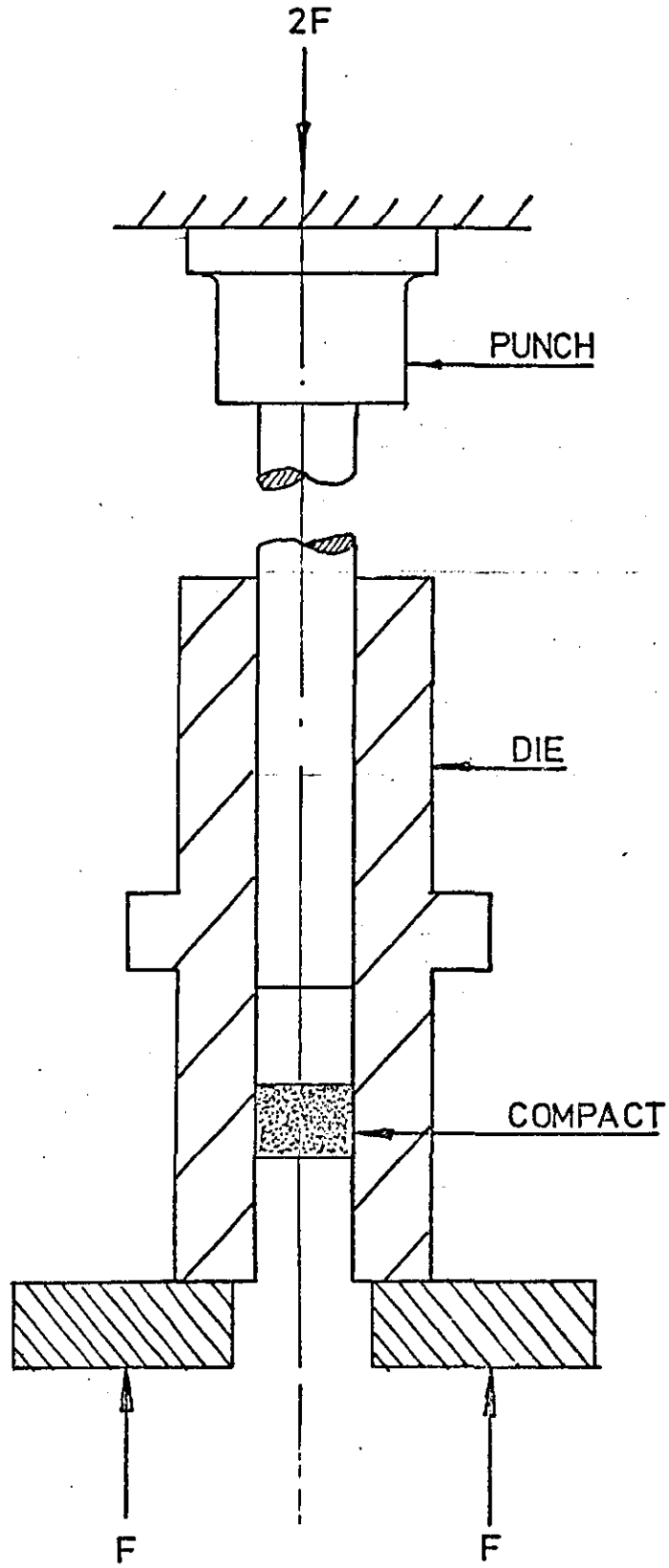

FIGURE 3

Pilot scale mechanical press used in this powder metallurgy research

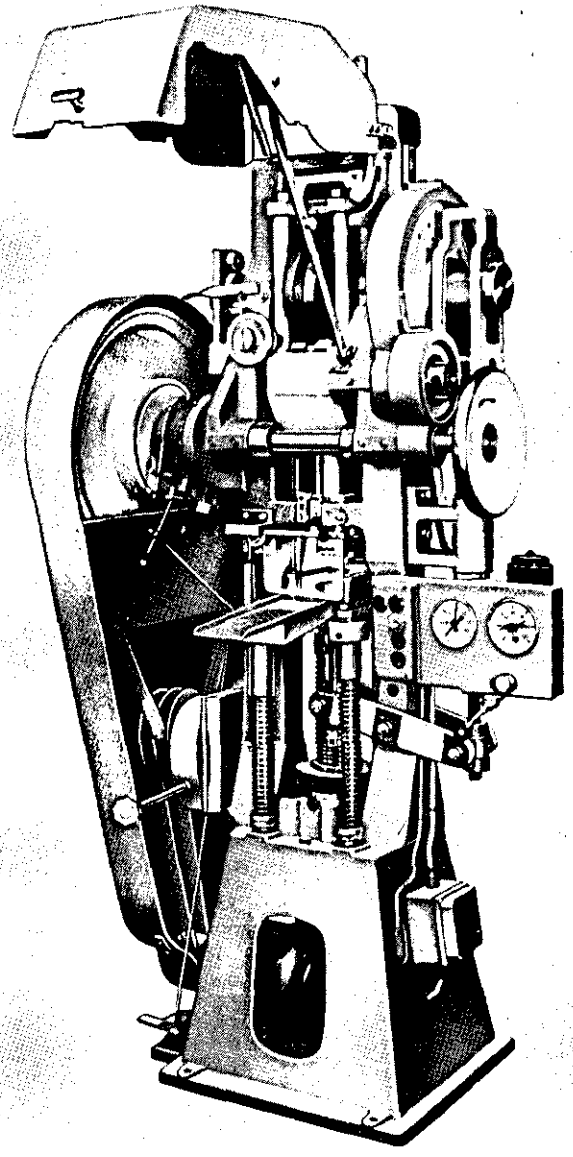

Fig.3.

FIGURE 4

Relative movements of punches and die table during press operation

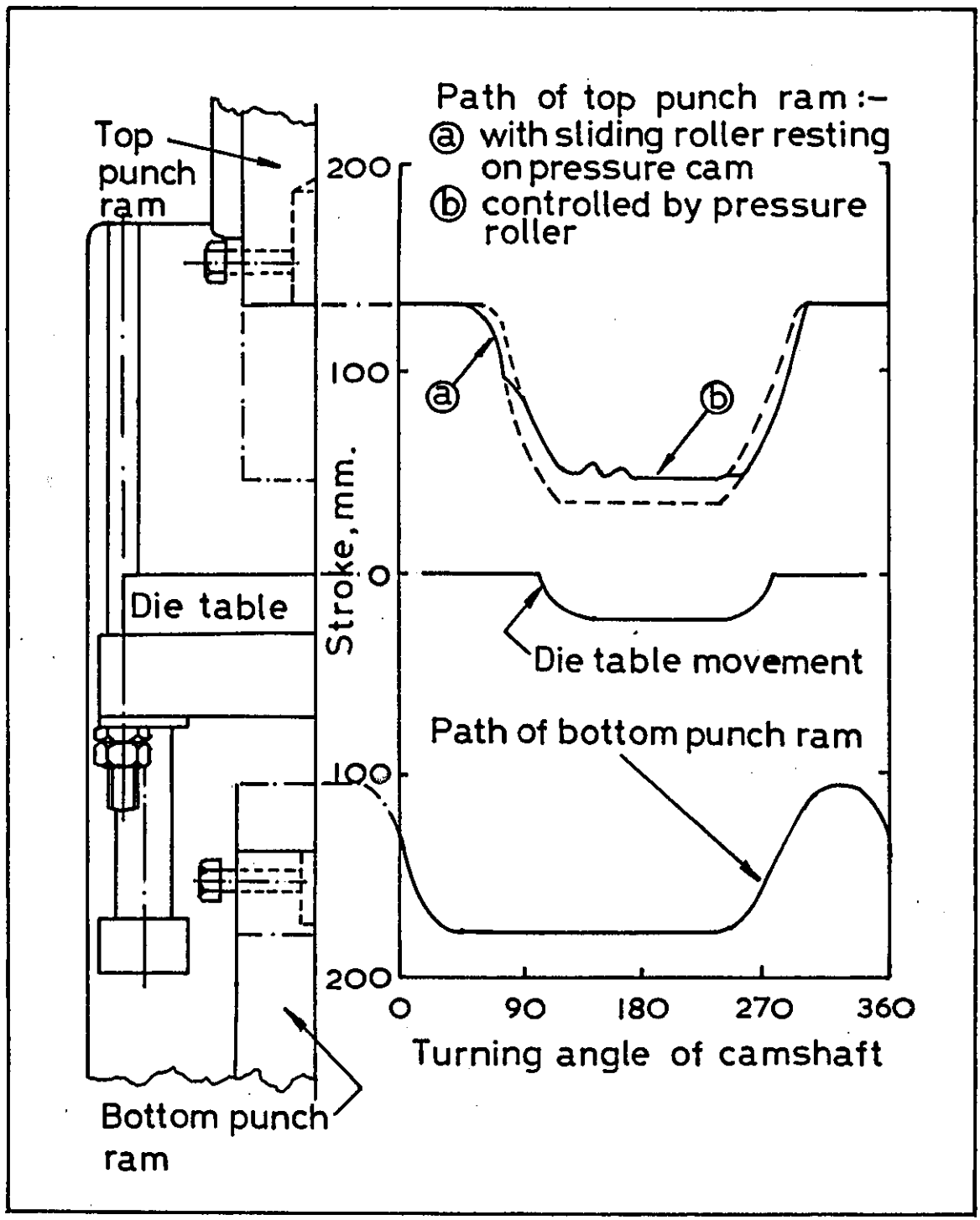
Top punch ram
Die table
Bottom punch ram
Stroke, mm.
200
100
0
100
200
Path of top punch ram :-
ⓐ with sliding roller resting on pressure cam
ⓑ controlled by pressure roller
ⓐ
ⓑ
Die table movement
Path of bottom punch ram
0
90
180
270
360
Turning angle of camshaft

Fig. 4.

FIGURE 5

(a) General layout of instrumented pilot scale powder metallurgy press
(b) Strain gauges attached to tools on press

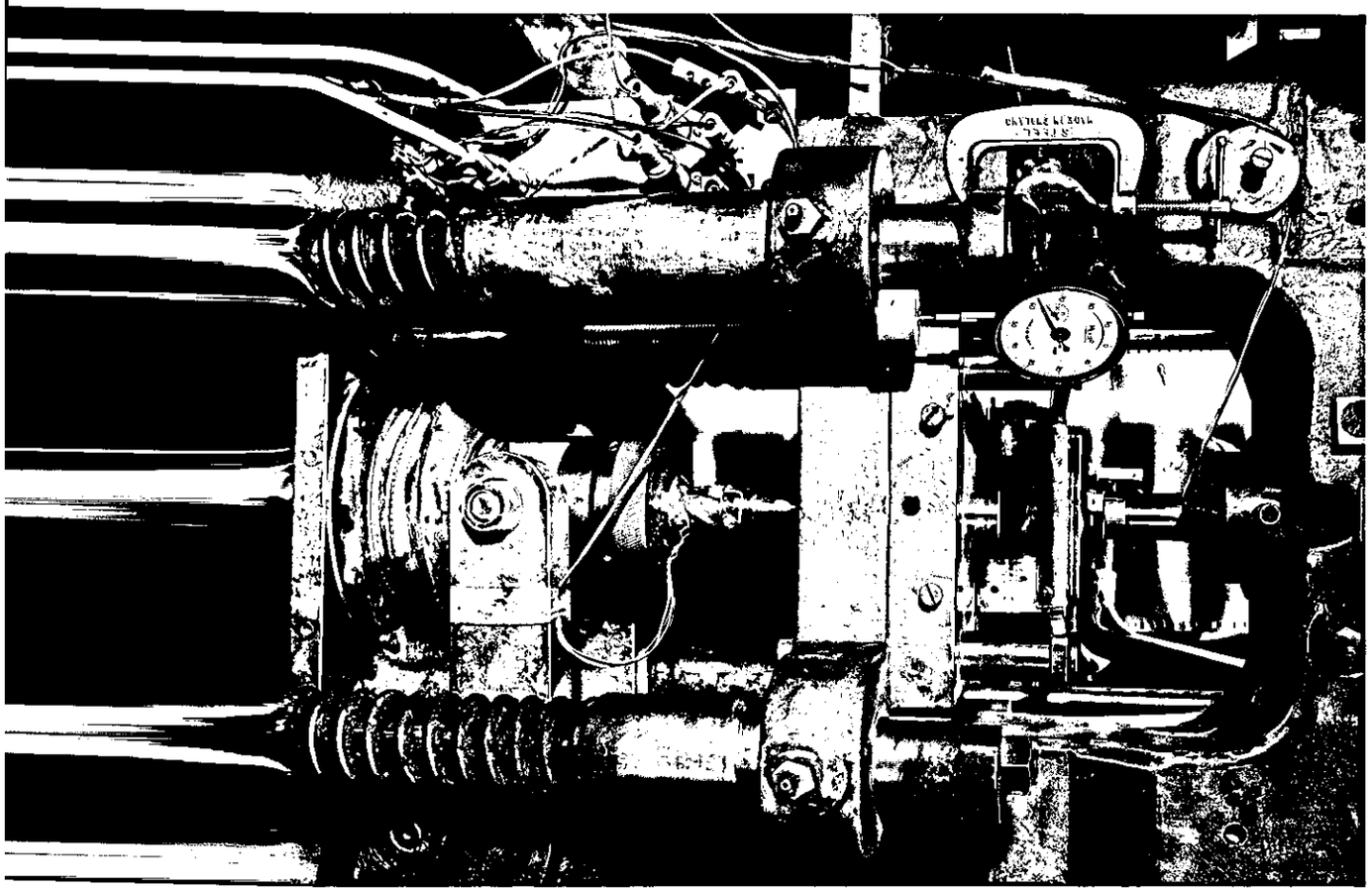

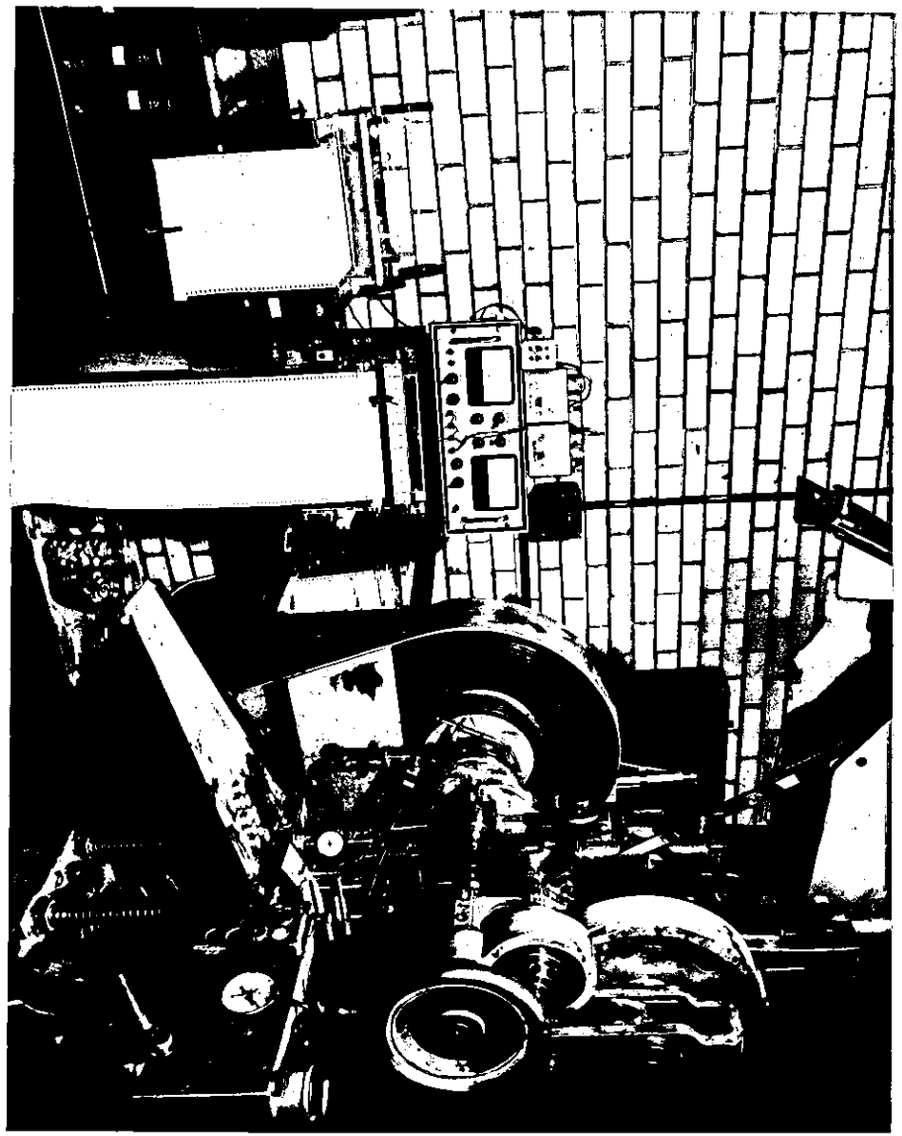

FIGURE 6

Detail of tool arrangement used in pilot plant press.

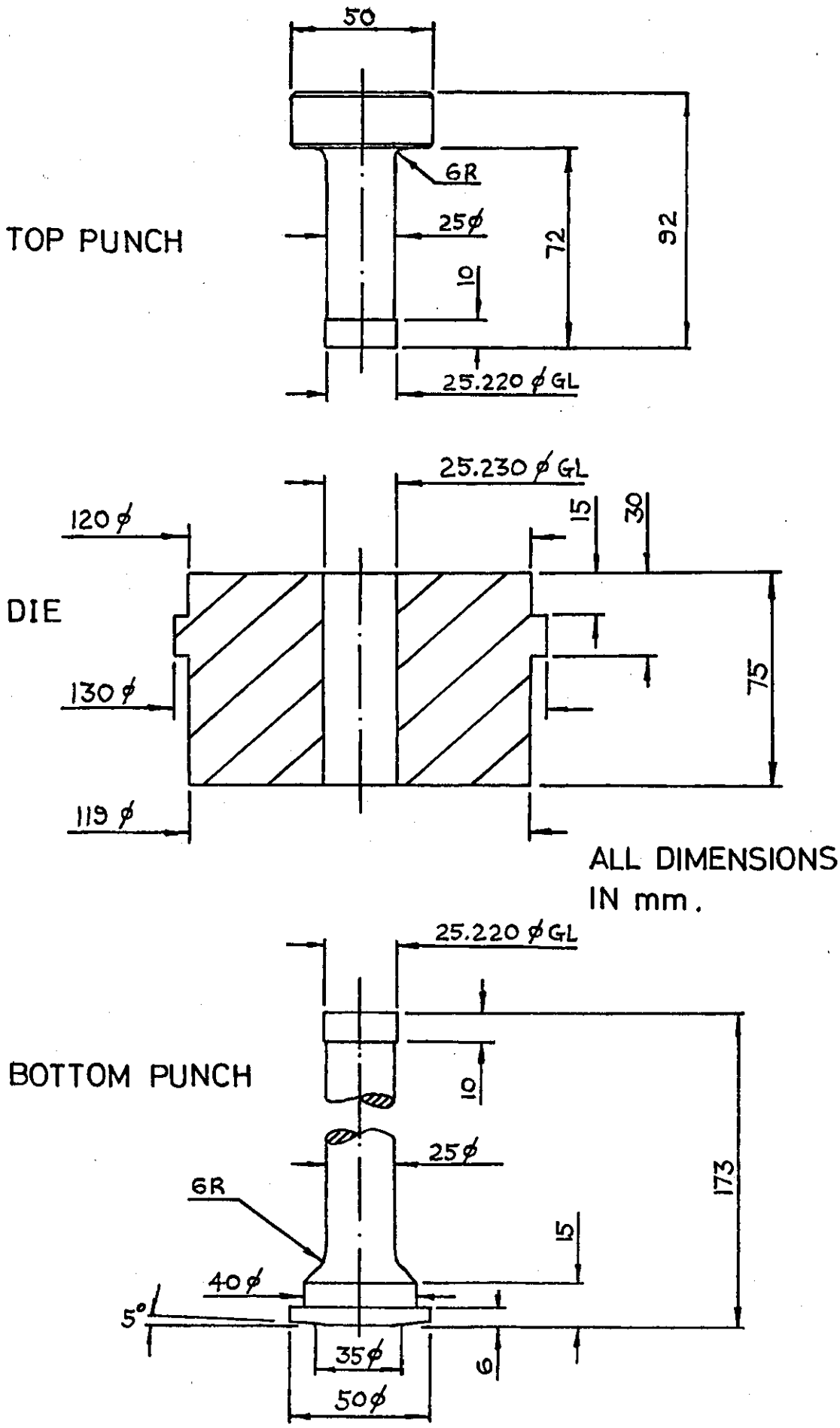

FIGURE 7

Electrical circuit and positioning of strain gauges on punches

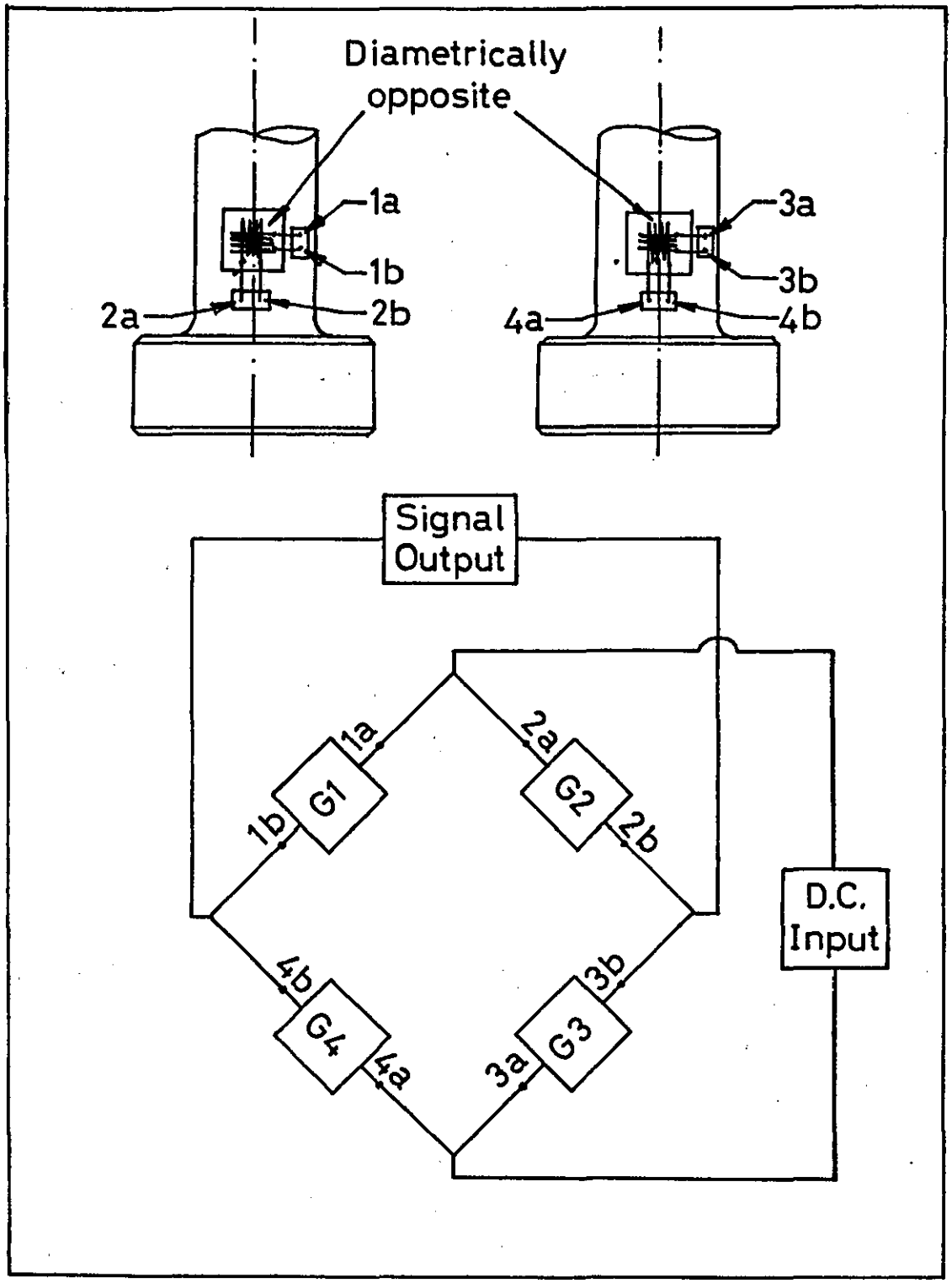
Diametrically
opposite
1a
1b
2a
2b
3a
3b
4a
4b
Signal
Output
G1
G2
G3
G4
D.C.
Input

Fig.7.

FIGURE 8

Positions of strain gauges on punches and die collar

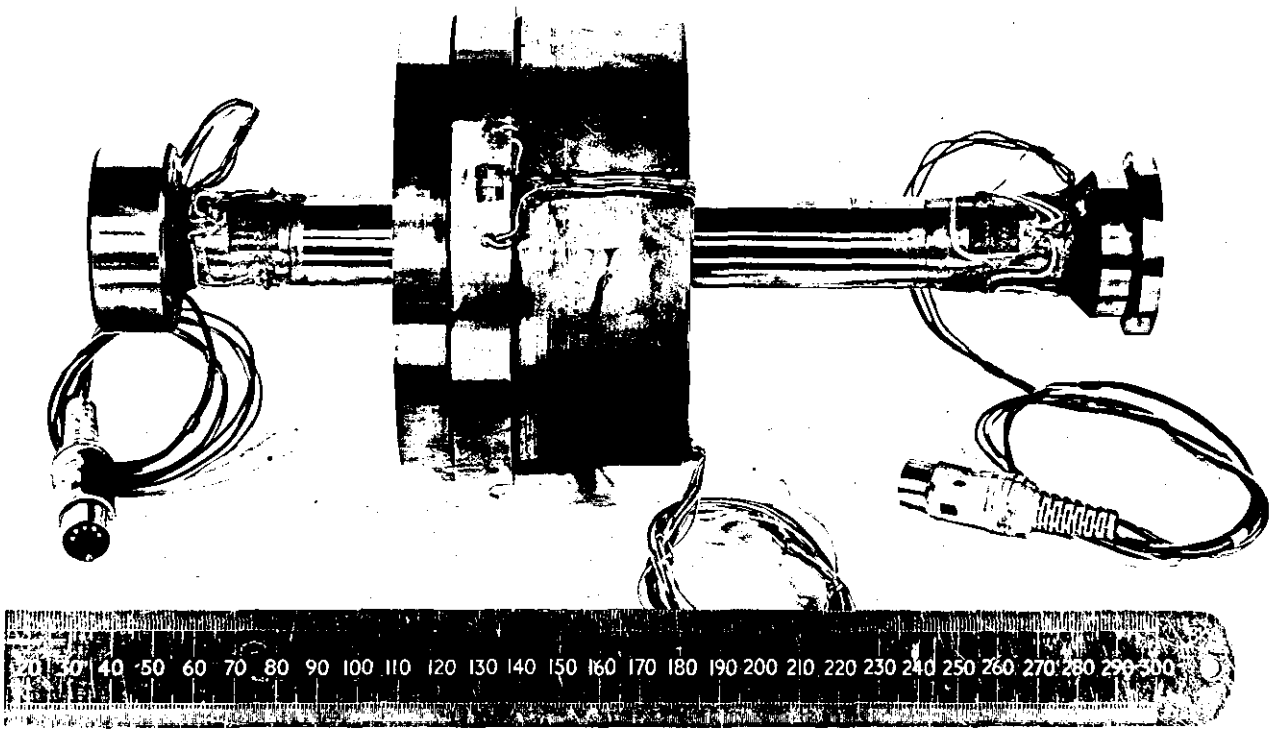
30 40 50 60 70 80 90 100 110 120 130 140 150 160 170 180 190 200 210 220 230 240 250 260 270 280 290 300

FIGURE 9

Electrical circuit for rectilinear potentiometer
to measure top punch motion

MEASUREMENT OF TOP PUNCH MOTION

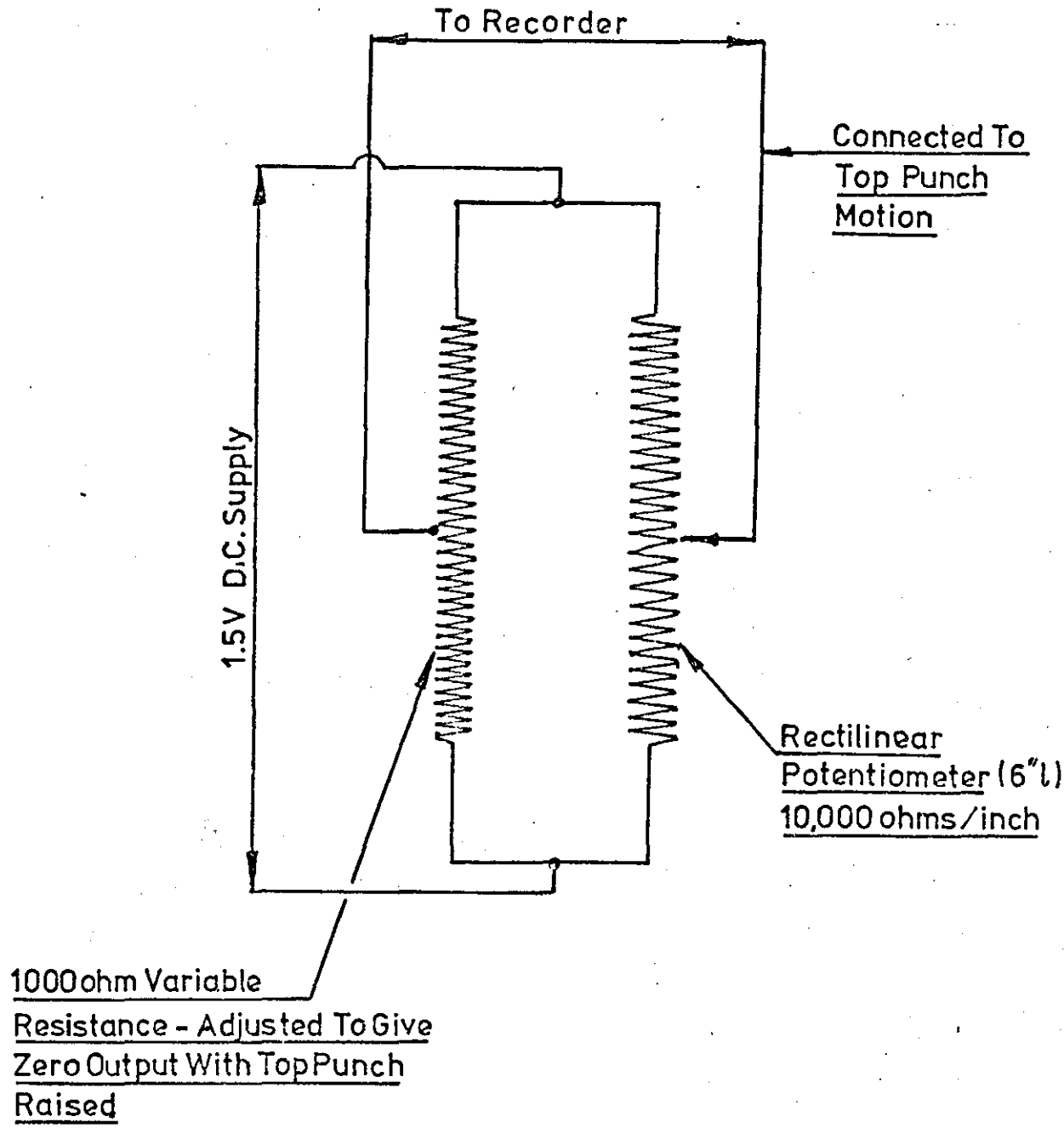

FIGURE 10

Method of die strain gauge calibration

DIE STRAIN GAUGE CALIBRATION
(Using Denison Mechanical Test M/C)

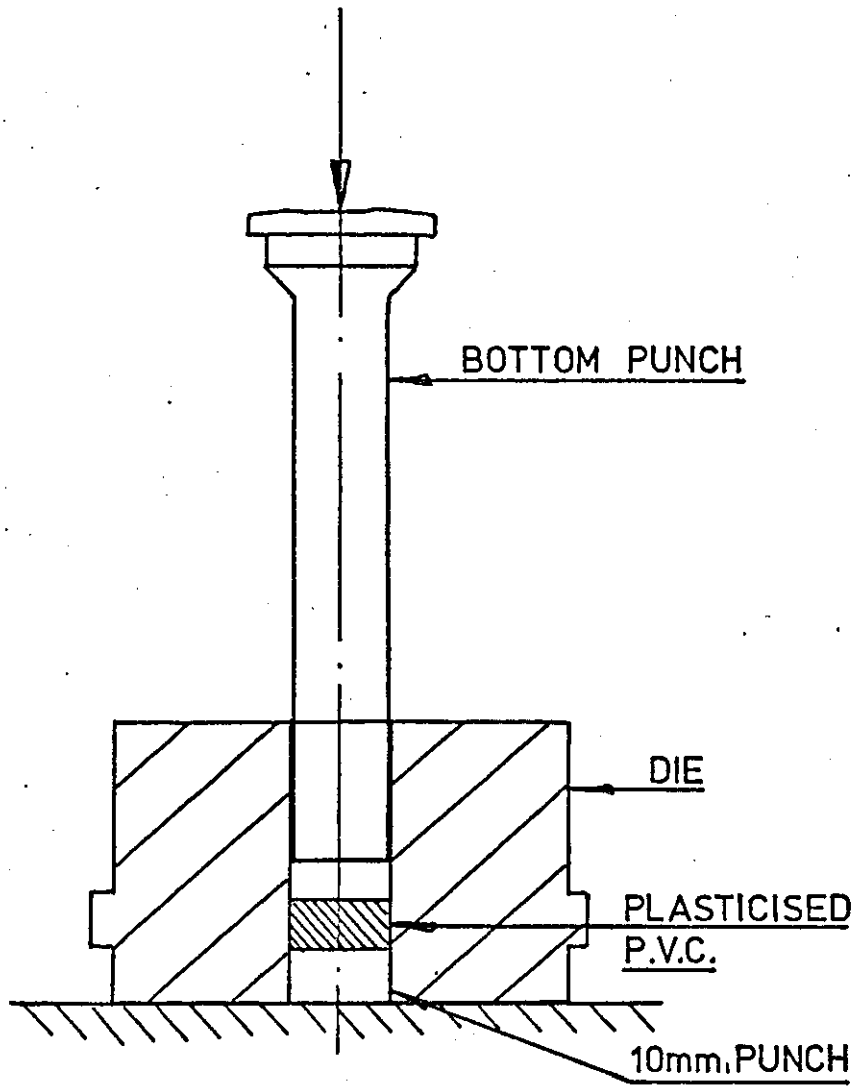

FIGURE 11

Apparatus for density measurement of irregular porous compacts - the Mercury Balance

APPARATUS FOR DENSITY MEASUREMENT OF IRREGULAR POROUS COMPACTS

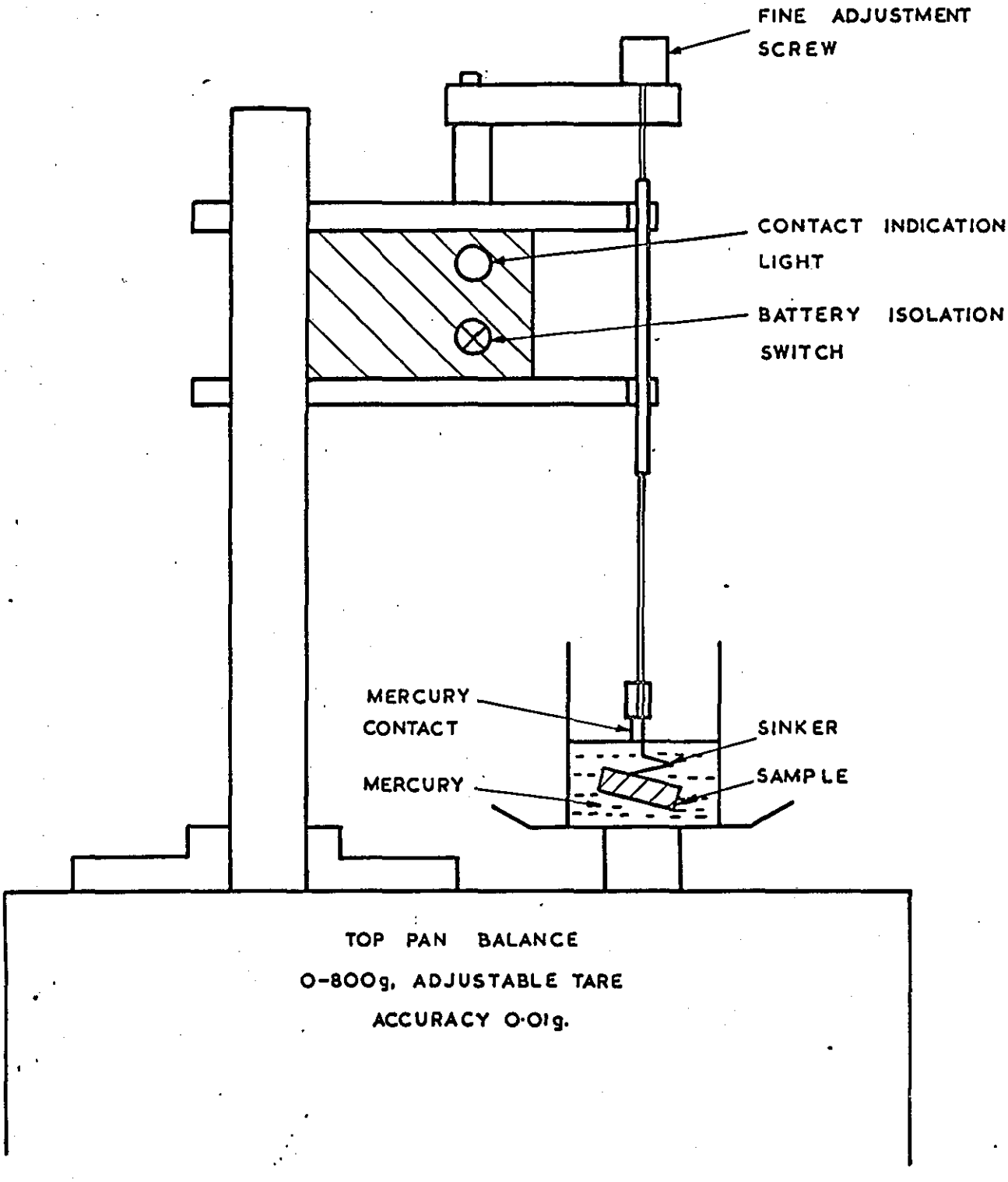

FIGURE 12

Method of compression testing of compacts
and typical stress-strain diagram obtained

(a)

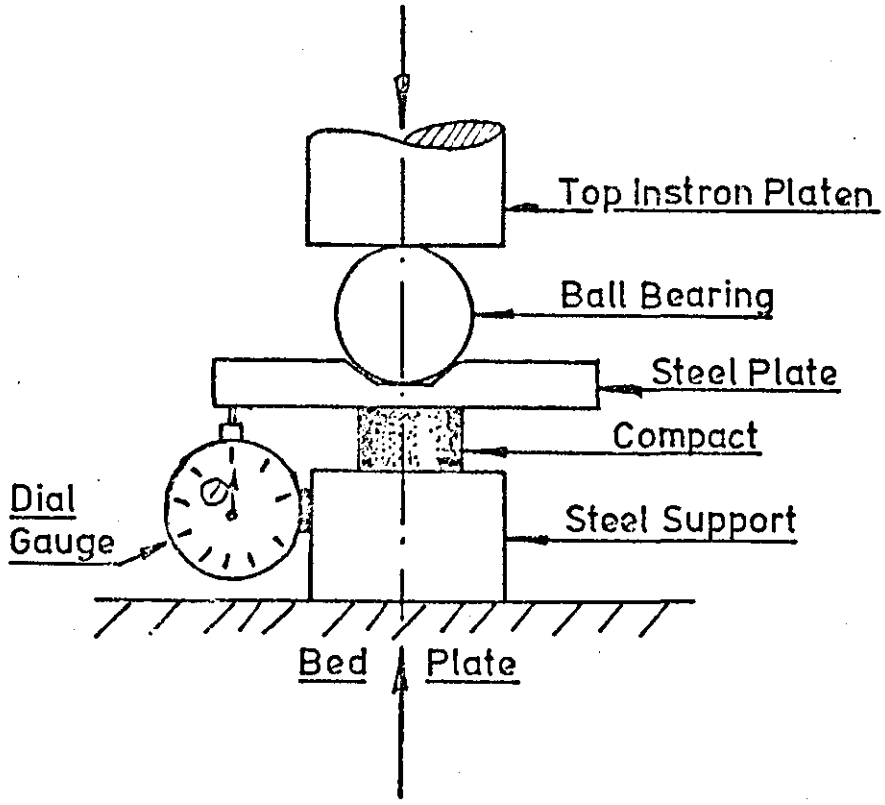

DETERMINATION OF ELASTIC BEHAVIOUR OF COMPACTS

(b)

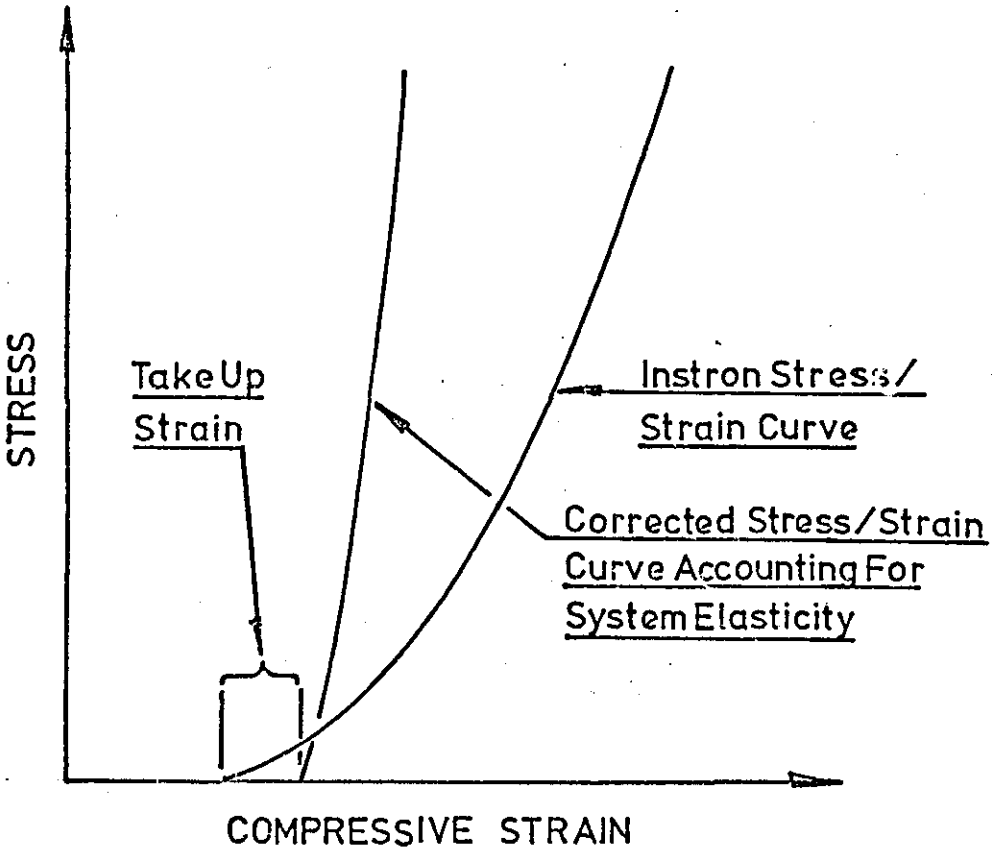

FIGURE 13

Graphical method for determination of secant modulus values

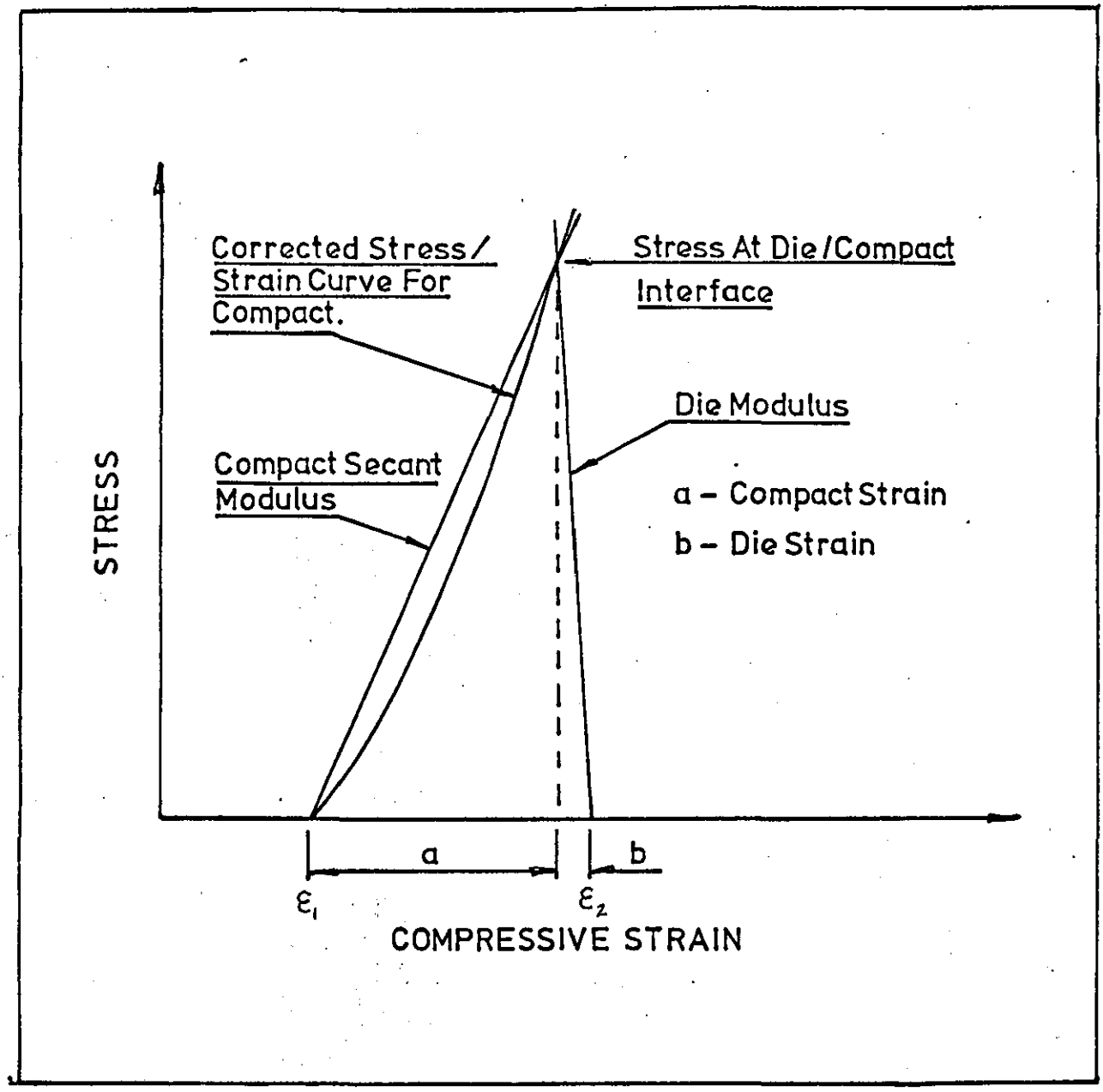
Corrected Stress / Strain Curve For Compact.
Stress At Die / Compact Interface
Die Modulus
Compact Secant Modulus
a – Compact Strain
b – Die Strain
STRESS
a
b
ε_1
ε_2
COMPRESSIVE STRAIN

FIGURE 14

"Pin and disc" apparatus for determination of friction coefficients

(a) General view of the apparatus

(b) View of "pin" mounting arm

(c) Overpage: view of wear traces on "discs": Disc A: High Chromium steel
Disc B: Tungsten Carbide
Disc C: Glass-ceramic

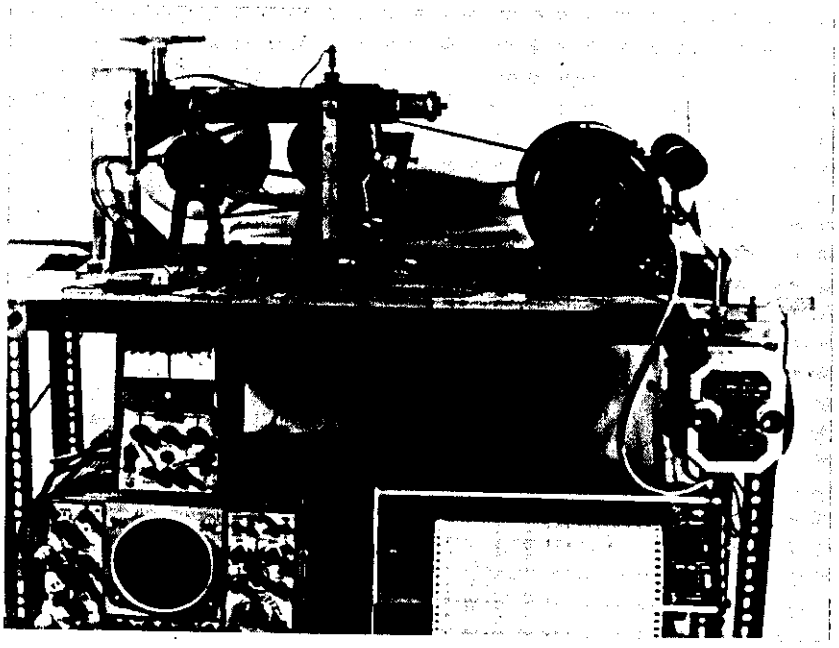

(a)

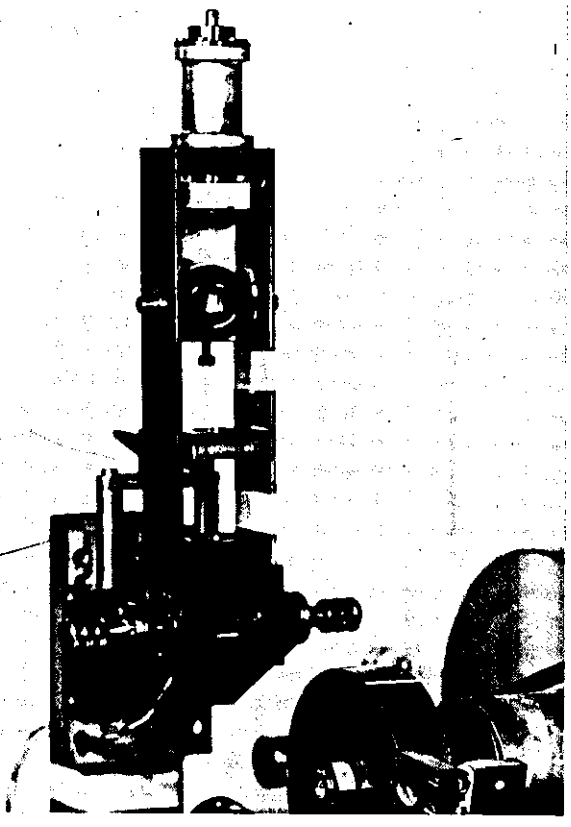

(b)

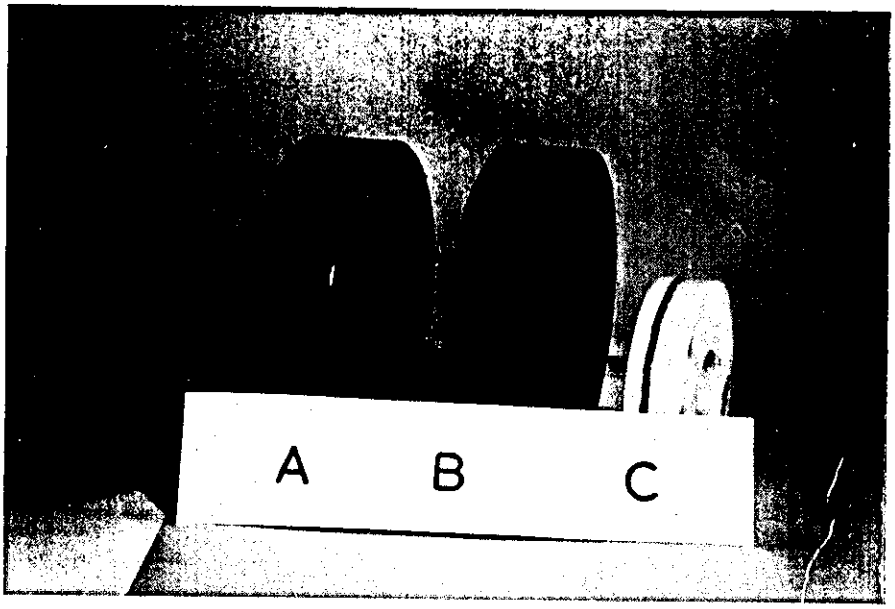

(c)

FIGURE 15

Method used to determine contact resistance

Circuit for measurement of electrical resistance

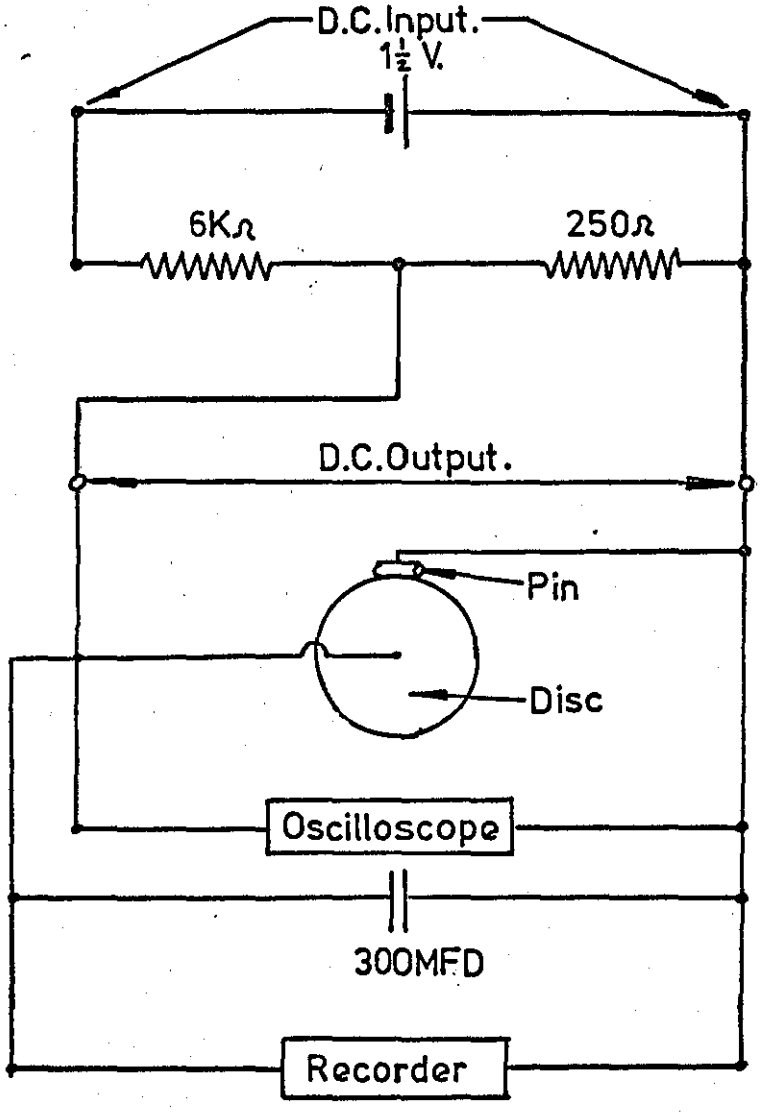

FIGURE 16

Graph of output versus contact resistance between pin and disc

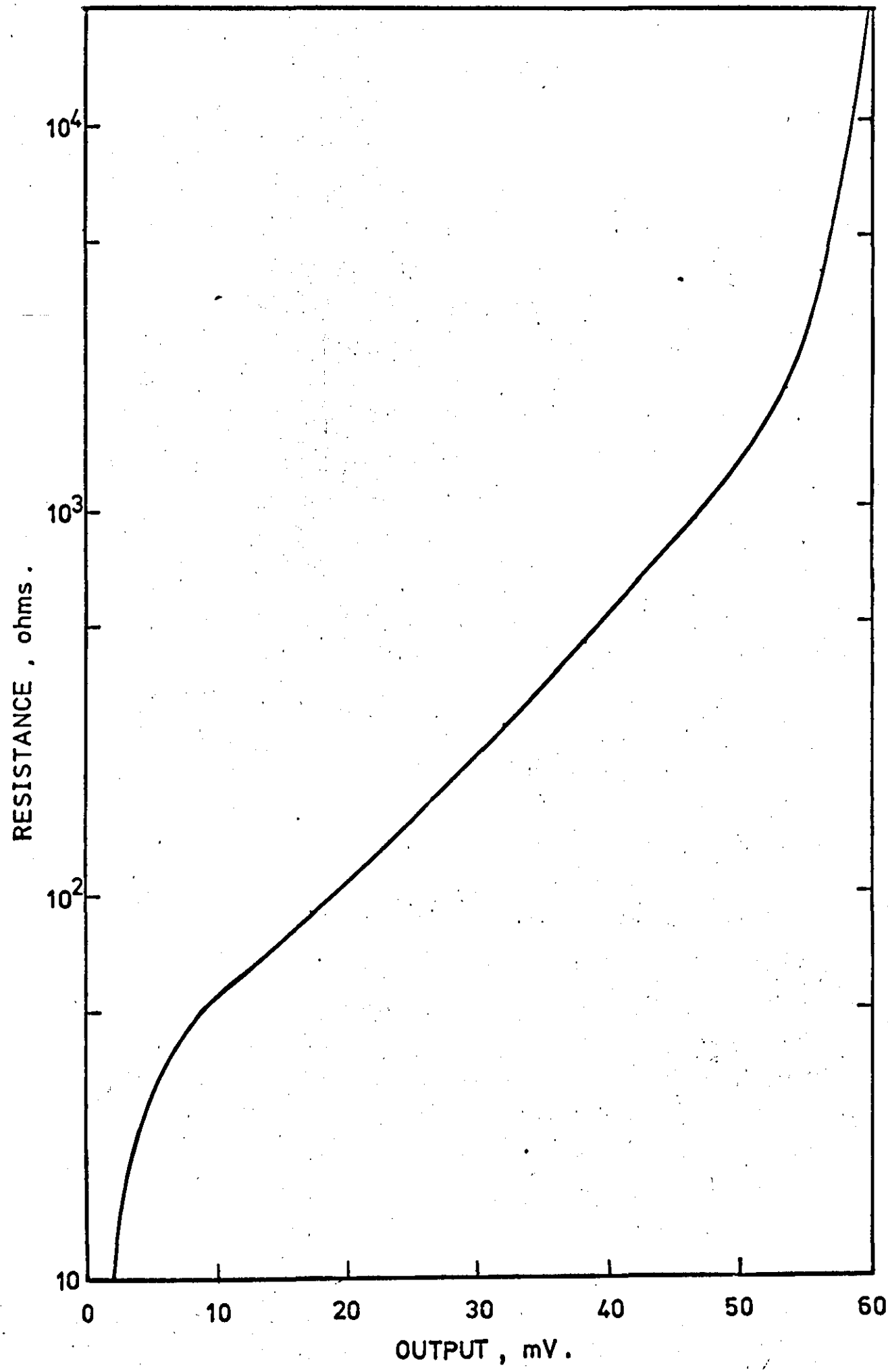
10^4
10^3
10^2
10
RESISTANCE , ohms .
0
10
20
30
40
50
60
OUTPUT , mV .

FIGURE 17

Particle size distribution for J.J.Makins 100 P.1 reduced iron powder

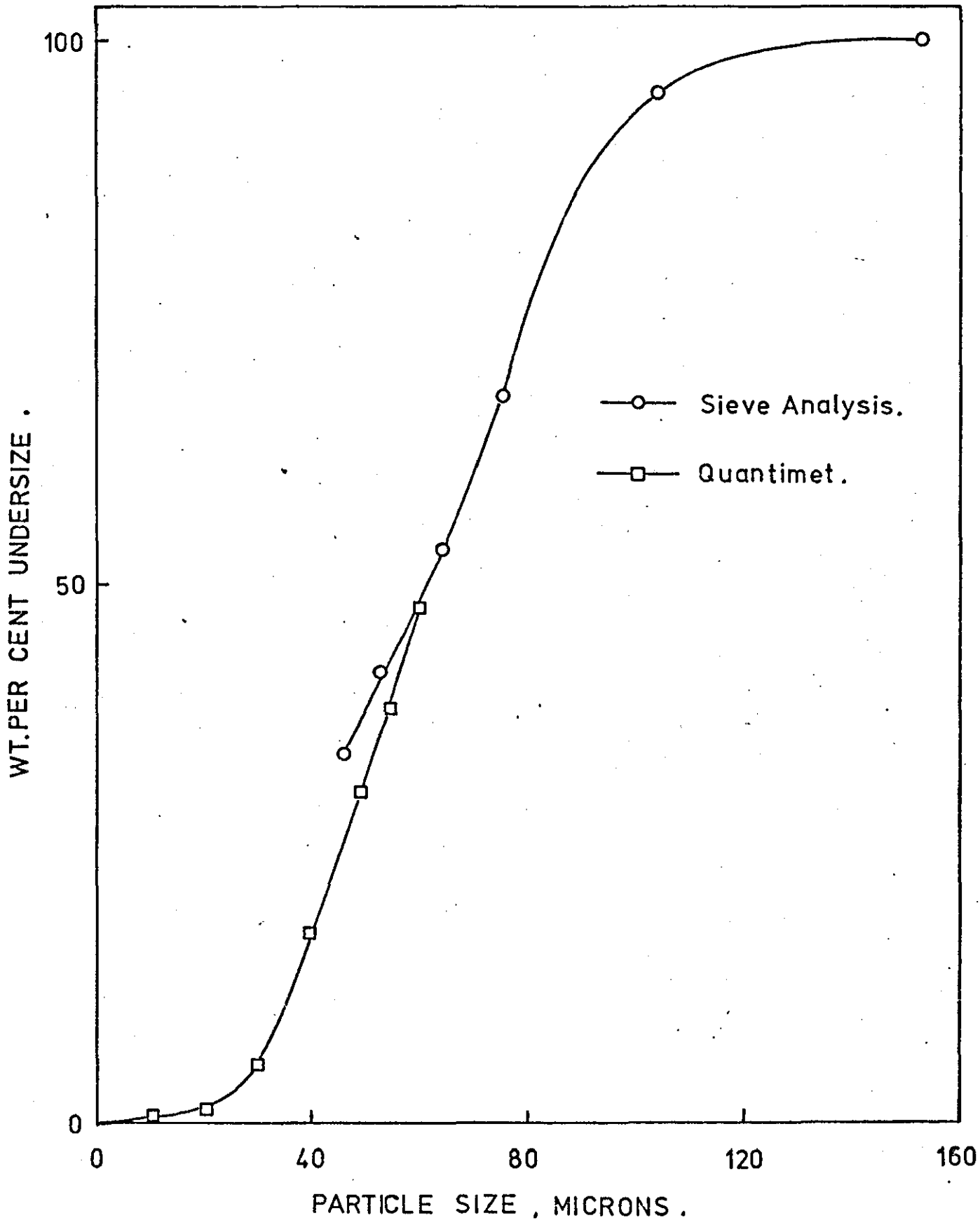
100
50
0
0
40
80
120
160
WT.PER CENT UNDERSIZE .
PARTICLE SIZE , MICRONS .
Sieve Analysis.
Quantimet .

FIGURE 18

Scanning Electron Microscope photographs of J. J. Makins 100 P1 reduced iron powder particles.

(a) Particles X 480

(b) Particles X 4800

(๙)

(๐)

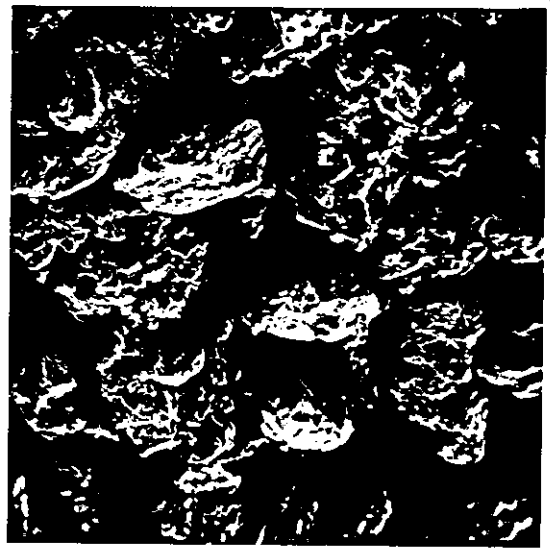

FIGURE 19

Scanning Electron Microscope photographs
of metal stearate particles

(a) Durham Zinc Stearate Grade 'S' X 11000

(b) Durham Zinc Stearate Grade 'A' X 5000

(c) Durham Calcium Stearate Grade 'A' X 5000

(d) Durham Lithium Stearate Grade 'A' X 5000

(a)

(b)

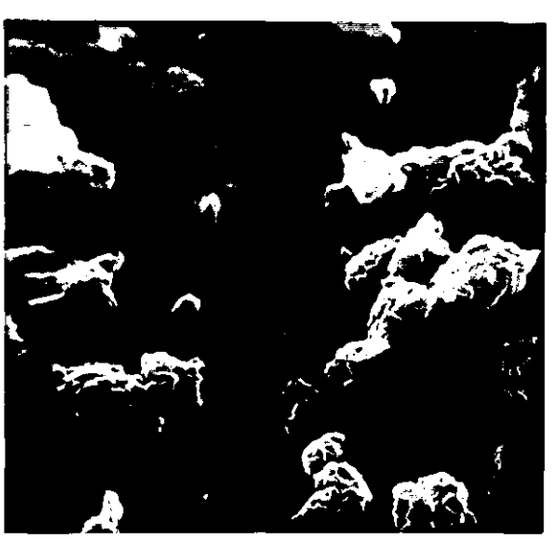

(c)

(d)

(a)

(b)

(c)

(d)

FIGURE 20

Iron Powder Particle surfaces before and after mixing with 1% zinc stearate 1:

(a) Particle having irregular surfaces

(b) Particle having more plain surfaces

(c) Particle having both plain and irregular surfaces

(b)

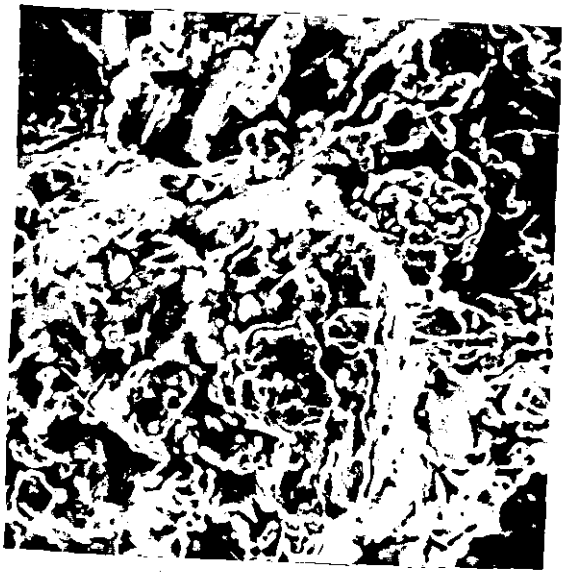

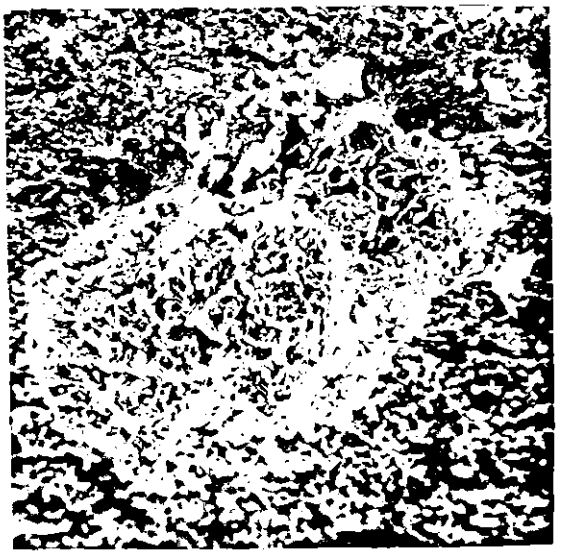

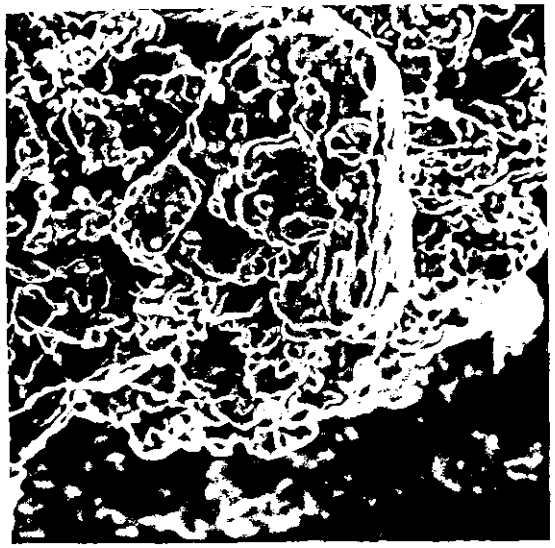

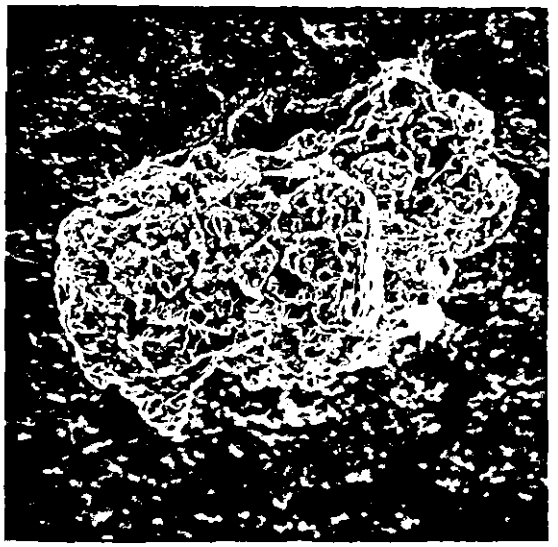

(b)

(c)

FIGURE 21

True Density - Compaction Pressure relationships obtained for unlubricated iron powder, showing the effect of Height/Diameter ratio on the compressibility.

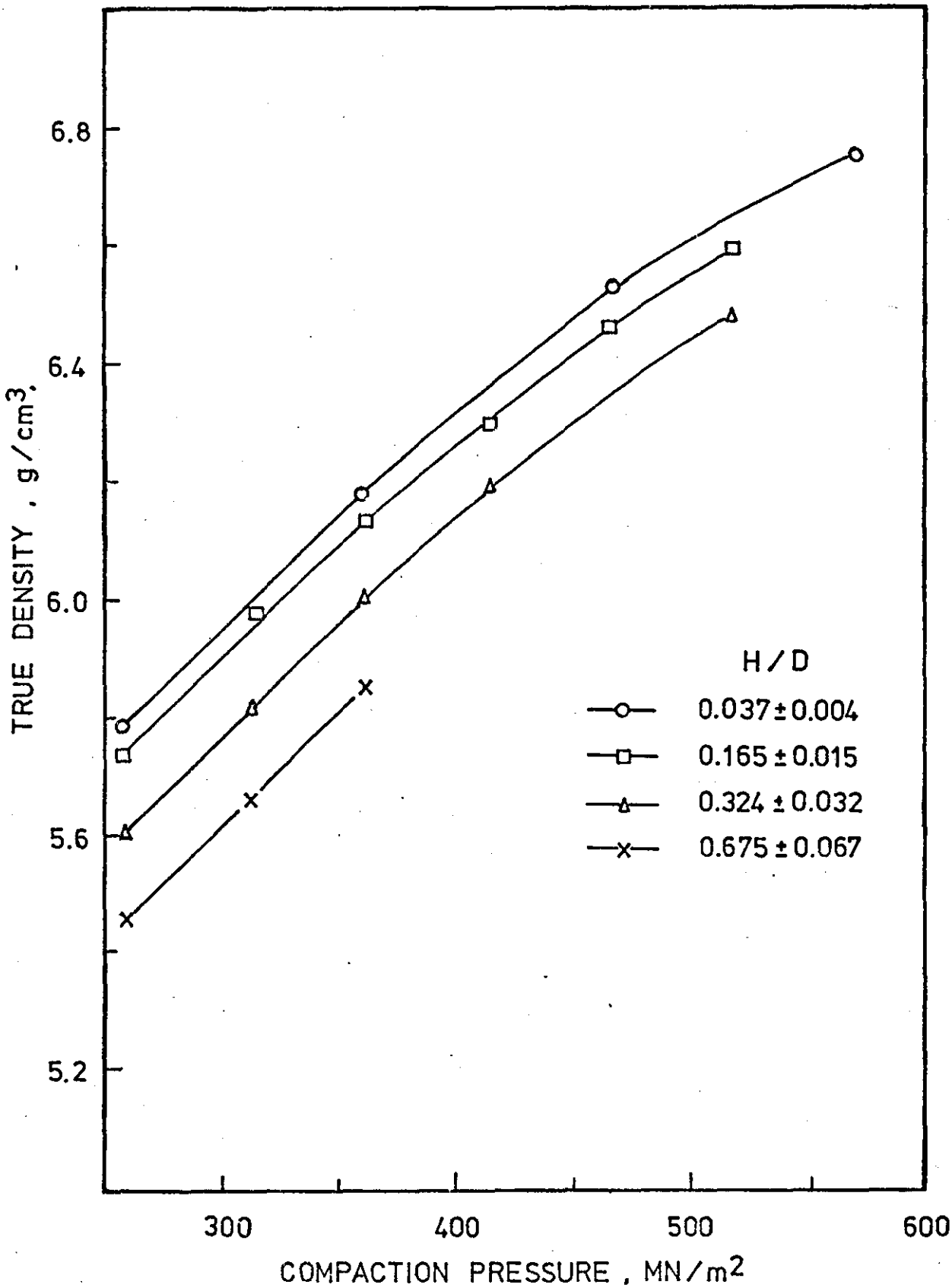
6.8
6.4
6.0
5.6
5.2
TRUE DENSITY , g/cm3.
300
400
500
600
COMPACTION PRESSURE , MN/m2
H/D
0.037±0.004
0.165±0.015
0.324±0.032
0.675±0.067

FIGURE 22

Typical Force - Distance curve obtained during the Laboratory Scale Studies of unlubricated iron compact ejection.

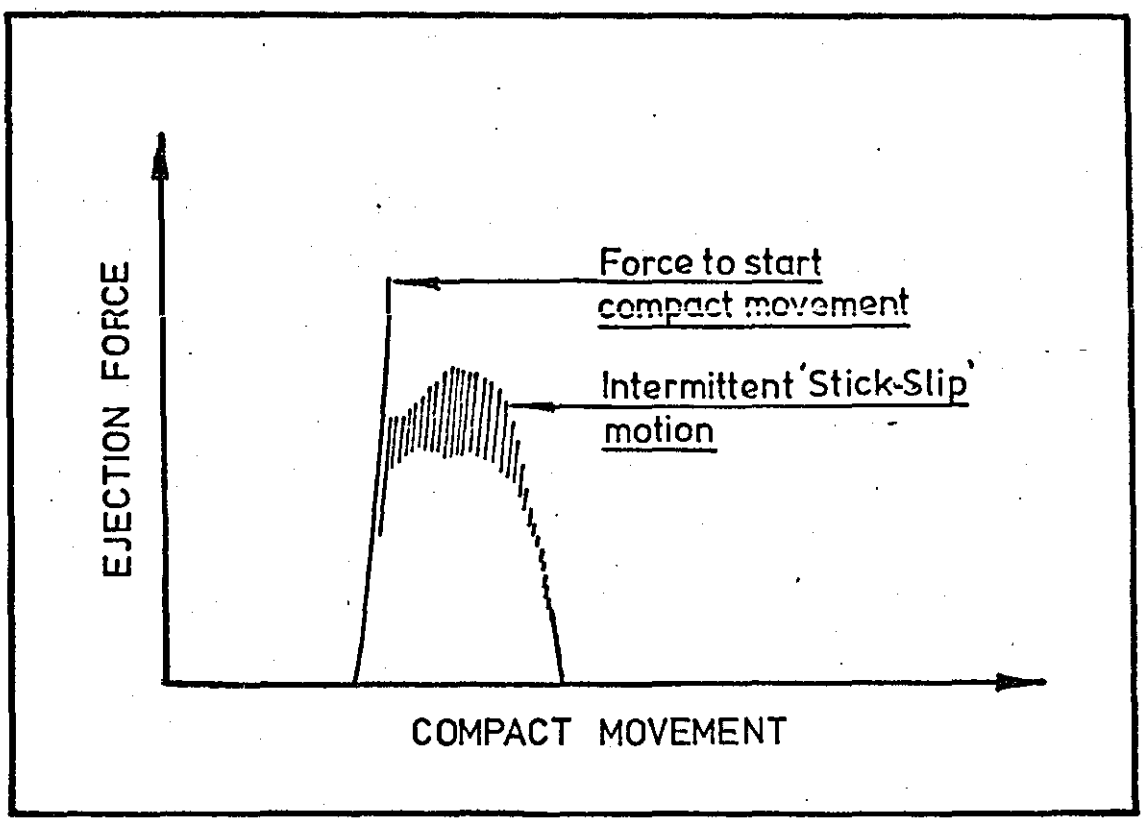
EJECTION FORCE
Force to start compact movement
Intermittent 'Stick-Slip' motion
COMPACT MOVEMENT

FIGURE 23

Ejection Stress - True Density relationships obtained for unlubricated iron powder, showing the effect of Height/Diameter ratio and Ejection Speed on the ejection behaviour.

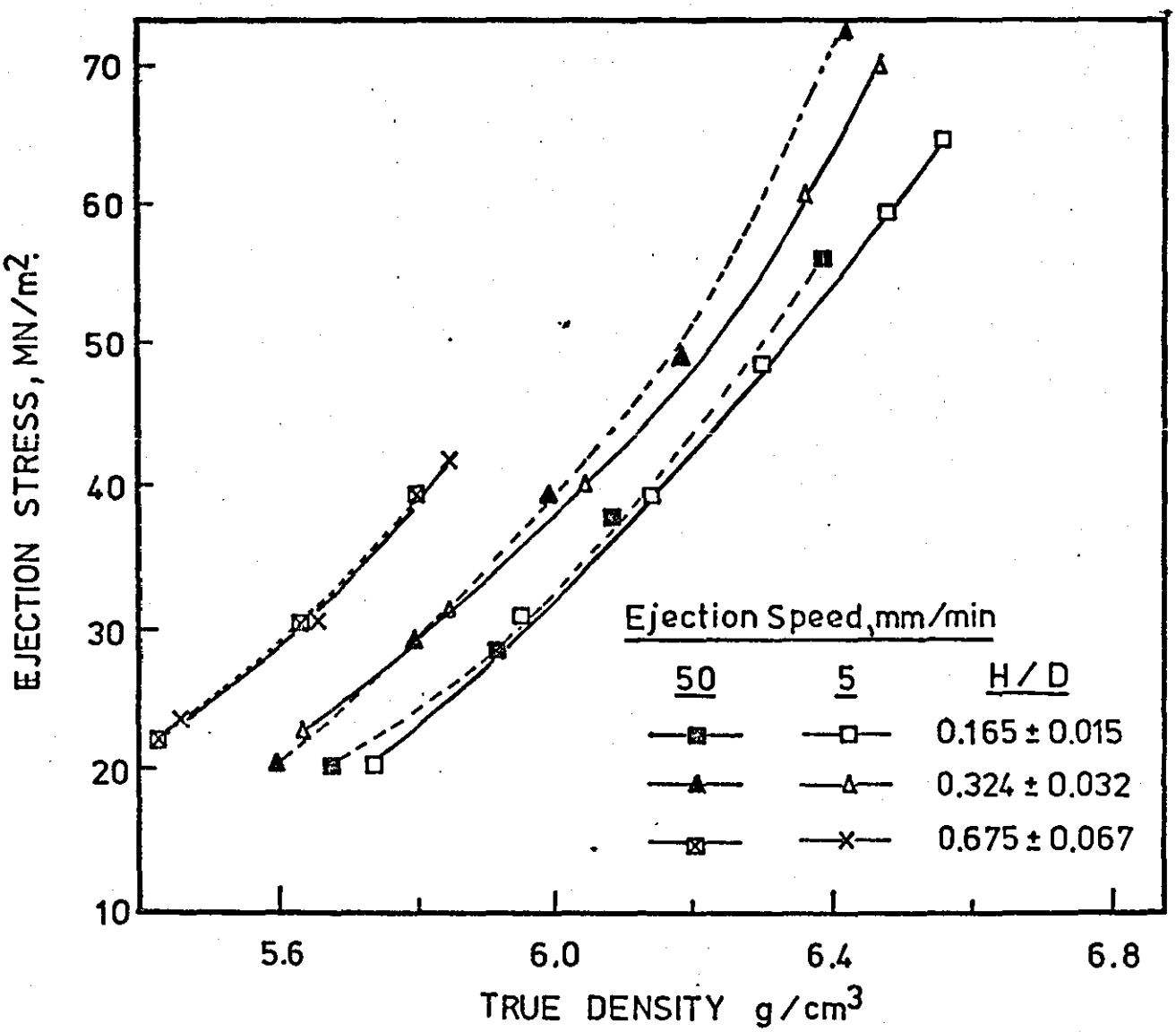
EJECTION STRESS, MN/m²
70
60
50
40
30
20
10
5.6
6.0
6.4
6.8
TRUE DENSITY g/cm³
Ejection Speed, mm/min
50
5
H/D
0.165 ± 0.015
0.324 ± 0.032
0.675 ± 0.067

FIGURE 24

True Density - Compaction Pressure relationship obtained for iron powder lubricated with 1 wt.% of zinc stearate I.

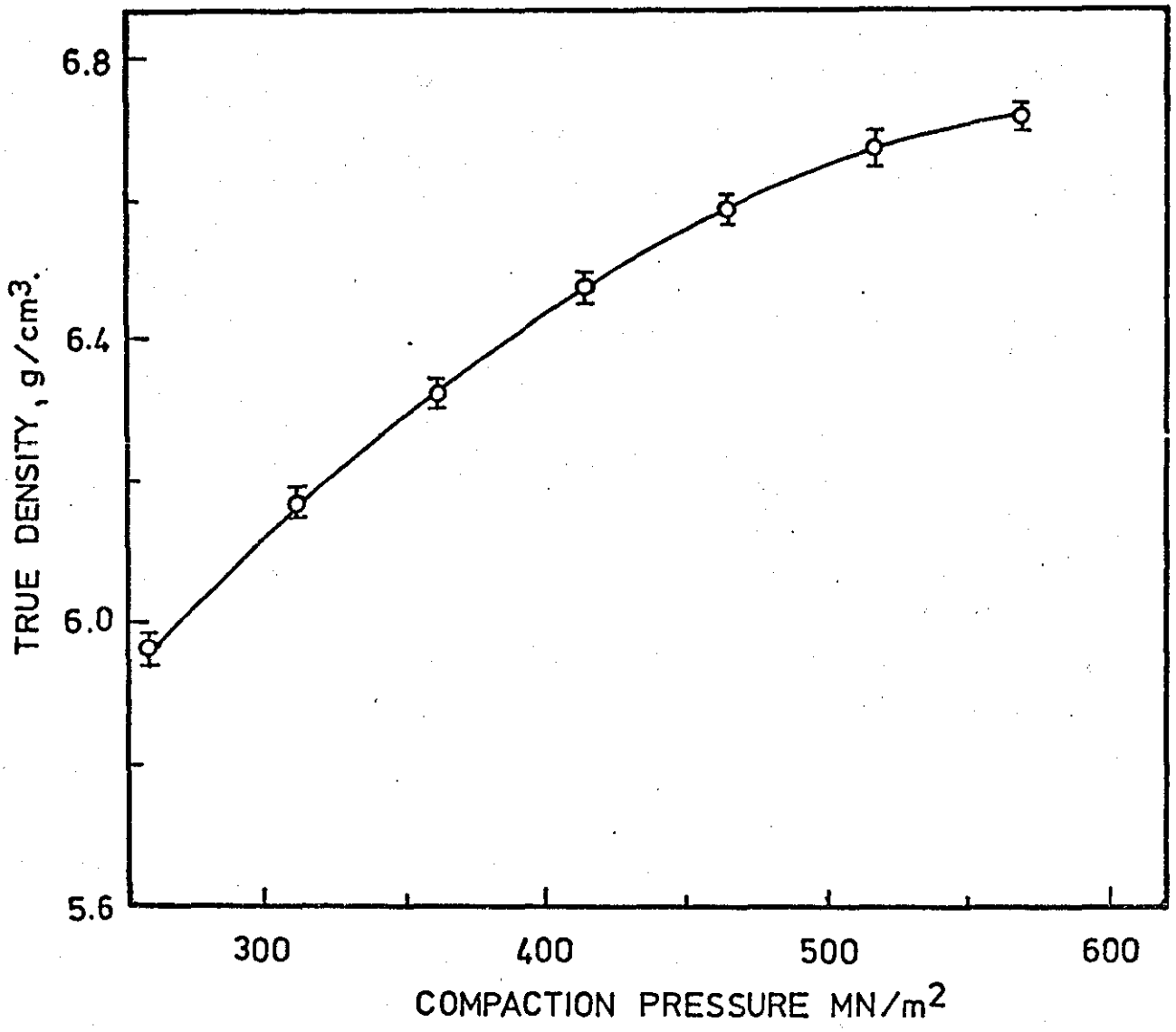
6.8
6.4
6.0
5.6
TRUE DENSITY, g/cm3.
300
400
500
600
COMPACTION PRESSURE MN/m2

FIGURE 25

Variation of True Density at constant pressure with Zinc Stearate I content for three compaction pressures during laboratory scale studies.

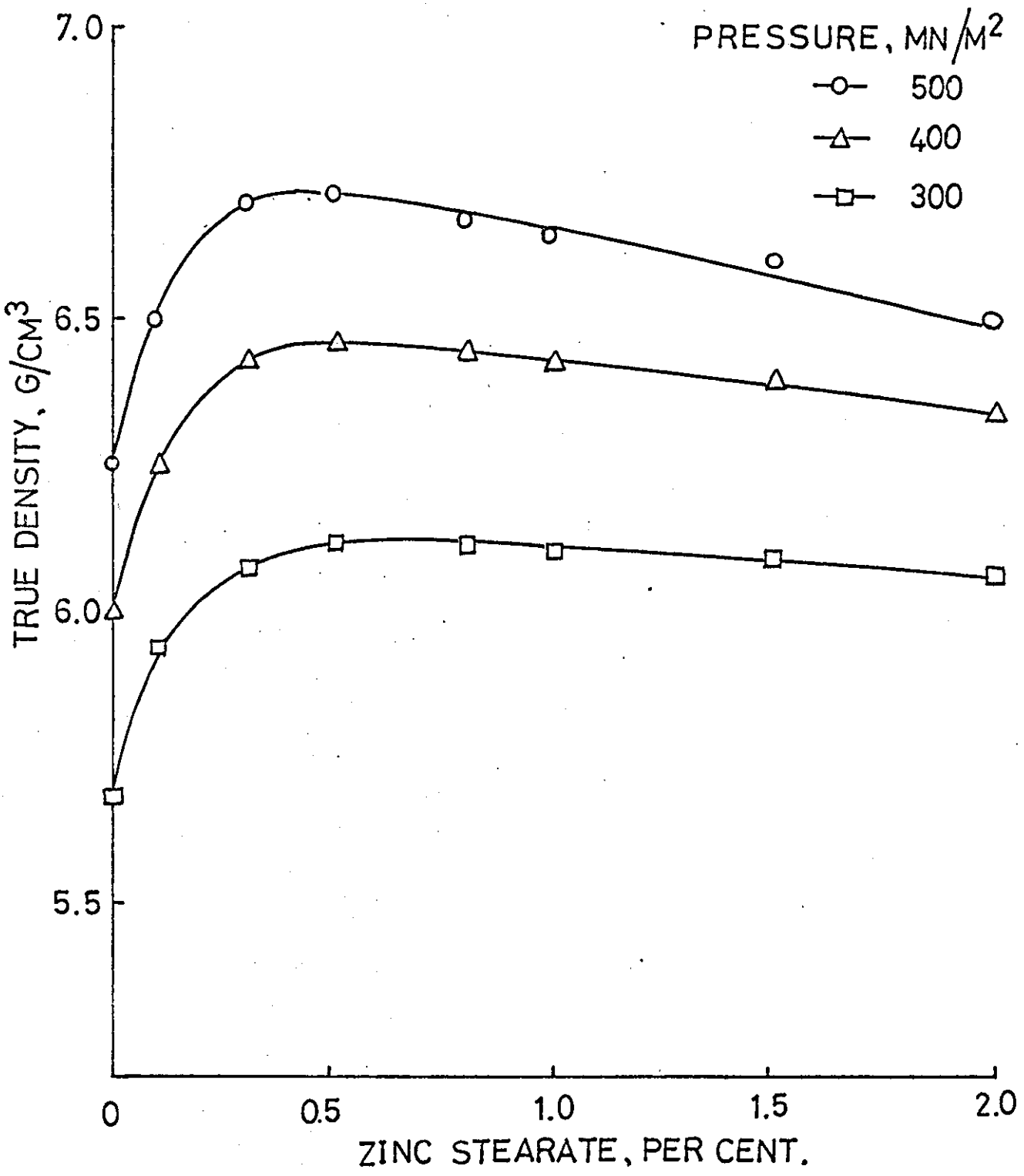
PRESSURE, MN/M2
500
400
300
7.0
6.5
6.0
5.5
TRUE DENSITY, G/CM3
0
0.5
1.0
1.5
2.0
ZINC STEARATE, PER CENT.

FIGURE 26

Comparison of Ejection Stress - True Density behaviour for compacts of different Height/Diameter ratio, with and without 1 wt. % Zinc Stearate 1.

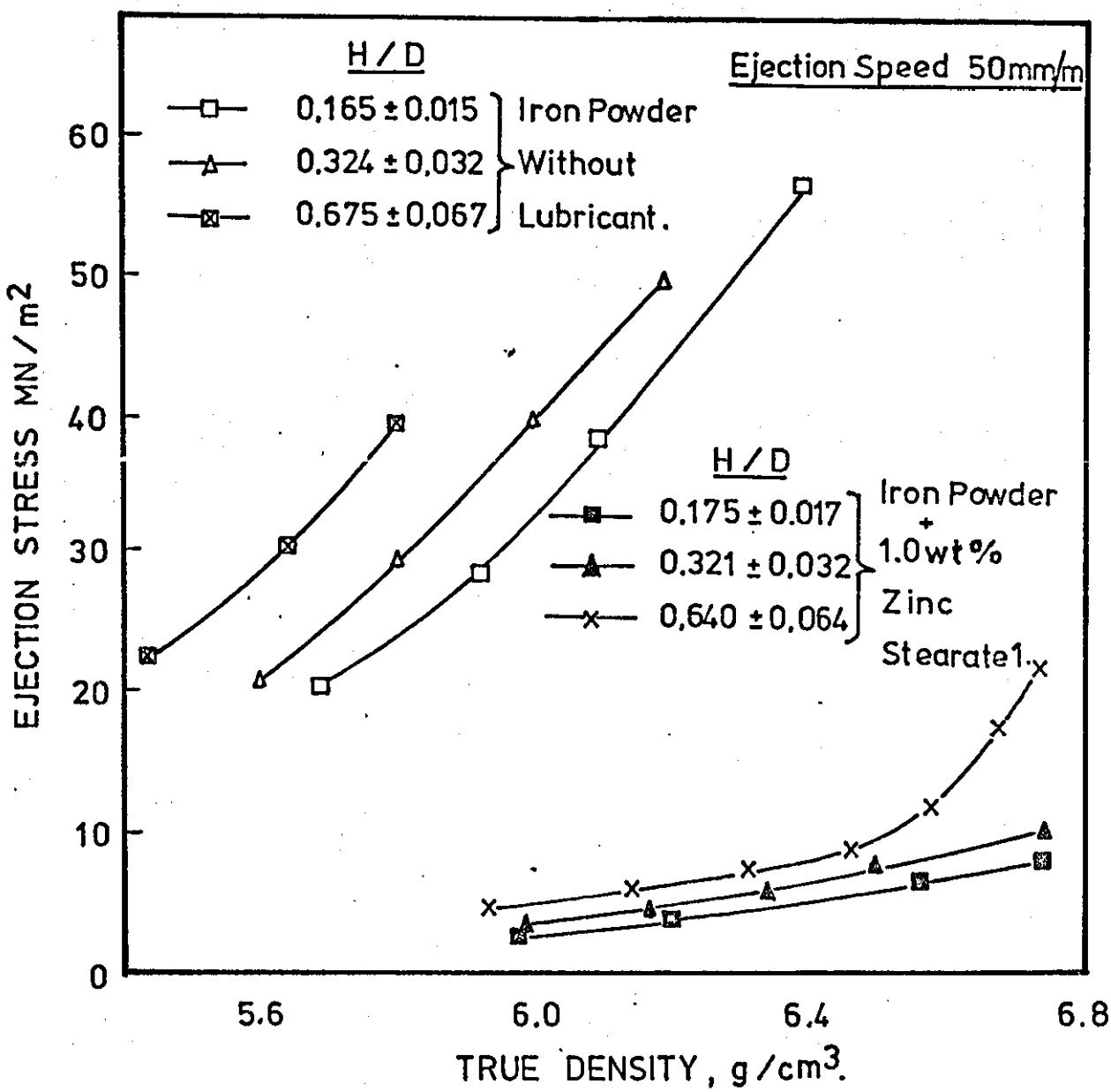
H / D
Ejection Speed 50mm/m
0.165 ± 0.015
0.324 ± 0.032
0.675 ± 0.067
Iron Powder
Without
Lubricant.
H / D
0.175 ± 0.017
0.321 ± 0.032
0.640 ± 0.064
Iron Powder
+
1.0 wt %
Zinc
Stearate1.
EJECTION STRESS MN / m2
TRUE DENSITY, g / cm3.
0
10
20
30
40
50
60
5.6
6.0
6.4
6.8

FIGURE 27

Effect of lubricant content on the Ejection Stress for compacts of the same true density.

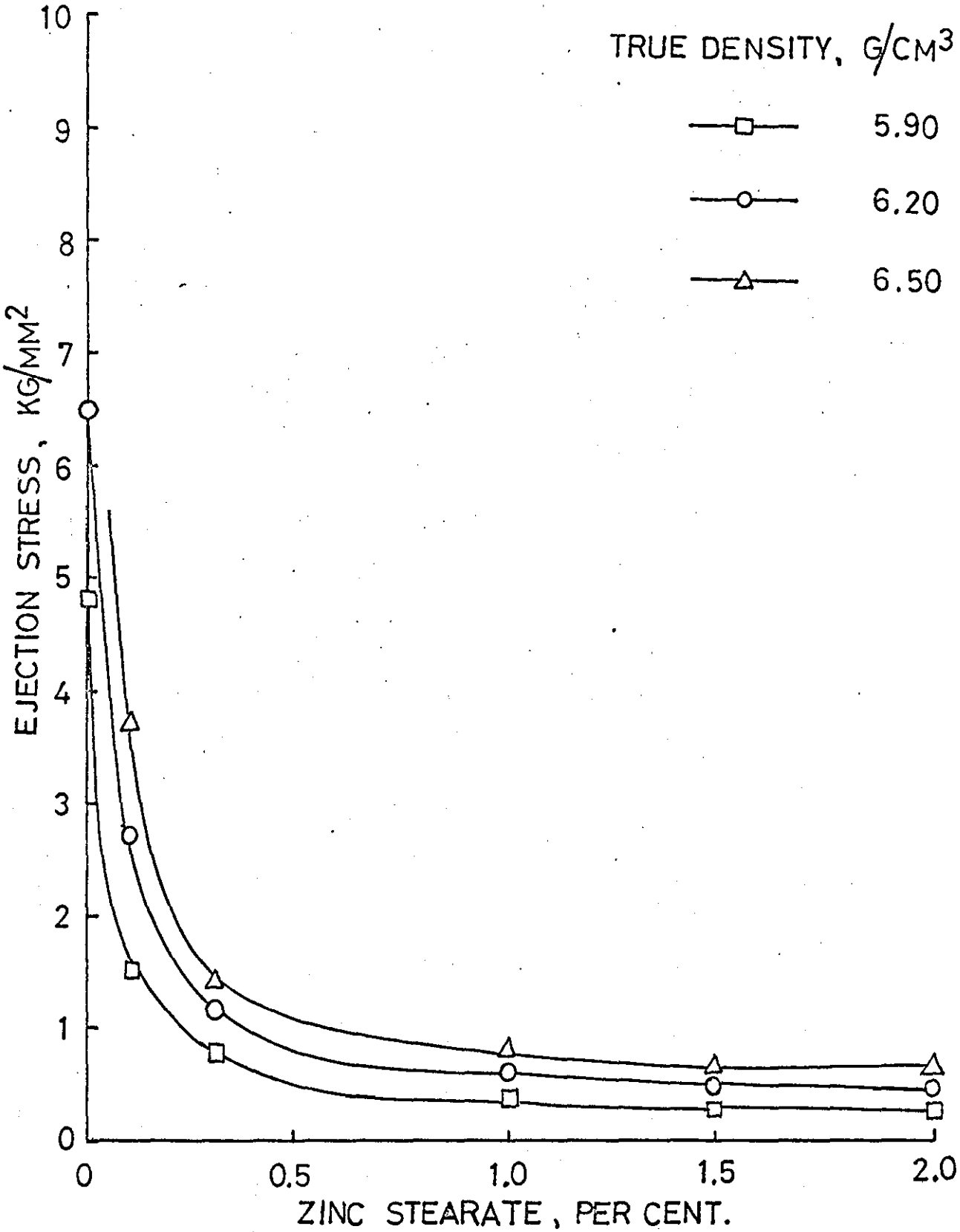
TRUE DENSITY, G/CM3
5.90
6.20
6.50
EJECTION STRESS, KG/MM2
10
9
8
7
6
5
4
3
2
1
0
0
0.5
1.0
1.5
2.0
ZINC STEARATE, PER CENT.

FIGURE 28

Ejection Stress - True Density relationships for compacts containing 1 wt.% Zinc Stearate from various sources. (See Appendix IV)

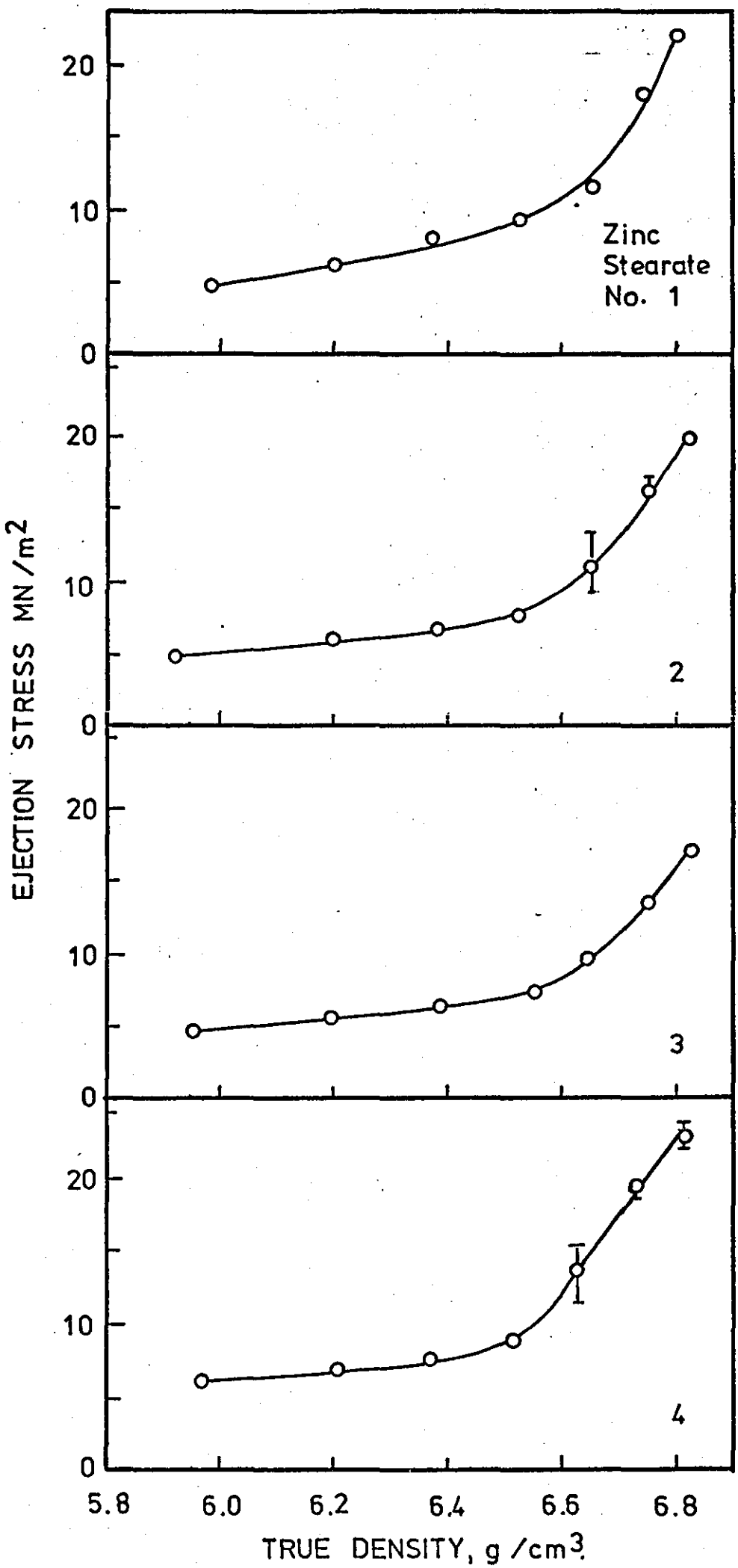
Zinc
Stearate
No. 1
2
3
4
EJECTION STRESS MN/m2
TRUE DENSITY, g/cm3
0
10
20
5.8
6.0
6.2
6.4
6.6
6.8

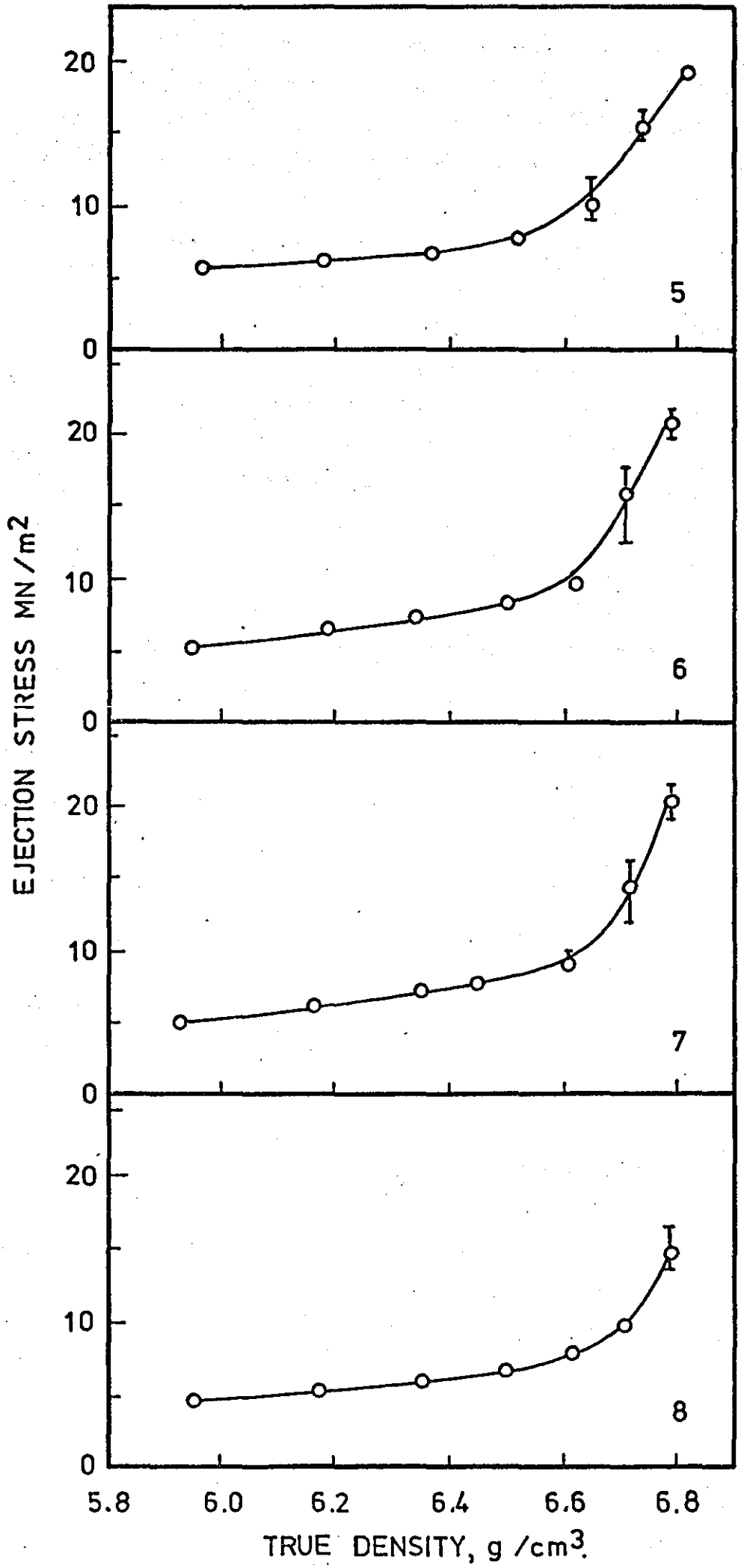
EJECTION STRESS MN/m2
20
10
0
5
6
7
8
5.8
6.0
6.2
6.4
6.6
6.8
TRUE DENSITY, g /cm3

FIGURE 29

Scanning Electron Microscope photographs of compact surfaces taken at intervals along the Ejection Stress - True Density curve.

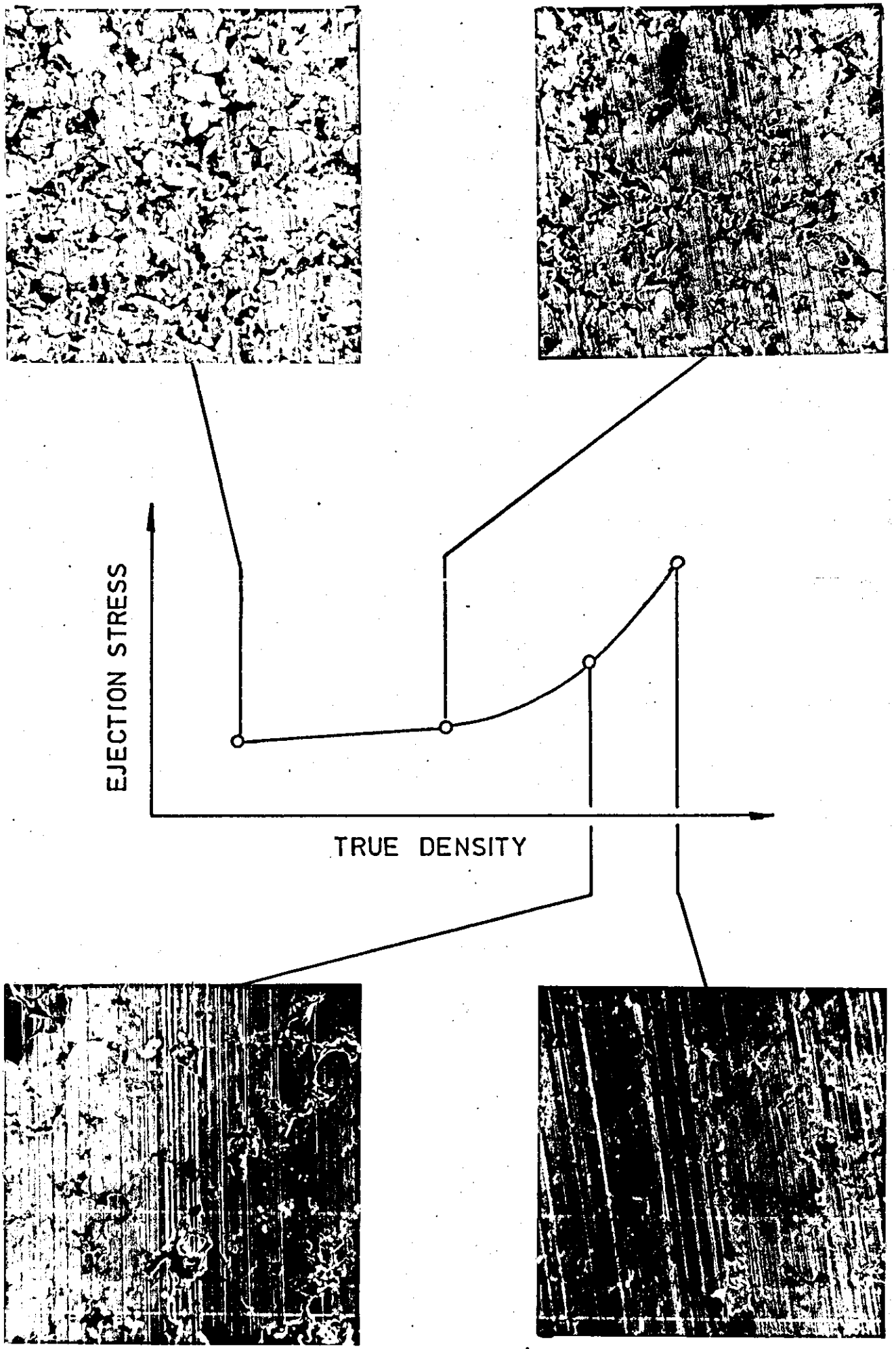
EJECTION STRESS
TRUE DENSITY

FIGURE 30

Ejection Stress - Compaction Pressure relationships for compacts containing 1 wt.% Zinc Stearate from various sources. (See Appendix IV).

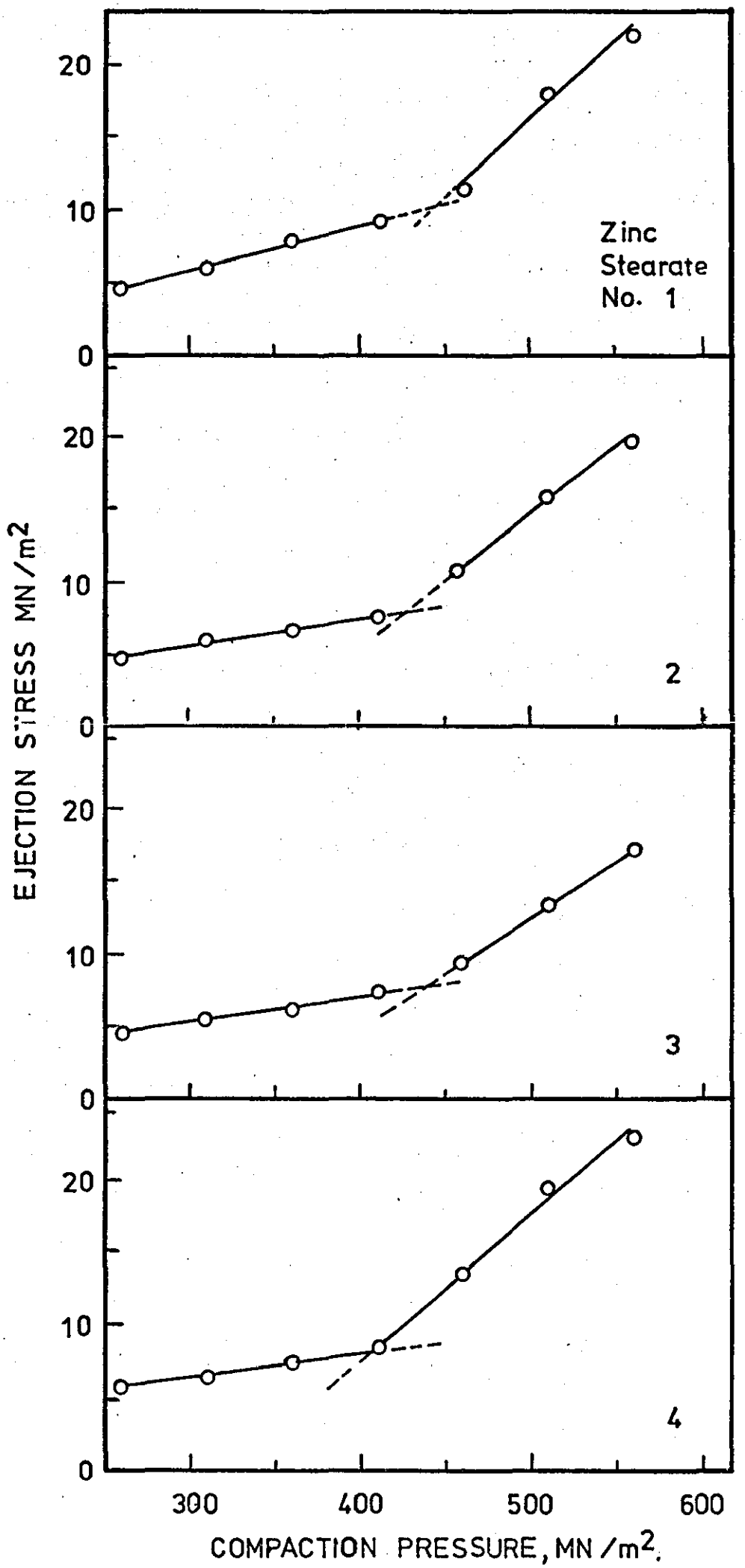
Zinc
Stearate
No. 1
2
3
4
EJECTION STRESS MN/m2
COMPACTION PRESSURE, MN/m2.
0
10
20
300
400
500
600

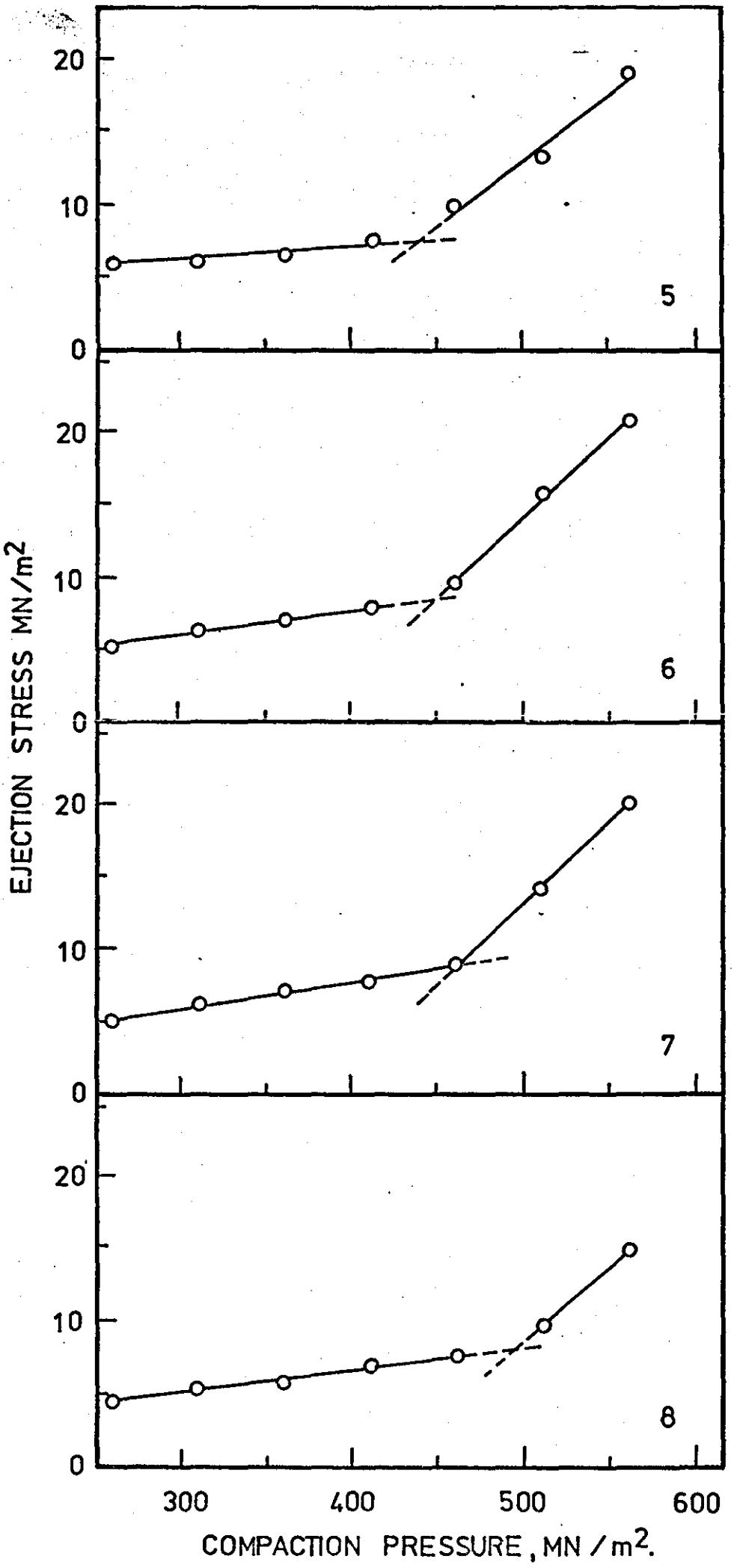
EJECTION STRESS MN/m2
20
10
0
5
6
7
8
300
400
500
600
COMPACTION PRESSURE, MN / m2.

FIGURE 31

Effect of Die Surface Finish upon Ejection Stress for compacts containing 1 wt.% Zinc Stearate I pressed to different density levels.

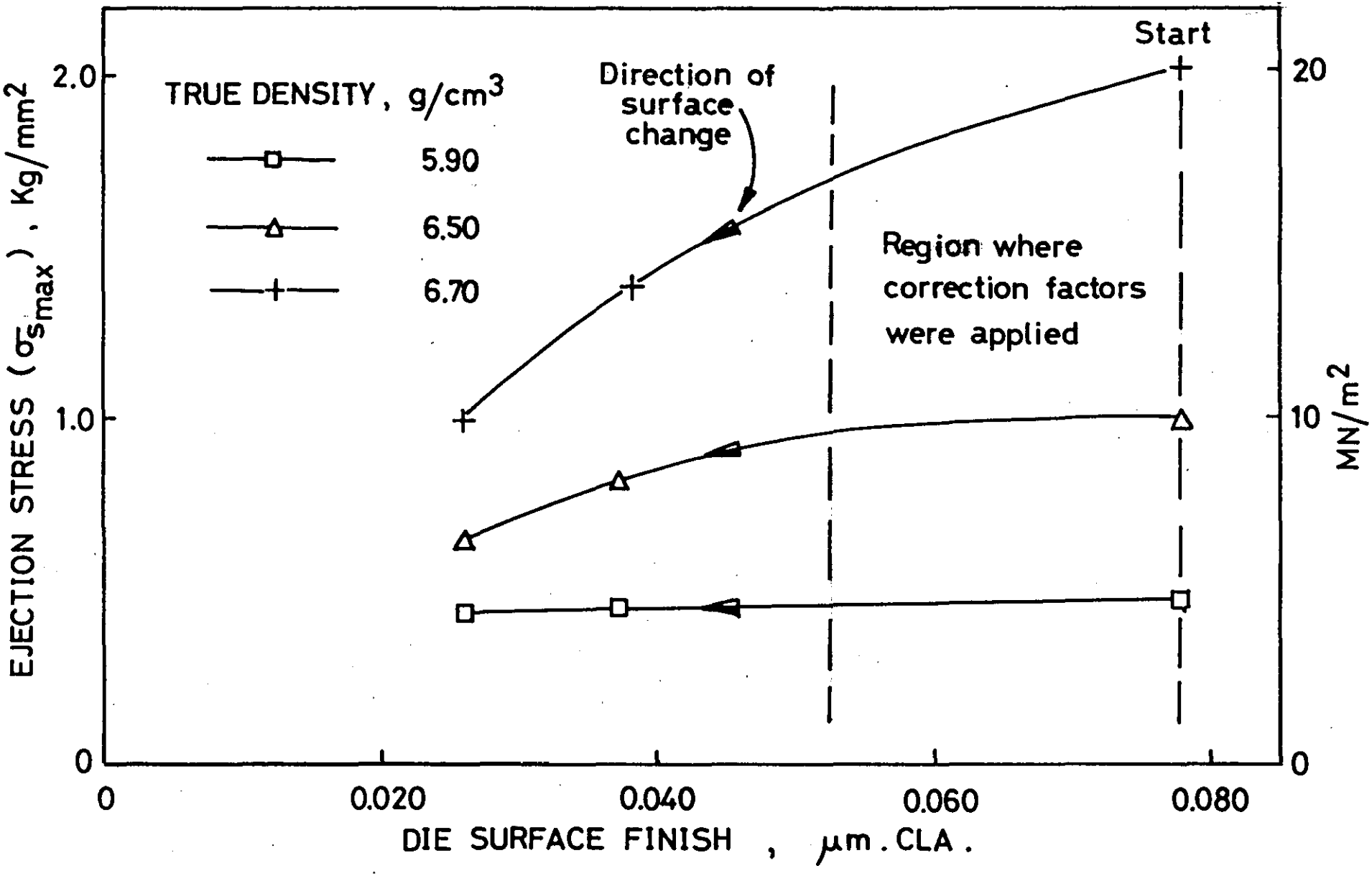
Start
Direction of surface change
TRUE DENSITY, g/cm3
5.90
6.50
6.70
Region where correction factors were applied
EJECTION STRESS (σsmax), Kg/mm2
MN/m2
2.0
1.0
0
20
10
0
0.020
0.040
0.060
0.080
DIE SURFACE FINISH, μm. CLA.

FIG. 31.

FIGURE 32

"Talysurf" traces obtained from the laboratory scale die during ejection studies.

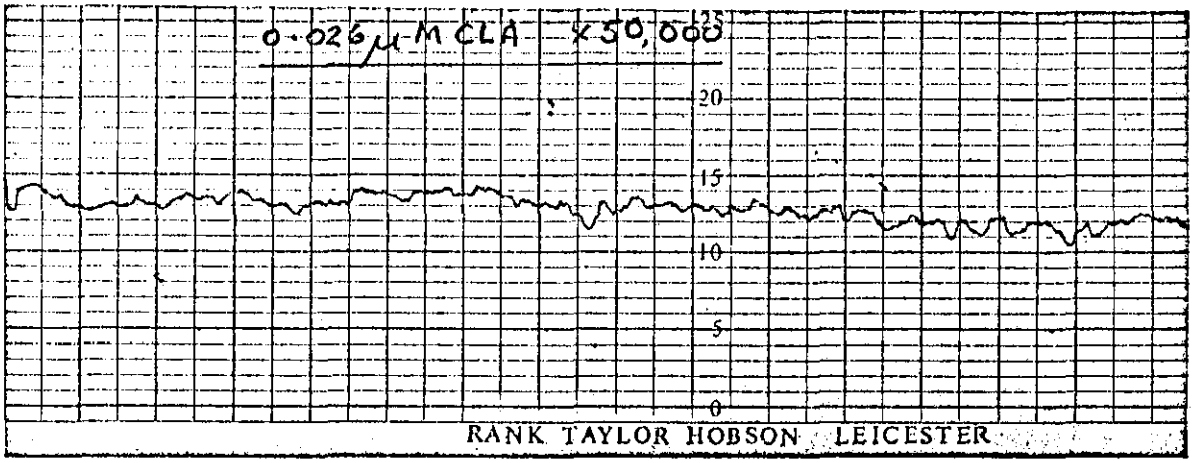
0·026 μM CLA ×50,000
25
20
15
10
5
0
RANK TAYLOR HOBSON LEICESTER

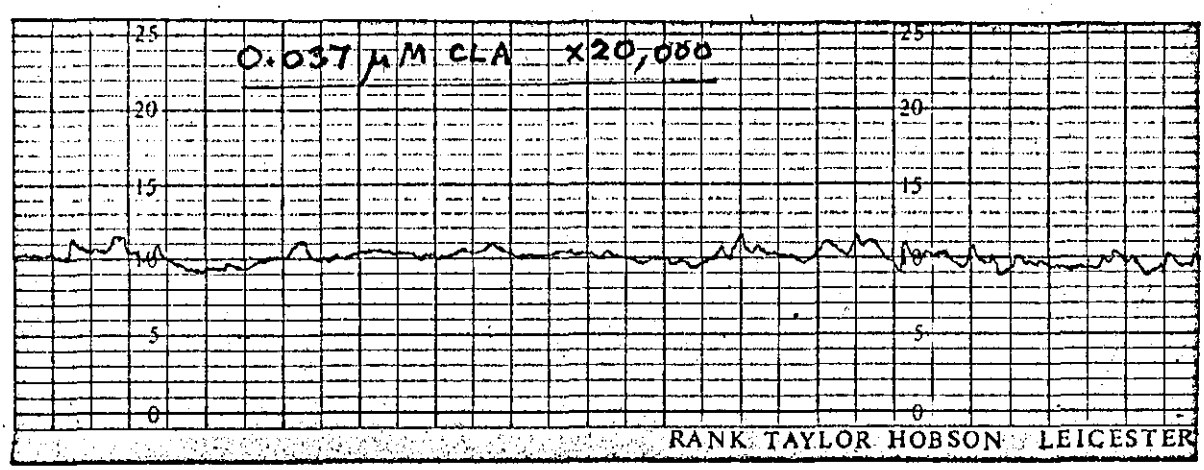
0·037 μM CLA ×20,000
25
20
15
10
5
0
RANK TAYLOR HOBSON LEICESTER

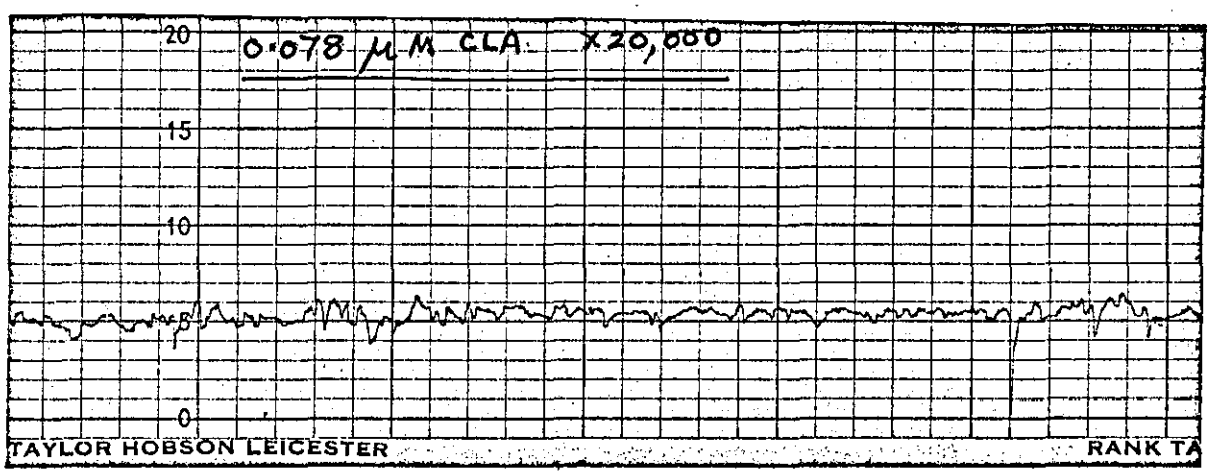
0·078 μM CLA ×20,000
20
15
10
0
TAYLOR HOBSON LEICESTER
RANK TA

FIGURE 33

Reciprocal Porosity - Compaction Pressure relationships for analysis of pressure - density data according to Kawakita for unlubricated compacts of various Height - Diameter ratios.

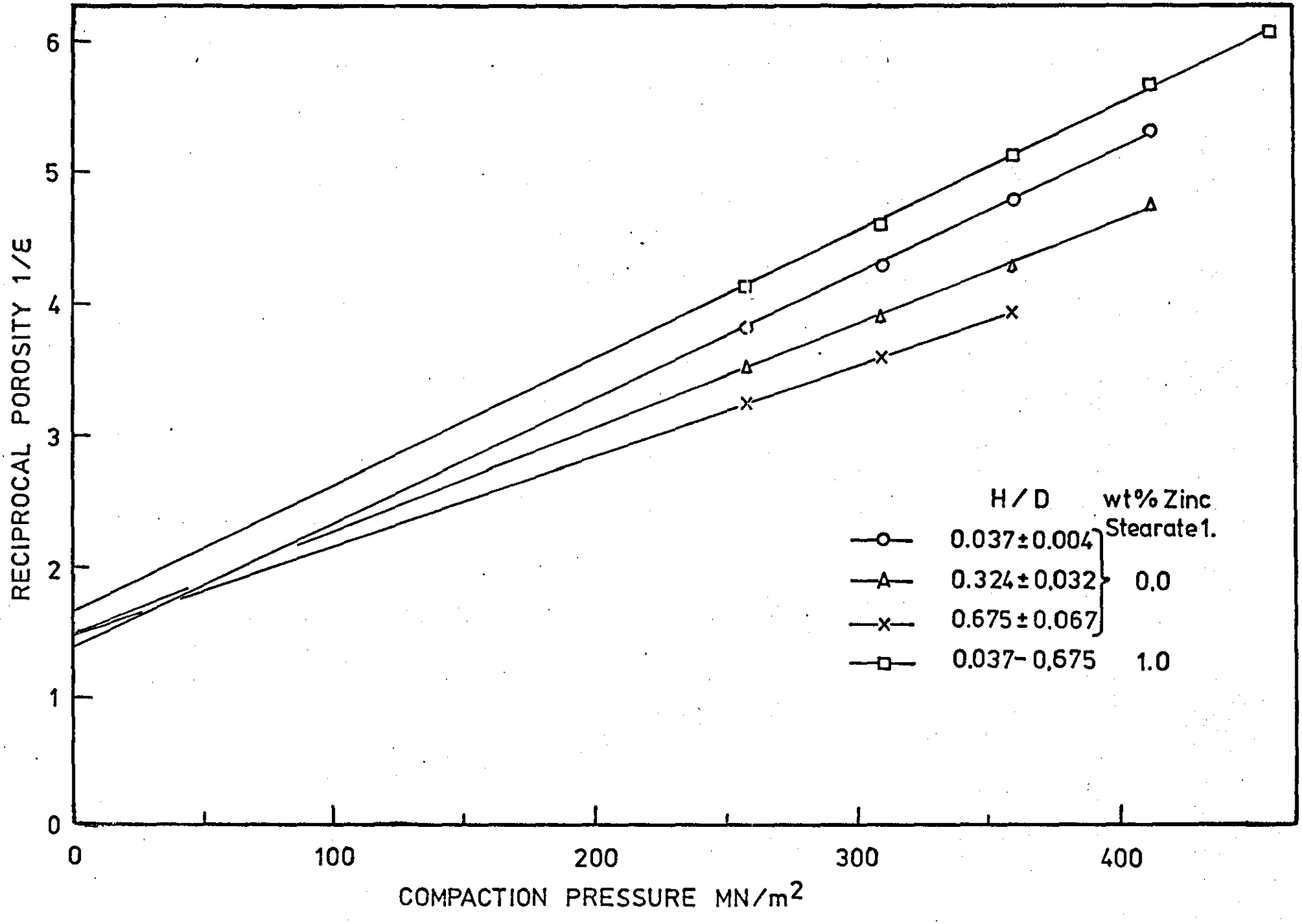
RECIPROCAL POROSITY 1/ε
0
1
2
3
4
5
6
0
100
200
300
400
COMPACTION PRESSURE MN/m²
H / D
wt% Zinc Stearate 1.
0.037 ± 0.004
0.324 ± 0.032
0.675 ± 0.067
0.0
0.037 - 0.675
1.0

FIGURE 34

Typical Force-Distance curves obtained during lubricated conpact ejection trials on laboratory (tensometer ejection) and production (press ejection) scales.

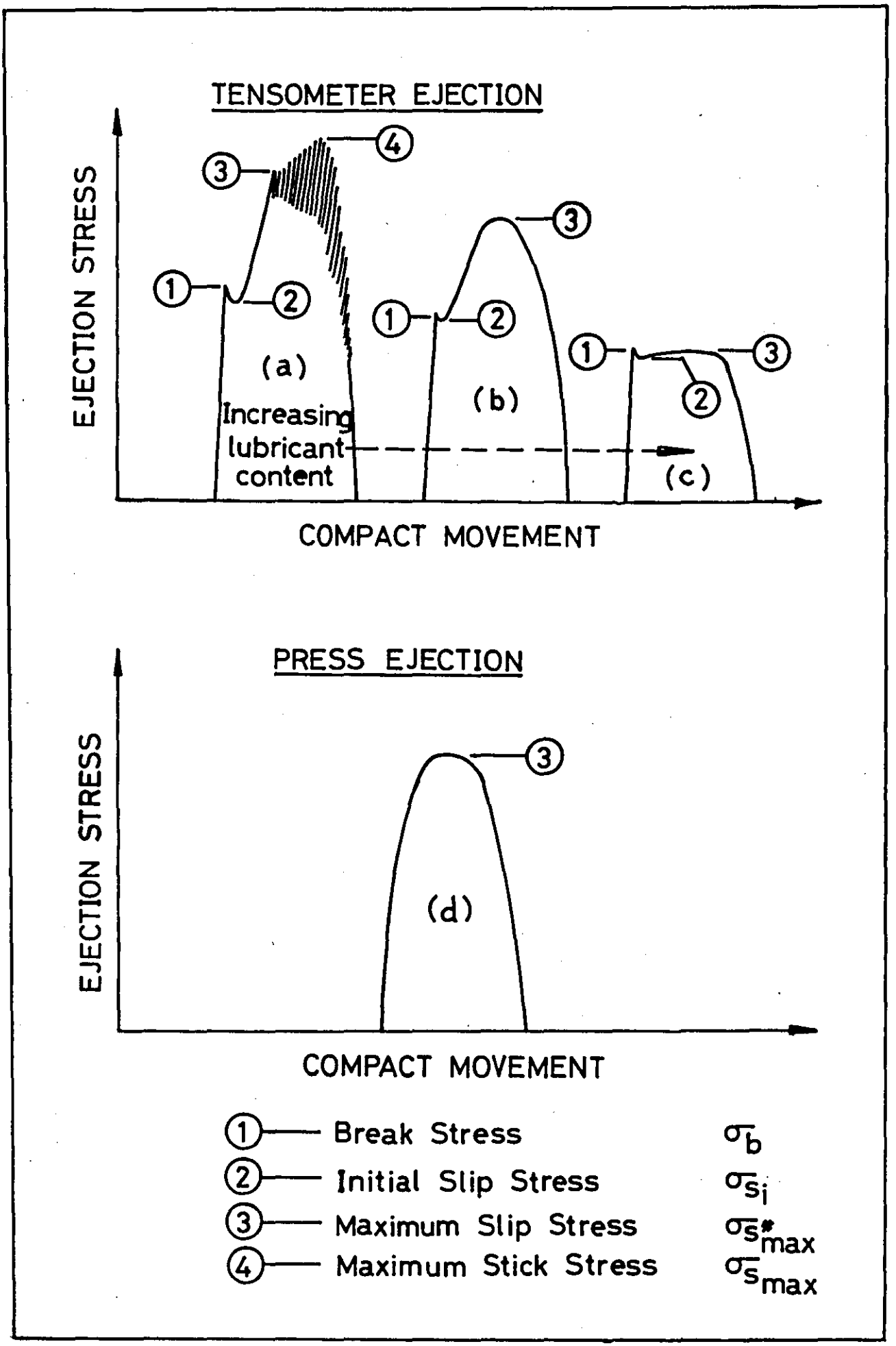
TENSOMETER EJECTION
EJECTION STRESS
(a)
Increasing lubricant content
(b)
(c)
COMPACT MOVEMENT
PRESS EJECTION
EJECTION STRESS
(d)
COMPACT MOVEMENT
1 Break Stress $\overline{\sigma_b}$
2 Initial Slip Stress $\overline{\sigma_{s_i}}$
3 Maximum Slip Stress $\overline{\sigma_s^*}_{max}$
4 Maximum Stick Stress $\overline{\sigma_s}_{max}$

FIG34.

FIGURE 35

Ejection Stress - TrueDensity relationships for analysis of ejection data for compacts containing between 0.3 and 2.0 wt. % zinc stearate 1.

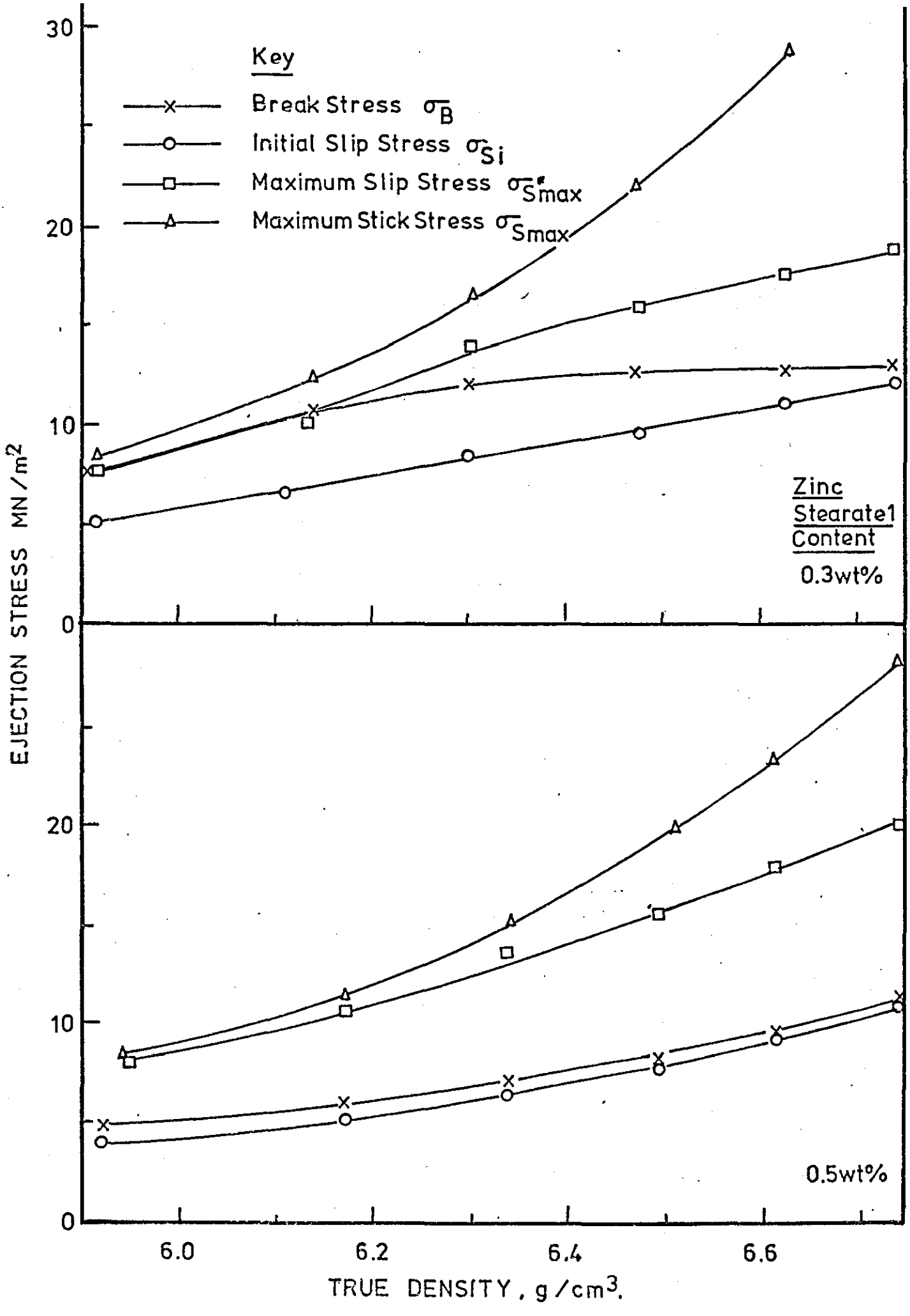
Key
Break Stress σ_B
Initial Slip Stress σ_{Si}
Maximum Slip Stress σ_{S^*max}
Maximum Stick Stress σ_{Smax}
Zinc Stearate1 Content
0.3wt%
0.5wt%
EJECTION STRESS MN/m^2
TRUE DENSITY, g/cm^3.
0
10
20
30
6.0
6.2
6.4
6.6

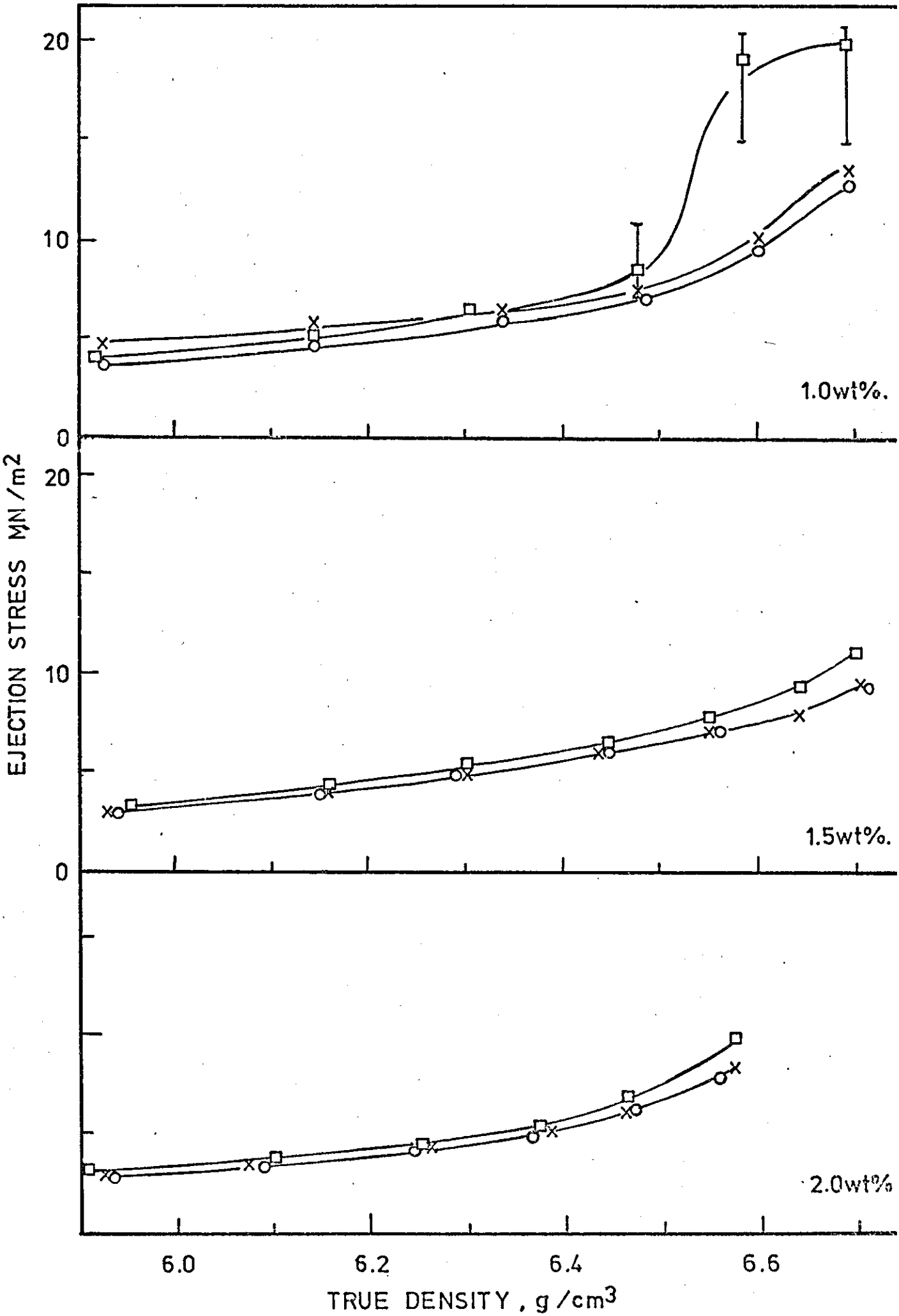
20
10
0
1.0wt%.
20
10
0
1.5wt%.
2.0wt%
EJECTION STRESS MN/m2
6.0
6.2
6.4
6.6
TRUE DENSITY , g /cm3

FIGURE 36

True Density - Zinc Stearate Content relationships for different compact densities, comparison between laboratory and production scale data

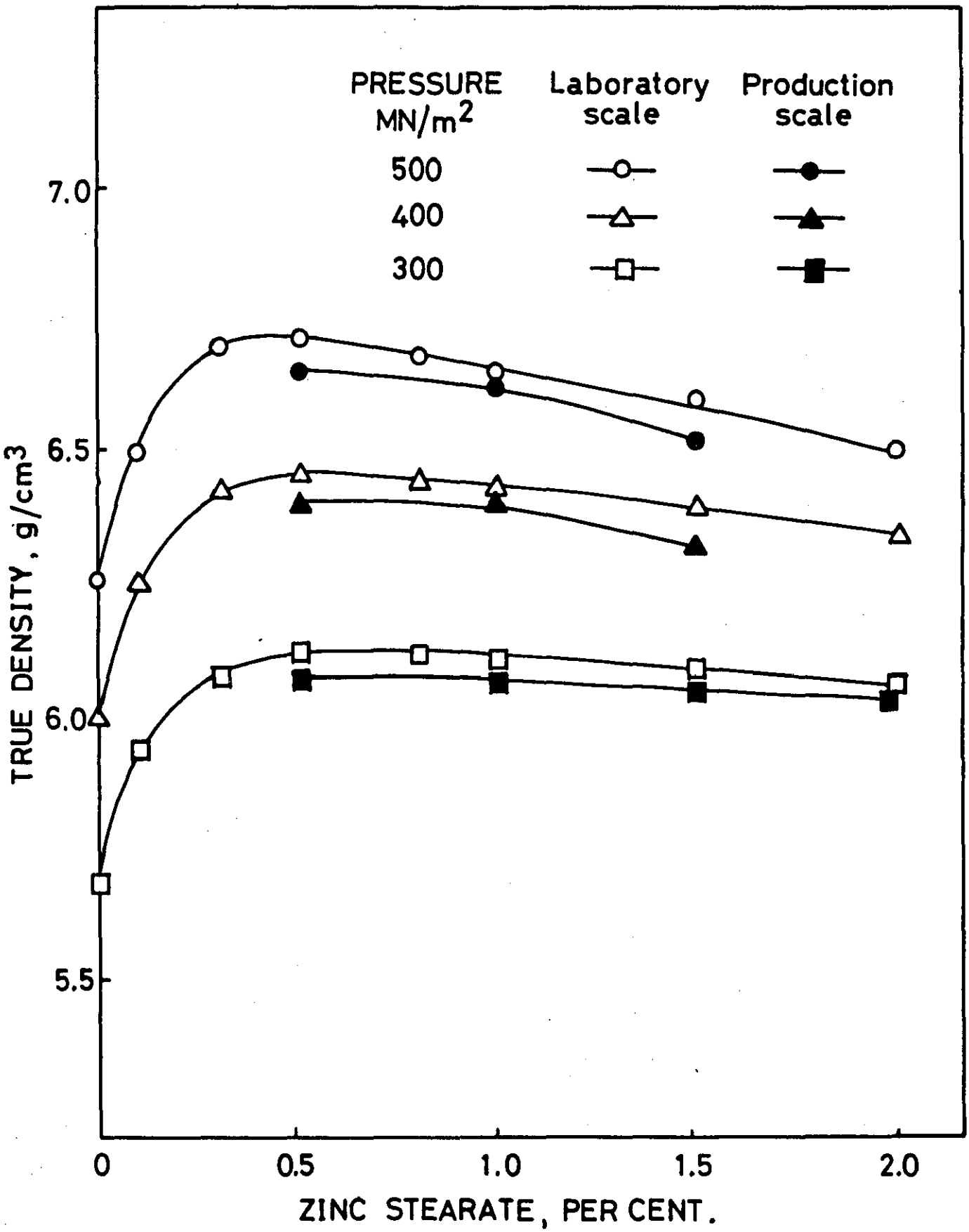
PRESSURE
MN/m2
Laboratory scale
Production scale
500
400
300
7.0
6.5
6.0
5.5
TRUE DENSITY, g/cm3
0
0.5
1.0
1.5
2.0
ZINC STEARATE, PER CENT.

FIG. 36.

FIGURE 37

Reciprocal Porosity - Compaction Pressure relationships for analysis of pressure-density data according to Kawa Kita in production scale trials.

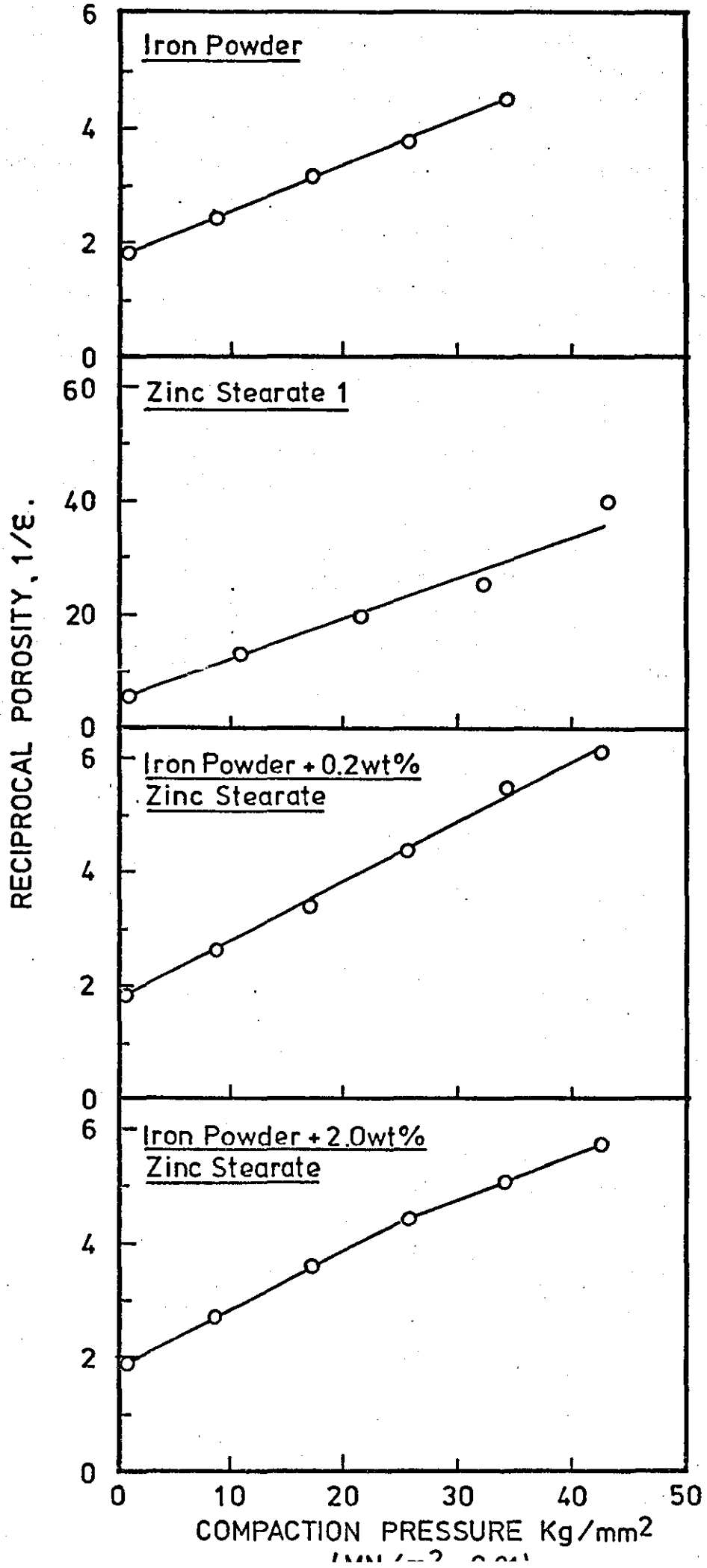
Iron Powder
Zinc Stearate 1
Iron Powder + 0.2wt% Zinc Stearate
Iron Powder + 2.0wt% Zinc Stearate
RECIPROCAL POROSITY, 1/ε.
COMPACTION PRESSURE Kg/mm2
0
2
4
6
20
40
60
10
30
50

FIGURE 38

Compaction Energy - True Density relationships for iron powder containing varying amounts of zinc stearate 1.

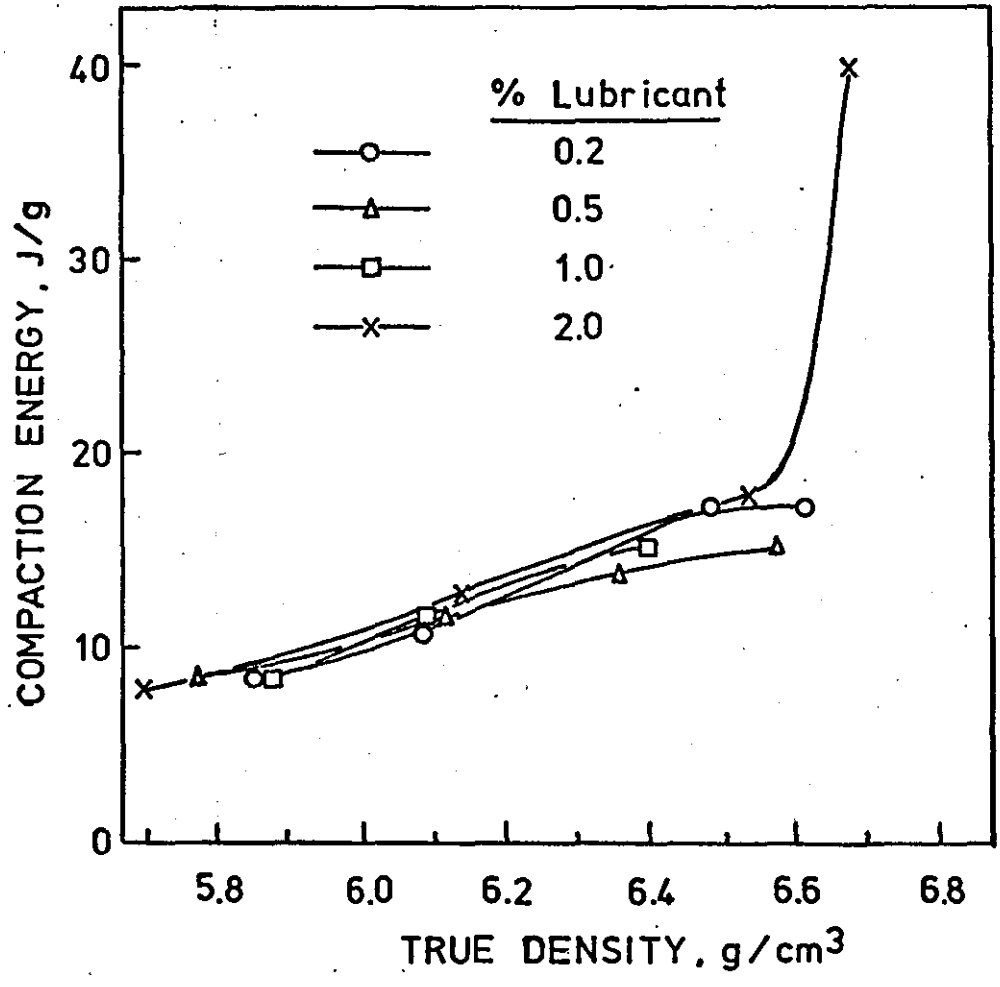
% Lubricant
0.2
0.5
1.0
2.0
COMPACTION ENERGY, J/g
TRUE DENSITY, g/cm3
0
10
20
30
40
5.8
6.0
6.2
6.4
6.6
6.8

FIGURE 33

Ejection Stress - Zinc Stearate Content relationships for different compact densities comparison between laboratory and production scale data.

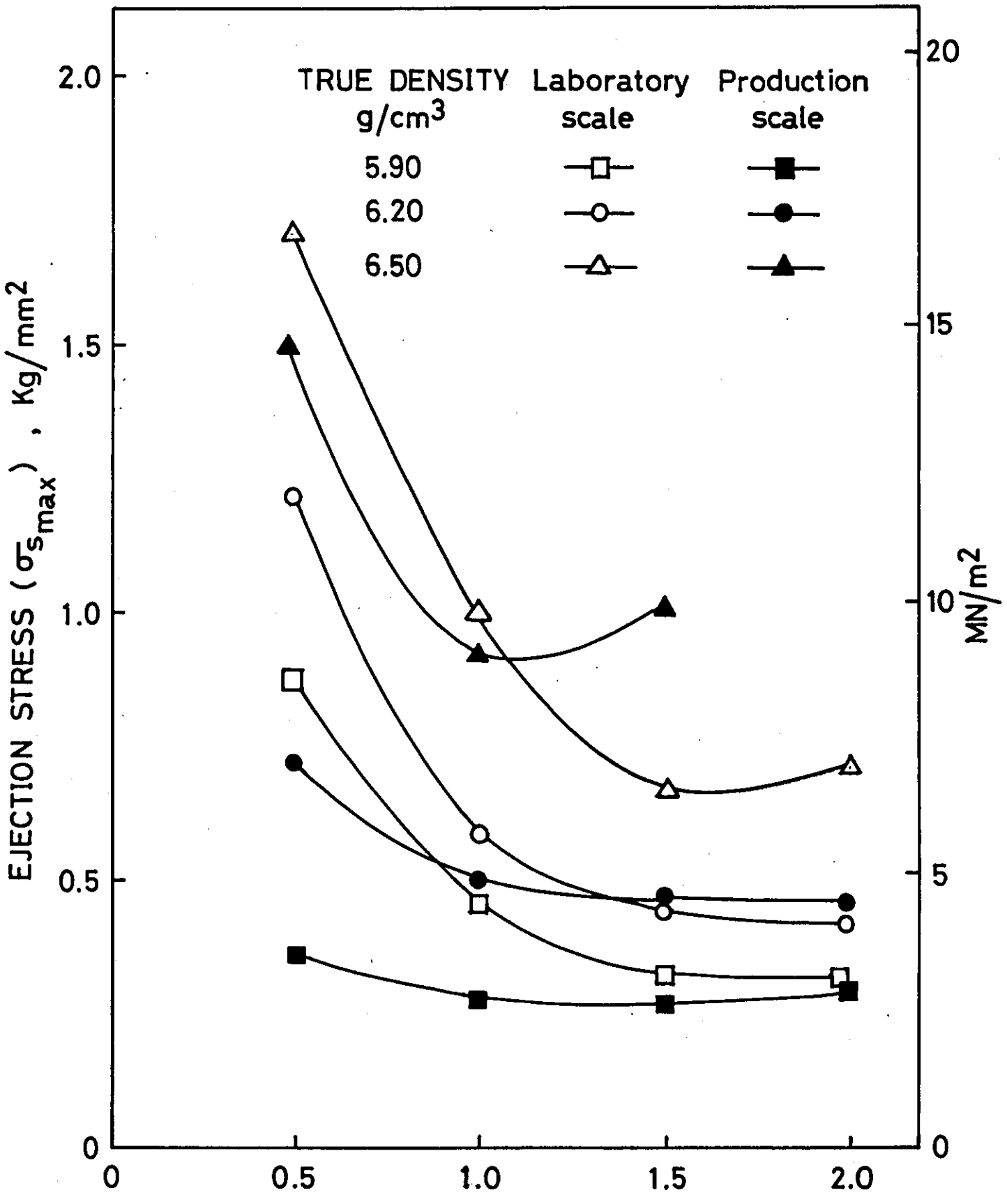
TRUE DENSITY g/cm3
Laboratory scale
Production scale
5.90
6.20
6.50
EJECTION STRESS (σsmax) , Kg/mm2
MN/m2
ZINC STEARATE , PER CENT .
0
0.5
1.0
1.5
2.0
5
10
15
20

FIG. 39.

FIGURE 40

Scanning Electron Microscope photographs of replicas of die surface:

(a) before compaction;
(b) after compaction to a high density, showing "cladding" of the die surface by iron powder.

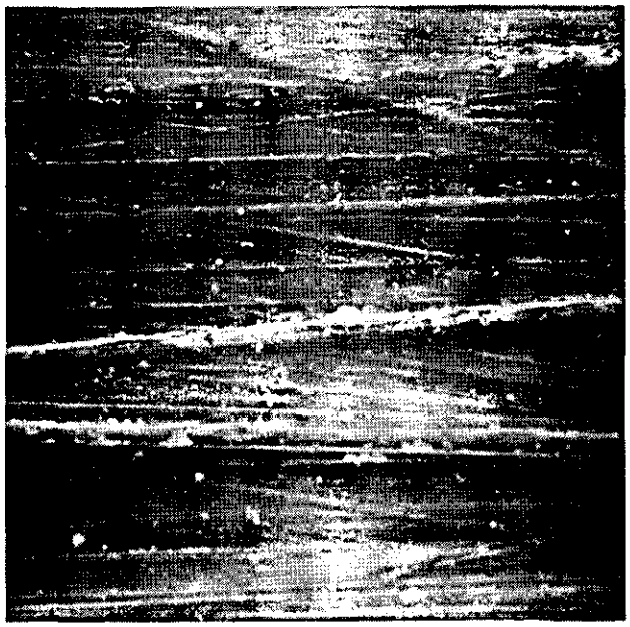

(a)

Scanning electron microscope photograph (X 500) of replica of die surface as received. Scoring marks are the result of final lapping of die to a finish of 0.07 M C.L.A.

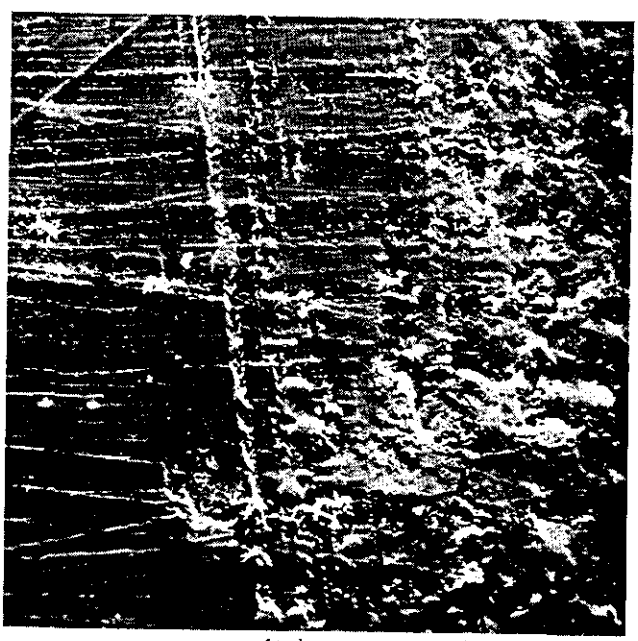

(b)

FIGURE 10

Scanning electron microscope photograph (X 500) of replica of die surface showing "cladding" by iron powder after compacting to a high true density with low lubricant content.

FIGURE 41

Ejection Stress - Compaction Pressure
relationships for different lubricants

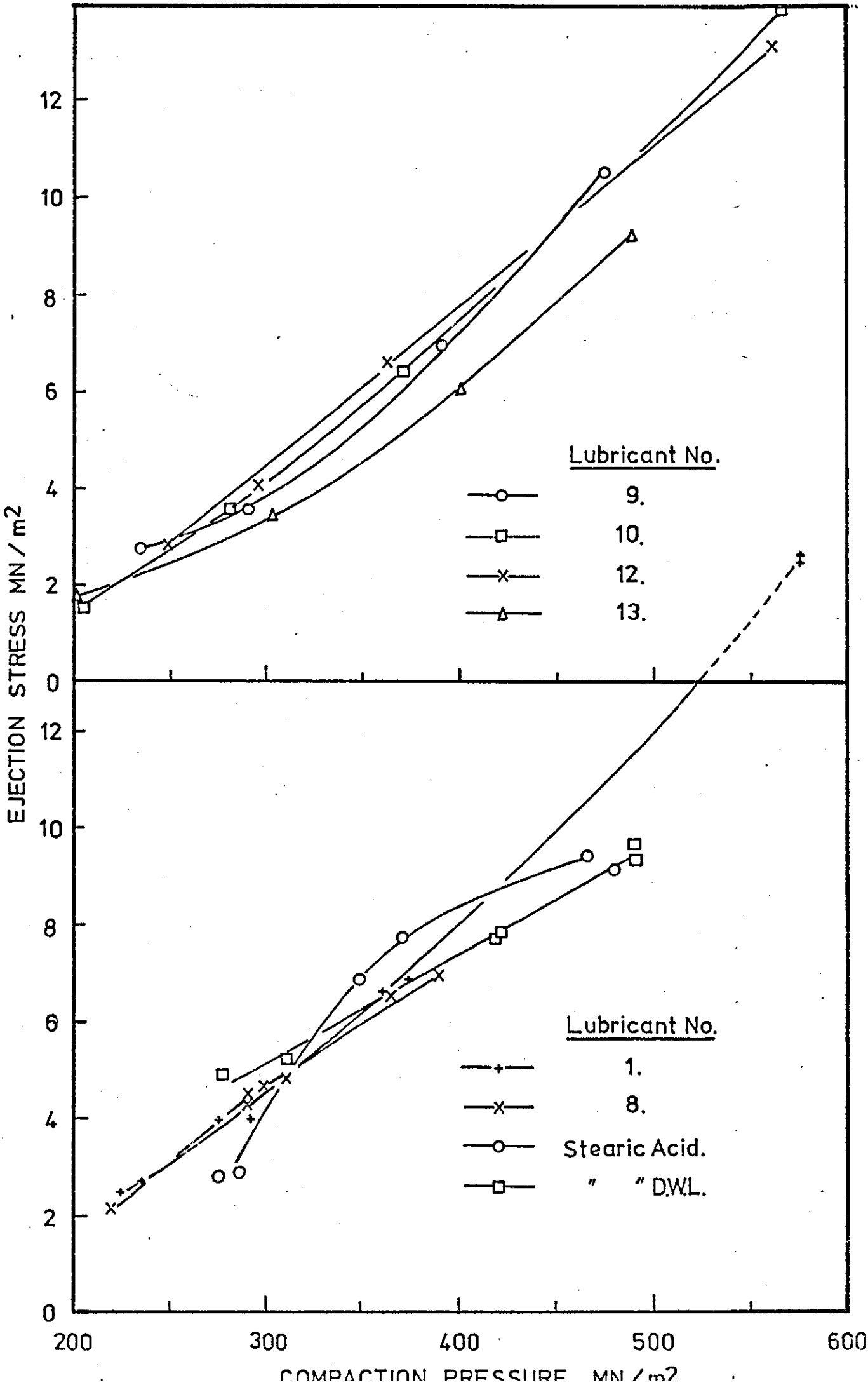
EJECTION STRESS MN / m2
COMPACTION PRESSURE MN / m2
0
2
4
6
8
10
12
200
300
400
500
600
Lubricant No.
9.
10.
12.
13.
Lubricant No.
1.
8.
Stearic Acid.
" " D.W.L.

FIGURE 42

Ejection Stress - Compaction Pressure relationships for different die materials, data obtained during production scale trials.

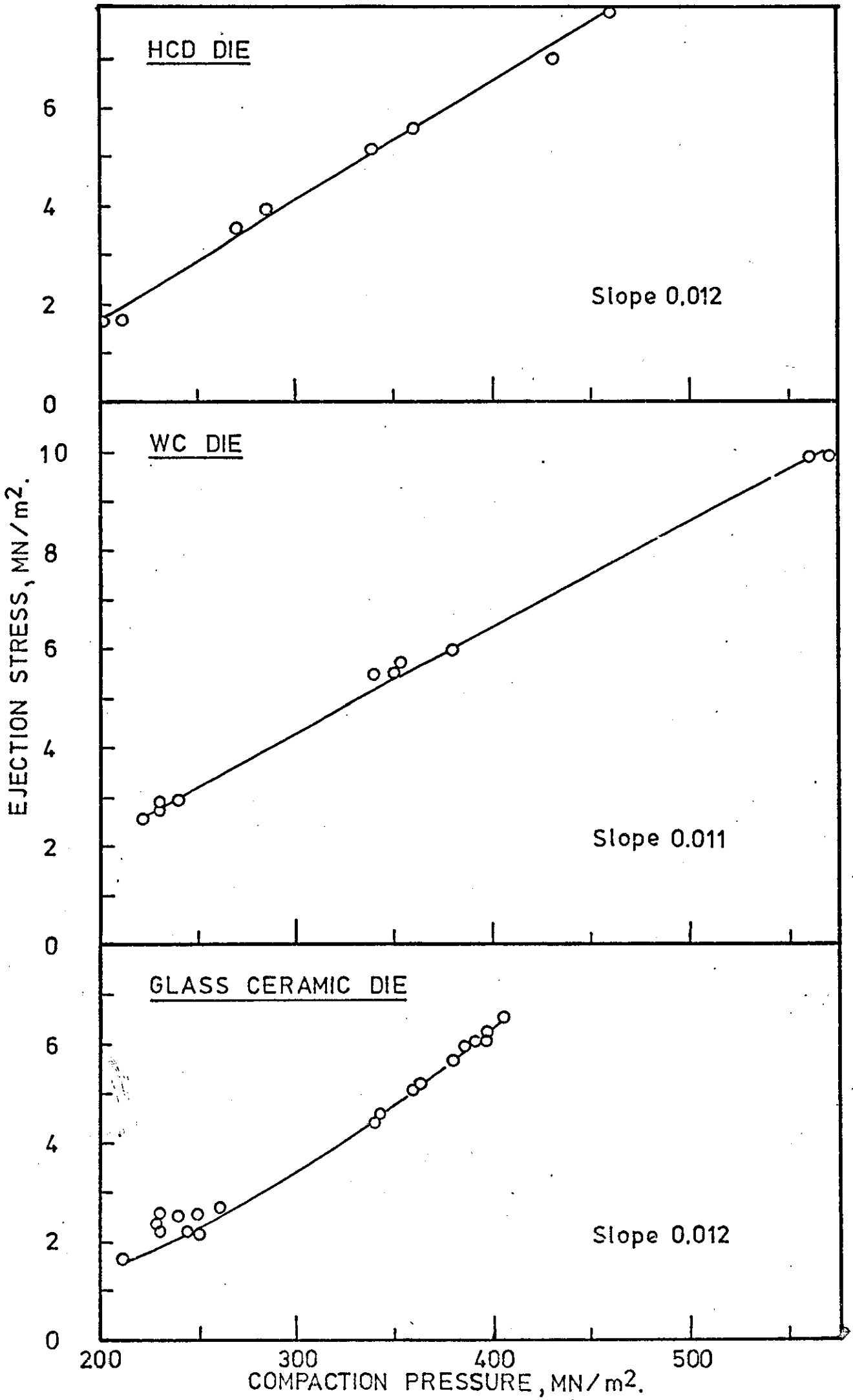
HCD DIE
Slope 0.012
WC DIE
Slope 0.011
GLASS CERAMIC DIE
Slope 0.012
EJECTION STRESS, MN/m2.
COMPACTION PRESSURE, MN/m2.
0
2
4
6
8
10
200
300
400
500

FIGURE 43

Scanning Electron Microscope photographs of compact surfaces (true density 6.2 g/cm^3) having zinc stearate 1 contents of:
(a) 0.5 ; (b) 1.0 ; (c) 1.5 ; (d) 2.0 wt.%

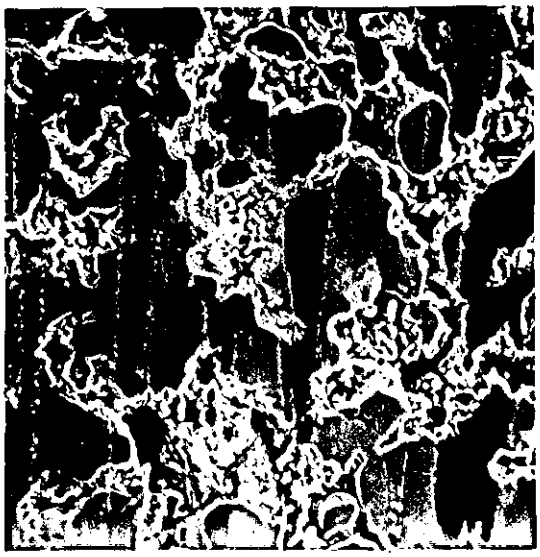

(a)

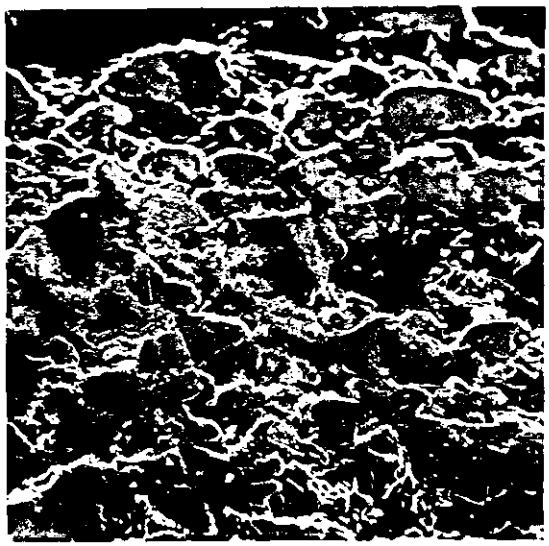

(b)

(c)

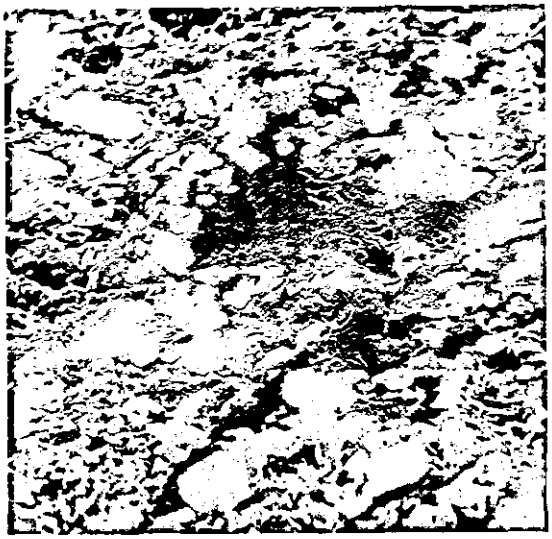

(d)

FIGURE 44

Scanning Electron Microscope photographs of compact surfaces:

(a) Compact density: 5.8 g/cm^3, 0.2 wt.% zinc stearate

(b) Compact density: 6.6 g/cm^3, 0.2 wt.% zinc stearate

(c) Compact density: 5.8 g/cm^3, 2.0 wt.% zinc stearate

(d) Compact density: 6.6 g/cm^3, 2.0 wt.% zinc stearate

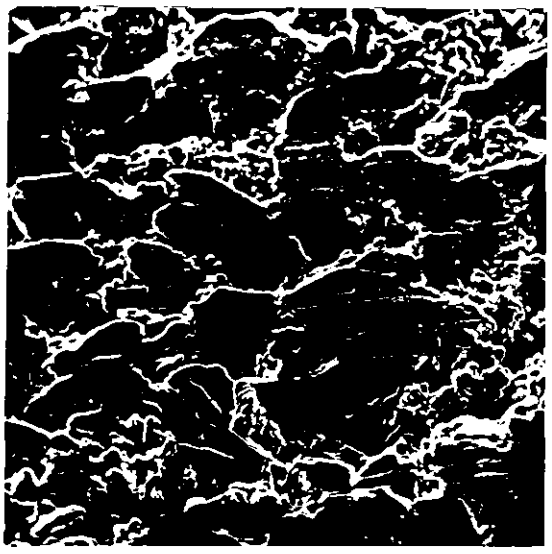

(a)

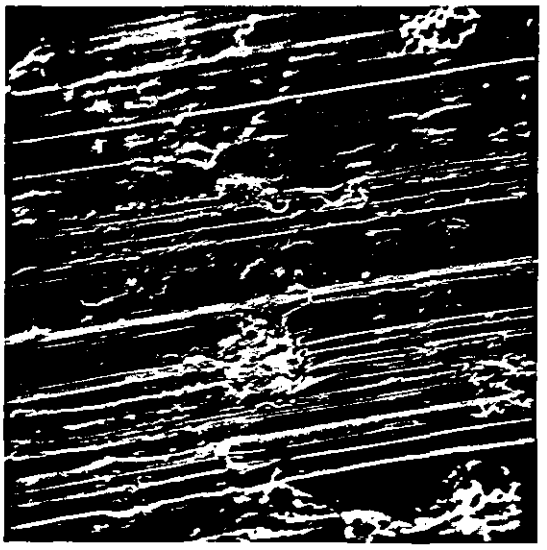

(b)

(c)

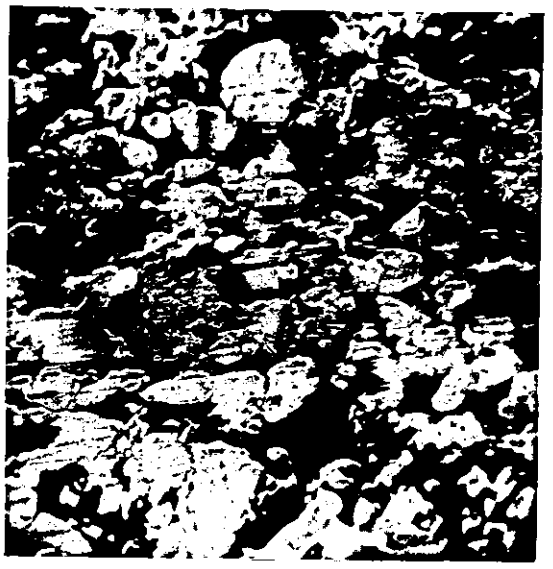

(d)

FIGURE 45

Scanning Electron Microscope photographs of fractured compact surfaces, showing free zinc stearate particles.

(a) Compact density: 5.8 g/cm^3, 2.0 wt. % zinc stearate.

(b) Compact density: 6.4 g/cm^3, 0.5 wt. % zinc stearate.

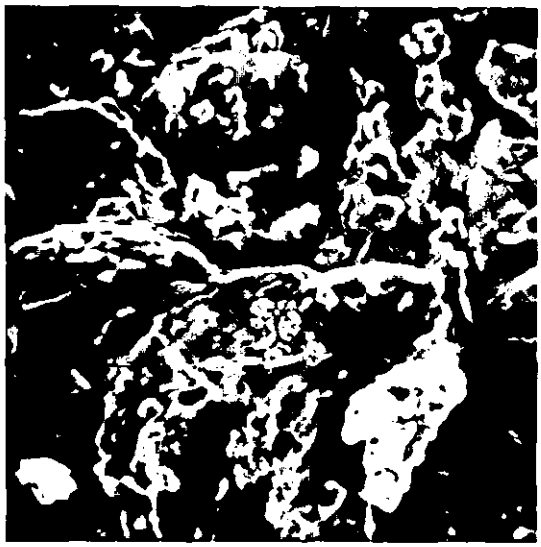

(a)

(b)

FIGURE 46

Compact Density distributions obtained using the mercury balance.

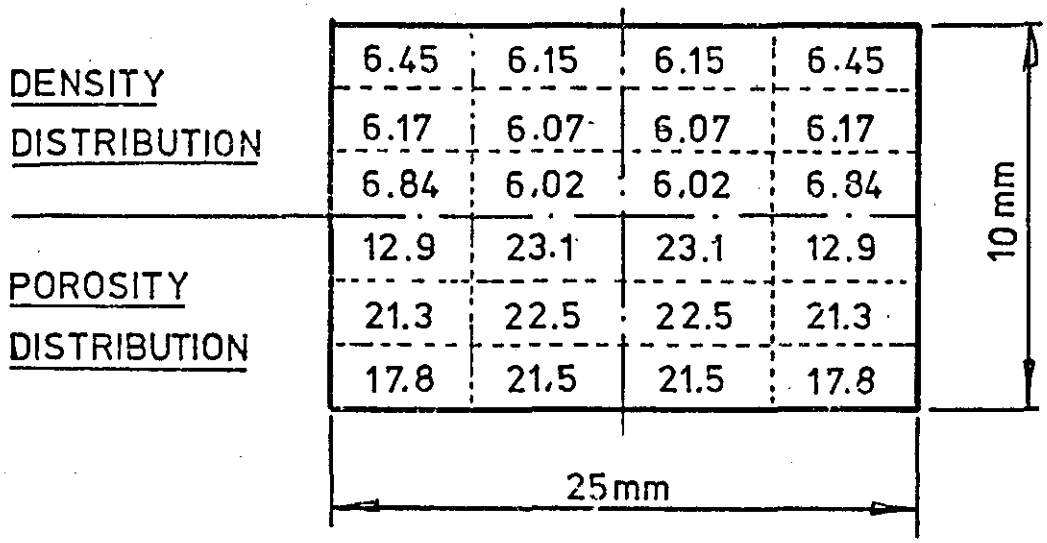
DENSITY DISTRIBUTION
POROSITY DISTRIBUTION
6.45 6.15 6.15 6.45
6.17 6.07 6.07 6.17
6.84 6.02 6.02 6.84
12.9 23.1 23.1 12.9
21.3 22.5 22.5 21.3
17.8 21.5 21.5 17.8
10 mm
25 mm

(a)

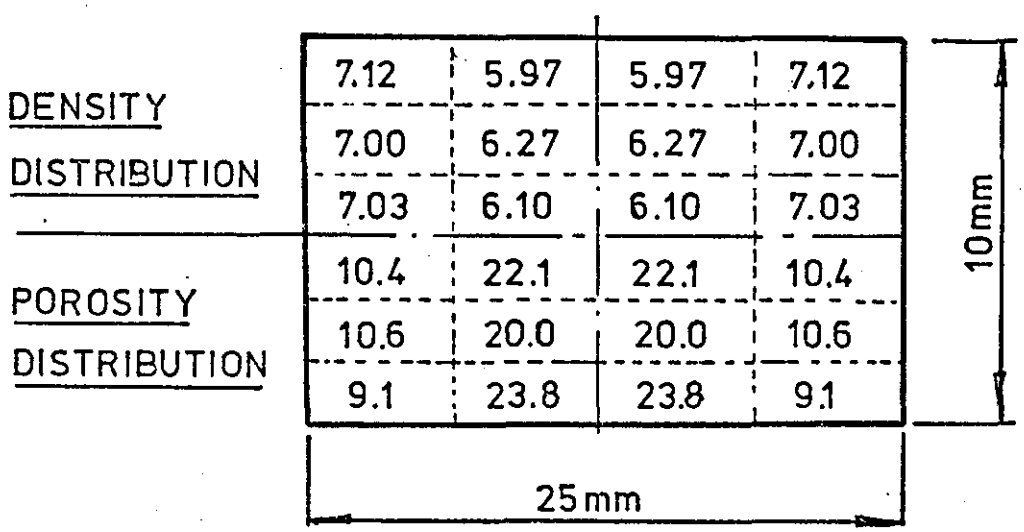
DENSITY DISTRIBUTION
POROSITY DISTRIBUTION
7.12 5.97 5.97 7.12
7.00 6.27 6.27 7.00
7.03 6.10 6.10 7.03
10.4 22.1 22.1 10.4
10.6 20.0 20.0 10.6
9.1 23.8 23.8 9.1
10 mm
25 mm

(b)

FIGURE 47

Area Porosity distributions obtained on the Automated Image Analysing Computer.

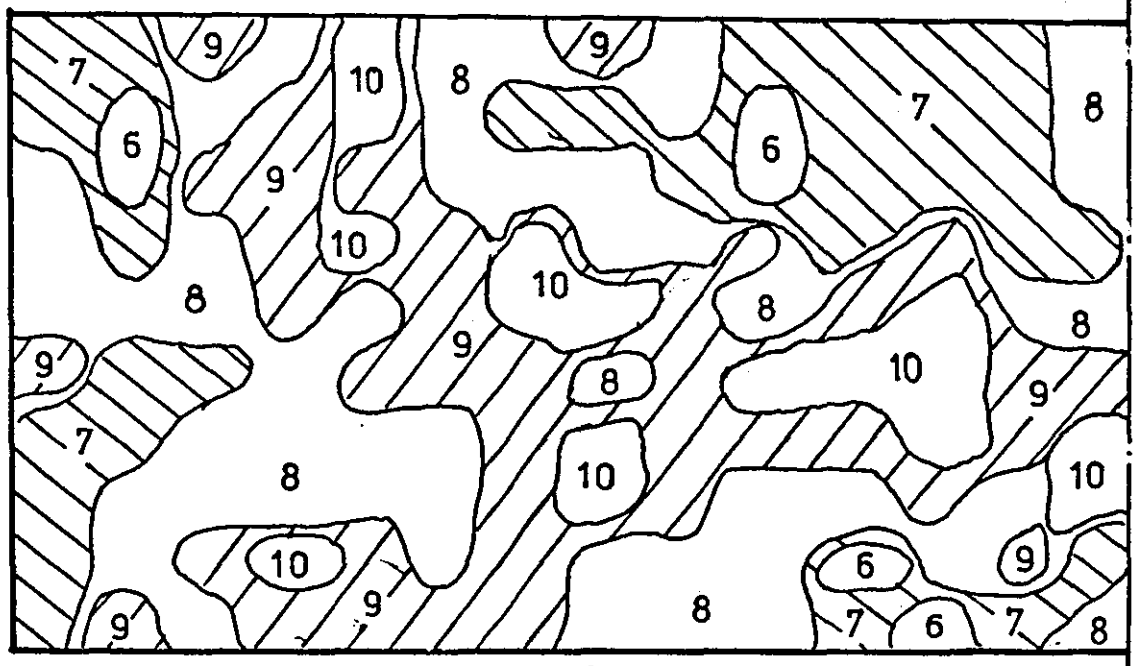
9
7
10
8
9
6
7
8
9
10
10
8
8
9
8
10
9
7
8
10
10
10
9
9
6
9
8
7
6
7
8

(a)

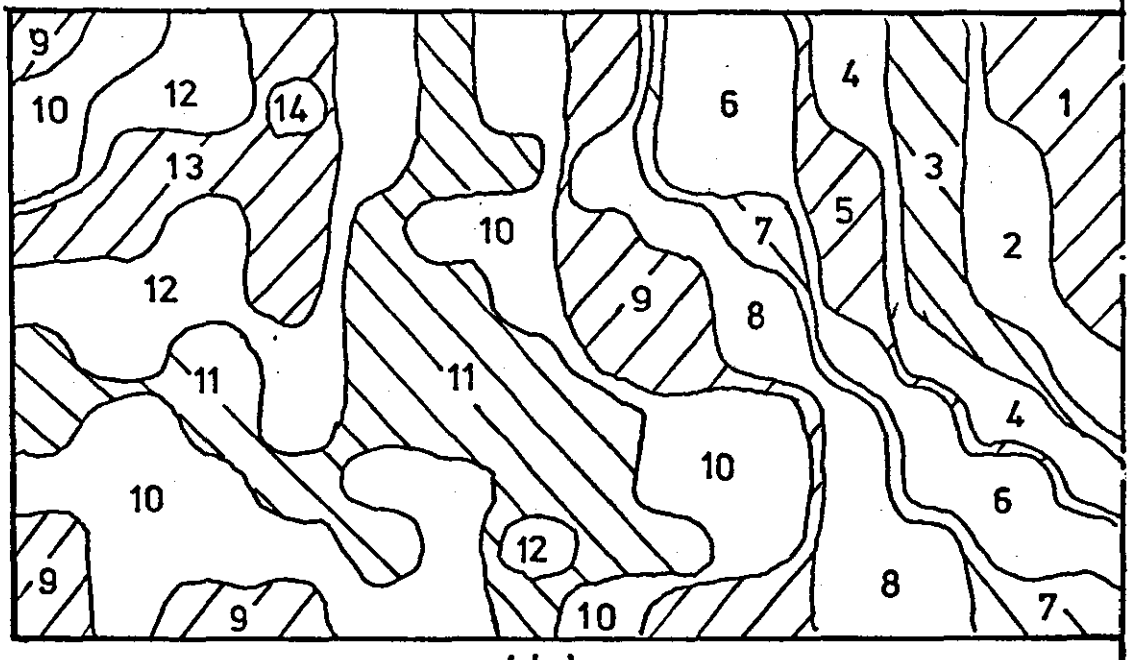
9
10
12
14
13
6
4
1
3
10
7
5
2
12
9
8
11
11
4
10
10
6
12
8
9
9
10
7

(b)

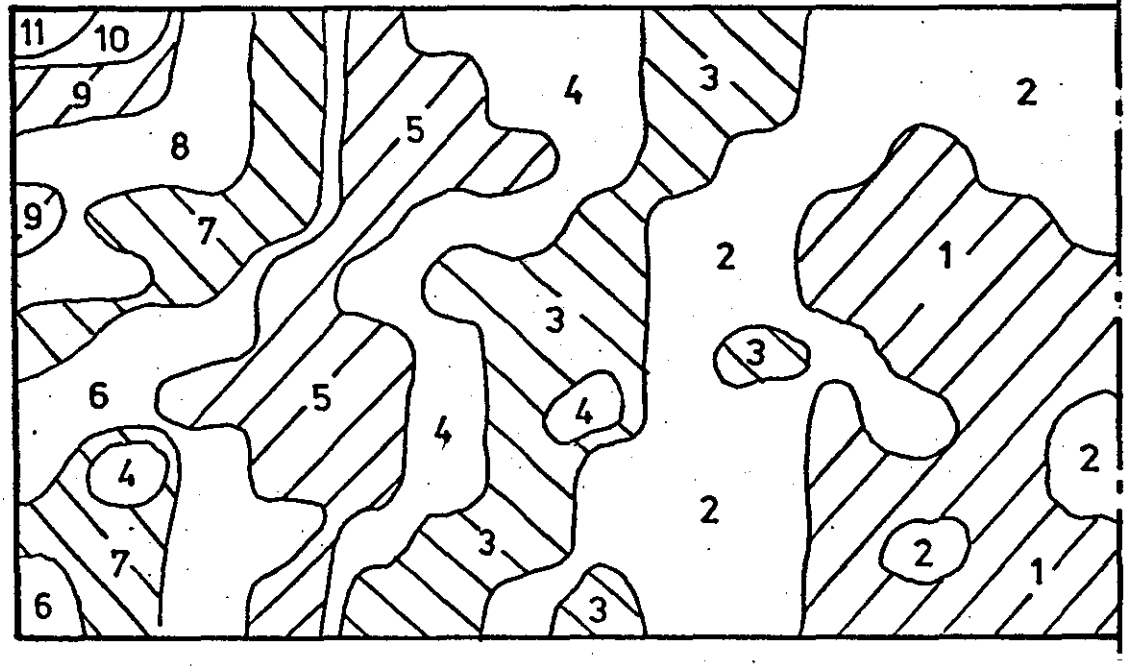
11
10
9
8
5
4
3
2
9
7
2
1
3
3
6
5
4
4
4
2
7
3
2
2
1
6
3

FIGURE 48

Green Strength - Zinc Stearate Content relationships for compacts of two different true densities.

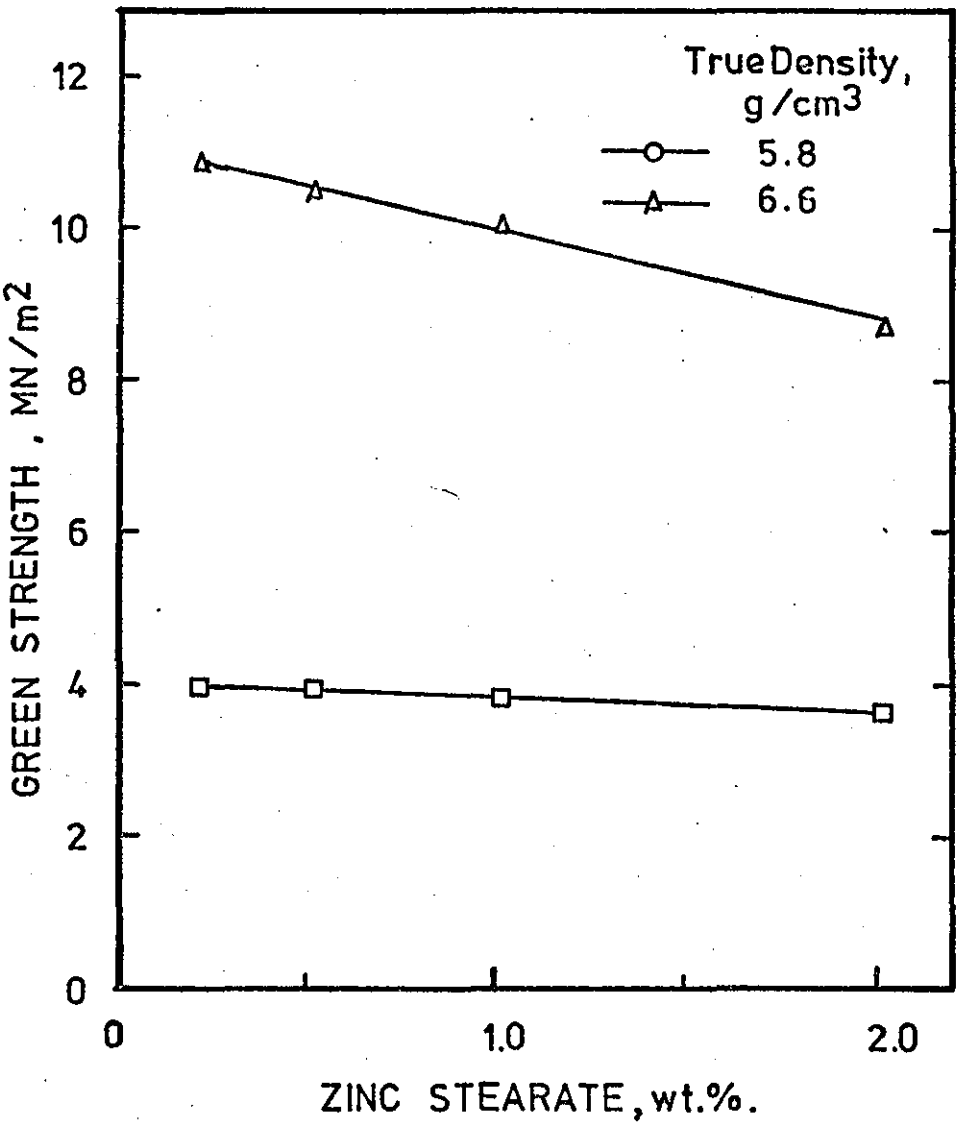
True Density,
g/cm3
5.8
6.6
GREEN STRENGTH , MN/m2
12
10
8
6
4
2
0
0
1.0
2.0
ZINC STEARATE, wt.%.

FIGURE 49

Percentage Spring of Die - True Density relationships for compacts containing varying zinc stearate 1 content.

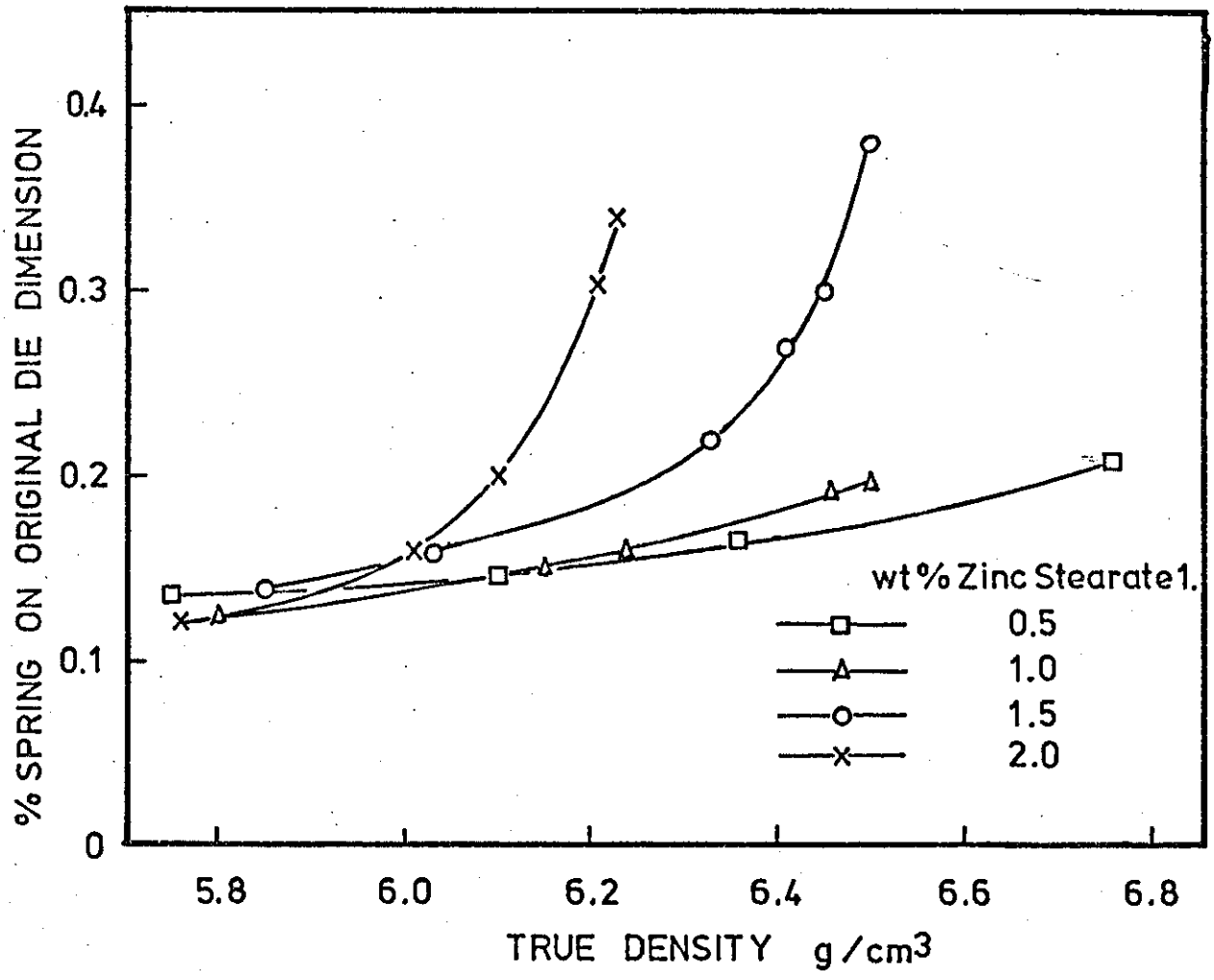
% SPRING ON ORIGINAL DIE DIMENSION
0.4
0.3
0.2
0.1
0
5.8
6.0
6.2
6.4
6.6
6.8
TRUE DENSITY g/cm3
wt % Zinc Stearate1.
0.5
1.0
1.5
2.0

FIGURE 50

Changes in die diameter during a pressing cycle

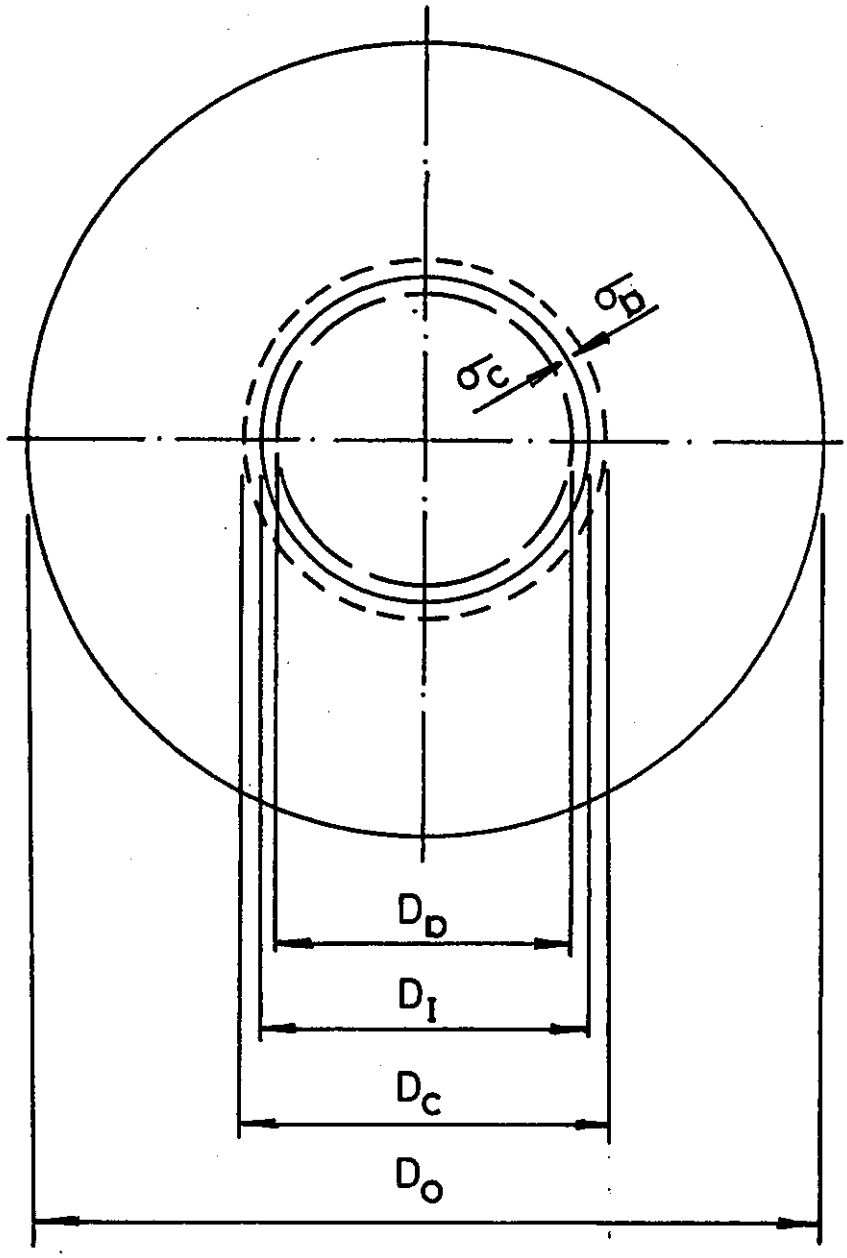

D_D = Dia. of empty die.

D_C = Dia. of free compact.

D_I = Dia. of interface at onset of ejection.

D_O = Outside dia. of die.

At equilibrium $\overline{\sigma_C} = \overline{\sigma_D} = \overline{\sigma_R}$

FIGURE 51

Youngs Modulus of "green" Compacts - True Density relationships for varying zinc stearate 1 content determined for stress levels of 3 and 120 MN/m^2

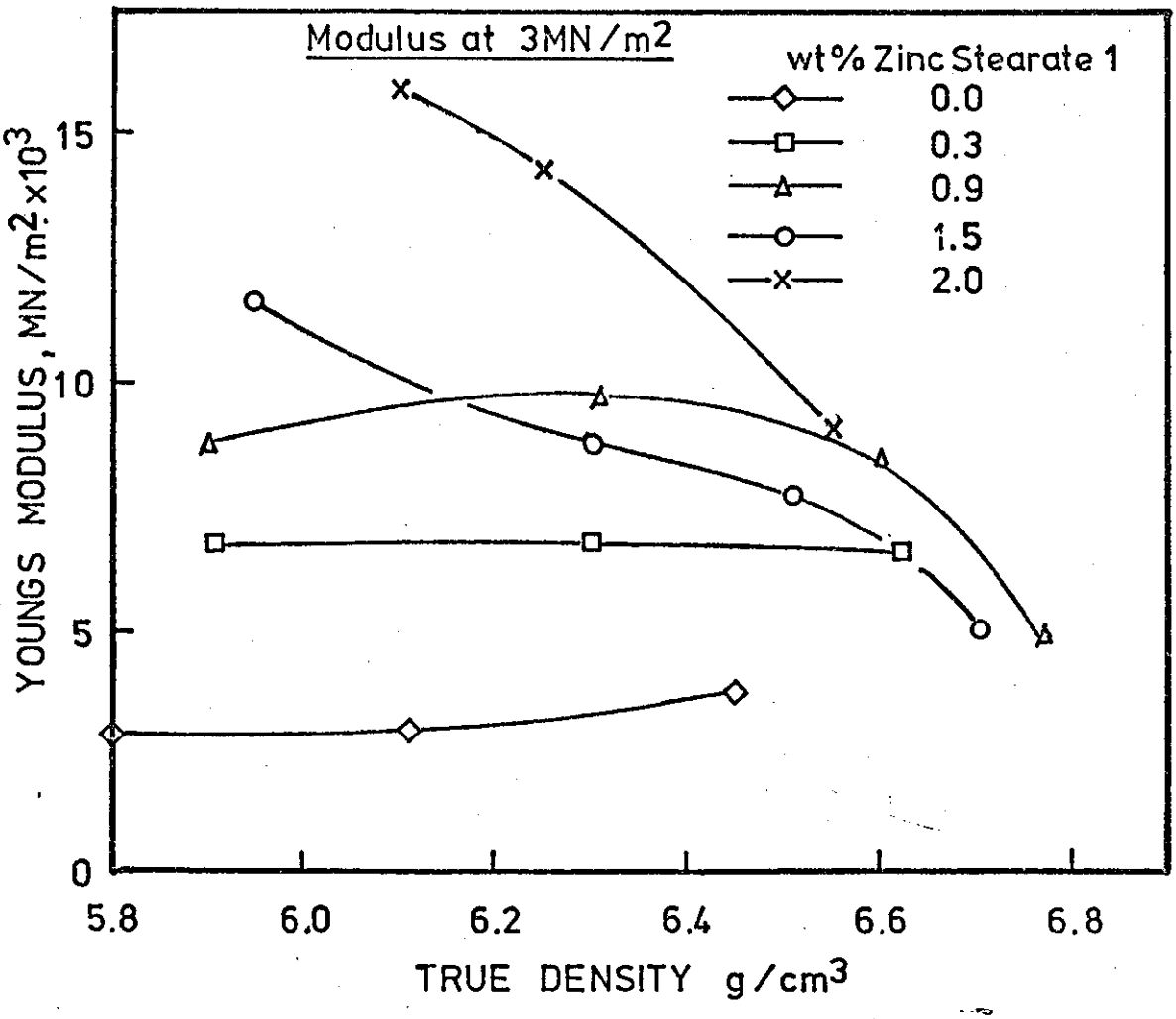
Modulus at 3MN/m2
wt% Zinc Stearate 1
0.0
0.3
0.9
1.5
2.0
YOUNGS MODULUS, MN/m2x10^3
15
10
5
0
5.8
6.0
6.2
6.4
6.6
6.8
TRUE DENSITY g/cm3

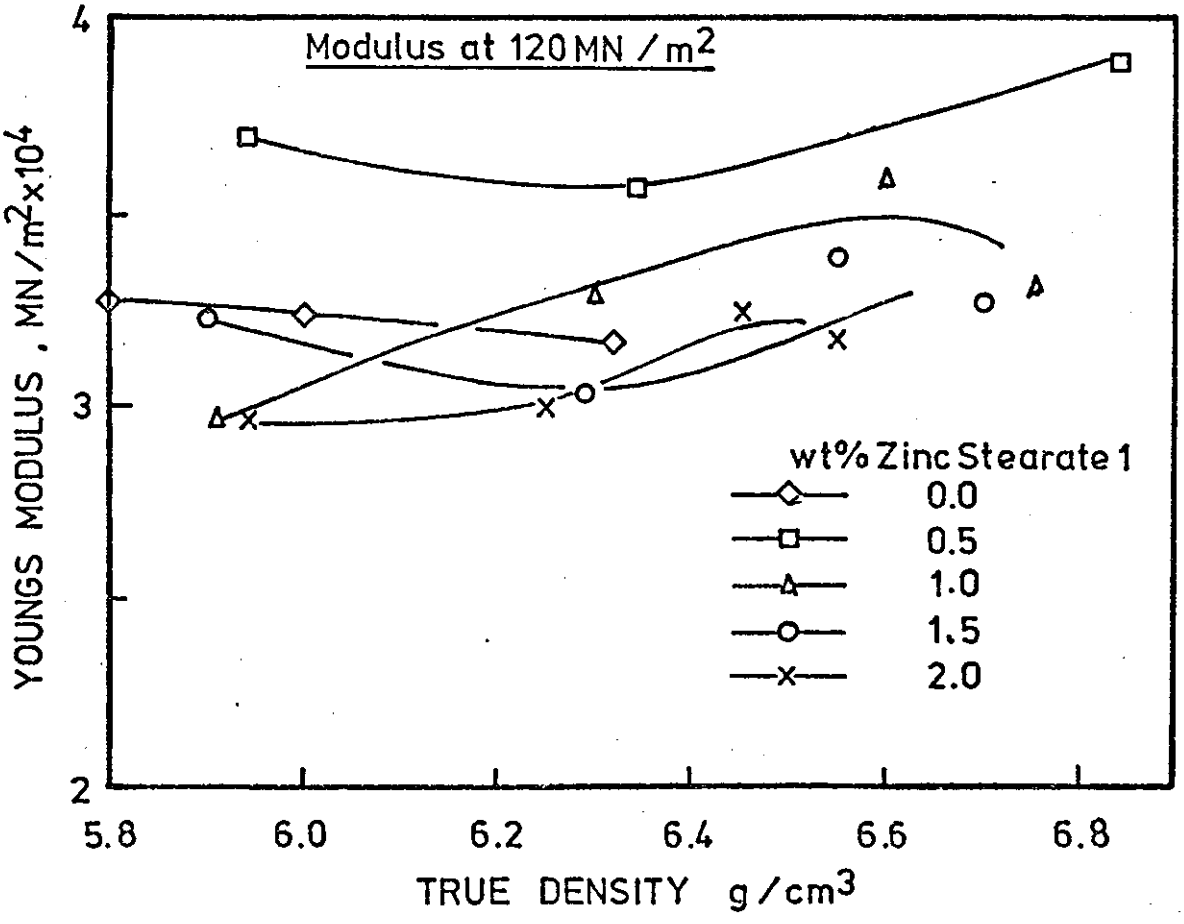
Modulus at 120 MN/m2
wt% Zinc Stearate 1
0.0
0.5
1.0
1.5
2.0
YOUNGS MODULUS, MN/m2x10^4
4
3
2
5.8
6.0
6.2
6.4
6.6
6.8
TRUE DENSITY g/cm3

FIGURE 52

Die Radial Stress - Compaction Pressure relationships for compacts pressed with varying zinc stearate 1 contents using a High Chromium Steel die (HCD)

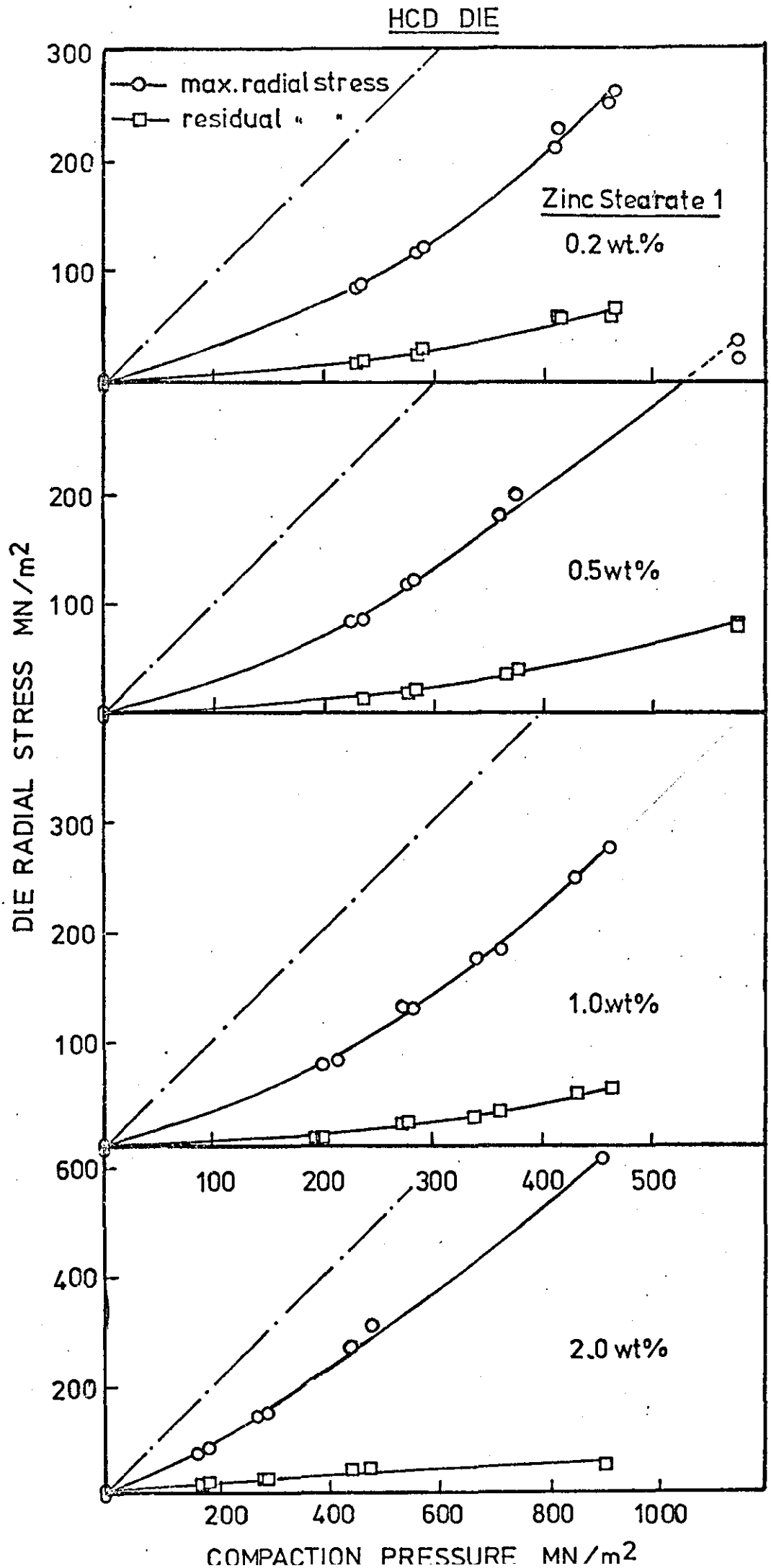
HCD DIE
max. radial stress
residual " "
Zinc Stearate 1
0.2 wt.%
0.5wt%
1.0wt%
2.0 wt%
DIE RADIAL STRESS MN/m2
COMPACTION PRESSURE MN/m2
300
200
100
600
400
100
200
300
400
500
200
400
600
800
1000

FIGURE 53

Die Radial Stress - Compaction Pressure relationships for compacts pressed with varying zinc stearate 1 contents using a Tungsten Carbide Die (WC).

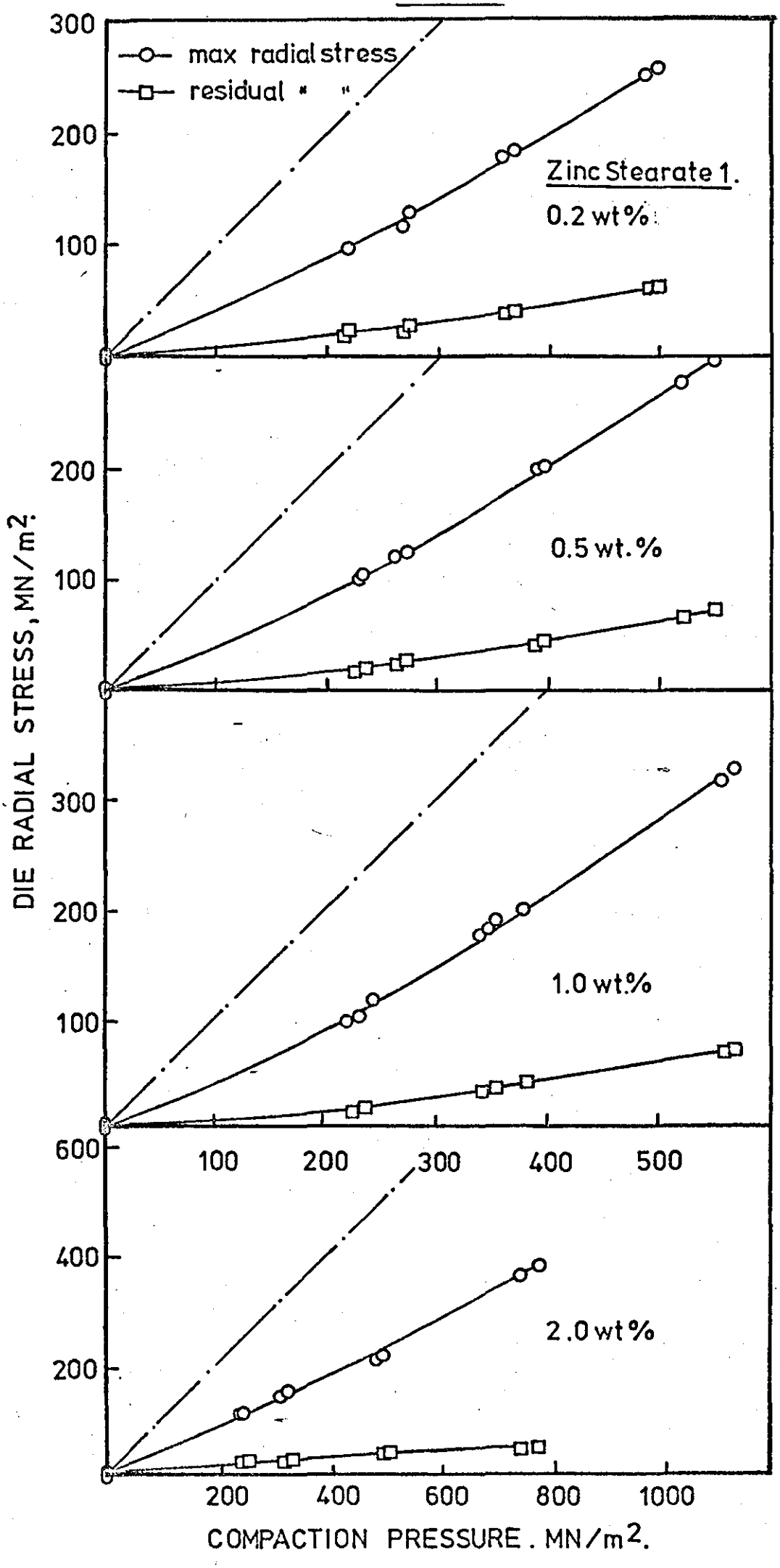
max radial stress
residual " "
Zinc Stearate 1.
0.2 wt%
0.5 wt.%
1.0 wt.%
2.0 wt%
DIE RADIAL STRESS, MN/m2.
COMPACTION PRESSURE . MN/m2.
300
200
100
600
400
100
200
300
400
500
200
400
600
800
1000

FIGURE 54

Coefficient of Friction - Lubricant Content relationships for compacts pressed at different densities in a High Chromium steel die (HCD)

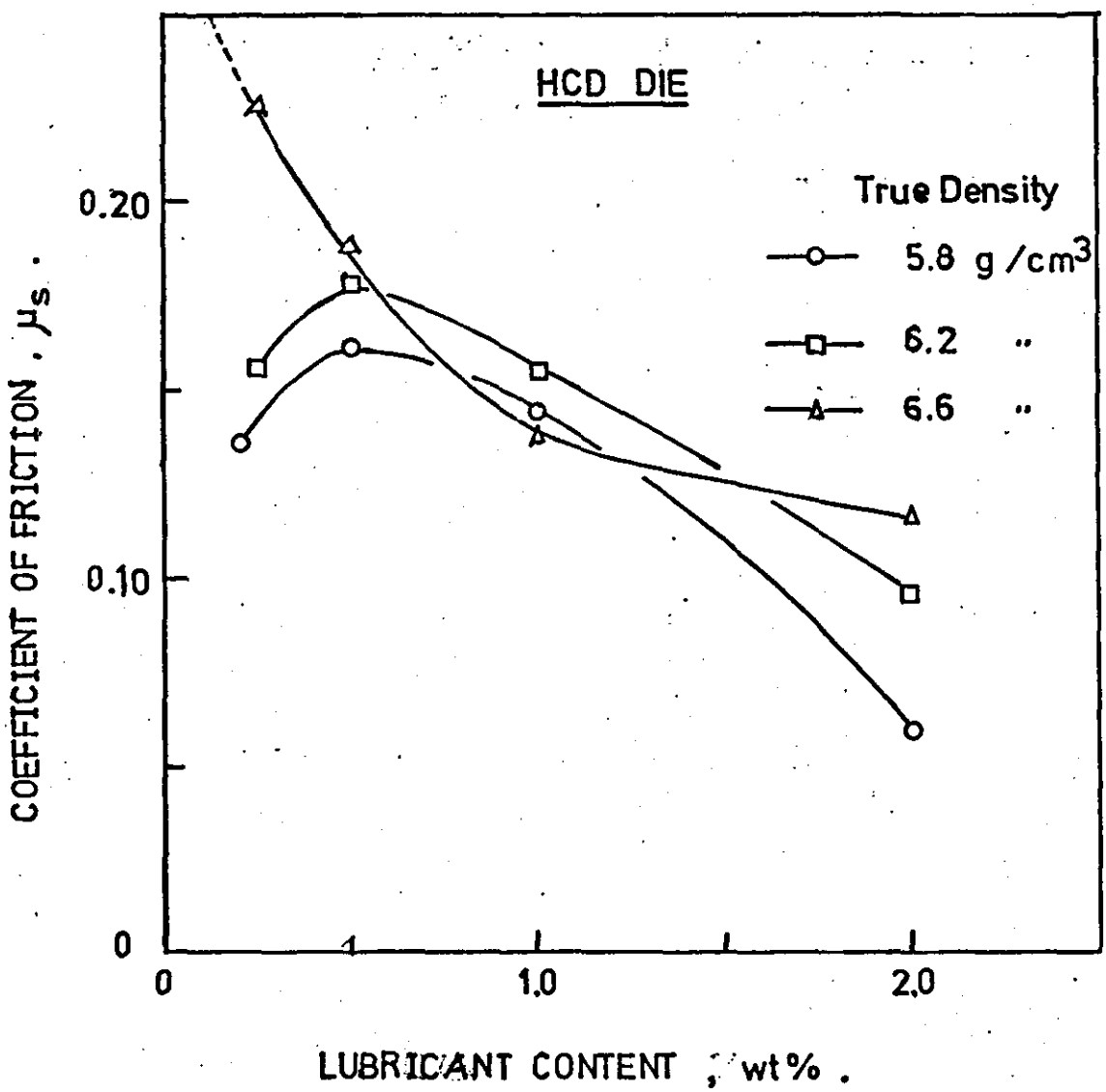
HCD DIE
True Density
5.8 g /cm3
6.2 ..
6.6 ..
0.20
0.10
0
0
1.0
2.0
COEFFICIENT OF FRICTION , μs .
LUBRICANT CONTENT , wt% .

FIGURE 55

Coefficient of Friction - Lubricant content relationships for compacts pressed at different densities in a Tungsten Carbide die (WC).

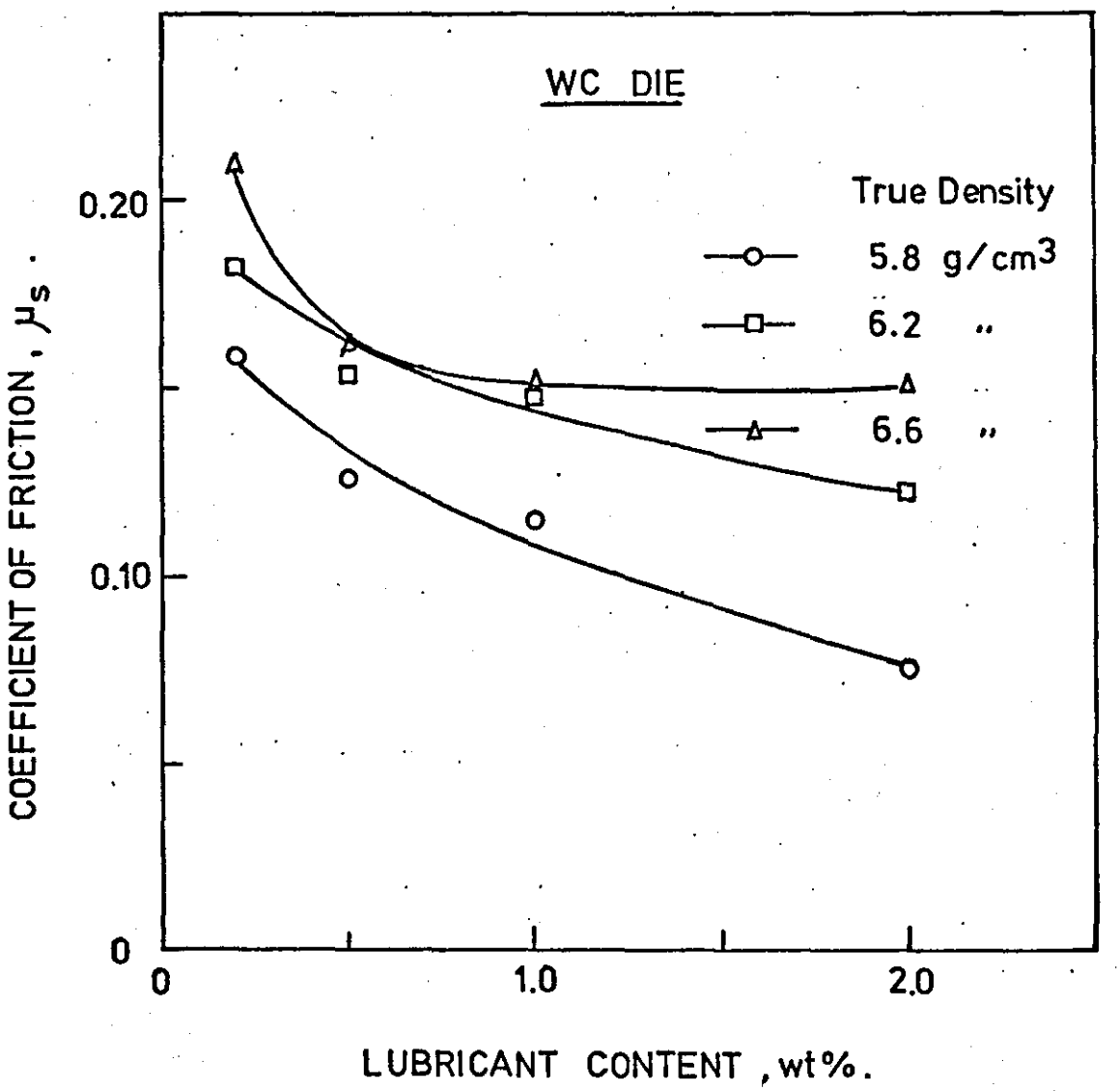
WC DIE
True Density
5.8 g/cm3
6.2 "
6.6 "
0.20
0.10
0
0
1.0
2.0
COEFFICIENT OF FRICTION, μ_s.
LUBRICANT CONTENT, wt%.

FIGURE 56

Typical traces obtained on instrumental press for bottom punch and die strain gauges in the determination of Poissons Ratio for green compacts.

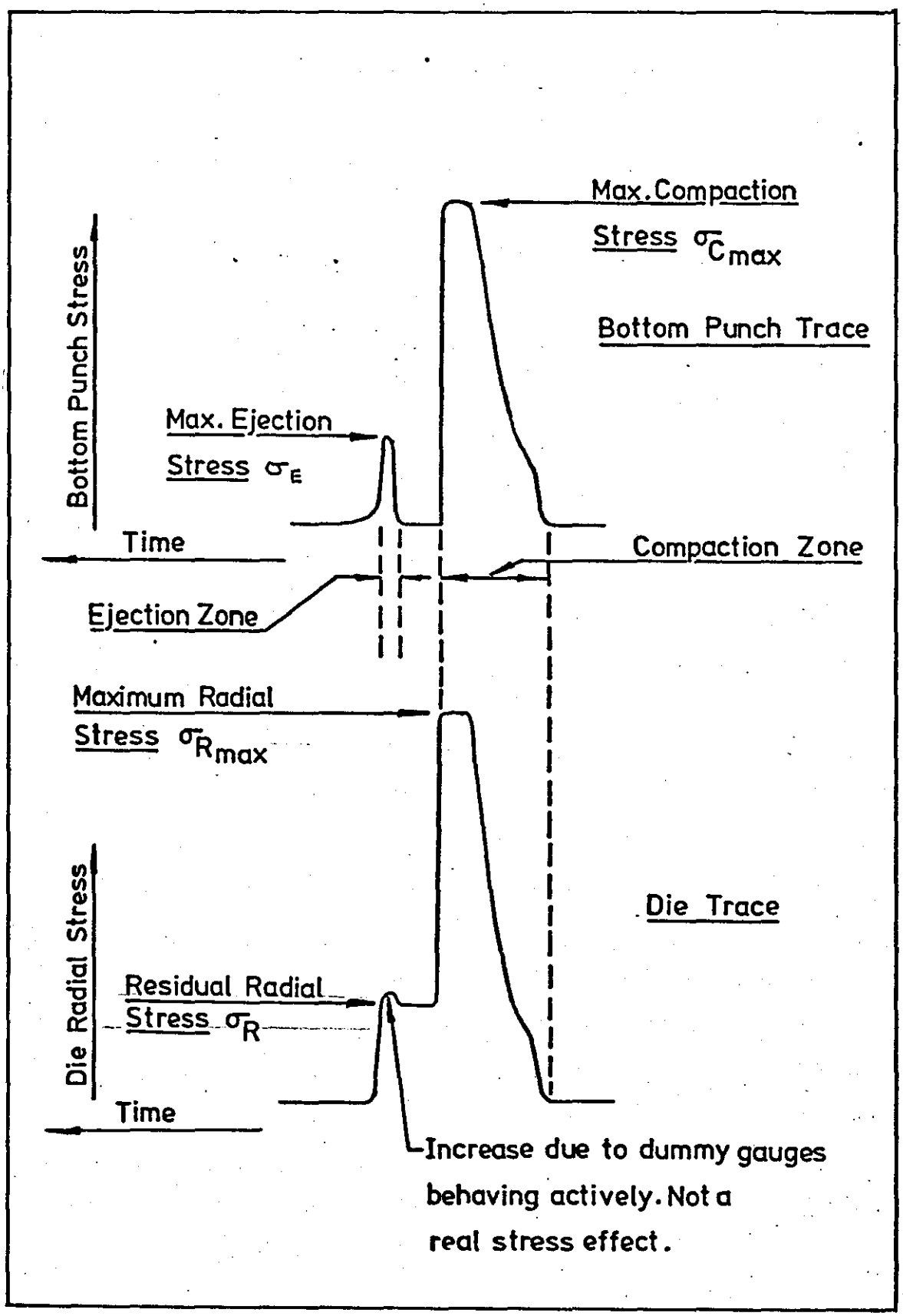
Max. Compaction
Stress $\sigma_{C_{max}}$
Bottom Punch Trace
Bottom Punch Stress
Max. Ejection
Stress σ_E
Time
Compaction Zone
Ejection Zone
Maximum Radial
Stress $\sigma_{R_{max}}$
Die Trace
Die Radial Stress
Residual Radial
Stress σ_R
Time
Increase due to dummy gauges
behaving actively. Not a
real stress effect.

FIGURE 57

Poissons Ratio - True Density relationships for compacts pressed with varying zinc stearate content in a High Chromium Steel die (HCD).

FIGURE 58

Poissons Ratio - True Density relationships for compacts pressed with varying zinc stearate content in a Tungsten Carbide die (WC).

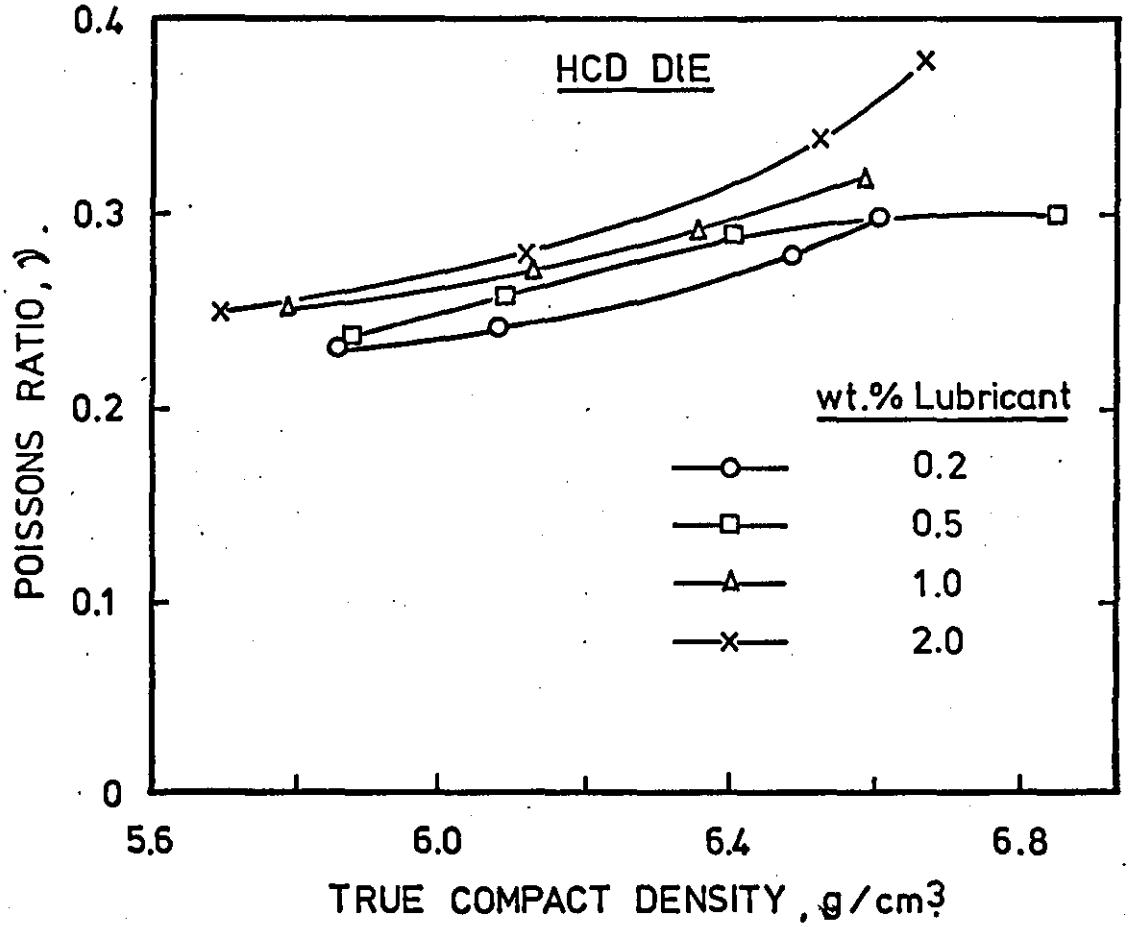
HCD DIE
POISSONS RATIO, ν.
0.4
0.3
0.2
0.1
0
5.6
6.0
6.4
6.8
TRUE COMPACT DENSITY, g/cm³
wt.% Lubricant
0.2
0.5
1.0
2.0

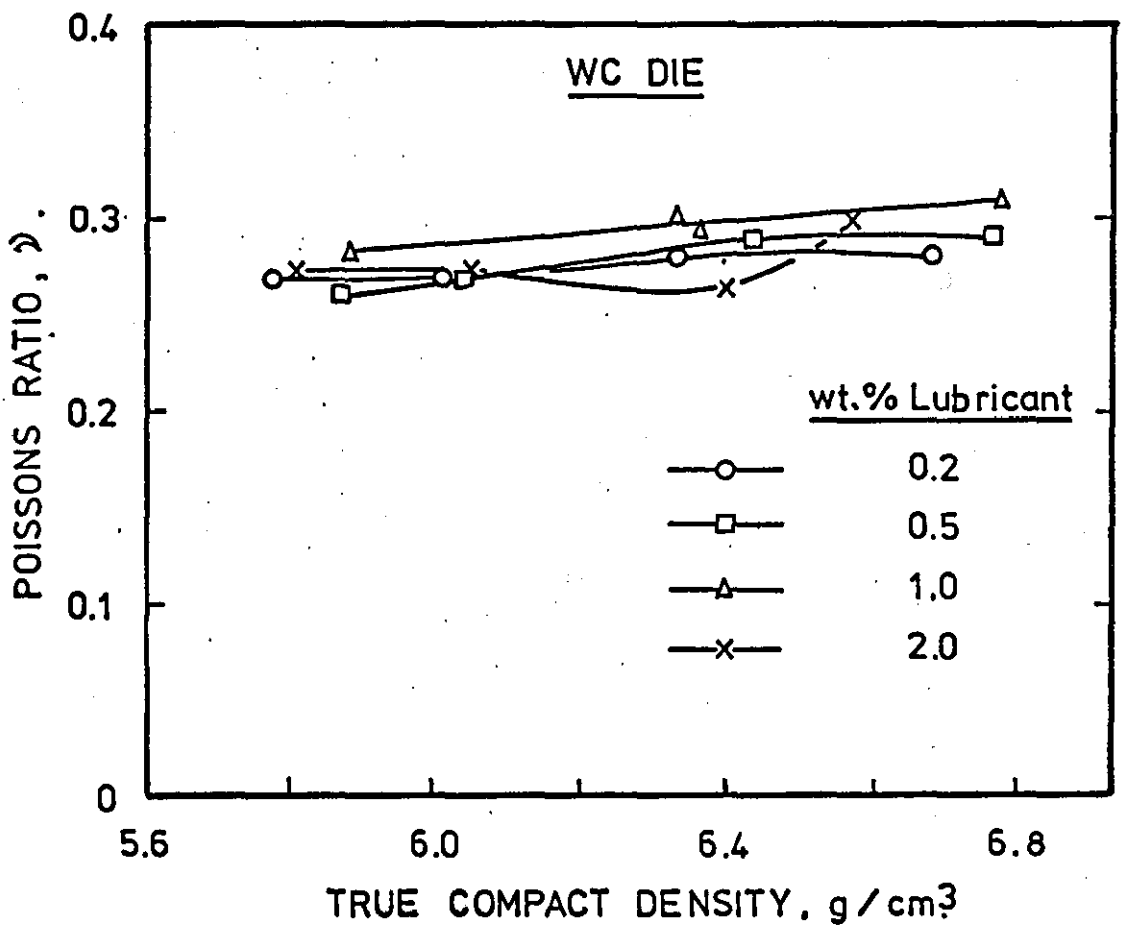
WC DIE
POISSONS RATIO, ν.
0.4
0.3
0.2
0.1
0
5.6
6.0
6.4
6.8
TRUE COMPACT DENSITY, g/cm³
wt.% Lubricant
0.2
0.5
1.0
2.0

FIGURE 59

Coefficient of Friction - contact Resistance relationships for Pin-and-Disc Apparatus for zinc stearates 1 and 8 lubricating iron compact "pins" under a load of 5kg.

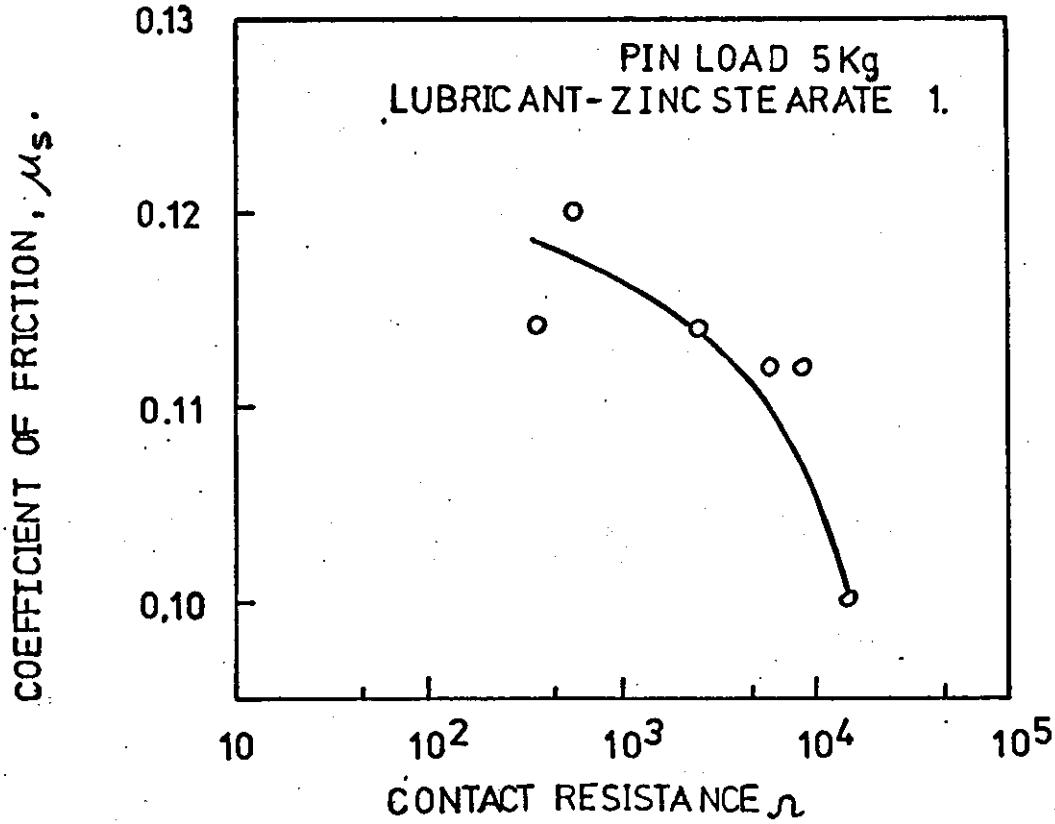
PIN LOAD 5Kg
LUBRICANT-ZINC STEARATE 1.
COEFFICIENT OF FRICTION, μ_s.
0.13
0.12
0.11
0.10
10
10^2
10^3
10^4
10^5
CONTACT RESISTANCE Ω

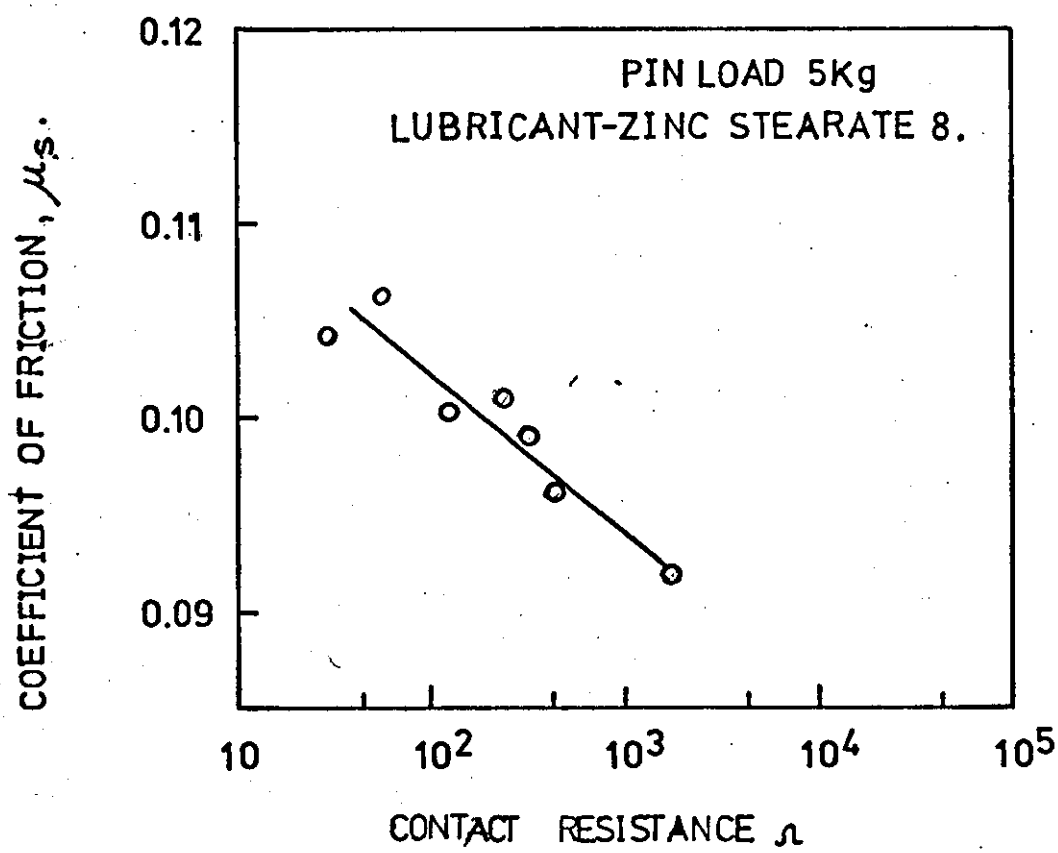
PIN LOAD 5Kg
LUBRICANT-ZINC STEARATE 8.
COEFFICIENT OF FRICTION, μ_s.
0.12
0.11
0.10
0.09
10
10^2
10^3
10^4
10^5
CONTACT RESISTANCE Ω

FIGURE 60

Coefficient of Friction - Pin Temperature relationships for Pin-and-Disc Apparatus for zinc stearate 1 lubricating and iron compact "pin" in contact with a High Chromium Steel disc (HCD)

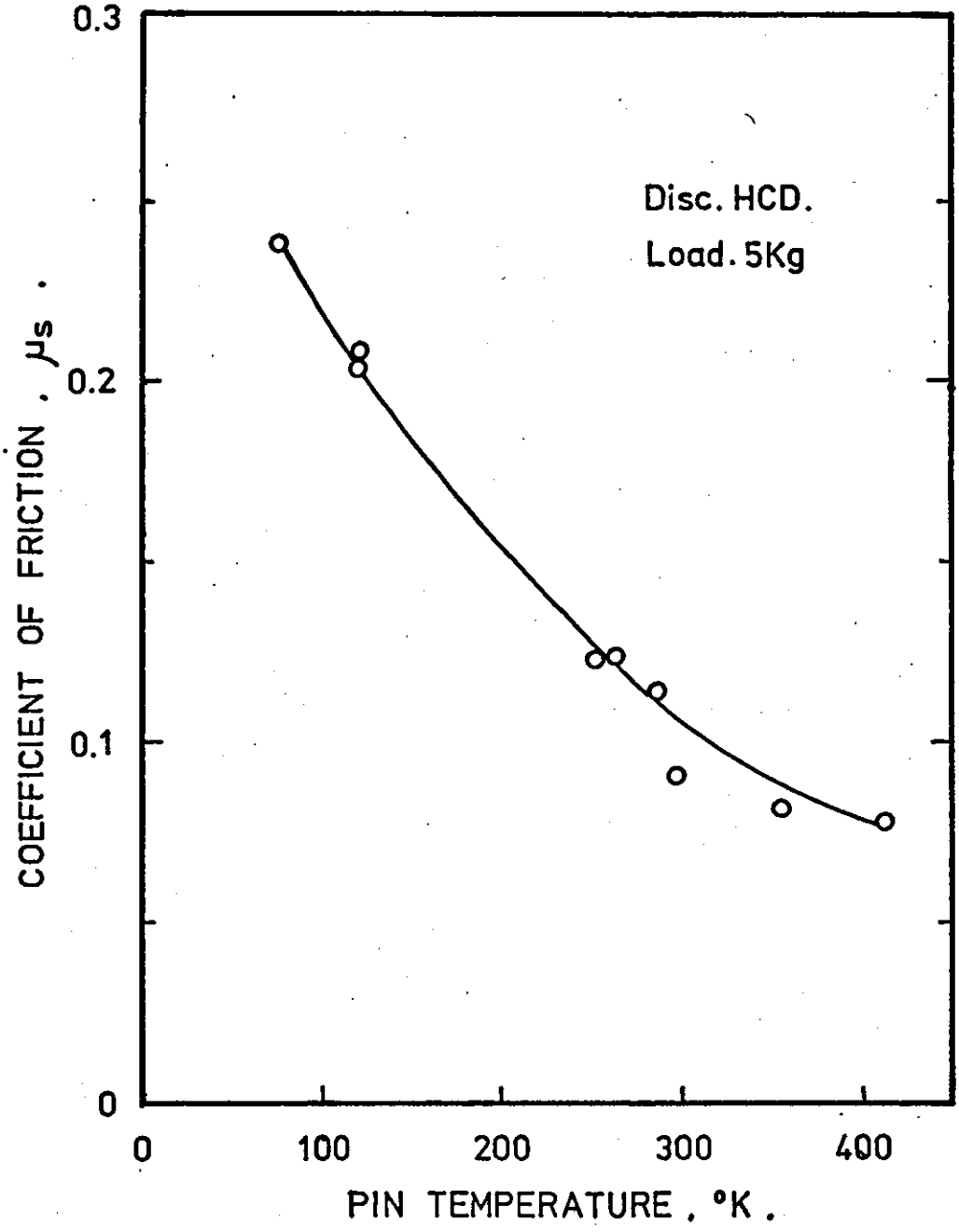
0.3
0.2
0.1
0
Disc. HCD.
Load. 5Kg
COEFFICIENT OF FRICTION , μ_s .
0
100
200
300
400
PIN TEMPERATURE , °K .

FIGURE 61

Variation of Coefficient of Friction with Sliding Distance in typical Pin-and-Disc studies

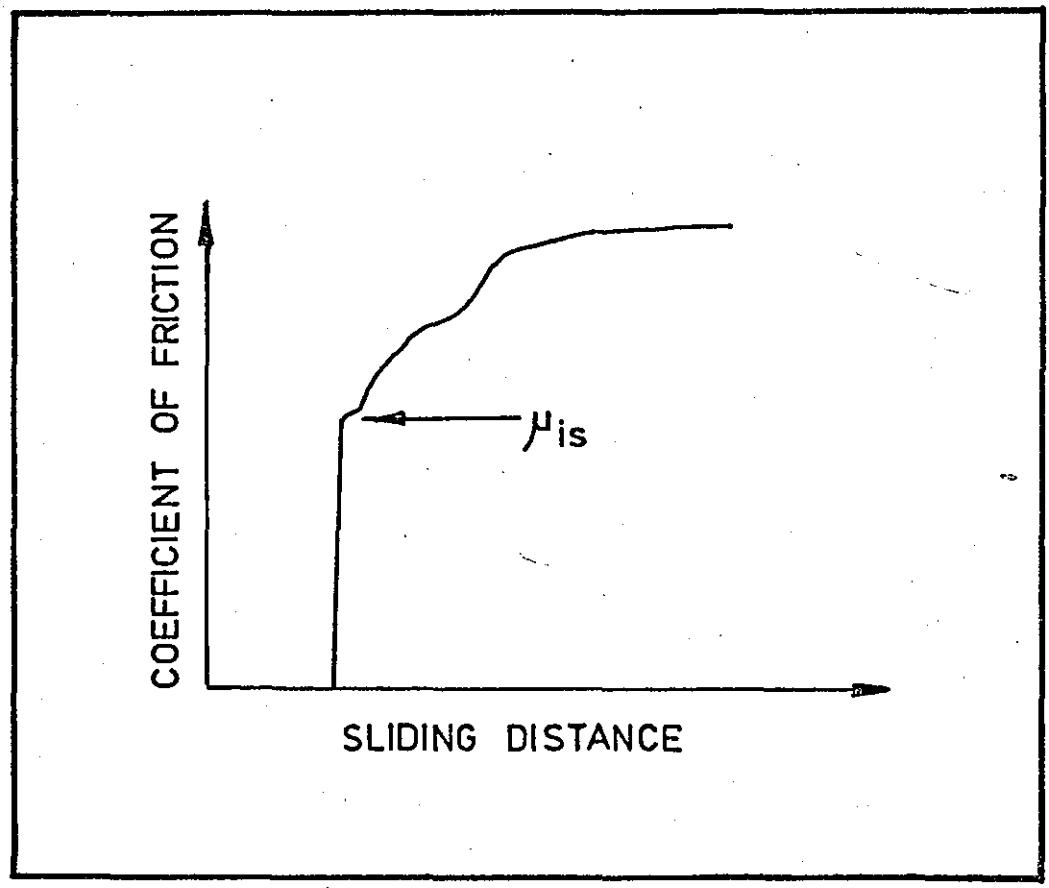
COEFFICIENT OF FRICTION
μ_{is}
SLIDING DISTANCE

Volume of Material Removed - Sliding Distance relationships for wear rate studies in Pin-and-Disc experiments for varying load and speed conditions with unlubricated iron compact "pins"

FIGURE 62: Varying load and constant speed of 156 cm/sec.

FIGURE 63: Varying speed and constant load of 1 kg.

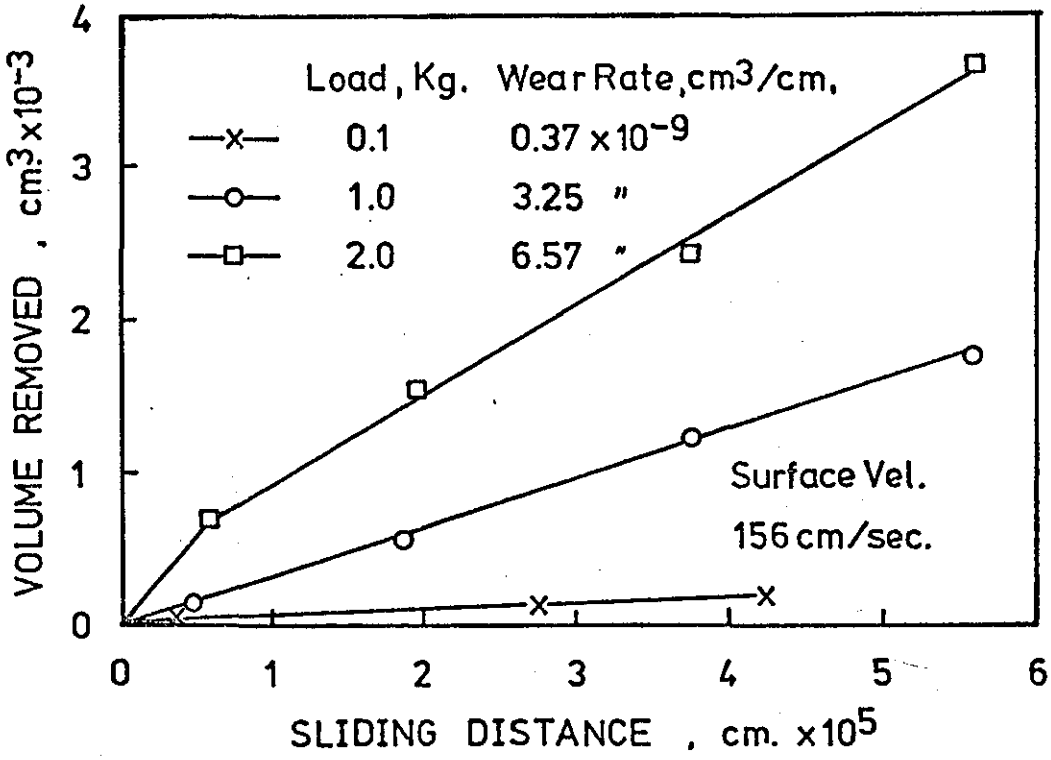
Load, Kg.
Wear Rate, cm3/cm.
0.1
0.37 x 10-9
1.0
3.25 "
2.0
6.57 "
Surface Vel.
156 cm/sec.
VOLUME REMOVED , cm.3 x10-3
SLIDING DISTANCE , cm. x105
0
1
2
3
4
5
6

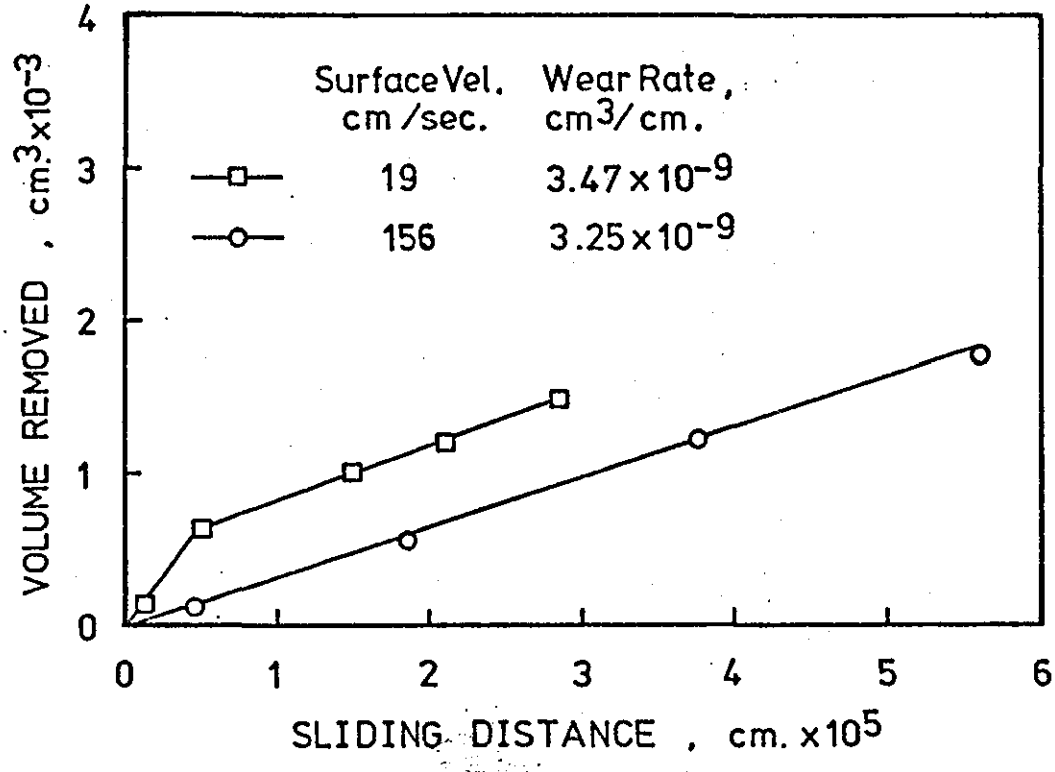
Surface Vel.
cm /sec.
Wear Rate,
cm3/ cm.
19
3.47 x 10-9
156
3.25 x 10-9
VOLUME REMOVED , cm.3 x10-3
SLIDING DISTANCE , cm. x105
0
1
2
3
4
5
6

Volume of Material Removed - Sliding Distance relationships for wear rate studies in Pin-and-Disc experiments for varying load and disc material conditions with iron compact "pins"

FIGURE 65: Varying disc materials for experiments at a speed of 19 cm/sec., load 1 kg., for unlubricated iron compact "pin".

FIGURE 64: Varying load for constant disc material (high chromium steel) and constant speed of 156 cm/sec.

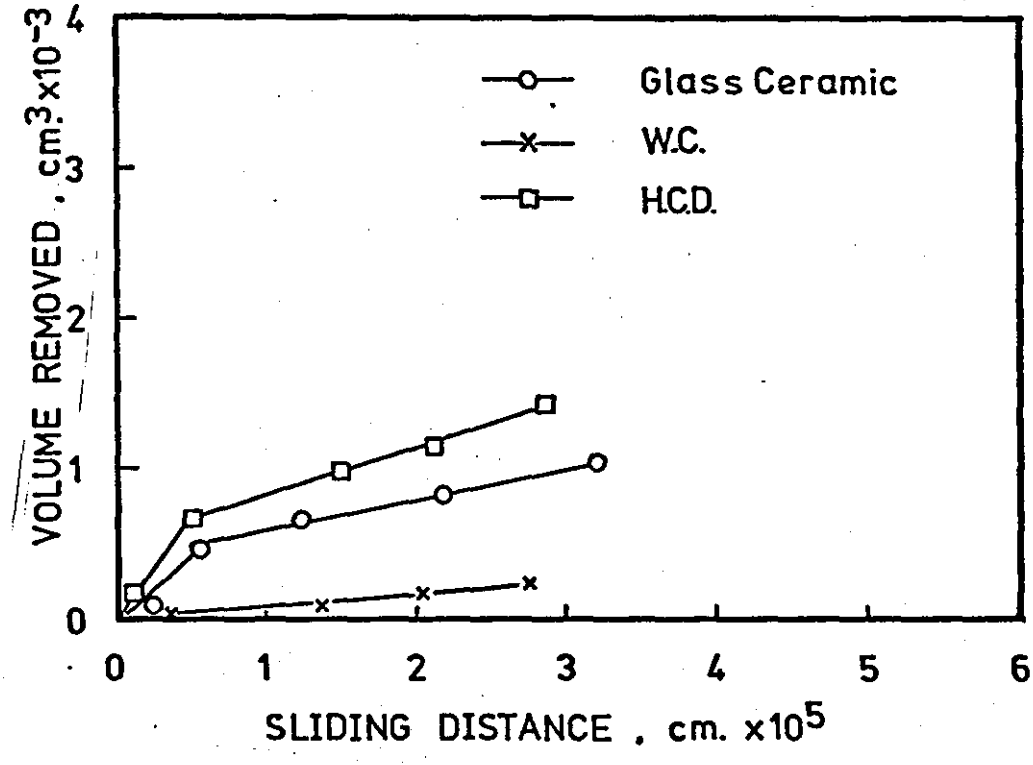
Glass Ceramic
W.C.
H.C.D.
VOLUME REMOVED , cm.^{3}x10^{-3}
SLIDING DISTANCE , cm. x10^5
0
1
2
3
4
5
6

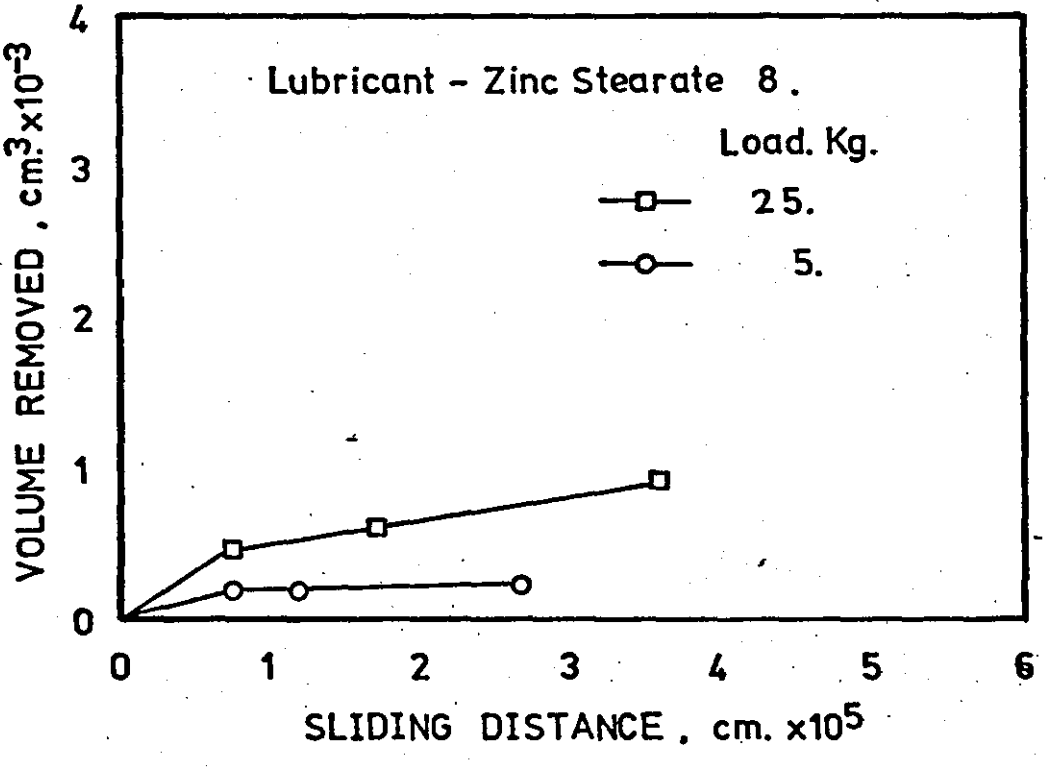
Lubricant - Zinc Stearate 8 .
Load. Kg.
25.
5.
VOLUME REMOVED , cm.^{3}x10^{-3}
SLIDING DISTANCE , cm. x10^5
0
1
2
3
4
5
6

FIGURE 66

Talysurf traces and Scanning Electron Microscope photographs of replicas of die surfaces taken during the unlubricated wear studies of iron powder compact running against a disc of high chromium steel

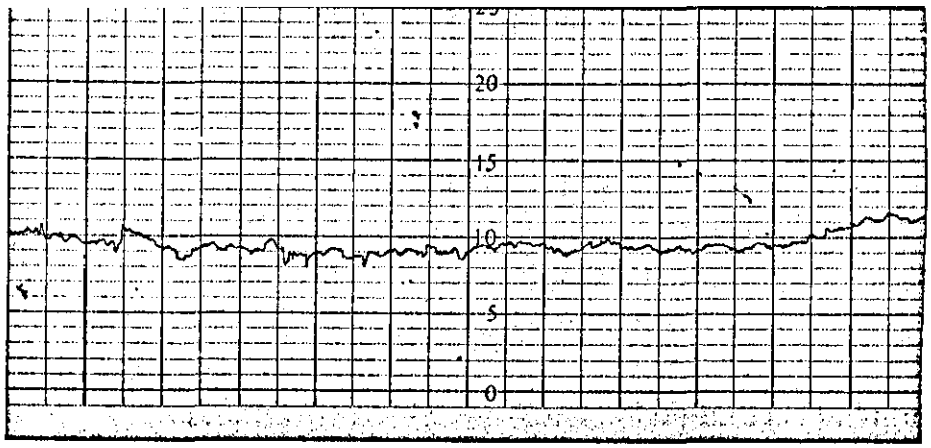
20
15
10
5
0

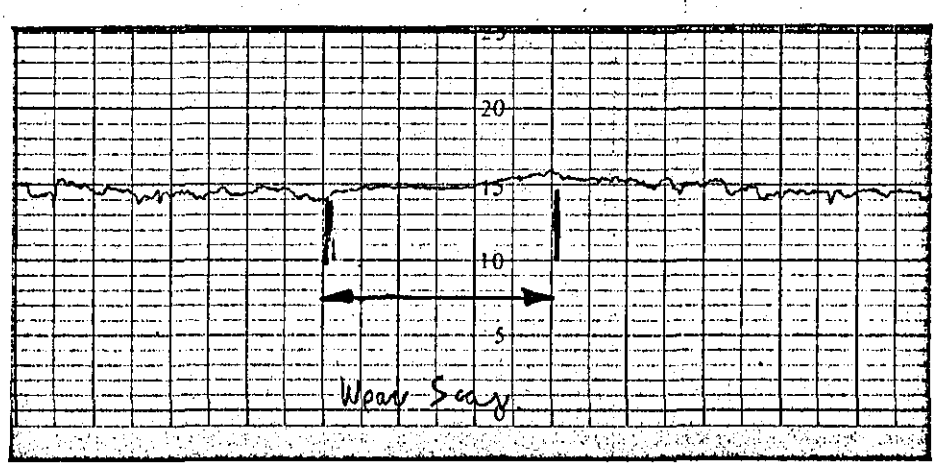
20
15
10
5
Wear Scar

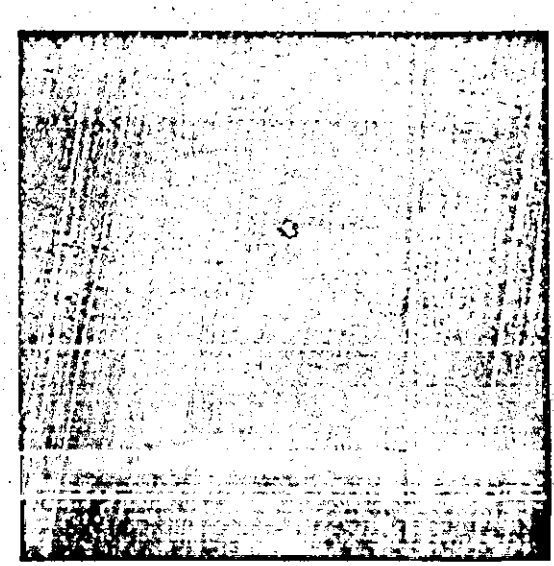

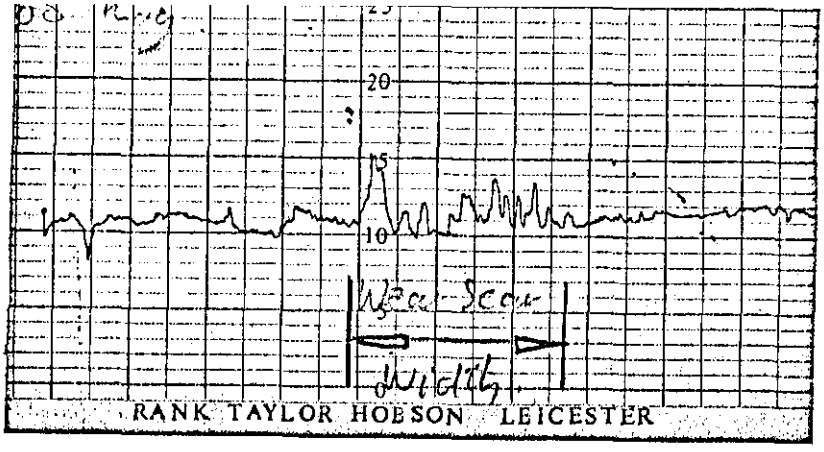
20
15
10
Wear Scar
Width
RANK TAYLOR HOBSON LEICESTER

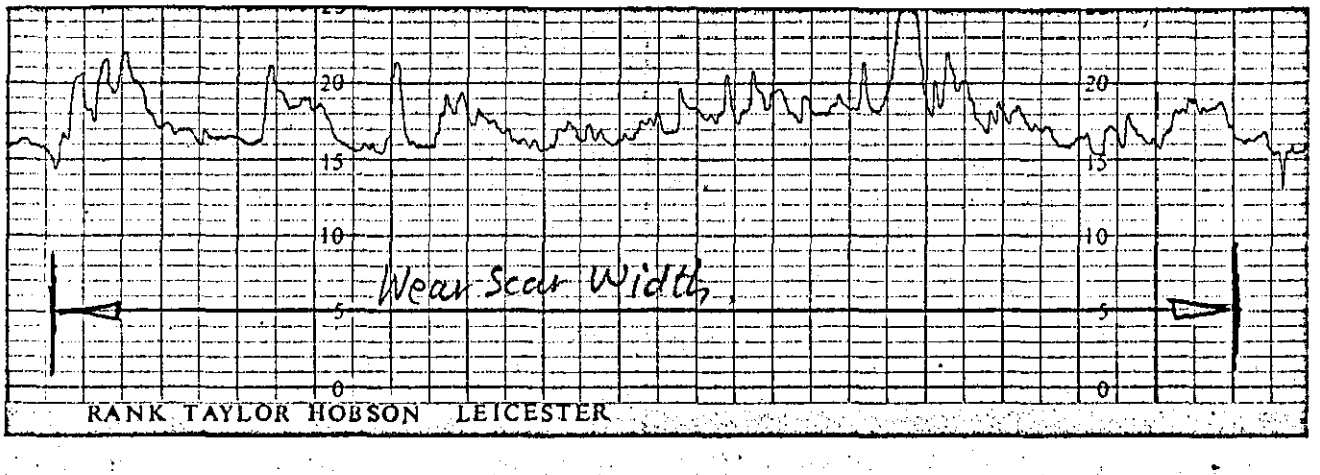
20
15
10
5
0
Wear Scar Width
RANK TAYLOR HOBSON LEICESTER

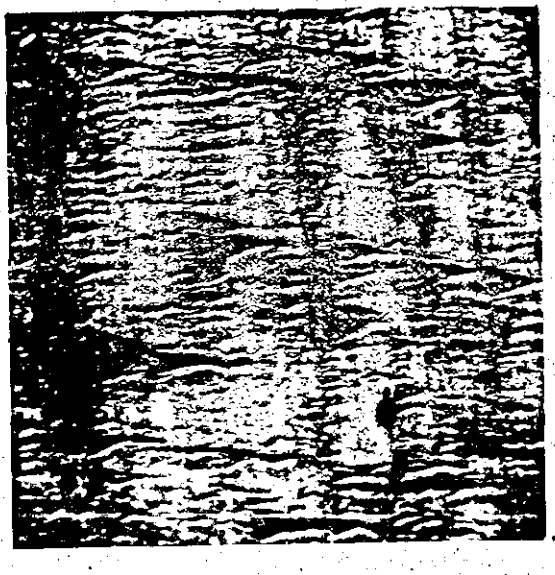

FIGURE 67

Compaction Pressure - True Density - Height/ Diameter ratio relationships for iron powder with 1% zinc stearate 1

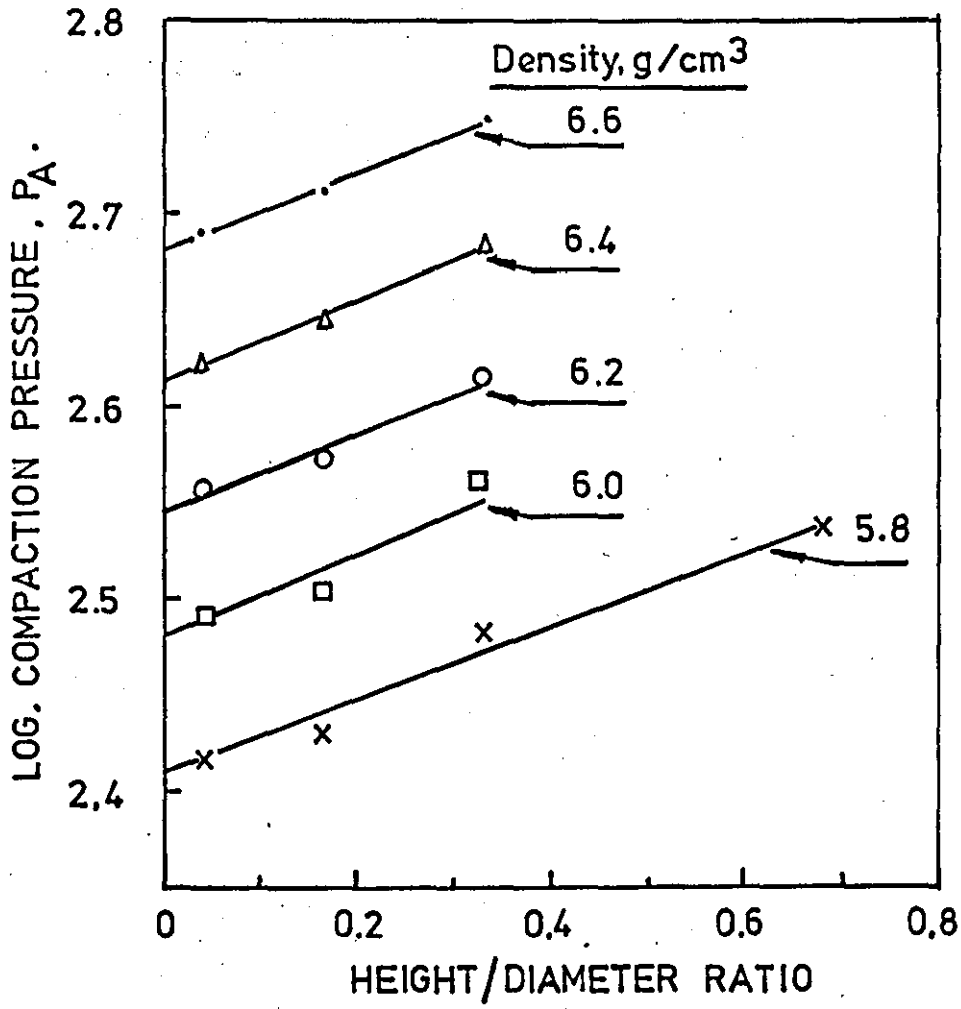
Density, g/cm3
6.6
6.4
6.2
6.0
5.8
LOG. COMPACTION PRESSURE, PA.
2.8
2.7
2.6
2.5
2.4
0
0.2
0.4
0.6
0.8
HEIGHT/DIAMETER RATIO

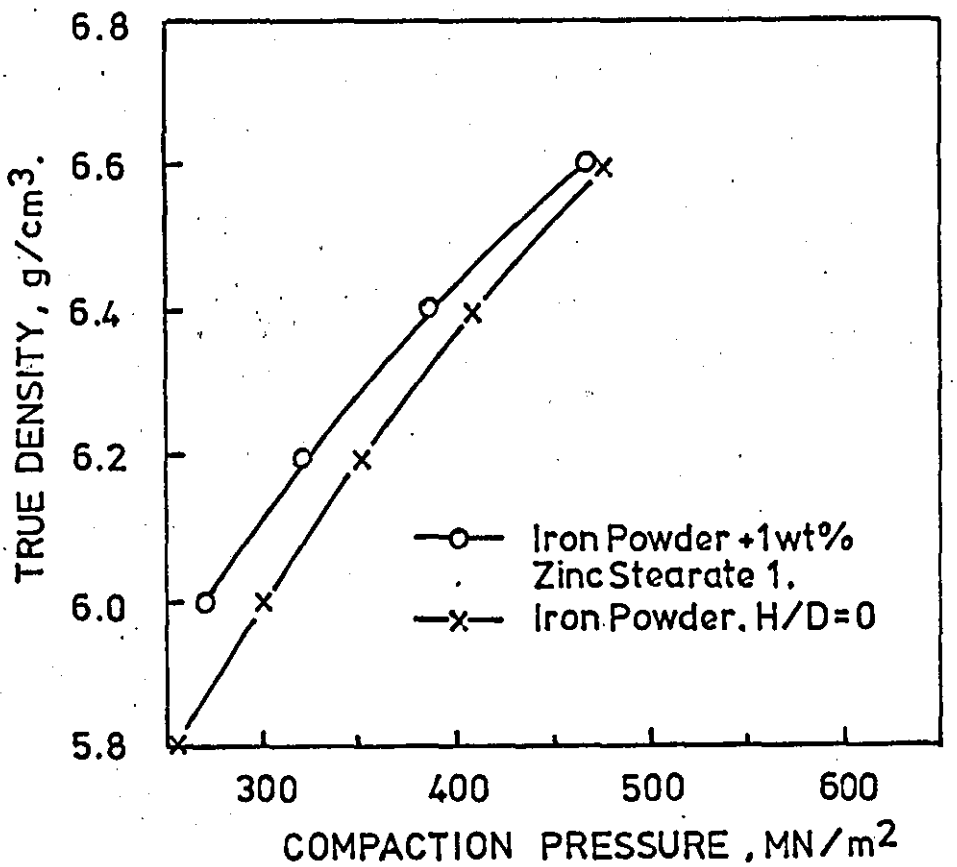
TRUE DENSITY, g/cm3.
6.8
6.6
6.4
6.2
6.0
5.8
Iron Powder +1wt%
Zinc Stearate 1.
Iron Powder. H/D=0
300
400
500
600
COMPACTION PRESSURE, MN/m2

FIGURE 68

Dependence of coefficient of sliding friction on zinc stearate medium particle size over a range of density levels in laboratory scale studies for the eight stearates.

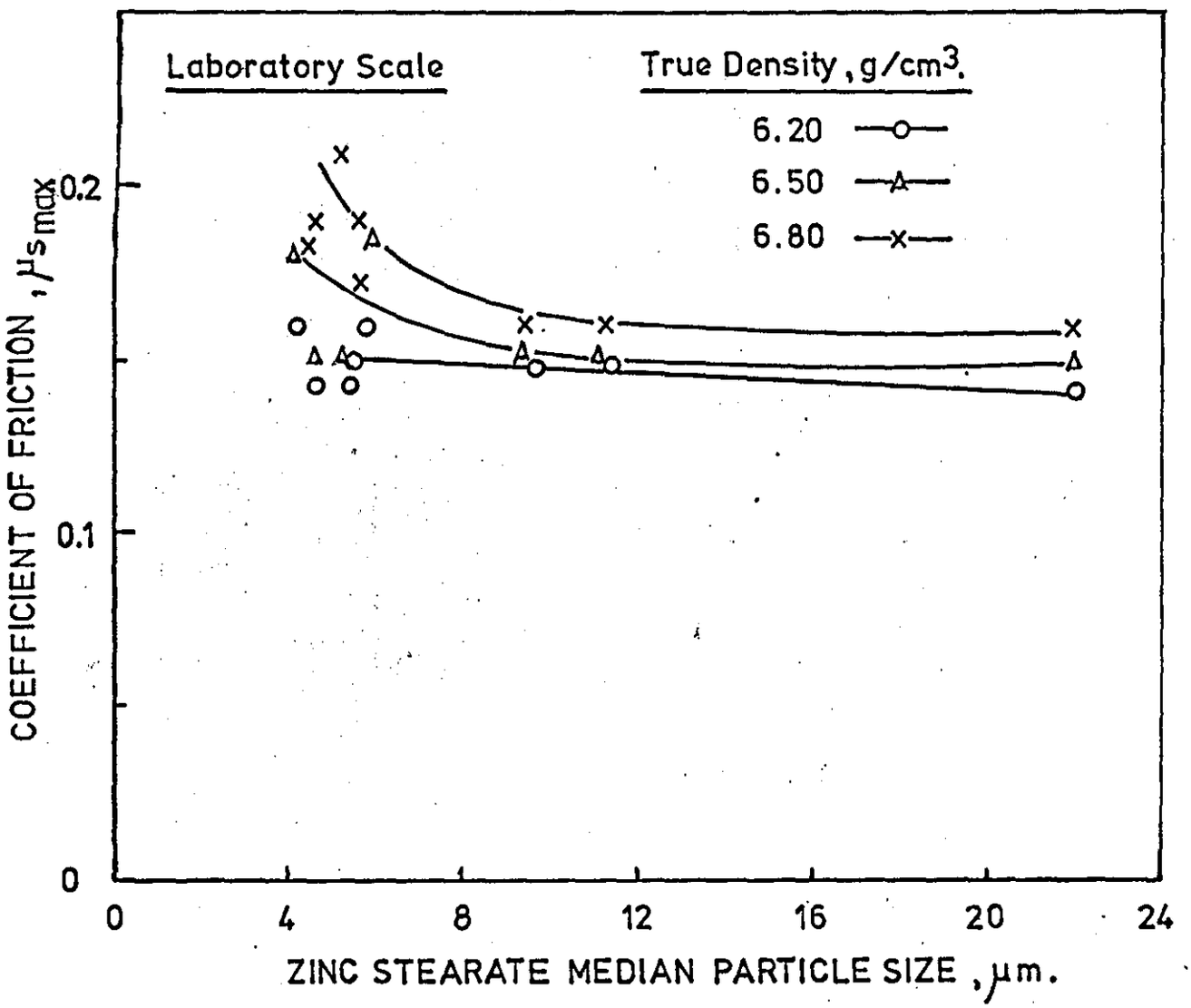
Laboratory Scale
True Density, g/cm3.
6.20
6.50
6.80
COEFFICIENT OF FRICTION, μsmax
0.2
0.1
0
0
4
8
12
16
20
24
ZINC STEARATE MEDIAN PARTICLE SIZE, μm.